UNIVERSITY OF SOUTHAMPTON

Imprinted Polymers and Templated Cyclic Peptides: a Combinatorial Approach

By

Loïc Le Strat

Doctor of Philosophy

Department of Chemistry

Faculty of Science

December 2002

UNIVERSITY OF SOUTHAMPTON

ABSTRACT

FACULTY OF SCIENCE

CHEMISTRY

Doctor of Philosophy

IMPRINTED POLYMERS AND TEMPLATED CYCLIC PEPTIDES: A COMBINATORIAL APPROACH

By Loïc Le Strat

The aims of this project were to apply the concept of combinatorial chemistry to two fields of supramolecular chemistry: molecular imprinted polymers (MIPs) and metal templated cyclo-oligomerisation of peptides.

A library of MIPs were synthesised as thin films. A range of aromatic and alkyl acrylamide monomer building blocks were synthesised and the binding properties of the polymers were investigated as a function of the polymerisation mixture. New screening methods were investigated to allow high-throughput screening of the MIPs. The results suggested the mixture methacrylic acid-toluene could give efficient MIPs.

Potential molecular imprinted polymers were prepared by bulk polymerisation and used as HPLC stationary phases. The properties of the polymers were investigated by resolution of the template and its enantiomer under a number of different elution conditions. Mobile phases with trifluoroacetic acid improved the resolution, but longer columns or high flow rate prevented base line resolution.

A range of dipeptides were synthesised and used in template mediated synthesis. The rates of peptide couplings around the metal ion, in solution and on solid support, were investigated as a function of the chain length and nature of the residues of the linear precursor. Although cyclo-oligomerisations were expected, only linear tetrapeptides were observed in the presence of the metal ion.

TABLE OF CONTENTS

ACKNOWLEDGEMENTS

I would like to thank my supervisor, Prof. Mark Bradley for his encouragement and help over the last three years. Thanks are also due to Dr. Richard Elliott for his support, comments and an extremely friendly welcome to GSK during my industrial placement.

My thanks go also to Julie Herniman and John Langley for running mass spec. samples and to Joan Street and Neil Wells for running NMR samples.

I would like to express my sincere thanks to the past Bradley group. First of all I thank Nathalie for her valuable help in the handling for the polymerisation, her suggestions, at least when her stress level allowed the dialogue. I thank also the past French post-doc connection: Fabrice for his help and kindness, Vincent, for his endless and contagious enthusiasm for mushroom picking and Christophe for his availability and friendship. Thanks to Thomas and Jürgen for their hoots of laughter, unforgettable.
Many thanks also to the present Bradley group: Mizio, for all the pizza parties, Boon-Ek. for his kindness (and spicy food), and Jeff (froggy) being just ...Jeff. Thanks to Mark, Katie, James and the others who helped me in one way or another during my PhD.
A big thanks to all those who proof read this thesis, which was very helpful.

Above all, I would like to thanks Cécile for her endless support, understanding and patience. Thank you for everything. I would like to thank my parents and my brother for their support and their faith in me.

ABBREVIATIONS

General

AcOEt	Ethyl Acetate
AcOH	Acetic acid
Boc	*tert*-Butoxycarbonyl
br.	broad
Calc.	Calculated
CSP	Chiral stationary phase
DCM	Dichloromethane
DIC	1,3-Diisopropylcarbodiimide
DIPEA	*N, N'*-Diisopropylethylamine
DMF	Dimethylformamide
DMSO	Dimethylsulfoxide
ELS	Evaporative light scattering
ESI	Electrospray Ionisation
Fmoc	Fluorenylmethoxycarbonyl
HCl	Hydrochloric acid
HOBt	*N*-Hydroxybenzotriazole
HPLC	High performance liquid chromatography
IBCF	Isobutylchloroformate
IR	Infra-red
J	Coupling constant
LC-MS	Liquid chromatography - Mass spectrometry
MeCN	Acetonitrile
MeOH	Methanol
Mp.	Melting point
NAD	Nicotinamide adenine dinucleotide
NMR	Nuclear Magnetic Resonance
NEt_3	Triethylamine
PE	Petroleum ether
R_f	Retention factor

RT	Room temperature
TFA	Trifluoroacetic acid
THF	Tetrahydrofuran
TLC	Thin Layer Chromatography
UV	Ultraviolet
δ_C	Carbon shift
δ_H	Proton shift

Polymerisation

AIBN	*azo-N,N'*-bisisobutyronitrile
EGDMA	Ethylene glycol dimethacrylate
HEMA	Hydroxyethyl methacrylate
MAA	Methacrylic acid
MIP	Molecular Imprinted Polymer
MMA	Methyl methacrylate
NBA	*N*-Benzylacrylamide
NBMA	*N*-Benzyl-2-methacrylamide
NEA	*N*-Ethylacrylamide
NEMA	*N*-Ethyl-2-methacrylamide
NHEA	*N*-(2-hydroxyethyl)acrylamide
NHEMA	*N*-(2-hydroxyethyl)methacrylamide
NVP	*N*-Vinyl-α-pyrrolidone
TFM	2-(Trifluoromethyl)acrylic acid
VPY	4-Vinylpyridine

CHAPTER 1: INTRODUCTION

1.1 SUPRAMOLECULAR CHEMISTRY: CHEMISTRY BEYOND THE MOLECULE

Evolution has produced compounds exquisitely organised to accomplish the most complicated and delicate of tasks such as cellular recognition, transcription and the regulation of gene expression or signal induction by neurotransmitters. Many organic chemists viewing crystal structures of enzymes, nucleic acids or observing the incredible specificity of the immune system have dreamt of reproducing in their test tubes compounds with similar molecular architectures and functions.

From this dream was born a new field in chemistry termed in the sixties supramolecular chemistry. Lehn has defined it as the chemistry of the intermolecular bond, covering the structure and functions of entities with higher organisation, resulting from the reversible association, by non covalent bonds, of two or more chemical species.[1] A new field requires new terms to simplify the reasoning by analogy. Thus supramolecular species have been termed hosts and guests as synthetic counterparts to the receptors sites and substrates of biological systems. Lehn, Cram and Pederson, pioneers in this area, understood the importance of the host-guest principle and developed synthetic macrocyclic structures to mimic some of the selective binding models observed in nature. Their works were awarded the Nobel Prize in 1987. Lehn[1] developed the concept of the macrocyclic cage, the cryptands, while Cram[2] focused on the paracyclophanes.[3] Pedersen[4] reported the synthesis of macrocyclic polyethers, such as the crown ethers, as another highly structured complex used as potential hosts. However, supramolecular chemistry is not limited to systems similar to those found in biology, but is free to create novel species and to invent processes. Molecular recognition, transformation and translocation are the basic functions of supramolecular species. The cyclic oligosaccharides (cyclodextrins)[5] are very promising hosts[6] especially in biomimetic reactions.[7] The macrocyclic frameworks are not the only models able to recognise their templates. Rebeck has reported the use of cleftlike structures (Kemp's triacid derivatives) for nucleotide fitting and asymmetric recognition.[8]

On the basis of the host-guest principle surprising discoveries in the field of the supramolecular chemistry have renewed interest. For instance, the synthesis of supramolecular species itself has been improved to lead to intricate variants, such as oligocatenanes[9], molecular necklaces[10] and cyclic daisy chains[11-13] to name but few.

Among the new applications, the development of self-replicating systems must be mentioned[7] as well as drug encapsulation by cyclodextrin derivatives with compound progressing well in clinical trials.[14] Finally, the synthesis of polymeric binding cavities for analytical applications can be performed using the host-guest concept.

1.2 "TEMPLATING CHEMISTRY" – AN OVERVIEW

1.2.1 Principles

The course of an organic reaction can be affected by numerous parameters, for example the temperature of a reaction can draw the equilibrium of the synthesis towards either the kinetic or thermodynamic product. A substitution reaction of a bifunctional substrate can yield the di-substituted product rather than the mono-substituted depending on the molar ratio of the reactants. Another method to "push" a reaction in a desired direction is the addition of a catalyst that is not engaged in the stoichiometry of the reaction. The catalyst increases the rate of the reaction. They can be divided into two broad classes: catalysts insoluble in the reaction medium (heterogeneous catalysts) like Raney Nickel[15] used in hydrogenations and catalysts soluble in the medium (homogeneous catalysts) such as rhodium derivatives $RhCl(Ph_3P)_3$[16] used for the hydrogenation of olefinic compounds. Based on the approach of involving a specific compound to drive the course of an organic reaction, a maybe more exquisite method must be cited: the template synthesis.[17] The term "template effect" was first used and defined at the beginning of the sixties (Scheme 1.1).[18]

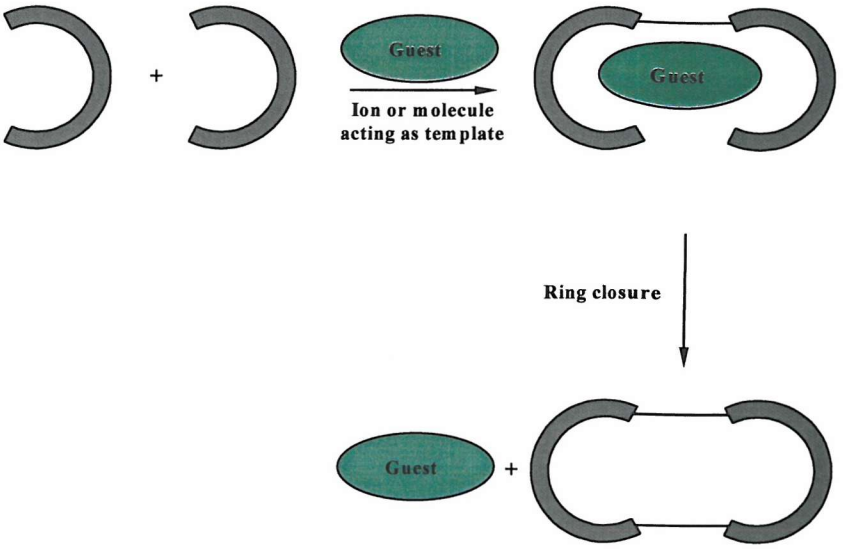

Scheme 1.1: Principle of the template effect.

A molecule called a "guest" which maybe a metal ion or a neutral compound, brings by coordination one or more molecules called "hosts" into a suitable conformation for the formation of a specific and structured product that is often cyclic. This effect is due to the stabilisation of the intermediate structure and the resulting site proximity. In the absence of the guest or template the desired product is actually formed, but with more side products that are often in equilibrium with each other. The presence of the guest directs the equilibrium in the desired direction. The formation of the polycondensation product is largely suppressed by the action of the template as a coordination centre. If no template is present in the media the two reagents can react to give a series of polymeric and cyclic products (Scheme 1.2).

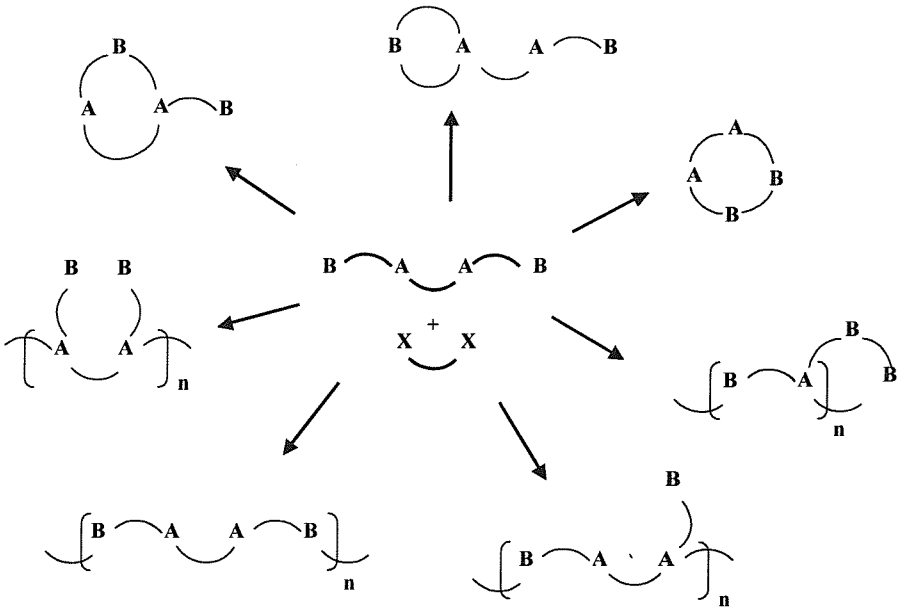

Scheme 1.2: Possible products of reaction not template induced.

The presence of the template (T) can steer the reaction (Scheme 1.3). If the template binds the linear reactive species selectively in a planar arrangement, the two functional groups (B) will be held adjacent to each other in a defined position to react with the second bifunctional substrate.

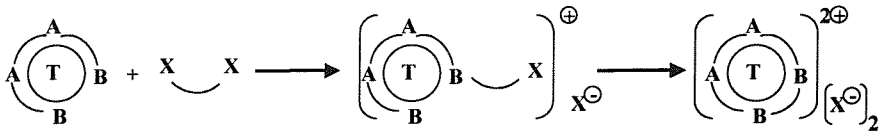

Scheme 1.3: Cyclisation reaction using a template effect.

According to its mode of action, the template has been named either positive or negative.[19] A positive template directs the approach of two reactive end groups wrapping the substrate around itself to lead to an intramolecular cyclisation. The negative template will keep the reactive groups far from the host compound (= substrate) preventing intramolecular cyclisation but, in contrast, favouring intermolecular polycondenstation. There are two types of template synthesis defined by

the nature of the bond between the guest and the host: non-covalent and covalent interactions.

1.2.2 Non covalent mediated template synthesis

Template synthesis consists mainly of synthesising macrocyclic compounds *via* hydrogen bonding, π-π stacking and metal-ligand interactions.

1.2.2.a Template synthesis with metal cations

The most frequently employed templates in syntheses are those based on metal ion chelates. The ligands building blocks wrap themselves around the metal ion to lead to the closure of the macrocycle (Scheme 1.4).

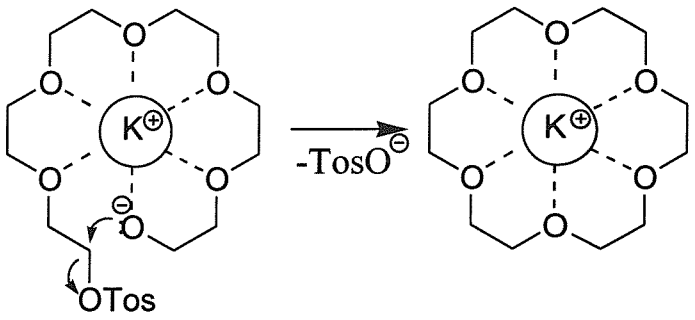

Scheme 1.4: Templated synthesis of [18] crown-6 ether.

Thus in Scheme 1.4, the potassium ion acts as a convex template to give a crown-ether complex. The total synthesis of enterobactin (Fig. 1.2) using the template approach was achieved involving tin in the cyclo-oligomerisation of β-lactones.[20]

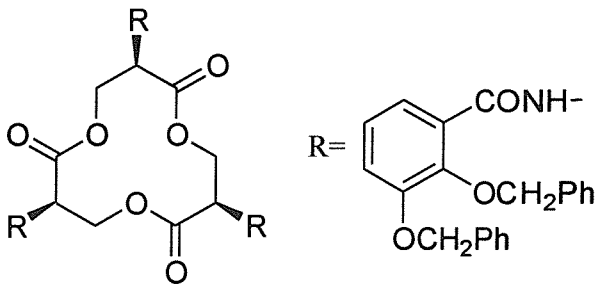

Fig. 1.2: Enterobactin synthesised by template chemistry.

Other supramolecular structures obtained by a metal ion convex template are the catenanes.[21] However, it is not just metal ions that can act as templates, neutral molecules can also participate in the process.

1.2.2.b Neutral molecules as templates

For this kind of template the driving forces are usually hydrogen bond interactions and π-π stacking. The first example reported in the literature was in 1988 by Hünig and described the use of a hydrocarbon guest.[22] One year later Kelly and co-workers carried out a template-promoted reaction between two substrates (Scheme 1.5).[23]

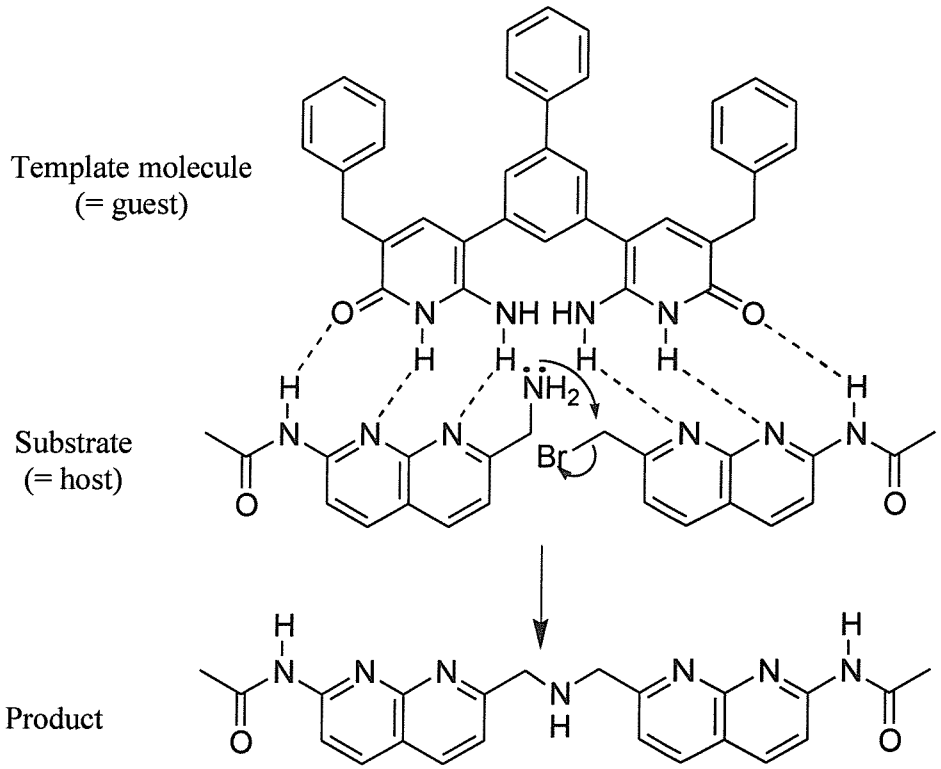

Scheme 1.5: Reaction induced by template.

The guest molecules were able to interact with two molecules of substrate, one alkyl amine and one alkyl bromide, to yield the condensation product. In this example the template molecule can be compared to an enzyme by its ability to bring the substrates into a close environment for reaction. Neutral templates were also successfully used in the inter-twined macrocyclic chain syntheses by Hunter[24] and Vögtle *et al.*[25]

1.2.3 Covalent mediated template synthesis

With this type of guest molecule the template effect is somewhat less obvious. There is a fundamental difference between this approach and supramolecular host-guest system since the molecular recognition is not necessary, rather the template and the host compounds are covalently bound together. The template can be called permanent or temporary according to its behaviour at the end of the reaction in which it participates.

1.2.3.a Permanent, covalently bound template

If the formation of a macrocyle is effected, for example, by expansion of a smaller ring *via* the insertion of a side chain already present (Scheme 1.6), the smaller ring is designated as a permanent template or endo-template, since all the molecular components originally present are also found in the final product.

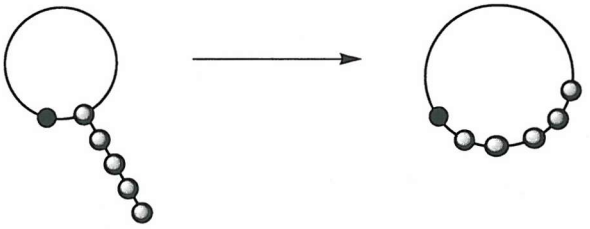

Scheme 1.6: Permanent, covalently bond template.

The most common example is probably the "zip" reaction for cyclic peptide synthesis.[26]

1.2.3.b Temporary, covalently bound template

A template is described as temporary or external if it is eliminated at the end of a synthesis and is therefore not incorporated into the structure of the final product. Leaving groups such as sulfur or nitrogen can be eliminated by pyrolysis. This approach has been used for the synthesis of asymmetrical [m,n]paracyclophane.[27] A selective chlorination reaction on the steroid backbone was also reported by the group of Breslow.[28]

1.2.4 Applications

Kool reported the use of a template to fold a synthetic oligonucleotide[30] into a triplex structure[29] while Ernest described the folding ofsynthetic peptide chains[31] into a characteristic three dimensional structure as a step toward achieving the folding of artificial proteins. Chiral cavities were obtained in a polymeric structure by imprinting of a template according to molecularly imprinted polymers (MIPs).[14]

1.3 MOLECULAR IMPRINTING POLYMERS (MIPS)

1.3.1 Concept of imprinting

The idea of template-mediated assembly in biological systems was first suggested by Linus Pauling to explain the mechanisms of the immune system.[32] Even though his theory is known now to be incorrect the principle of using a target molecule to create its own recognition sites has been applied in the preparation of artificial polymeric receptors. Molecular imprinting is a technique for the fabrication of mimetic polymeric recognition sites. In this way, recognition matrices can in theory be prepared from substrates with high selectivity and specificity. In this technology macromolecular entities are prepared by polymerisation processes in which sites are introduced using a given compound as a template in a casting procedure. The technique is schematically depicted in Fig. 1.3.

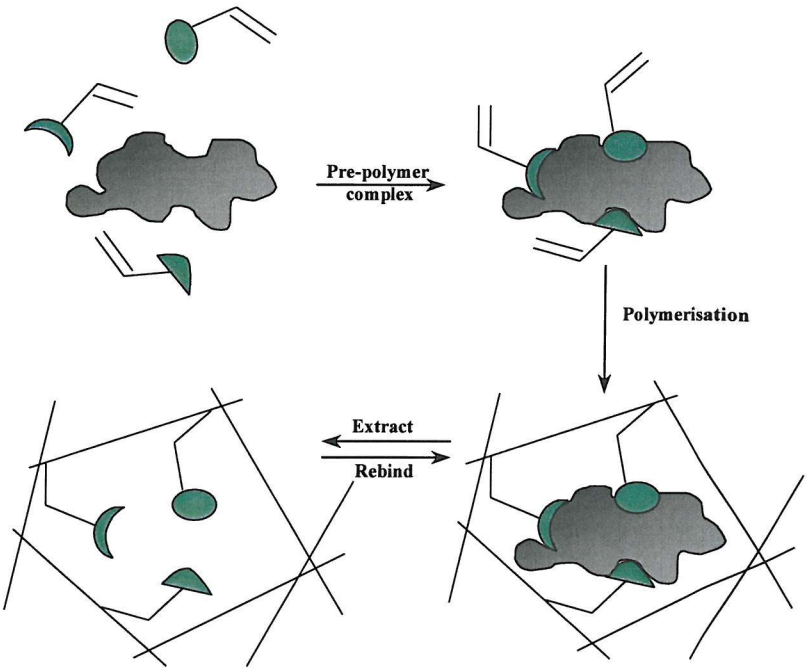

Fig. 1.3: Principle of molecular imprinted polymer.

The selected template (or imprint molecule) is first allowed to establish "binding" interactions with polymerisable chemical functionalities and the resulting complexes or adducts are subsequently copolymerised with a high level of cross-linkers to give a rigid polymer. Although usually the template is free in solution, the β-blocker theophylline has recently been used as an immobilised template on aminopropyl silica.[33] After extraction of the template, specific recognition sites are left in the polymeric network in which the spatial arrangement of the functional groups together with the shape are complementary to the imprinted molecule. The relationship of the template to the imprinted cavity corresponds to the key/lock principle proposed by Fischer for enzyme catalysis about 100 years ago.[34] In the imprinting procedure, the binding groups have several functions. The bond between the template and the binding group should be as strong as possible during the polymerisation to enable the binding groups to be fixed by the template in the definite orientation in the polymer chains during cross linking. However the template should be removed as completely as possible. Another very important function is the interaction of the binding groups with the substrate to be bound. This process should be as fast and reversible as possible to enable applications in separation or catalysis.

Since the work of Dickey and attempts at imprinting dyes in gel silica by precipitation, many other substances have been used as templates to produce imprinted polymers. Some of them are listed in Table 1.1.

Template	Ref.
Amino acids	35 - 37
Amino acid derivatives	38 - 44
Peptides	38, 45 - 48
Proteins	38 & 49
Dyes	45 & 51
Diols and polyols	52 - 54
Hydroxycarboxylic acids	55 & 56
Sugars and derivatives	57 - 61
Nucleosides and nucleotides	62 & 63
Purine	64
Steroids	65 - 69
Drugs	70 - 82
Dialdehydes	83
Diketones	84 - 86
Dicarboxylic acid	38, 49, 87
Vitamins	88
Herbicides	89 - 92
Bacteria	93
Co-factors	94 & 95
Crystals	96
Polychlorinated aromatic compounds	97
Polycyclic aromatic compounds	86, 98 - 101
Metal cations	102 - 104

Table 1.1: Examples of templates used for imprinted polymers.

1.3.2 Molecular recognition

Molecular recognition is a process involving both the binding and selection of a substrate for a given receptor molecule. In order to achieve good recognition it is desirable that receptor and substrate be in contact over a large surface area. This occurs when the synthetic receptor is able to wrap around its guest so as to establish numerous non-covalent binding interactions and to sense its molecular size, shape and architecture. Molecular recognition thus is a question of information storage at the supramolecular level. Information may be stored in the architecture of the ligand or in its binding sites (nature, number, arrangement). Binding of substrate and host forms a complex characterised by its selectivity and by its thermodynamic and kinetic stability.

These stabilities determine the rate of formation and dissociation of the complex. All these parameters lead to a double complementarily principle extending over energetic and geometrical features i.e. the "lock and key" concept of Fischer.[105] The balance between rigidity and flexibility is of particular importance for the dynamic properties of host and guest. Although strong recognition may be achieved with rigidly organised receptors, the processes of exchange, regulation, and cooperativity require built-in flexibility so that the receptor may adapt and respond to change.[111]

1.3.3 Imprinted cavities: scope of base material

Initial attempts at imprinted polymers were the experiments described by Dickey. He precipitated silica gel in the presence of dyes. During the formation of a matrix around the template it was expected that specific interactions between the silanol groups and the functional groups of the template occur. In a further development of this experiment, imprinted layers of cross-linked polysiloxane were produced on the surface of the silica particles. In this case, instead of polymerisable double bonds, polycondensable silane groups were attached to the binding groups. Non-covalent interactions during the imprint process were exploited with dye substrates[106] while covalent interactions with NAD-dimers[95] and sugars[107] were also explored.

An alternative method is to use organic macroporous imprinted polymers produced as thin layers (5 – 10 nm) on the surface of wide pore silica particles. For this process, methacrylate groups are bound covalently to the surface of the microparticles silica.[50] The surface is further coated with a monomer mixture, which is then polymerised allowing for molecular recognition of the template.

Another kind of imprint is the surface modification of wide-pore silica gels. The template is derivatised with two binding groups (usually $RSi(CH_3)(OCH_3)_2$) able to react with the silanol groups of silica gel.[83] After splitting the template off by hydrolysis the selectivity is obtained by the defined distance of the two binding groups on the silica particle surface. In a similar way the remaining silanol groups can be capped with space-filling silanes as phenyldimethylmethoxysilane after condensation of the template to lead, after removal of the latter, to an imprint although not a real cavity. This method was also investigated using the self-assembly approach for imprinting of dyes.[108]

Surface imprints on monolayers and vesicles have been reported for protein recognition.[49, 109] Finally, as a last example of surface imprinting, a selective chelate

resin has been prepared by emulsion polymerisation with methacrylic acid in order to obtain microparticles able to recognise a specific metal cation template (Cu^{2+}).[110]

1.3.4 Nature of the interactions

According to the interaction involved in molecular imprinting, the technique can be subdivided into covalent and non-covalent based molecular imprinting.

1.3.4.a Covalent interactions: pre-organisation approach

Wulff and coworkers have made an intensive study of covalent imprinted polymers and their pioneering work has led to further development of novel molecular imprinted systems.[111]

This method usually involves the synthesis of a molecule that is a composite of the imprint molecule and the binding monomer linked by covalent bonds. Removal of the imprint by chemical reaction from the imprinted polymer leaves the residual binding monomers in the position precisely determining in space by the imprint molecule. This method is claimed to lead to more uniform imprinted sites than the non-covalent approach, and shows only a very weak selectivity dependence on the solvent that is used during the polymerisation. However, several drawbacks such as slow binding kinetics, and also the lack of suitable covalent bonds exist since the bonds should be cleaved easily and rebound.[112] The most typically used covalent interactions during the imprinting process are summarised in Table 1.2.

Binding group	Binding site to the template	Type of bond	Ref.
Boronic acid	Diol	Boronic ester	113 & 58
Boronaphthalide	Alcohol	Boronic ester	114
Amine	Aldehyde	Schiffs base	83 & 115
Aldehyde	Amine	Schiffs base	114 & 116
Diols	Ketone	Ketal	84 - 86
Acrylic acid	Amine	Amide	53 & 117
Acrylic acid	Alcohol	Ester	69, 118 & 119
Carbonate ester	Alcohol	Ester	65
Alcohols	Carboxylic acid	Ester	120
Cobalt chelate	Amino acid	Chelate complex	121 & 122
Vinylimidazole + Co^{2+}	Amino acids	Chelate complex	104
Copper chelate	Imidazole	Chelate complex	49, 95, 114 & 124
	Amino acid		35

Table 1.2: Examples of covalent interactions between template and functional monomer.

1.3.4.b Non-covalent interactions: self-assembly approach

With the non-covalent method, the binding monomer and imprint molecule are allowed to self-assemble in a "pre-polymerisation mixture" in a way that maximises the binding interactions between the two species. The most important type of non-covalent interactions is electrostatic. However electrostatic interactions alone lead to relatively low selectivity; therefore other interactions must be present. Table 1.3 lists some possible non-covalent interactions. After polymerisation, the imprint is extracted from the polymerised material by "simple" washing, leaving a cavity in theory selective for the template.

Binding group	Binding site to the matrix	Type of interaction	Ref.
Acrylic acid, Methacrylic acid	Amine	Electrostatic	99 & 125
Acrylic acid	Amidine	Electrostatic	126 & 127
Itaconic acid	Amine	Electrostatic	70
Sulfonic Acid	Amine	Electrostatic	101
2-Vinylpyridine, 4-Vinylpyridine	In combination with carboxylic acid binding groups	Electrostatic	128
Acrylic acid, Methacrylic acid	Amide	Hydrogen bond formation	129
	Amide in combination with electrostatic interaction	Hydrogen bond formation	130 & 131
Acrylic acid	Purine base	Hydrogen bond formation	132 & 133
Boronic acid	With covalent interaction	Charge transfer interactions	55
Glyceric acid	With covalent interaction	Hydrophobic interactions	56

Table 1.3: Non-covalent interactions between template and functional monomers.

1.3.4 c Combination of covalent and non-covalent interactions

Experiments have been carried out to combine the homogenous imprint process based on reversible covalent bond formation and the versatility of a non-covalent interaction rebinding process (hydrogen bonding).[65, 69, 84, 97 & 119] This approach, although requiring a template derivative for reversible covalent binding as the first step, seems to be promising even for applications requiring fast kinetics of rebinding.

Non-covalent interactions can be partitioned into various categories: electrostatic, induction, charge transfer and dispersion terms are the main interactions involved.

1.4 CLASSIFICATION OF NON-COVALENT INTERACTIONS

1.4.1 Hydrogen bonds

These interactions are by far the most important in non-covalent complexes since they determine the structure of many bio-macromolecules and play a key role in many processes of molecular recognition and regulation (immune system, DNA replication,

etc.). Hydrogen bonding is a charge transfer from the lone pairs of the electron donor to the antibonding orbitals of the X-H bond of the electron acceptor that can be symbolised by X-H•Y. The atom X is usually electronegative and Y is either an electronegative atom with one or two lone pairs. The concept has been extended to C-H•Y bonds although leading to much weaker bonds than those in OH•Y or NH•Y bonds. The directional nature of hydrogen bonds allows exquisite recognition in host-guest complexes. Often hydrogen bonds provide organisation and selectivity in clusters but the strength is enhanced by the use of other interactions.

1.4.2 Electrostatic interactions

Electrostatic interactions are based on Coulombic attractions between oppositely charged species such as ion-ion, ion-dipole or dipole-dipole. The high strength of this kind of interaction (250 kJ/mol for good ion-ion interactions) has made them the primary choice in the design of molecular imprinted polymers. There are many receptors both natural and synthetic that use electrostatic interactions to bind the substrate such as crown ethers or cryptands. However entropic balance is an important balance which often negates the strength of this binding effect.

1.4.3 π-π stacking interactions

These interactions arise between systems containing aromatic rings. Current theories suggest that these attractive forces are electrostatic in nature.[134] They can take place in a "face-to-face" manner where the aromatic rings are parallel together to maximise the overlapping (maximal attractive force). On the other hand, in order to decrease the dispersion energy the aromatic moieties can take an "edge-to-face" conformation where they are located in perpendicular planes.

1.4.4 Dispersion interactions

The dispersion forces are attractive forces between molecules that occur when instantaneous dipoles in the electron clouds around each molecule interact favourably. These van der Waals forces are less directionally specific than electrostatic interactions but contribute to the stability of a cluster.

1.4.5 Metal coordination

In this interaction the ligand donates two electrons to the metal ion centre to lead to an interaction that is a non-covalent bond. From this coordination results strong directionality as well as large stabilisation of the complex.

1.4.6 Hydrophobic interactions

Hydrophobic interactions represent the driving force for the association of apolar groups in aqueous solution. This effect is connected to the extraction of polar compounds (water molecules for instance) from the hydrophobic cavities where they form clusters. This results in a favourable increase in their disorder, thus a favourable entropy term, which differs from some of the previous interactions based on energy stabilisation.

1.5 STRUCTURE OF THE POLYMERIC MATRIX

The quality of the imprint process is controlled by the structure of the matrix. The cavities must be able to retain their shape even after removal of the template. However, a compromise must be found between an inflexible arrangement of the polymer chains to give high selectivity and an appropriate degree of flexibility, which is necessary to obtain a fast equilibrium with the substrate to be embedded. Good mass transfer is also essential to allow as many cavities as possible to be accessed. Finally for broad application, the imprinted polymers must show mechanical and thermal stability.

The stiffness, and consequently the selectivity, of the polymer is obtained by a high degree of cross-linking. Usually polymerisation mixtures containing up to 90% of cross-linker are used. Two different types of cross-linker have been investigated: divinyl benzene (DVB) and ethylene glycol dimethacrylate (EGDMA).[57] The better performance of EGDMA as a cross-linking agent over DVB is suggested by the higher selectivity observed versus the ratio of the cross-linker in the polymerisation mixture. Several reasons for this exist, for instance non-specific hydrophobic interactions with the racemate are less important for the ethylene dimethacrylate cross-linked polymer.[135] Moreover the flexibility of the polymer chains with this cross-linking agent are higher, resulting in a faster equilibrium of uptake and release of the template. The use of tri– and tetra-functional methacrylates as cross-linkers has been investigated with the hope that the resulting recognition sites would be more well-defined.[136] The imprinted

polymer prepared with the trifunctional cross-linkers pentaerythritol triacrylate (PETRA) and 2,2-bis-(hydroxymethyl)butanol trimethacrylate (TRIM) were shown to have higher loading capacities and better resolution than those prepared from the usual EGDMA and even than the tetrafunctional cross-linker pentaerythritol tetraacrylate (PETEA). The higher average pore volume for TRIM and PETRA-based polymers could be an explanation. On the other hand, the introduction of methylene spacers in the cross-linker EGDMA did not affect the observed molecular recognition characteristics.[137]

To improve the selectivity of the MIP the use of optically active cross-linker agents based on dimethacrylate is of special interest.[135] However, no effect on the selectivity has been observed. A decisive factor for high selectivity as well as for stability is the type and the amount of cross-linking agent used to prepare the polymer. The porogen has small effect on selectivity but controls the morphology of the polymer *i.e.* the accessibility to the cavities. A study was performed using fluorescent monomers covalently bound to the matrix of a styrene-divinylbenzene copolymer.[135] According to the porogenic solvent used the accessibility of the solvent to the fluorescent probes, measured by solvatochromic shift, was shown to be different. To control as much as possible the structure of the matrix an interesting approach to the hierarchically imprinted sorbents was reported by Dai.[102] A polymerisation mixture containing metal cation (as a template for the usual imprint), and surfactant micelles (for a pore size control) was thermally polymerised. After removal of both templates, a selective polymer for the metal cation was obtained with a highly homogeneous matrix. Such polymers exhibited high capacities and fast binding kinetics.

1.6 Potential applications of MIPs

1.6.1 Adsorbents for screening of chemical and biological combinatorial libraries

The use of MIPs as specific sorbents for the screening of chemical combinatorial libraries was successfully applied to a library of twelve closely related steroids.[66] The screening of phage display peptide libraries was also performed with synthetic receptors prepared against yohimbine, an α-adrenergic antagonist.[138] Although the results are

somewhat preliminary in nature, the indications are that MIPs have a good potential in this new field.

1.6.2 Immunoassay

It has been demonstrated that MIPs can be a substitute for antibodies in immunoassay protocols. The assay format has mainly used imprinted polymers with a radio ligand displacement assay. In the first study of this type, theophylline and diazepam imprints were successfully used by Mosbach et al. for the accurate determination of concentrations of these drugs in human serum.[64] An excellent correlation was observed between the results obtained using the MIPs format and a commercial immunoassay for the determination of theophylline. In subsequent studies on anti-morphine and anti-enkephalin MIPs[139] the imprints showed binding affinities approaching those demonstrated by the antigen-antibody system in both organic solvents and aqueous media. The development of aqueous buffer and organic solvent based radio-ligand binding assays was carried out with the imprint of S-propranolol[71] to lead to a material so efficient that the direct determination of S-propranolol was possible in human plasma and urine without prior sample clean up.[140] Recently, new molecularly imprinted affinity sorbents against theophylline and 17β-estradiol were synthesised *via* precipitation polymerisation, a synthetic method that yields monodisperse, spherical polymer particles in the micron scale-range.[141] The cross-reactions that occur with drugs of similar structure were the same as those of antibodies.

Since this work, non-isotopic assays have been reported in which a fluorescence template (coumarin analogues of 2,4-dichlorophenoxyacetic acid (2,4-D)) was used as the labelled ligand, avoiding the handling of the radioactive materials.[142] The detection limit and the cross-reactivities were similar to those obtained with the radioassay reported earlier.[143]

Until only two years ago no imprinted polymer-based assays using non-isotopic labelled ligands had been reported. The first was accomplished by Takeuchi *et al.* with the imprint of biotin derivatives.[144]

The idea behind the use of such compounds is the application of avidin-biotin systems in conjunction with enzymes opens up the route to MIPs in ELISA (Enzyme Linked Immuno Sorbent Assay). A molecularly imprinted polymer specific for epinephrine was coated on the surface of microplate wells and the affinity was determined by an

enzyme-linked assay using a conjugate of horseradish peroxidase and norepinephrine.[145] Polymer microspheres imprinted with 2,4-dichlorophenoxyacetic acid (2,4-D) were also added to the microtite plate.[146] For the assay, based on chemiluminescence, the analyte 2,4-D was labelled with tobacco peroxidase. Using a competitive format, the amount of polymer-bound 2,4-D-peroxidase conjugate was quantified using luminol as the chemiluminescent substrate.

1.6.3 Sensors

Another area for which imprints have been tested is their use as chemo-sensor mimics. A chemical sensor selectively recognises a target molecule in a complex mixture and generates a quantifiable output signal using a transducer that correlates to the concentration of the analyte. This signal is a change in one or more physiochemical parameters associated with the interaction occurring and can produce ions, electrons, gases, heat, mass change or light.[147] Unfortunately these devices often lack stability over long storage periods and operational stability at high temperature and in harsh chemical environments due to fragile biological recognition elements such as enzymes or antibodies.[148] An appealing alternative is the imprinted polymer membranes or polymer surfaces that could be used as robust chemosensors with the same general principles (Fig. 1.4).[149]

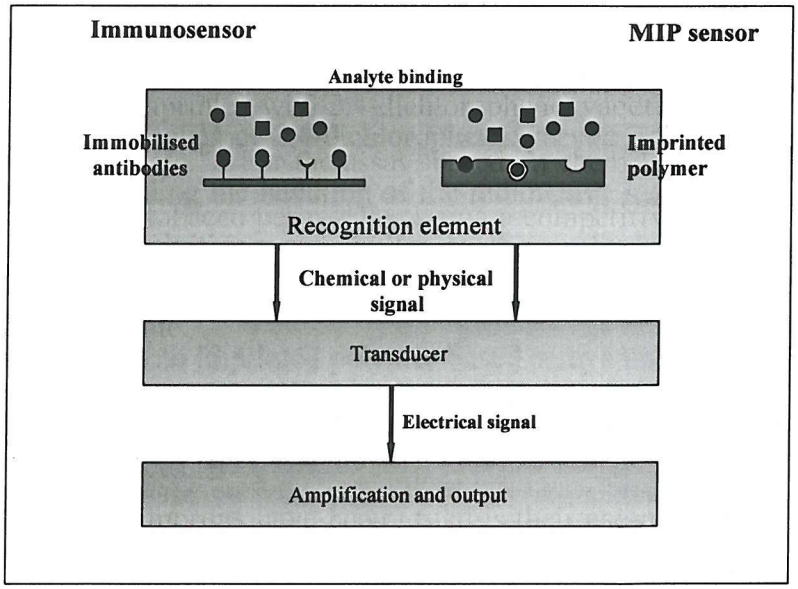

Fig. 1.4: Schematic representation of a MIP-based biomimetic sensor compared to an immunosensor.[147]

In this case certain general properties of the analyte, or changes in one or more physicochemical parameters of the system upon analyte binding, are used for detection. Alternatively, reporter groups can be incorporated into the polymer to generate or enhance the sensor response. In other cases, the analyte may possess a specific property that can be used for the design of a MIP-based sensor. The table 1.4 summarises different transducer types that have been or could be used with MIPs.

Format	Transducer	Analyte	Ref.
General formats	Ellipsometry	Vitamin K_1	88
	Surface plasmon resonance	Theophylline	150
	Capacitance	Phenylalanine anilde Phenylalanine	44 & 151
	Conductometry	Atrazine	152
	Field effect transistors	Chloroaromatic acids	153
	Quartz crystal microbalance	Hormone Glucose Propranolol	100 61 154
	Infrared evanescent wave	2,4-D	89
Analyte generates signal	Fibre optic fluorescence	Dansyl phenylalanine	155
	Fluorescence	PAH (pyrene) Morphine Cinchona alkaloid	98 156 157
Competitive binding format	Colorimetry	Chloramphenicol	82
	Voltammetry	2,4-D	90
Polymer generates signal	Fluorescence	cAMP D-fructose Heteroarylcarboxa-midrazone L-Tryptophan	94 158 159 37
	Fibre optic luminescence	Sarin and Soman	160

Table 1.4: Examples of transducers employed in imprinted-based sensors.

1.6.4 Catalytic reactors

Stereoselective and regioselective reactions in the cavities of imprinted polymers have also been developed for applications in synthesis. The cavity is first imprinted with the

end products of the reaction, and a precursor is then embedded into the cavity to be converted into the product (cf. catalytic antibodies).

The use of the imprinted recognition site as a microreactor for enantioselective synthesis was first described by the research groups of Shea[120] and Neckers.[161] Synthetic transformations including enantioselective protonation-deprotonation[162] and selective hydrolysis[163] have also been carried out in imprinted polymers. However, the most popular example of microreactors was described by Wulff[164] with an imprint by L-DOPA leading to cavities with chiral alkylation properties of glycine.

Another field investigated is the use of MIPs as polymer supported.[69] Polymer beads were imprinted with sterols and converted to the acrylate esters at the 3- or 17-positions. The resultant polymers gave selective reduction of the hydroxyl group of androstan-3, 17-dione.

The use of imprinted polymers in protecting group strategies has also been reported. For example, simply reacting D- or L-Phenylalanine anilide with dansyl chloride, in the presence of a polymer imprinted with L-Phenylalanine anilide, resulted in 46% less L-dansyl derivative than D.[165] A fundamentally different approach is to direct the site of substitution by performing reactions with ligands bound to imprinted polymers. This was demonstrated with the acylation of di- and tri-hydroxysteroids bound to polymers imprinted with structurally related diols.[52]

Finally catalytic turnover has been investigated by a number of groups, who have generally adopted an approach analogous to the raising of catalytic antibodies (but without the same level of success),[166] by imprinting polymers or silica with a transition state analogue for the reaction of interest. The applications of such polymers are summarised in Table 1.5.

Catalytic reaction	**Ref.**
Hydrolysis	167-173
Transesterification	174
Dinitrophenolysis of benzoic anhydride and derivatives	175-177
Dehydrofluorination	178 & 179
Class II aldolase mimic	180
Isomerisation	181
Enantioselective hydride transfer to aryl ketones	182
Butanolysis of benzoic anhydride	183

Table 1.5: Some catalytic reactions performed with MIPs.

1.6.5 Chromatography

Imprinted materials can be used as stationary phases in chromatography, especially for the separation of racemates. Early value of MIP systems in chromatography was demonstrated by non-covalent imprinting of dyes in a thin shell of acrylic polymer on porous silica.[50] Since this time, a large diversity of templates has been investigated such as amino acids[184-185] and their derivatives,[136, 186] sugars and derivatives,[58, 111, 187] peptides,[136] sterols,[84] rigid aromatic compounds,[188-189] drugs[190-192] and pesticides.[192-195] All of these templates were used following either a covalent approach or by non-covalent interactions. Even though the covalent imprinting method is known to yield more uniform imprinted sites, the self-assembly approach is preferred in terms of kinetics of separation.[196] The most commonly used monomers are methacrylates, such as methacrylic acid or 2-(trifluoromethyl)methyl acid (TFMAA),[156, 157, 197] and heteroaromatic monomers, such as vinylpyridine.[193]

MIPs can be prepared in several formats for use in chromatography. Polymer production techniques normally used are the bulk polymerisation of the mixture of monomers around the imprint molecules, followed by grinding and extraction of the print species. Particle sizes usually in the 25 μm range, suitable for HPLC are used.[196] By this method numerous resolutions of racemates have been obtained on the base line. Recently a polymer was imprinted by several templates at the same time for multiple simultaneous chiral separations.[198] The grinding and the sieving steps were found to be the weakest link of the procedure leading to polydispersity in shape and size of the particles, which limits efficiency and resolution. Efforts have been made to address this problem.[199] A layer of MIP has been grafted into wide-pore silica particles and packed into HPLC columns to perform a molecularly imprinted ligand-exchange adsorbents.[35] The drawback of this kind of surface-imprinting approach, as well as the one described by Norrlow,[50] is the potential occluding of the small pores of the supporting silica particles by the MIP layer, thereby reducing the surface area available for interaction for the small imprint molecule. It may work better for imprinting bulky molecules such as proteins, which would not ordinarily occupy the pore space to a significant degree anyway.

Polystyrene particles have also been used as shape templates for synthesising MIPs via a two-stage swelling seed-polymerisation technique.[200] Particles obtained using this technique are monodisperse in size (6 μm) and shape and well suited for

chromatographic applications. However the typical two-step swelling and polymerisation method requires water as the suspension medium, which could interfere with the non-covalent interactions between the imprint molecule and the monomers. To avoid such interferences, suspension polymerisation in perfluorocarbon solvents has been investigated.[201] Polymer beads produced using this method showed excellent chromatographic performance and good selectivity even at high flow rates. Unfortunately, the high density of the perfluororcarbon solvent causes rapid "creaming" of the solution, and fluorinated surfactant has a poor solubility capacity, which imposes limits on the applicability and practicality of this method.

To eliminate the need for packing the columns a general procedure has been described by Sellergren and Svec[202] for the *in situ* preparation of continuous rods of macroporous polymer for liquid chromatography (LC) separation. This method has been employed in several studies for the preparation of imprinted polymer rods for use in LC and capillary electrophoresis (CE).

Matsui *et al.*[99] used this approach to imprint aminonaphthalene derivatives by heating at 70°C stainless steel columns filled with appropriate solutions for the MIP. Although columns exhibiting reasonable selectivity were obtained in a single step, the poor efficiencies resulted in low resolution separation. Some improvements in selectivity were obtained with columns imprinted with the cinchona alkaloid in presence of TFMMA as the functional monomer.[197] Sellergren also reported the use of a variant of the dispersion polymerisation technique to prepare porous MIPs in glass tubes for LC separation.[75, 127] A mixture of isopropanol and water was used as solvent to yield an unstabilised dispersion polymerisation. The process produces random precipitates rather than regular beads and a correct selectivity was observed for only highly charged print molecules such as pentamidine and tri-*O*-acetyl adenosine. Finally, this dispersion polymerisation method was applied to the preparation of stationary phases in fused silica capillaries, using pentamidine as template or phenylalanine anilide.[203] Efficient bulk flow through the rods was used in the LC and LCE modes. The enantiomeric separations recorded in the LC mode were, however, much less efficient than those obtained using the traditional packed imprinted columns, and such separations were not achieved at all in the CE mode. The drawback of this method is the use of porogenic agents such as cyclohexanol and 1-dodecanol. These are added as pore formers to make the polymer rods sufficiently porous, but they interfere with the interactions between template and functional monomer required for the formation of well-defined imprints.

Porous monoliths of MIPs have also been prepared *in situ* in fused silica capillaries for enantiomeric separation of β-adrenergic antagonist propranolol and metoprolol.[190]
MIP capillary columns can also be prepared for both open tubular liquid chromatography (OT-LC) and capillary electrochromatography (OT-CEC) applications. Thin films of imprinted polymers bonded to the inner walls of 25 μm ID were prepared for the enantiomeric separation of D- and L-dansyl phenylalanine anilides.[184]

1.6.6 Solid phase extraction

Molecularly imprinted polymers sometimes possess far too strong an affinity for their template to allow a quick binding release equilibrium of the substrate compatible with chromatographic applications. However, this feature is perfect for solid-phase extraction where an on-off-type separation is required. In this case, the substance of interest is first absorbed from the crude sample, followed by an affinity separation based on the molecular recognition to elute the compound used as template in the imprint process. By this way extractions of herbicides from water[92] or organic tissue extracts[204] can be performed.

1.6.7 Controlled release matrices

Another area for which MIPs could be investigated in the future is in the area of the controlled release matrices.[205] The binding strength of the compounds may be sufficiently regulated in an on-off-manner, such that the binding can be reduced, either totally in one step or gradually, by means of simple external influences as pH, light or heat, then polymers can be made to release at a certain position and time.[206] Thus, if the ligand is a drug compound and the polymeric matrix is biocompatible, such devices may be employed to control drug delivery *in vivo*. Other applications of this technique could be the control released of antibiotics in solutions sensitive to bacterial degradation.

CHAPTER 2: MOLECULAR IMPRINTED POLYMERS – A CONVENTIONAL APPROACH

2.1 INTRODUCTION

The purification of compounds after synthesis is one of the most important and time-consuming parts of chemistry. For achiral compounds purification techniques are well established and applied on a large scale in industry, using for instance acid or base extractions, crystallisations or chromatographic separation. However purification of racemates requires more exquisite methods. Enantiomers have exactly the same chemical and generally physical characteristics (except for the direction in which they rotate the plan of polarised light). For these reasons the interaction of enantiomers with other achiral molecules or phases will be identical, so that they can not be separated using usual HPLC procedures. However, even if enantiomers of chiral drugs have identical physical and chemical properties, they may have drastically different pharmacological and pharmacokinetic profiles. For instance, the β-adrenergic antagonist propranolol was launched as a racemate, despite the S-form being approximately 100 times as potent as the R-form.[207] Horrific examples are known such as D-penicillamine which is active against biliary cirrhosis, whereas the L- enantiomer atrophies the optic nerve, or thalidomide where R-thalidomide is a sedative and S-thalidomide is teratogenic.[208] However despite this, ten years ago, out of the 500 chiral drugs on the market, some 90% were still administrated as racemic mixtures. During this time the Food and Drugs Administration (USA) has required that for any new optically active drug to be approved, both enantiomers must be treated as separate substances in pharmacokinetic and toxicological profiling.[147] This has led to an emphasis and development by pharmaceutical industries of novel and improved techniques for both analytical and preparative-scale chiral separations.

To achieve the resolution of racemates the use of differential crystallisation or specific enzymes have been investigated to yield an excess of one of the enantiomers but separation of these can still be problematic and scale up can be an issue.

Two others approaches have been further investigated by both using indirect and direct methods.[209] The first consists of derivatising the enantiomers into two diastereoisomers by treatment of the racemate with an enantiomerically pure chiral derivatising agent

(either covalent or ionic pairing). Having different chemical and physical properties the diastereoisomers can be separated by chromatography, crystallisation, etc.

The second approach, the direct method, is based on chiral chromatography. Chiral chromatography includes the use of gas chromatography, supercritical fluid chromatography, capillary electrophoresis and HPLC, the last being the most widely used. This approach does not require derivatisation of the chiral molecules since a transient diastereomeric complex is formed with the analyte directly on the column. This complex can be obtained by adding an enantiomerically pure compound to the mobile-phase (for example quinine has been used as a chiral mobile-phase additive (CMPA)). Thus, for example, Bergholdt reported the use of a sulphated β-cyclodextrin as chiral buffer additive for capillary electrophoresis separation of omeloxifene enantiomers.[210] Due to its cost, this procedure is rarely used. Another direct method uses a chiral substance that is chemically bonded to a stationary-phase support to form a chiral stationary phase (CSP). The CSP interacts with the analyte enantiomers to form short-lived transient diastereomeric complexes. The binding strength of one of these complexes will be stronger than the other leading to differences in retention time and thus a separation of the enantiomers. To obtain this chiral recognition it has been suggested that a three-point interaction must be formed between the CSP and the most retained enantiomer.[211] The CSP can be attached to the support in various ways: covalently, ionically or coated physically. Depending on the nature of the CSP the transient diastereomeric complexes will be formed utilising hydrogen bonding, π-π stacking, dipole interactions, inclusion complexing and steric bulk effects, but an enantio separation will be obtained only if the analyte exhibits adequate functional groups to interact with the CSP. The table 2.1 shows some of the different CSP commercially available.

Type of CSP	Chiral recognition Mechanism	Analyte Requirement
Protein based[212]	Hydrophobic and electrostatic interactions	Ionisable groups (ie. amines or acids), aromatic groups
Cyclodextrin[213, 214]	Inclusion complexation, H-bonding	Polar and aromatic groups
Polymer-based carbohydrates[215, 216]	Inclusion complexation, H-bonding and dipole interactions	Ability to H-bond, bulky group near chiral center helps
Pirkle type[217]	H-bonding, π-π stacking, dipole interactions	Ability to π or H-bond; aromatic group helpful

Table 2.1: Characterisation of some commercially available chiral stationary phases (CSPs).

Unfortunately even though chiral stationary phase chromatography is a powerful tool for analytical and preparative HPLC, the choice of the CSP for a given racemate and the elution conditions for the best enantio-separation remains empirical. Moreover this type of material is expensive and does not allow prediction of the elution order of the enantiomers.

To over-come these drawbacks molecular imprinted polymers (MIPs) could afford a low-cost alternative to CSP's with a tailor-made material for a given compound where the elution order of the enantiomers is known. Such an application requires fast binding and release of the substrate. A metal-coordinating template usually shows too strong an interaction with the substrate and leads to excessive retention. A smart approach called "bait-and-switch", consists of replacing the strong metal centre (Cu^{2+}) of the initial polymerisation step by a weaker one (Zn^{2+}) for the rebinding experiment, seems to be promising but is at an early age.[127] The most appropriate approach is the use of non-covalent interactions.

MIPs can be prepared in several formats for use in chromatography. The conventional approach is to synthesise the MIP in bulk, grind the resulting polymer block into particles, and sieve the particles into the desired size range.[147] Particles of 25 μm or below are generally used in chromatography studies.[196] Such ground and sieved particles can be packed into conventional HPLC columns,[136, 218] immobilised onto TLC plate[185] and entrapped in capillary columns.[219] Bulk polymerisation by UV or thermal initiation is simple, and optimisation of imprinting conditions is in theory relatively straightforward. However, the grinding and the sieving steps are tedious and unsatisfactory for several reasons. It inevitably produces irregular particles as well as a

considerable quantity of "fines" which have to be removed (by sedimentation for example). Typically less than 50% of the ground polymer is recovered as useable particles.[188] Irregular particles can affect the general characteristics of the columns and often prove troublesome in process scale up. However this approach is the most commonly used method and is the basis of the work presented in this chapter.

An HPLC column is defined by several standard parameters (Fig. 2.1).[220]

HPLC parameters.

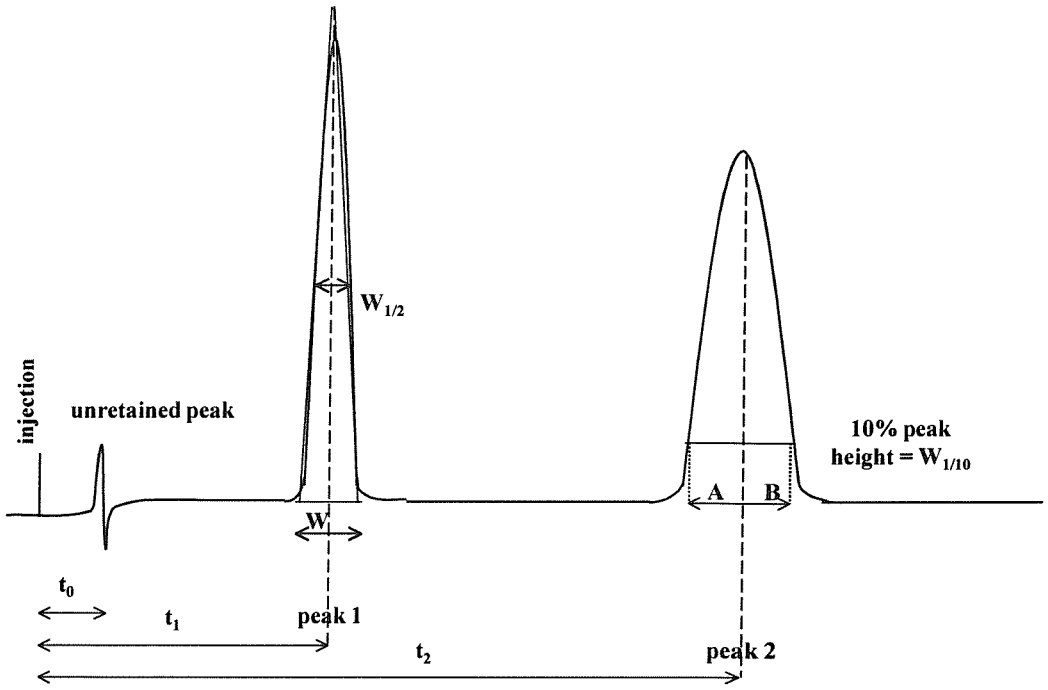

Fig. 2.1: Standard chromatographic parameters (idealised).

Capacity factor (relative retention):

The capacity factor, k_r', of a sample component is a measurement of the degree to which that component is retained by the column relative to an unretained component (such as acetone).

$$k_r' = (t_r - t_0) / t_0$$

Where t_r is the elution time of retained component, and t_0 is the elution time of the unretained component giving by this way the void volume of the column. The unretained peak is often referred as the solvent front. The higher the value, the stronger the interactions are between the eluted compound and the stationary phase.

Selectivity:

The selectivity parameter, α, is the measurement of peak spacing between components 1 and 2 due to different affinity and therefore retention. It is expressed as:

$$\alpha = k'_2 / k'_1$$

The higher the value, the better selectivity is. A value of $\alpha = 1$ means that both enatiomers are eluted with the same retention time.

Number of theoretical plates (N):

$$N = 16 (t_1 / W_1)^2 = 5.54 (t_1 / W_{1/2})^2$$

Where W_1 is the peak width of the solute 1, $W_{½}$ is the width at half the peak height, 16 is a factor carried over from distillation theory. N is a measurement of zone or band spread of a peak throughout the chromatographic system. The smaller the band spread the bigger the N value and the more efficient column.

Height equivalent to a theoretical plate (H):

$$H = L / N$$

Where L is the column length. H measures the column efficiency and is a more important parameter as it is independent of the column length. The lower this value is the better the efficiency of the column.

Reduced plate height (h):

$$h = H / dp$$

Where dp is the mean particle diameter of the packing material, h is the measurement of the degree of band dispersion produced by the packing considered in relation to the particle size. It is the best parameter for determining peak efficiency. It has no dimensions thus allowing different columns to be compared.

Peak asymmetry factor (A_S):

The peak shape is reflected in the peak asymmetry factor and determined at 10% of the peak maximum (Fig. 2.1) as:

$$A_S = B / A$$

The peak shape is informative about the existence of non-linear binding isotherms and slow adsorption or desorption of solute to the stationary phase.

Resolution factor (R_s):

R_s, defined as the amount of separation between two adjacent peaks, is given by:

$$R_s = (t_2 - t_1) / ½ (W_2 + W_1)$$

Since R_s is dependent on the capacity factor k', α and N, the resolution equation can be expressed as

$$Rs = ¼ \sqrt{N} (\alpha\text{-}1/\alpha) (k' / k' + 1)$$

The most important practical parameter that must be controlled is the mono-dispersity of the size and shape of the particles packed to obtain homogenous diffusion through the column (Fig. 2.2).

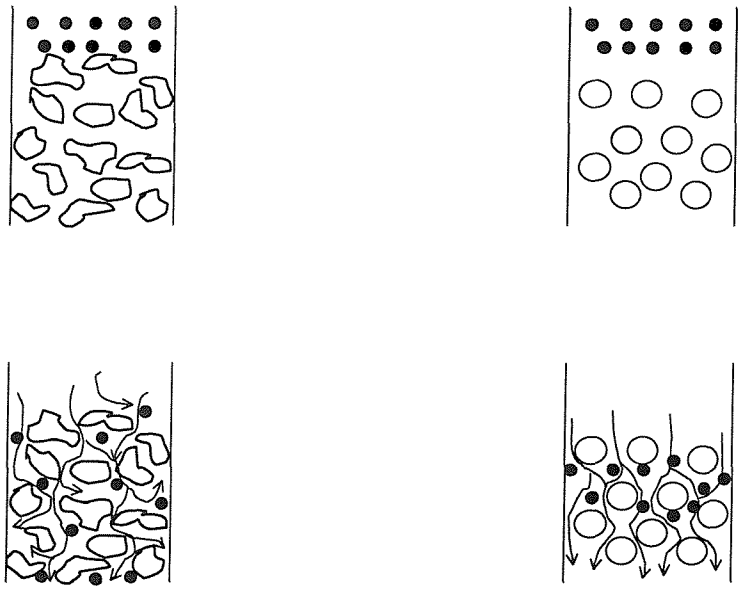

Fig. 2.2: Effect of the particle shape on the diffusion

The small size of the particles provides good diffusion properties and thus rapid access of the sample to the imprinted sited in the particles. Unfortunately the packing of small particles increases drastically the backpressure and limits the resolution factor of the columns.

2.2 RESULTS AND DISCUSSION

2.2.1 Synthesis of H-Phe-NHPh (3) and H-D-Phe-NHPh (4)

Amino acids and their derivatives are often chosen as model compounds for imprinting polymers because they are inexpensive, stable, possess a range of functional groups and are soluble in convenient solvents. Among the different amino acids derivatives used L-phenylalanine anilide is often chosen due to the various non-covalent interactions that are possible, namely electrostatic, hydrogen bonding and π-π stacking. The synthesis method previously described by Obrecht[242] was followed, the carboxyl group of Boc-Phe-OH was activated with isobutyl chloroformate (IBCF) in the presence of base (*N*-methylmorpholine) to give the corresponding mixed anhydride (Scheme 2.1). Nucleophilic attack on the mixed anhydride by aniline followed by an aqueous work-up afforded Boc-Phe-NHPh **(1)** (63%). The deprotection of the *N*-terminal amino group by TFA was followed by a neutralisation step to give the free amine H-Phe-NHPh **(3)** (52%). The enantiomer H-D-Phe-NHPh **(4)** was obtained from **(2)** in the same manner in a 22% yield.

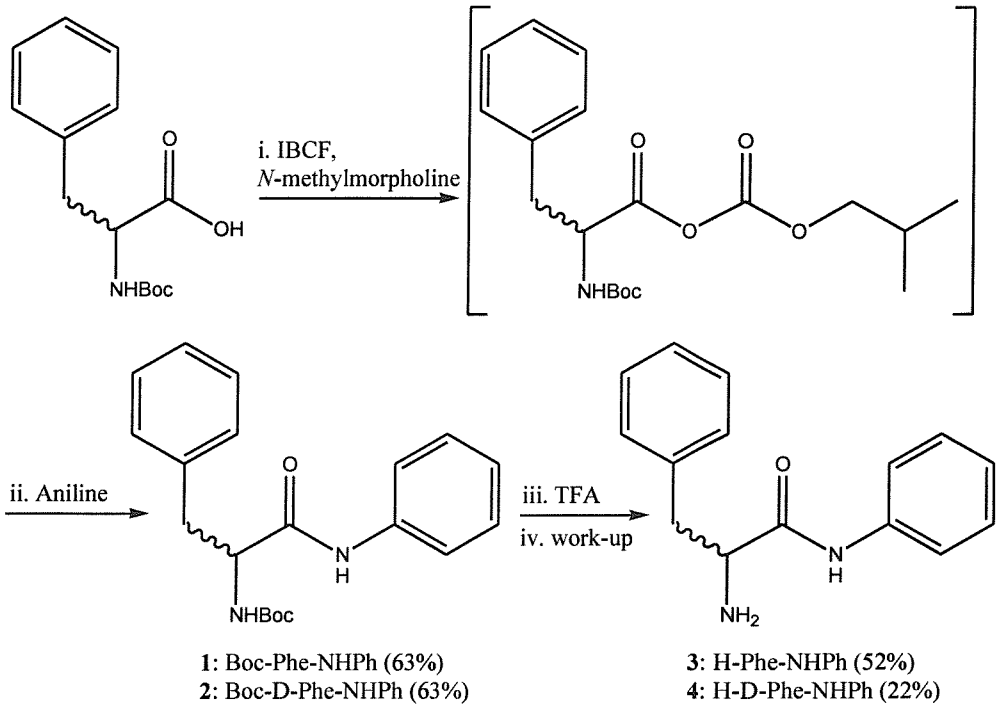

Scheme 2.1: Synthesis of the template H-Phe-NHPh and its antipode.

2.2.2 Bulk polymerisation of imprinted polymer

Four basic methods of polymerisation exist: emulsion, dispersion, suspension and bulk. The last approach being the most convenient. Bulk polymerisation has been defined as the formation of polymer from pure, undiluted monomers (i.e. single phase in contrast to the other methods), resulting in the generation of high molecular weight polymers. Incidental amounts of solvent and small amounts of chain transfer agent, dye and anti-oxidant may also be present. Bulk polymerisation has recently been applied to the molecularly imprinted polymer (MIP) area. Free radical polymerisations proceed by a mechanism of initiation, propagation and termination. Initiation can be achieved by thermal or photochemical decomposition of a radical initiator. Due to its capability to undergo both types of decomposition, AIBN (an azo derivative) has been used for the experiments described in this chapter to initiate the copolymerisation between the cross-linker (EGDMA) and monomer (MAA) (Scheme 2.2).

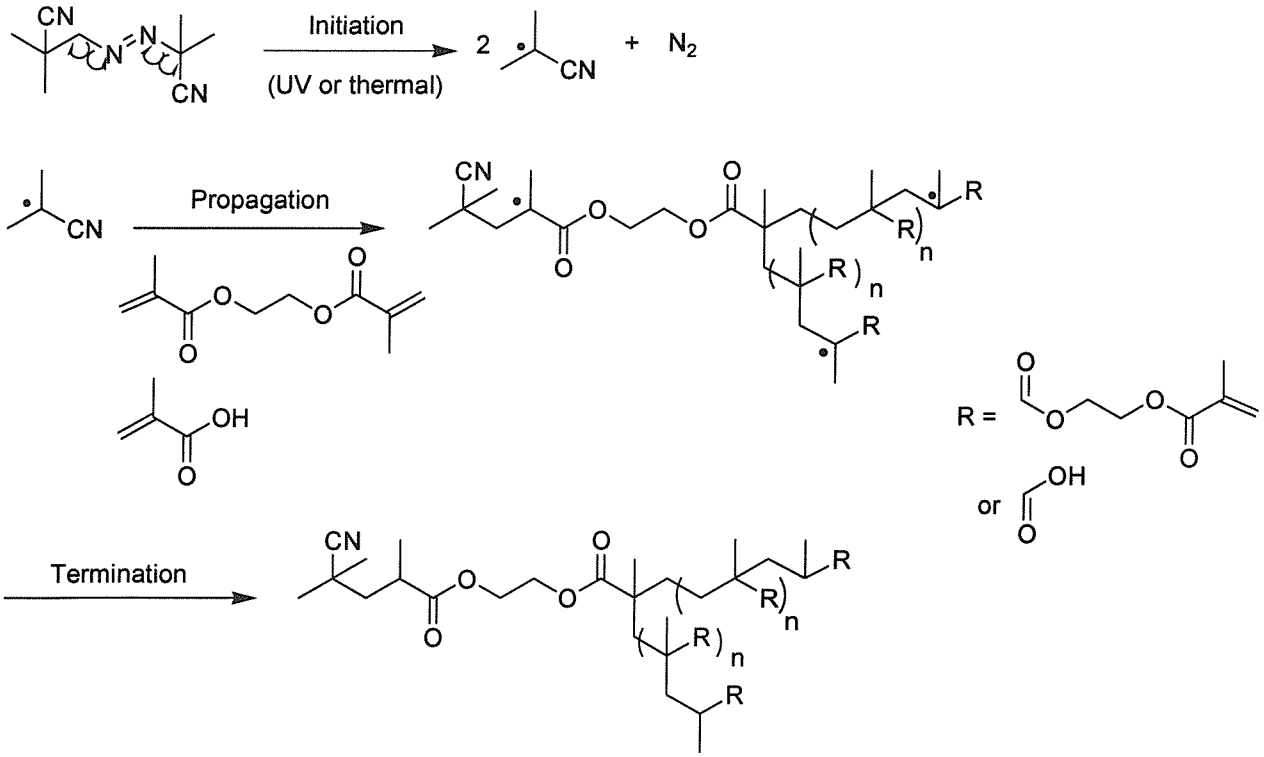

Scheme 2.2: Synthesis of polymeric matrix via radical copolymerisation.

In order to maximise the non-covalent interactions between the template **(3)** and the functional monomer (MAA), the polymerisation mixtures in these studies consisted of a

porogenic solvent (acetonitrile **(P1)**, DCM **(P2)** or toluene **(P3)**) in the presence of cross-linker (EGDMA), which were polymerised by UV irradiation for 24 hours at 15°C. Polymerisation at low temperatures is known to stabilise the pre-polymerisation complex but give incomplete reactions (6 – 9% of unreacted double bonds).[39] Hence, the polymers were subsequently heated at 65°C for 18 hours to achieve full polymerisation. A similar procedure was followed for the synthesis of the respective non-imprinted polymers (blank polymers). Such polymers were used as references to confirm that selectivity was due to the imprint process inside the polymeric matrix of the MIPs.

The interactions expected between the functional monomers (MAA) and the template **(3)** are electrostatic and hydrogen bonding (Fig. 2.3).

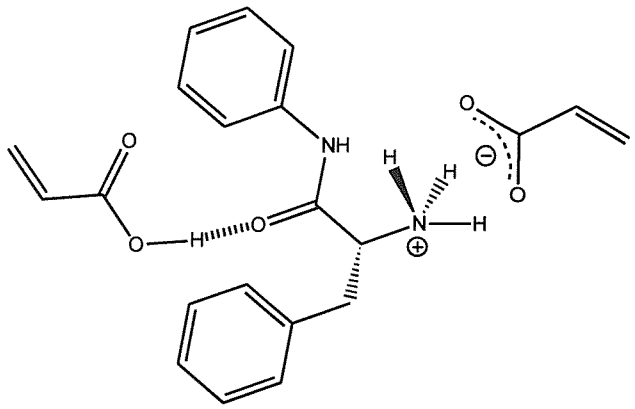

*Fig. 2.3: Non-covalent interactions between methacrylic acid and H-Phe-NHPh **(3)** in the pre-polymerisation complex.*

The porogenic solvents were selected according to their ability to enhance, or alter, template-monomer interactions and alter matrix morphology (the hydrogen bond capacity being acetonitrile > DCM > toluene). The first effect noticed of these porogenic solvents was the colour of the polymer. The polymer formed in acetonitrile was a white and opaque block, while the polymers prepared in DCM and toluene were glassy. After grinding and drying all became white and opaque. The fraction 45 – 75 μm was retained by sieving for subsequent slurry packing in acetonitrile. The particles observed under an optical microscope show, in comparison with commercial beads, an extremely heterogeneous distribution of particles (Fig. 2.4)

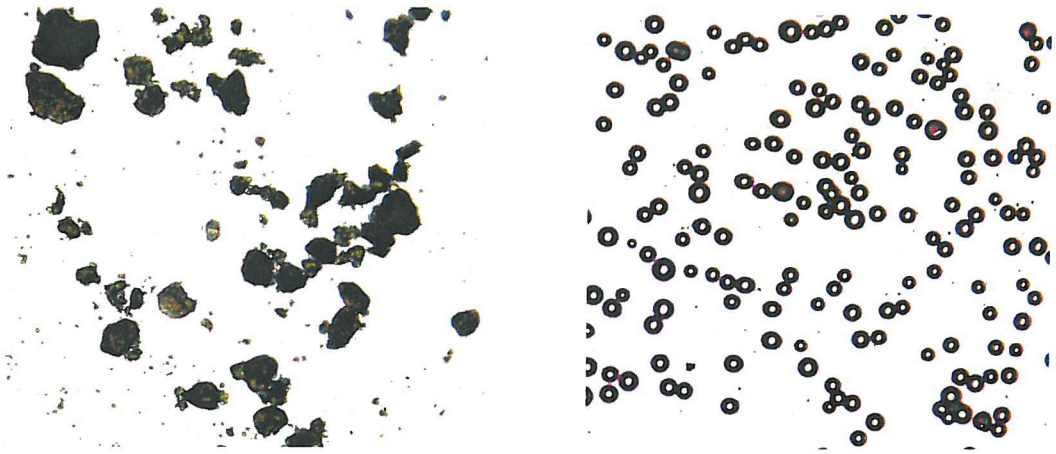

Fig 2.4 Comparison between particles of ground polymer (left) and commercial bead polymers (right) used as a conventional HPLC stationary phase.

As explained above (2.1 Introduction) such polydispersity will affect the resolution properties of the columns. Several columns were used to evaluate the effect the resolution of the racemate (60 x 4.6 mm, 150 x 4.6 mm and 250 x 4.6 mm), all under isocratic elution.

2.2.3 Effect of the mobile phase nature on the selectivity

In order to improve the resolution of the racemate mixture, several mobile phases have been investigated. Assessment of the first polymer **(P1)** (porogen MeCN, in a 60 x 4.6 mm column) was performed by injecting a solution of template **(3)** or its enantiomer **(4)** or the racemate (20 µL of MeCN 0.5 mM) with MeCN - AcOH 5% as the mobile phase, with a flow rate of 0.3 mL / min. Unfortunately although this eluent is commonly reported in the literature, no elution was observed after injection of the template H-Phe-NHPh **(3)**, suggesting very strong binding of the template to the stationary phase. On the other hand, elution of the antipode H-D-Phe-NHPh **(4)** was observed with a value of $K'_D = 3.4$. To decrease the strength of the electrostatic interactions between the template **(3)** and the stationary phase, AcOH (pKa = 4.7) was replaced by a stronger acid TFA (pKa = 0) in a mixture MeCN-TFA 0.042%. In this case the template and its isomer were recovered after injection ($\alpha = 3.20$), the polymer showing a preferential binding for the template compound (Spectra 2.1).

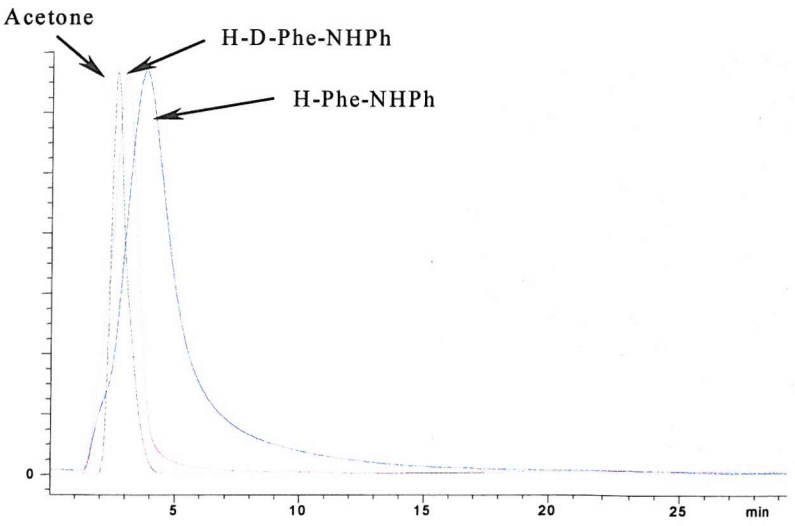

*Spectra 2.1: Elution profiles of acetone, **(3)** and **(4)** with **(P1)** (polymer made with MeCN as the porogen, in a 60 x 4.6 mm column). Elution: MeCN – TFA 0.04% , 0.3 mL / min.*

It was presumed that TFA protonated the amine group of the template H-Phe-NHPh **(3)** while the carboxylic groups of MAA located on the stationary phase were in the acid form.

To test the first hypothesis, 20 µL of the template solution (0.5 mM in MeCN - TFA 0.042%) was eluted with MeCN - AcOH 5% as a mobile phase. Although two peaks were expected (one for the template•TFA salt, showing weak binding in the imprinted cavities, and one delayed for the free template), no elution for the template H-Phe-NHPh **(3)** was observed.

Possible protonation of the carboxylic groups of MAA by TFA to the acid form was then investigated. For this two series of experiments were carried out. Initially, the column was washed for 30 minutes with MeCN – TFA 0.042% then the samples (**(3)**, **(4)** 0.5 mM in MeCN and acetone to determine the void volume) were eluted with MeCN – AcOH 5%. The retention times observed were similar to those obtained with the mobile phase MeCN – TFA 0.042% (Spectra 2.2).

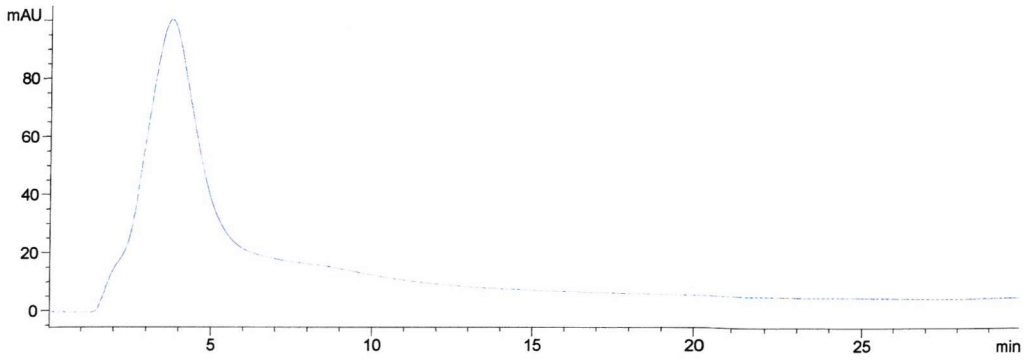

Spectra 2.2: Elution profile of H-Phe-NHPh ***(3)*** *with* ***(P1)*** *(polymer done with MeCN as the porogen, in a 60 x 4.6 mm column). Elution: MeCN – AcOH 5% , 0.3 mL / min.*

It was noteworthy that a tail was present on the elution trace in this case suggesting that, during the run, the interaction between the template **(3)** and the stationary phase increased. A second series of assessments was therefore carried out. After washing for 30 minutes with MeCN - TFA 0.042% the column was equilibrated for an additional 30 minutes with MeCN - AcOH 5%. No elution was observed for the template H-Phe-NHPh **(3)** while its antipode H-D-Phe-NHPh **(4)** showed a retention time of 4.6 min., in between those obtained with mobile phases MeCN – AcOH 5% and MeCN – TFA 0.042%. From these results it was concluded that TFA competed with the template by interacting with the stationary phase. Different ratios of MeCN - AcOH 5% / MeCN - TFA 0.042% (A / B) were then investigated in an isocratic manner: 100% A, 98 / 2, 95 / 5, 90 / 10, 75 / 25, 50 / 50, 100% B. The retention times relative to acetone of H-Phe-NHPh and H-D-Phe-NHPh are plotted in Graph. 2.1.

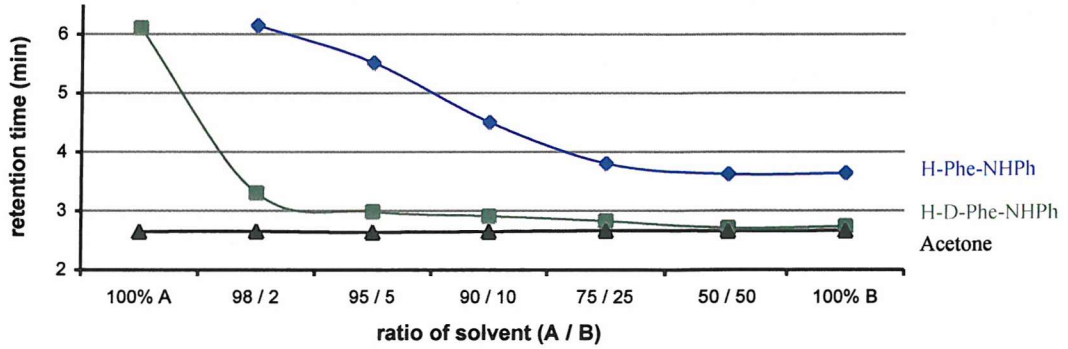

Graph. 2.1: Mobile phase effect on the retention time on ***(P1)*** *(polymer done with MeCN as the porogen, in a 60 x 4.6 mm column) (A: MeCN – AcOH 5%, B: MeCN – TFA 0.042%).*

A decrease in the retention times of H-Phe-NHPh **(3)** and H-D-Phe-NHPh **(4)** was observed, while that of acetone stayed constant (2.6 min) as expected. The retention time of H-D-Phe-NHPh stayed roughly constant (2.8 min) but for H-Phe-NHPh the curve reached a plateau (3.6 min) only from A / B = 75 / 25. With this mobile phase H-D-Phe-NHPh and the acetone have the same retention times while the template was still slightly retained. The binding of H-D-Phe-NHPh **(4)** on the column could be compared with a usual ion-exchange separation. The same trend was observed with the polymer prepared in DCM as porogenic solvent **(P2)** (Graph. 2.2). This porogen, which is less polar than MeCN, should improve non-covalent interactions between the template and the functional monomer leading to better quality imprinted cavities.

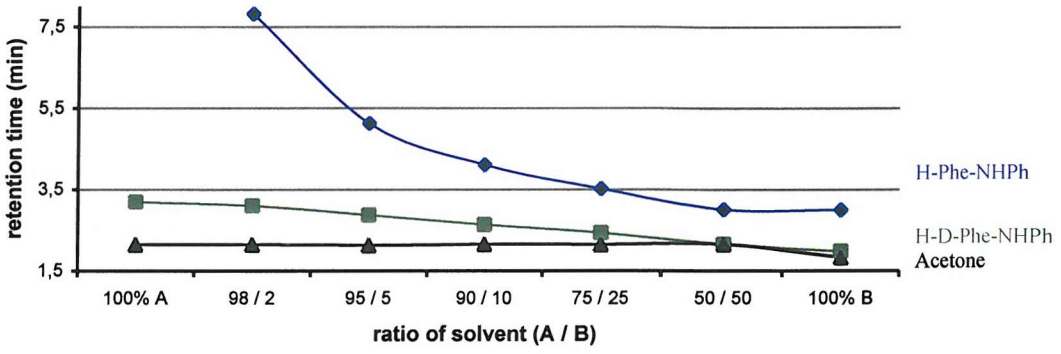

*Graph. 2.2: Mobile phase effect on retention time on polymer **(P2)** (polymer made with DCM as the porogen, in a 60 x 4.6 mm column) (A: MeCN – AcOH 5%, B: MeCN – TFA 0.042%).*

The binding properties of polymer **(P2)** seemed to be more sensitive to the eluent than the polymer made in acetonitrile **(P1)** since the relative retention times for the template decreased faster. On the other hand polymer **(P3)** made with toluene as the porogen showed very strong binding of the template, since a mobile phase with 2% of the mixture B (MeCN – TFA 0.042%) did not elute the template (Graph. 2.3).

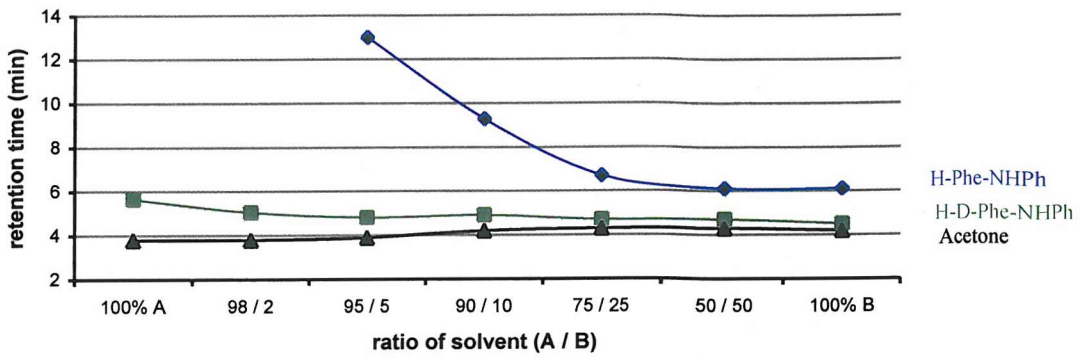

Graph. 2.3: Mobile phase effect on the retention time on ***(P3)*** *(polymer made with toluene as the porogen, in a 60 x 4.6 mm column) (A: MeCN – AcOH 5%, B: MeCN – TFA 0.042%).*

Toluene is a well known aprotic solvent able to maximise non-covalent interactions between templates and functional monomers. The retention time of acetone (4 min) was much higher than that of other polymers and stayed, as expected, absolutely constant under the different eluting conditions. This high retention time is due to the network of the matrix and not packing since the backpressure was lower than in the previous polymers.

The different retention times give indications about characteristics of the column such as selectivity (α) and the relative retention factor (K') for the template H-Phe-NHPh **(3)** and its enantiomer H-D-Phe-NHPh **(4)**. An amazing selectivity (α = 20) for the template was obtained with polymer **(P1)** (made with MeCN as the porogen) due to the lack of accurate measurement since the retention times were close using 50% B as eluent (Graph. 2.4).

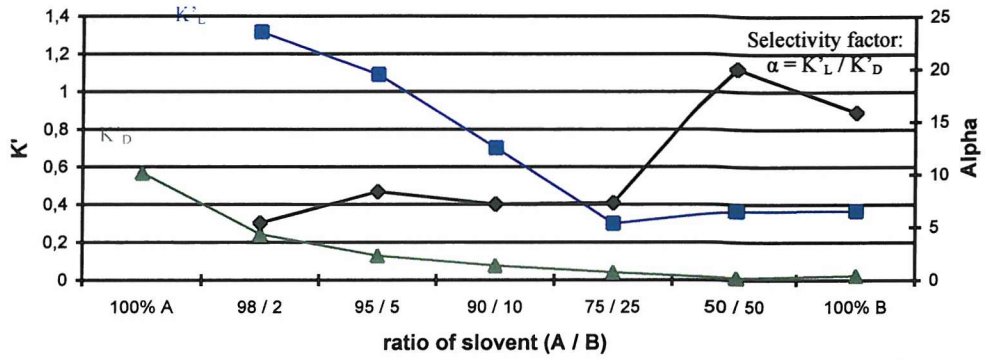

Graph. 2.4: Capacity factors and selectivity with different mobile phases on ***(P1)*** *(polymer made with MeCN as the porogen, in a 60 x 4.6 mm column) (A: MeCN – AcOH 5%, B: MeCN – TFA 0.042%).*

Polymer **(P2)** (made with DCM as the porogen) showed its best selectivity (α = 6) with only 2% B (MeCN – TFA 0.042%) in the eluent (Graph. 2.5). However, the selectivity remained good (α = 4) when using an eluent composed of 100% B.

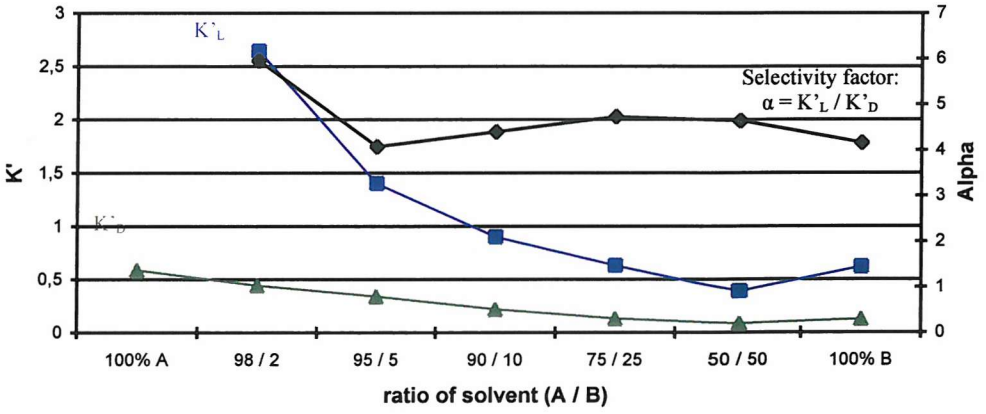

Graph. 2.5: Capacity factors and selectivity with different mobile phases on ***(P2)*** *(polymer made with DCM as the porogen, in a 60 x 4.6 mm column) (A: MeCN – AcOH 5%, B: MeCN – TFA 0.042%).*

The best selectivity for the polymer **(P3)** (made with the toluene as the porogen) was achieved when 5% B were used in the mobile phase since the capacity factor of H-D-Phe-NHPh (K'_D) was close to zero (Graph. 2.6).

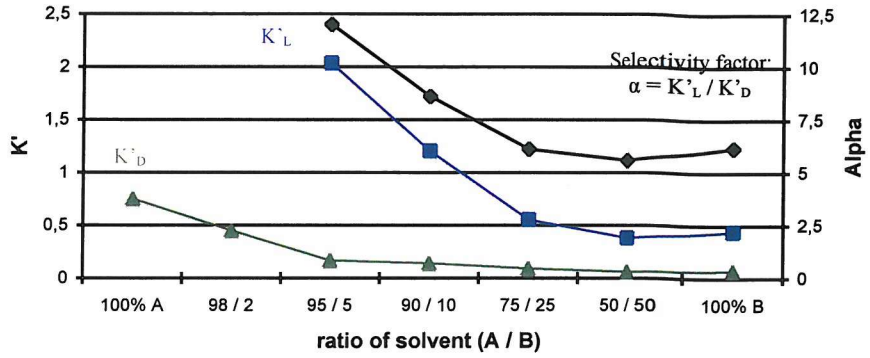

Graph. 2.6: Capacity factors and selectivity at different mobile phase on ***(P3)*** *(polymer made with toluene as the porogen, in a 60 x 4.6 mm column) (A: MeCN – AcOH 5%, B: MeCN – TFA 0.042%).*

From the data the peak efficiencies given by the reduced plate height values were calculated according to the following equation for each polymer.

$$h = H / dp$$

Where d*p* is the mean particle diameter of the packing material, H is the height equivalent to a theoretical plate and *h* is the measurement of the degree of band dispersion produced by the packing considered in relation to the particle size. It is the best parameter for determining peak efficiency. It has no dimensions thus allowing different columns to be compared (the lower this value the better the efficiency of the column) (Graph. 2.7). In every case the efficiency was highly dependent on the nature of the mobile phase used.

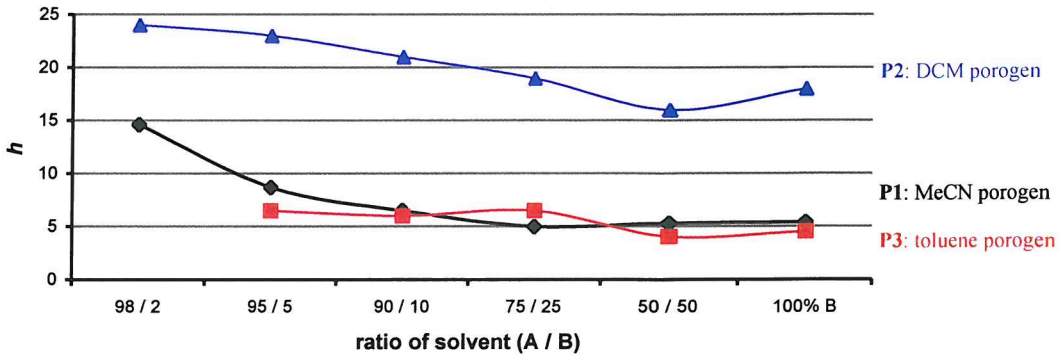

Graph. 2.7: Mobile phase effect on reduced plate height values (h) for the three polymers (A: MeCN – AcOH 5%, B: MeCN – TFA 0.042%).

The reduced plate height values (h) for column **(P1)** reached a plateau with 25% of mixture B and levelled off. The polymer **(P3)** showed the lowest dependence on solvent with an h value about 5. Column **(P2)** seemed to be less efficient than the counterparts made in MeCN or toluene.

The criteria to evaluate the capability of a column to resolve a racemic mixture are not only based on the selectivity factor but strongly depend on K'_D (as discussed previously). The shape of the peaks is also a critical parameter. For the same amount of template injected on the column the asymmetry peak factor was two fold higher for polymer prepared with DCM **(P2)** than for the two other columns (Graph. 2.8).

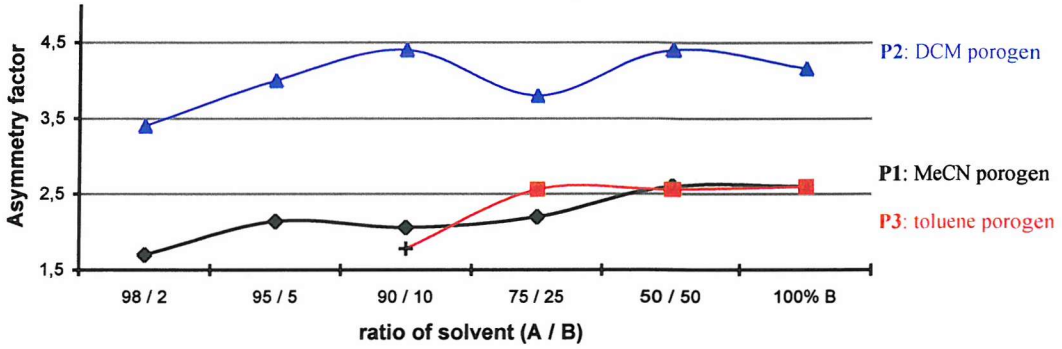

Graph. 2.8: Mobile phase effect on peak asymmetry factors after injection of ***(3)*** *(A: MeCN – AcOH 5%, B: MeCN – TFA 0.042%).*

The asymmetry factor stayed roughly constant under the different eluting conditions. Although H-D-Phe-NHPh **(4)** showed the lowest values, the same profile was obtained. The mobile phase did not affect this parameter. An asymmetry for acetone was also observed suggesting an inherent heterogeneity of the packing material. Moreover, the broadness of the peaks (width at 1 / 10 of the peak height ($W_{1/10}$)) was also the highest for the polymer **(P2)** (Graph. 2.9).

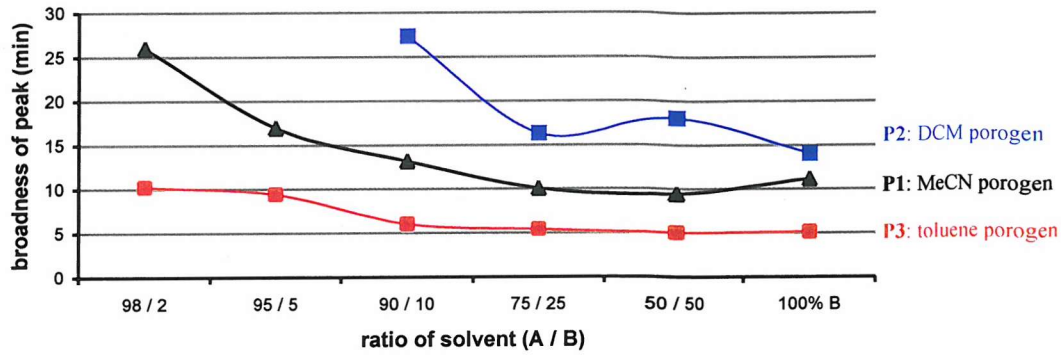

Graph. 2.9: Mobile phase effect on peaks broadness. ***(3)*** *eluted on the three polymers (A: MeCN – AcOH 5%, B: MeCN – TFA 0.042%).*

There was a correlation between the decrease in peak broadness and the level of B in the eluent. The broadness could be due to the "polyclonal" behaviour of the cavities. The template - monomer complex formed before the actual polymerisation is based on the weak non-covalent interactions and is known to give a population of heterogeneous sites in terms of recognition properties, comparable to the polyclonal behaviour of some antibodies.[111] Since polymer **(P1)** showed the highest $W_{1/10}$ values it can be suggested that the cavities are less well defined around the template (as expected since acetonitrile is the most polar solvent of the series investigated). This is confirmed by the fact that the peak broadness in the control polymers (non imprinted) was not sensitive to the nature of the eluent.

Owing to the excessive asymmetry and broadness of the peaks, and despite very good selectivity values, the resolution on base line of the racemic mixture by **(P1)** was not achieved (Spectra 2.3).

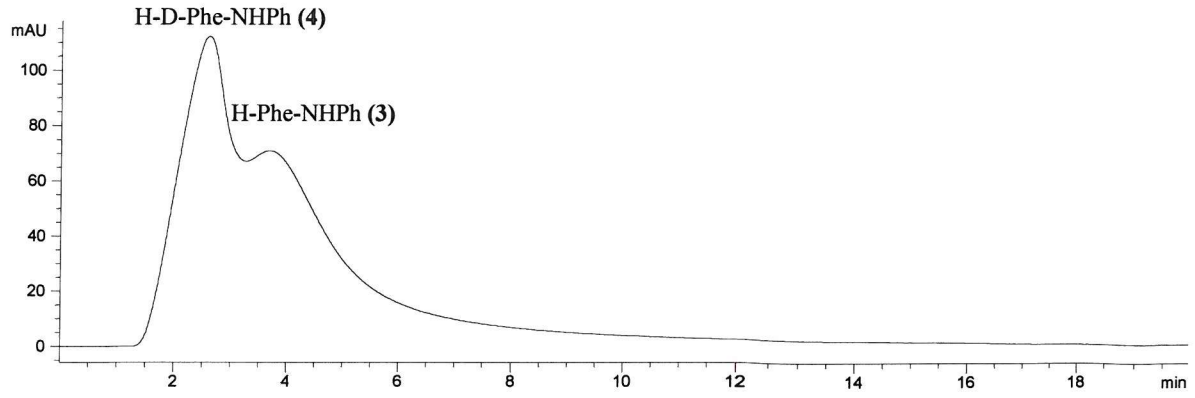

*Spectra 2.3: Elution profile of a racemic mixture **(3) / (4)** by **(P1)** (polymer made with MeCN as the porogen, in a 60 x 4.6 mm column).*

For polymer **(P2)** (prepared in DCM as the porogen) the injection of the enantiomers was carried out separately to measure their retention times more accurately (Spectra 2.4).

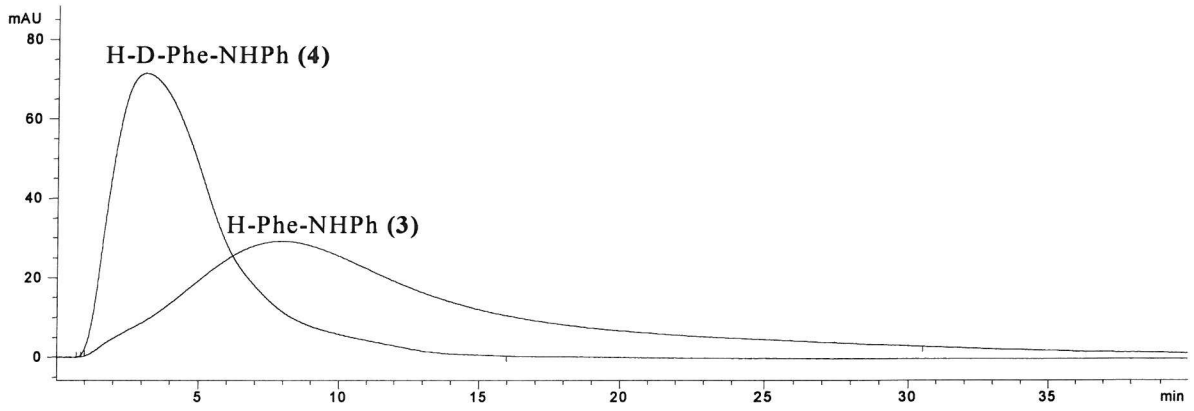

*Spectra 2.4: Elution profile of **(3)** and **(4)** by **(P2)** (polymer made with DCM as the porogen, in a 60 x 4.6 mm column).*

The polymer formed in toluene **(P3)** showed the best resolution, allowing a base line resolution (Spectra 2.5).

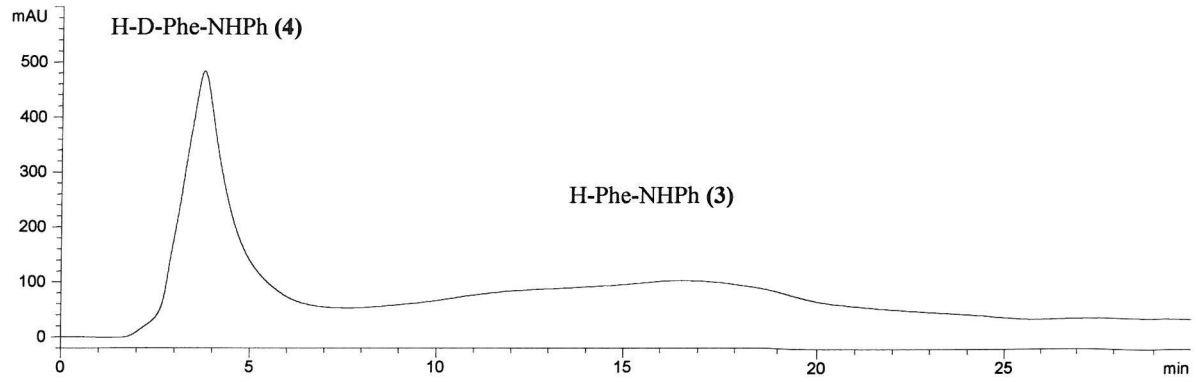

Spectra 2.5: Elution profile of a racemic mixture of ***(3) – (4)*** *by* ***(P3)*** *(polymer made with toluene as the porogen, in a 60 x 4.6 mm column).*

However due to the broadness of the peak of elution it was not possible to calculate the resolution factor (R_s).

More acidic mobile phases were used to investigate the recognition ability under these conditions. To this end, a higher concentration of TFA in the eluent B was used. The assessments were carried out on the polymers **(P1)** (Graph. 2.10) and **(P2)**.

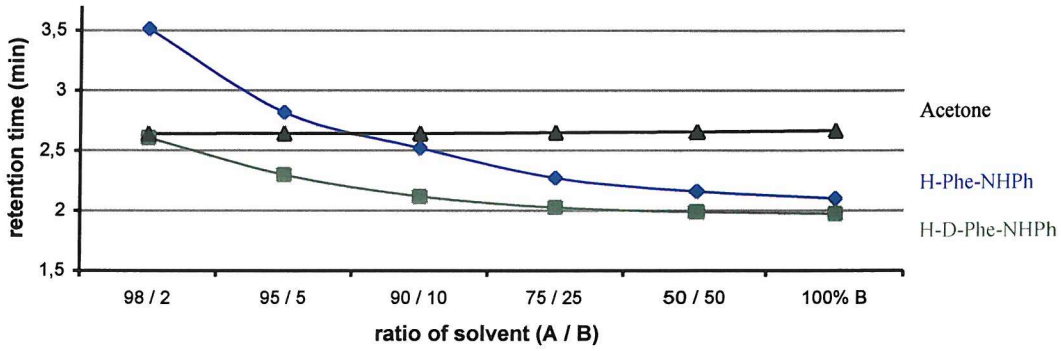

Graph. 2.10: Mobile phase effect on the retention time of ***(3)*** *and* ***(4)*** *on* ***(P1)*** *(polymer made with toluene as the porogen, in a 60 x 4.6 mm column) (A: MeCN – AcOH 5%, B: MeCN – TFA 0.3%).*

The retention time of acetone was similar to that previously observed (2.6 min) and stayed constant under the different eluting conditions. The interactions of the template H-Phe-NHPh **(3)** and its enantiomer H-D-Phe-NHPh **(4)** with the stationary phase decreased. Compound **(4)** ran faster than acetone while **(3)** showed little retention.

Apparently acetone, that was expected to have no retention, was interacting with the stationary phase. The strong effect of the eluent on the $W_{1/10}$ value was once again observed for the template (from 3.1 to 0.8 min.) while for the enantiomer and acetone the value stayed around 0.8 min. Since the retention time of the inert compound was higher than those of **(3)** and **(4)**, the capacity factor and the selectivity was not calculated. Similar results were obtained with polymer **(P2)** (Graph. 2.11).

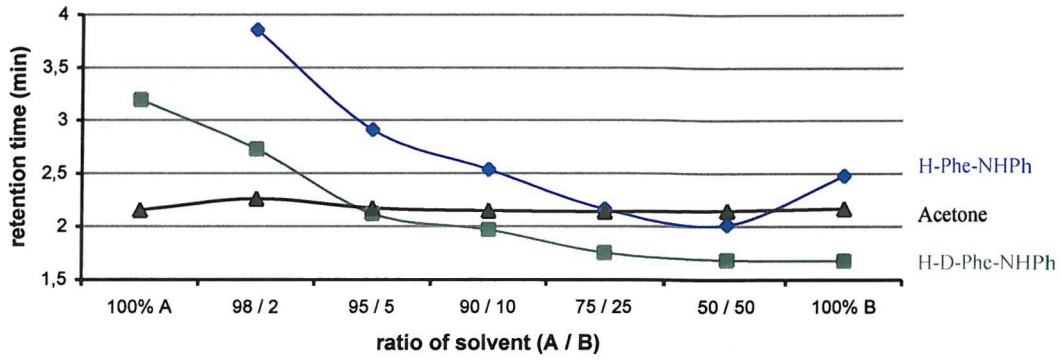

Graph. 2.11: Mobile phase effect on the retention time of ***(3)*** *and* ***(4)*** *on* ***(P2)*** *(polymer made with DCM as the porogen, in a 60 x 4.6 mm column) (A: MeCN – AcOH 5%, B: MeCN – TFA 0.3%).*

An inorganic acid (HCl) was used instead of TFA at 0.03% in MeCN. The effect on the retention time is shown on Graph. 2.12 for the polymer **(P2)**.

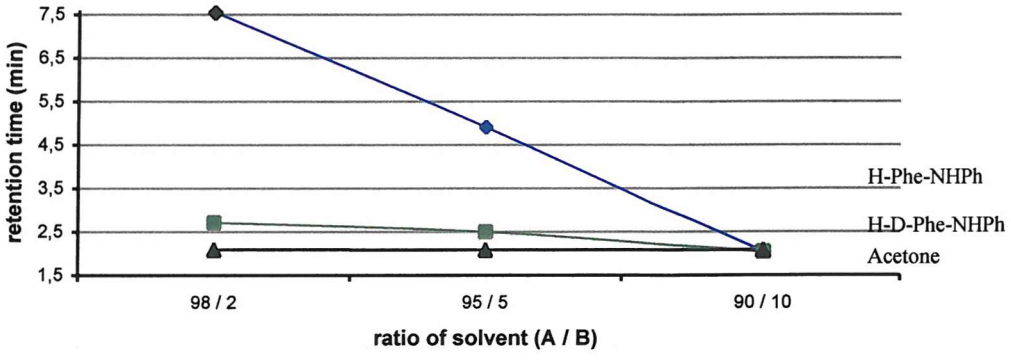

Graph. 2.12: Mobile phase effect on the retention time on ***(P2)*** *(polymer made with DCM as the porogen, in a 60 x 4.6 mm column) (A: MeCN – AcOH 5%, B: MeCN – HCl 0.03%).*

Low levels of HCl seemed to limit the interactions between the stationary phase and compounds H-Phe-NHPh **(3)** and H-D-Phe-NHPh **(4)** as suggested by their short retention times. When the ratio of B (MeCN - HCl 0.03%) was increased to 25%, peak splitting was observed on the elution profiles of acetone, **(3)**, **(4)** and blank injections (20 µL of MeCN). Mass spectroscopy failed to identify the compound corresponding to this additional peak. It was suggested that high levels of HCl in the mobile phase could damage the stationary phase. However, when acetone, **(3)** and **(4)** were again eluted with low levels of HCl (5% of MeCN - HCl 0.03%) elution profiles show a single peak. Weak interactions between the stationary phase and **(3)** and **(4)** were also observed with low levels of HCl in the eluent with **(P1)** (Graph. 2.13).

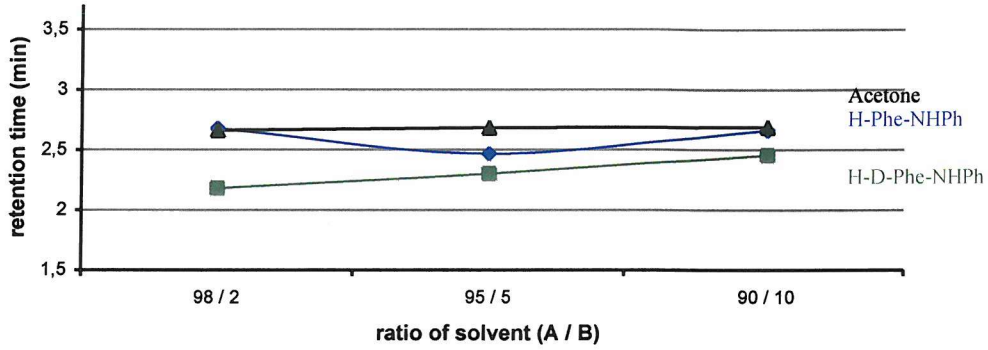

*Graph. 2.13: Mobile phase effect on the retention time on **(P1)** (polymer made with MeCN as the porogen, in a 60 x 4.6 mm column) (A: MeCN – AcOH 5%, B: MeCN – HCl 0.03%).*

Inconsistent split peaks were also observed when ratio of B was increased to 25% in the eluent. The assessments performed with the blank polymer **(B1)** (MeCN as the porogen) gave the same behaviour as the imprinted polymer **(P1)**.

Several hypotheses have been suggested to explain the inconsistent results with high levels of HCl in the eluent. First of all it was assumed that MeCN, the solvent used to prepare samples of **(3)**, **(4)** and acetone, could disturb the column during the elution. 20 µL of a mixture A / B (50 / 50) have been eluted with A / B: 50 / 50 as mobile phase. The elution profile showed once again a split peak. The second hypothesis suggested was the presence of water in the HCl.

Water was therefore used instead of HCl at 0.03% in MeCN. The effect on the retention time for polymer **(P2)** is shown on Graph. 2.14.

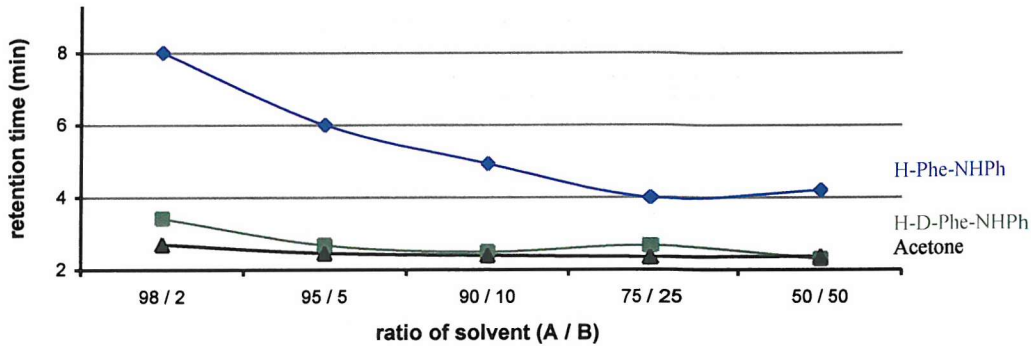

Graph. 2.14: Mobile phase effect on the retention time on ***(P2)*** *(polymer made with DCM as the porogen, in a 60 x 4.6 mm column) (A: MeCN – AcOH 5%, B: MeCN – H_2O 0.03%).*

At low water levels in the eluent a decrease in retention times was observed for H-Phe-NHPh **(3)** and H-D-Phe-NHPh **(4)**, while for acetone it stayed constant (2.5 min). The solvatation of the ammonium ions was suggested. However, when the ratio of B (MeCN - H_2O 0.03%) was increased to 75% no peak was observed on the elution profiles of **(3)** and **(4)**, while that of acetone was still observed (2.5 min). At this level of water in the eluent hydrophobic interactions could take place increasing, paradoxically, the binding strength between the stationary phase and H-Phe-NHPh **(3)** and H-D-Phe-NHPh **(4)**.
The presence of water seemed to improve chromatographic performances, since the *h* values (degree of band dispersion) of H-D-Phe-NHPh **(4)** decreased at high levels of water in the eluent while they stayed constant for acetone (Graph. 2.15).

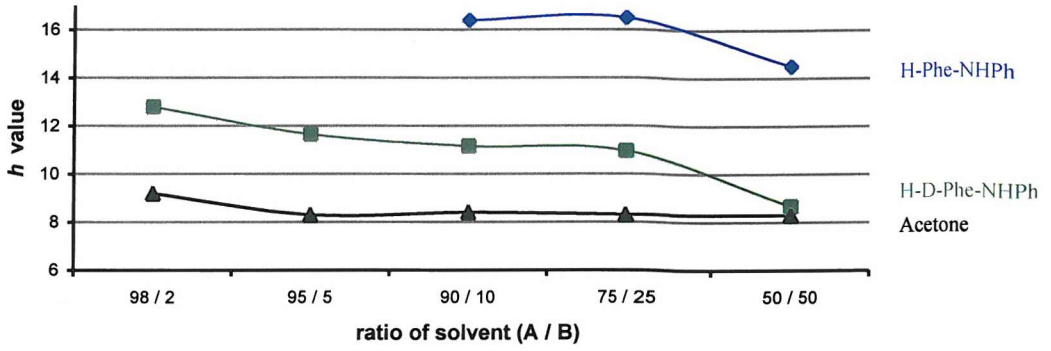

Graph. 2.15: Mobile phase effect on the reduced plate heights (h) with ***(P2)*** *(polymer made with DCM as the porogen, in a 60 x 4.6 mm column) (A: MeCN – AcOH 5%, B: MeCN – H_2O 0.03%).*

The broadness of peak obtained during the elution of H-Phe-NHPh **(3)** at low levels of water prevented the evaluation of h values. The use of water in the mobile phase did not allow an explanation of the results obtained with high levels of HCl in the eluent. Another inorganic acid (H_2SO_4) was used in order to see if results similar to those obtained with HCl could be also observed. The effects on the retention times were investigated with polymer **(P1)** (Graph. 2.16).

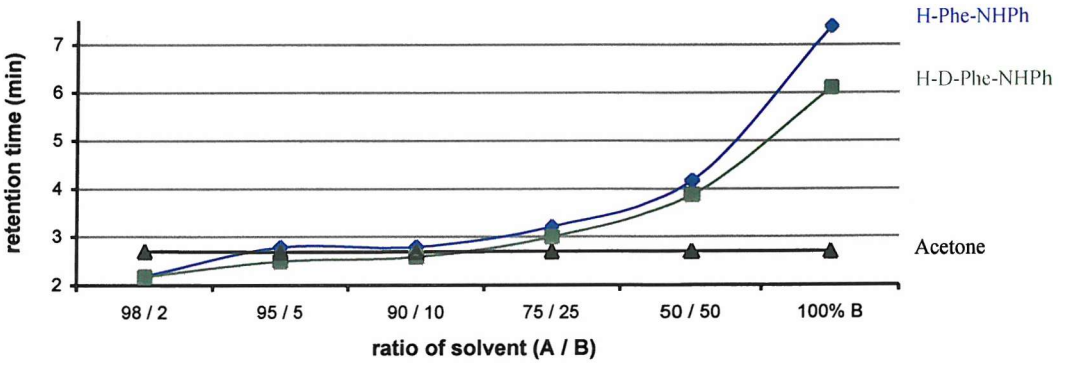

Graph. 2.16: Mobile phase effect on the retention time investigated with ***(P1)*** *(polymer made with MeCN as the porogen, in a 60 x 4.6 mm column) (A: MeCN – AcOH 5%, B: MeCN – H_2SO_4 0.03%).*

High levels of H_2SO_4 seemed to increase the interactions between the stationary phase and H-Phe-NHPh **(3)** and its antipode **(4)** as suggested by the longer retention times. The general trend was that the template H-Phe-NHPh **(3)** was retained more on the stationary phase than the enantiomer **(4)**. However the selectivity factor (α) did not vary greatly (1.4 ± 0.2). The stronger binding of compounds, without improvement in selectivity, could come from unspecific binding by the matrix. On the other hand the efficiency of the column was decreased as observed by the values of the reduced plate heights (*h*) (Graph. 2.17).

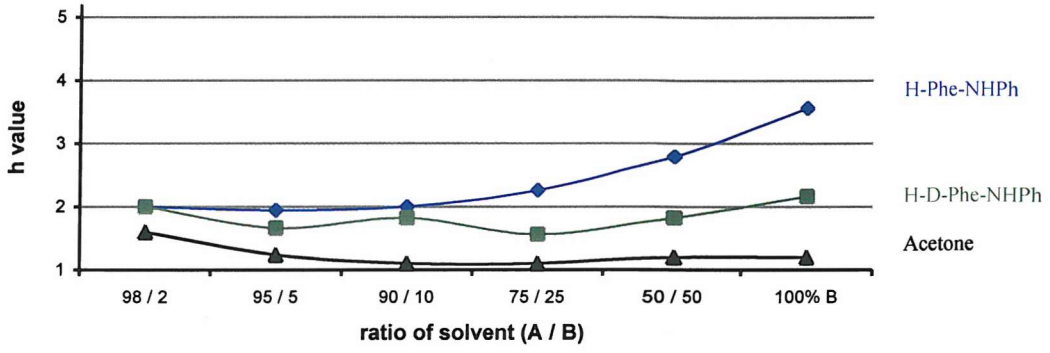

Graph. 2.17: Mobile phase effect on the reduced plate heights (h) with ***(P1)*** *(polymer made with MeCN as the porogen, in a 60 x 4.6 mm column) (A: MeCN – AcOH 5%, B: MeCN – H_2SO_4 0.03%).*

It has been reported that carboxylic acids close together in cavities are able to form dimers[39] and decrease the swelling capacity of the imprinted polymer compared to the non-imprinted polymer where the carboxylic groups are randomly present. Sulphuric acid (pKa H_2SO_4 / $HSO_4^{(-)}$ = -9) could form in a similar way dimers with the carboxylic acid (pKa RCO_2H / $RCO_2^{(-)}$ = 4) in the cavities of the polymer. On the wall of the cavities, and in the same spatial orientation as the carboxylic acid, the sulphuric acid groups could interact strongly with the amine of the template H-Phe-NHPh **(3)** and its enantiomer **(4)** and give therefore higher retention times.

A basic eluent (0.03% NEt_3 in MeCN) never allowed even a flat base line to be obtained.

2.2.4 Effect of the size of the column

In order to investigate the plate number effect on the selectivity, the influence of different sizes of column was explored. A longer column could lead to better resolution of a racemic mixture since the amount of imprinted polymer and consequently the number of cavities would be greater. To this end polymers prepared in acetonitrile and toluene as porogenic solvent **(P1 & P3)** were packed in 150 x 4.6 mm HPLC columns. The retention time of acetone for polymer **(P3)** and packed in a 60 x 4.6 mm column shifted from 4.0 min to 6.5 min compared to the polymer packed in a 150 x 4.6 mm column. The retention time of H-Phe-NHPh **(3)** and its antipode **(4)** should shift in the same proportion (i.e. 2.5 min). However the retention time of template **(3)** was delayed by 15 min when the longest column was used with 5% of B in the mobile phase (B: MeCN – TFA 0.03%). This delay was reduced to only 4 min at 100% of B. The same trend was observed for H-D-Phe-NHPh **(4)**. Template elution seemed to be more dependant on the column size than **(4)** and acetone. The reason for this may be slow kinetics of adsorption – desorption. This hypothesis was confirmed by the broadness of peaks (Graph. 2.18).

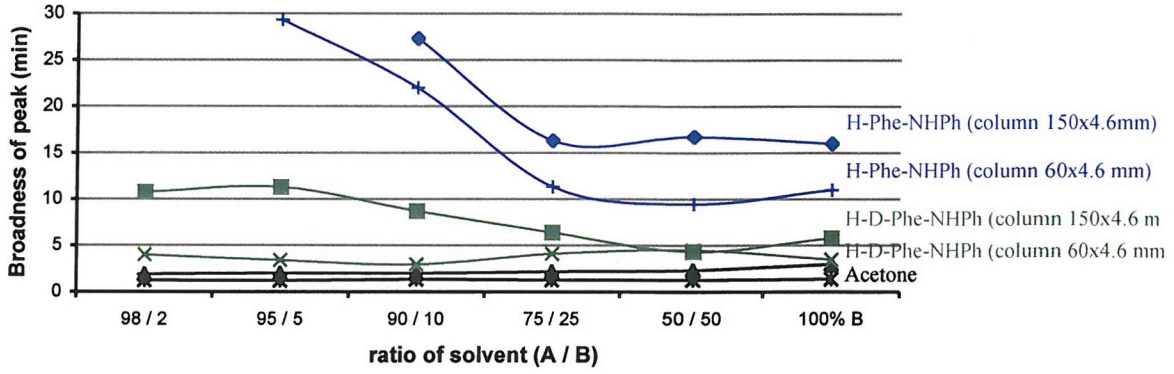

*Graph. 2.18: Size column effect on the peak broadness obtained with **(P3)** (polymer made with toluene as the porogen, in 60 x 4.6 and 150 x 4.6 mm columns) (A: MeCN – AcOH 5%, B: MeCN – TFA 0.03%).*

Acetone did not show a strong dependence on the column size since the broadness of the peak ($W_{1/10}$) was 1.3 min with the 60 x 4.6 mm column versus 2 min with the 150 x 4.6 mm column. This was consistent since acetone was expected not to interact with the

imprinted cavities. The slight increase in $W_{1/10}$ value could be explained by a diffusion phenomenon, usually increasing with the size of the column, although in this case it stayed quite reasonable. On the other hand, the template H-Phe-NHPh **(3)** was eluted more slowly with the longer column whatever the eluent used. The peak was therefore too broad to allow an accurate evaluation of the $W_{1/10}$ value. The enantiomer H-D-Phe-NHPh **(4)** showed a similar increase in eluting time ($W_{1/10}$), at least with the mobile phase having a low level of TFA. In both cases the diffusion phenomenon already observed for acetone was dramatically amplified, since the template, and in a smaller proportion the enantiomer, showed slow kinetics of adsorption – desorption due to strong interactions with the stationary phase.

Unlike polymer **(P3)** packed in a 150 x 4.6 mm column, polymer **(P1)** showed an increase in the broadness of the peaks even for acetone (about 4 min). The reason for this may be the column packing. The increase of the $W_{1/10}$ value for H-D-Phe-NHPh **(4)** was also about 4 min while for template **(3)** was 20 min.

The selectivity for the columns **(P3)** (toluene as porogen) is reported in Graph. 2.19. Both columns (60 x 4.6 and 150 x 4.6 mm) presented similar α values except at low level of B (MeCN – TFA 0.03%).

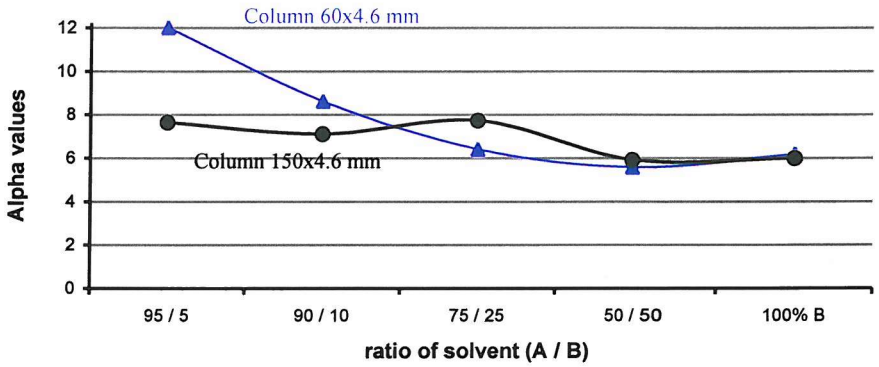

*Graph. 2.19: Selectivity factor for the columns **(P3)** (polymer made with toluene as the porogen, in 60 x 4.6 and 150 x 4.6 mm columns) (A: MeCN – AcOH 5%, B: MeCN – TFA 0.03%).*

A longer column did not improve the resolution of the racemic mixture. It was confirmed by the evaluation of the reduced plate height since the highest values were

obtained for the 150 x 4.6 mm column, probably due to the polydispersity in the shape of the packing material (Graph. 2.20).

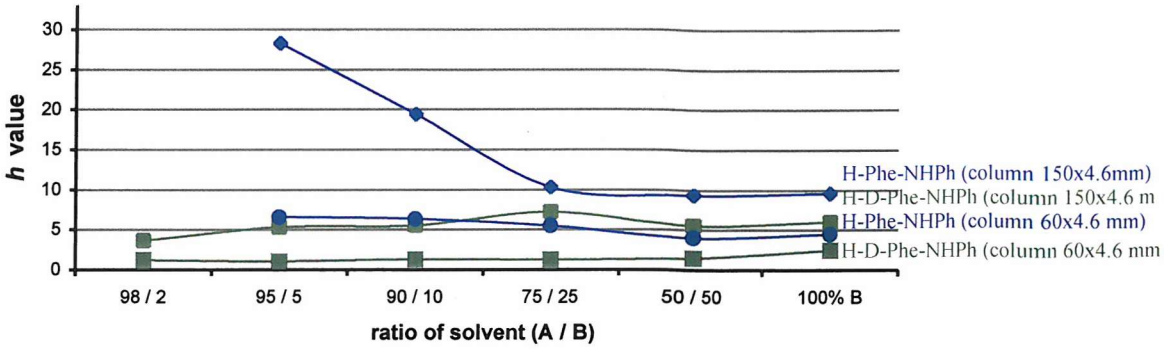

Graph. 2.20: Peak efficiency for ***(P3)*** *(polymer made with toluene as the porogen, in 60 x 4.6 and 150 x 4.6 mm columns) (A: MeCN – AcOH 5%, B: MeCN – TFA 0.03%).*

The HPLC assessments of a polymer made in toluene and packed in a 250 x 4.6 mm column failed due to a problem with high back pressures.

2.2.5 Effect of the flow rate on the peak asymmetry and selectivity

In order to study the binding kinetics and to determine if the selectivity could be improved, the effect of the flow rate was investigated. Polymer **(P3)** (toluene as the porogen) packed in 60 x 4.6 and 150 x 4.6 mm columns was used at 0.3 and 0.5 mL / min with the same eluents as previously (A: MeCN – AcOH 5%, B: MeCN – TFA 0.03%). The broadness of the peak for the template decreased by a factor of 1.3 for both columns at the higher flow rate, but the asymmetry factor did not change proportionally since the 150 x 4.6 mm column gave a value of 2.5 at 0.3 mL / min and 2.8 at 0.5 mL / min while the 60 x 4.6 mm column gave a slightly higher difference: 2.5 at 0.3 mL / min and 1.6 at 0.5 mL / min. At 0.5 mL / min it was expected that the polyclonal behaviour of the polymer would be decreased with the use of only the more selective recognition sites. The selectivity of the columns decreased at higher flow rates (Graph. 2.21).

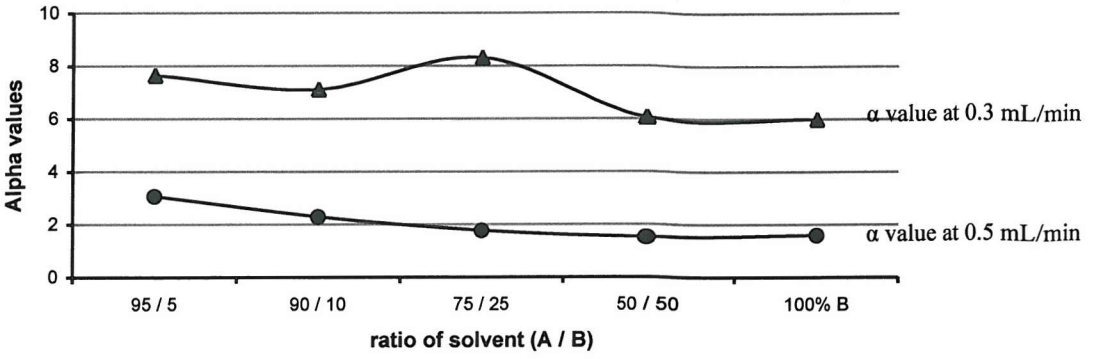

Graph. 2.21: Selectivity for polymer ***(P3)*** *(made with toluene as the porogen, in a 150 x 4.6 mm column at 0.3 and 0.5 mL / min. (A: MeCN – AcOH 5%, B: MeCN – TFA 0.03%).*

However the resolution of the racemic mixture **(3)** / **(4)** was still acceptable at 0.5 mL / min for both columns (Spectra 2.6).

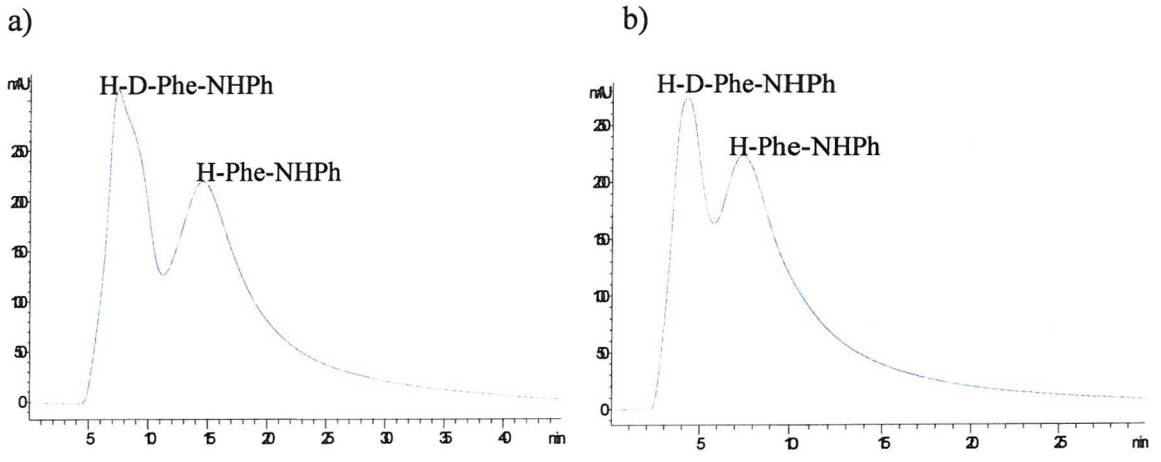

Spectra 2.6: Elution profile of a racemic mixture ***(3)*** */* ***(4)*** *by* ***(P3)*** *(polymer made with toluene as the porogen, in a 150 x 4.6 mm column). a) 0.3 mL / min, b) 0.5 mL / min.*

A polymer **(P4)** was imprinted with H-Phe-NHPh **(3)** in presence of the porogenic solvent toluene and *N*-vinylpyrolidone as a functional monomer. Despite several attempts of packing, the back pressures obtained when the columns were placed on the HPLC were too high to allow any assessment. This problem of back pressure prevented the assessment of columns packed with particles with a size below 30 µm.

2.2.6 Monolith synthesis[190]

To overcome the problem of grinding and packing of the polymer, thermal polymerisation *in situ* was investigated. The polymerisation mixture consisting of MAA, L-Phe-NHPh, AIBN and acetonitrile was degassed and poured into 30 x 4.6 mm **(P5)** and 150 x 4.6 mm **(P6)** columns. Similar mixtures in toluene were also used to fill 30 x 4.6 mm **(P7)** and 150 x 4.6 mm **(P8)** columns. After polymerisation, assessment of the columns was attempted but all the columns, except the polymer **(P5)** made with MeCN in a 30 x 4.6 mm column, gave a far too high back pressure to allow the HPLC assessments. The polymerisation *in situ* seemed to lead to an impermeable material preventing the flow of eluent. Unfortunately when column **(P5)** was assessed the retention times of H-Phe-NHPh **(3)**, H-D-Phe-NHPh **(4)** and acetone were extremely close (about 0.4 min of difference). Either the thermal conditions used during the polymerisation prevented the formation of the pre-complex functional monomer – template, or the column was too short to allow racemic resolution.

2.3 CONCLUSION

In this chapter molecular imprinted polymers (MIPs) as chiral stationary phases (CSPs) have been synthesised in different porogenic solvents in order to determine which one would give the best MIP. To improve the selectivity of CSPs several parameters have been investigated namely mobile phase composition, size of columns and flow rate. It was concluded that:

- toluene as porogenic solvent gave the most selective MIP.
- the nature of the mobile phase could change the selectivity by disturbing the interactions template-stationary phase (TFA in the mobile phase interacted with stationary phase to compete with the template, while H_2SO_4 increased binding strength between the template and stationary phase).
- unexpectedly acetone interacted with the stationary phase, distorting the selectivity factor assessment.
- the size of the column did not seem to have an effect on resolution while higher flow rates decreased the selectivity value. Such behaviour is consistent with commercial chiral stationary phases.

- bulk polymerisation *in situ* did not seem to be a promising approach for preparing imprinted polymers.

The conventional approach used in this chapter to synthesise the MIPs showed the limits (time consuming, problem of back pressure due to polydispersity of the particule shape, etc) to find quickly the best polymer among only a series of three. A combinatorial approach could be an appealing alternative to speed up the process.

CHAPTER 3: MOLECULAR IMPRINTED POLYMERS – A COMBINATORIAL APPROACH

3.1 INTRODUCTION

As reviewed in numerous papers, a vast range of variables affects the characteristics of molecularly imprinted polymers (MIPs). The use of different cross-linking agents[135-137, 200] to increase the flexibility of the matrix, functional monomers,[35, 112, 214, 221] polymerisation temperature[39] and pressure[223] to improve the template-monomers complex stability, the hierarchically imprinted sorbents[102] to create a homogenous pore distribution in the network, have all been reported. From all of these parameters the most investigated is the nature of the functional monomer. For example, chiral monomers have been synthesised by the group of Nicholls to try to improve, without success, the molecular binding of the substrate.[224] To widen the range of possible interactions, several groups have investigated hydrophobic interaction-based recognition with macrocyclic compounds such as vinyl β-cyclodextrin derivatives for the recognition of large guests such as steroids.[225-227] Ramström reported the use of crown ethers to improve the solubility of template-monomer complexes.[228] Recently a polymerisable valine derivative was synthesised for use as a functional monomer in the imprinting of peptides,[229] and showed a remarkable imprinting effect for the template H-Phe-Ala-OH.

To date, to find the best reaction conditions for a given imprinted molecule, the common approach consists of preparing a series of polymerisation mixtures differing by only one parameter (amount of monomer, nature of monomer...) and then applying the overall bulk polymerisation procedure. This approach means that the time and tedious consuming steps of crushing, sieving and packing of the material for use in HPLC stationary phases, which takes several days to complete, must be undertaken for the whole procedure to prepare and evaluate new molecularly imprinted polymers. The limits of this approach have already been highlighted in the previous chapter. It requires long and careful work to find an optimal functional monomer by this method of assessment. To speed up the process, two new concepts have recently been reported. The first one is the rational design of non-covalent imprinted polymers based on a theoretical understanding and use of thermodynamic principles.[230] Since the basis for the molecular memory of MIPs lies in the formation of template-functional monomer

solution adducts in the pre-polymerisation step, the system is under thermodynamic control and the relative strength of these interactions is critical. Andrews's group[231] has developed a "back of the envelope" approach for the evaluation of ligand-receptor binding constants, while the group of Williams[232-233] proposed an equation to determine the energetic contributions to binding. These studies, especially the latter, have been utilised as a basis for a general theory describing molecular recognition phenomena with respect to molecular imprinted systems, which was drawn under a factorisation form (Equation 3.1).[234]

$$\Delta G_{bind} = \Delta G_{t+r} + \Delta G_r + \Delta G_h + \Delta G_{vib} + \sum \Delta G_p \text{ (Equation 3.1)}$$

where the Gibbs free energy changes are: ΔG_{bind}, complex formation; ΔG_{t+r}, translational and rotational; ΔG_r, restriction of rotors under complexation; ΔG_h, hydrophobic interactions; ΔG_{vib}, residual soft vibrational modes; $\sum \Delta G_p$, the sum of interacting polar group contributions.

This thermodynamic treatment can be used to identify factors influencing site formation and consequently to improve polymer design. By considering the various terms in this thermodynamic model (Equation 3.1) the following general conclusions may be drawn in regard to the design of MIPs.[235] The ΔG_{t+r} term defines the order (number of components) of complexes which may be formed. Multivalent monomers could offer energetic advantages due to a reduction in the number of degrees of freedom lost upon complex formation minimising the ΔG_{t+r}. A direct consequence of the ΔG_r term is that a rigid template used in the polymerisation mixture should lead to MIPs with a higher selectivity than those prepared with a less rigid template. This is due to the fact that the more rigid the structure, the lower the number of possible conformations which leads to a narrower site distribution in the resulting polymer. The number and relative strength of interaction ($\sum \Delta G_p$) between the substrate and the monomer control the degree of selectivity of the imprinted polymer. The ΔG_h term reflects the hydrophobic interaction contribution in the imprint process in aqueous media. The optimisation of interactions between hydrophobic moieties of the template structure and suitable hydrophobic interacting functional monomers should enhance the stability of complex formation in aqueous media. Finally from the ΔG_{vib} term we can presume that low temperatures reduce the influence of residual vibrational modes (reducing ΔG_{vib}) and thus contributes to the solution adduct homogeneity. All these parameters determine the position of the equilibrium, ΔG_{bind}, for the formation of self-assembly complexes between the template

and the monomers. On this term the number and the degree of the receptor site heterogeneity depends. The more stable and regular the template – functional monomer complex, the greater the number and fidelity of the resulting cavities. On the basis of purely theoretical assumptions, the formation of molecular imprints in polymers has been investigated. By computer simulation Pande identified the formation of non-random polymer sequences arising from a preferred selection of various monomers by a given template.[236] The application of the Freundlich adsorption isotherm in the characterisation of MIPs gives a good mathematical approximation of the binding characteristics for non-covalent imprinted polymers.[237] More recently UV titration methods have been used to calculate dissociation constants and in this way possible candidate functional monomers able to interact with a template can be screened.[238, 239] However, the success of most imprinting protocols has relied more on chemical intuition than on rational design. In view of the many synthetic parameters that need to be optimised in order to obtain the desired recognition properties, practical techniques for the rapid synthesis and screening of large groups of molecularly imprinted polymers are required. Accordingly, a method involving the molecular imprinting concept and a combinatorial chemistry based strategy has been reported (during this PhD programme), which can readily perform the preparation and evaluation of MIPs thus establishing an optimal monomer system in a short time. Combinatorial chemistry is a recent approach for organic synthesis by which various compounds (called libraries) can straightforwardly be obtained. This library may be prepared in solution or on solid support. Takeuchi and co-workers have recently applied this concept to molecular imprinting.[240] MIPs were explored as artificial receptors for triazine herbicides, ametryn and atrazine, but only two functional monomers, methacrylic acid (MAA) and 2-(trifluoromethyl)acrylic acid (TFMAA) were evaluated. To this end a new *in situ* molecular imprinting protocol was proposed, by automated liquid handling, to prepare plates of imprinted polymer films on the bottom surface of glass vials and for direct assessment of binding. The evaluation of the MIPs was carried out using two types of assessment. In the "first screening" the affinity of the polymer was roughly evaluated by adding a fixed amount of solvent immediately after polymerisation in order to wash the polymers. The affinity was estimated by subtracting the amount of template released from the original amount added in polymerisation solution. A smaller amount of template released translates to a higher affinity. After exhaustive washing of the polymers to extract as much as possible of the substrate (template), the polymers were

incubated in the presence of the imprint molecule to evaluate the ability of the polymer to rebind the template. The assessments of these steps are performed by HPLC quantification of each supernatant. A similar experiment was published by Sellergren and co-workers[91] with a library of imprinted polymers using also a triazine herbicide named terbutylazine. In this approach the monomer which gave the best imprint was screened among a library of six monomers (Fig. 3.1).

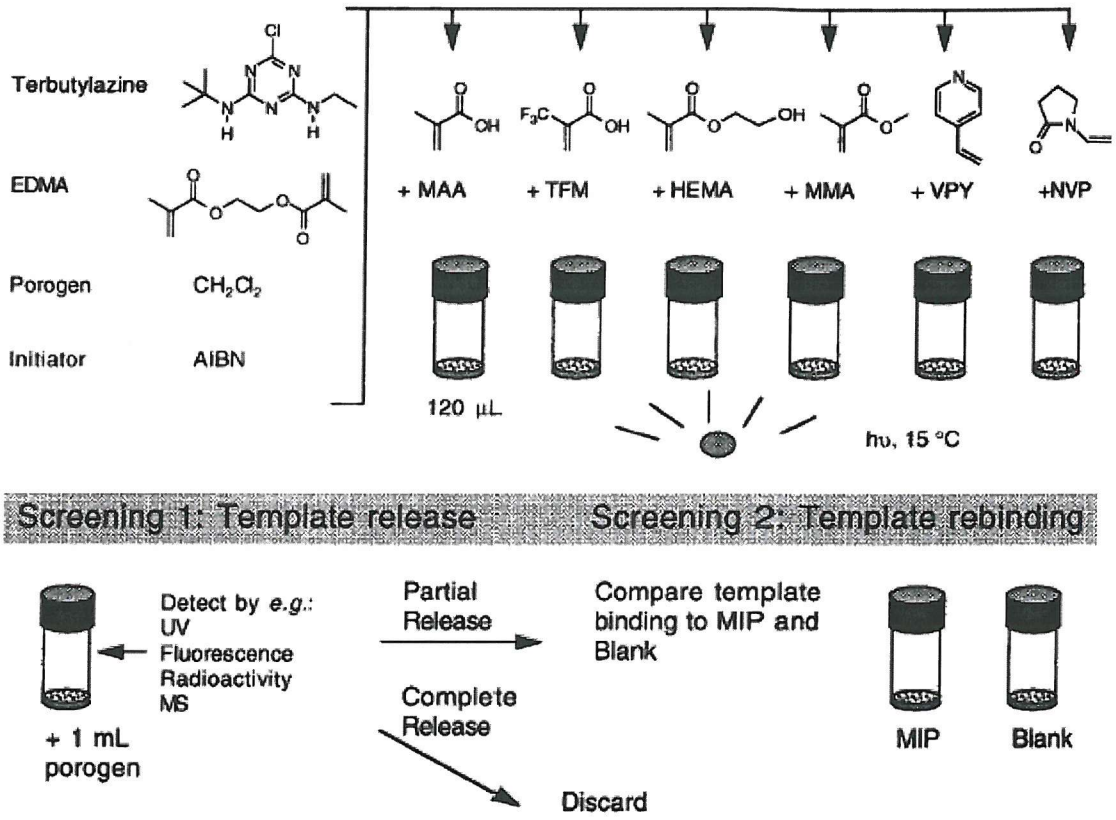

Fig. 3.1: Principle of the MIPs library via combinatorial based approach.[91]

A couple of years later the same group published an optimised version with respect to full automation.[241] In this new study the optimisation of the small scale synthesis was addressed: the choice of the initiation (photo- or thermo-chemical) and of the azo-initiator as well as the degassing and polymerisation times were investigated. Finally the best polymerisation mixture was found by this combinatorial approach for the poorly soluble template (phenytoin) and for a substrate containing poor sterically hindered functionalities for imprinting (nifedipine).

The combinatorial approach developed in this chapter was designed to investigate some of the parameters (nature and amount of porogen, functional monomer, etc.) on the quality and efficiency of the imprint process. New high throughput screening methods were also investigated, answering better the requirements of the combinatorial chemist. The method developed would theoretically offer the ability to screen thousands of MIPs within days.

3.2 RESULTS AND DISCUSSION

3.2.1 Synthesis of templates

3.2.1.a H-Phe-NH-C_6D_5 (6)

D_5-aniline was purchased deuteriated and coupled to Boc-Phe-OH as previously described for the synthesis of **(1)**.[242] After removing the *N*-terminal protecting group from the Boc-Phe-NH-C_6D_5 **(5)** by TFA cleavage and neutralisation of the amine salt (NEt_3), **(6)** was obtained as a white solid in 67% yield.

3.2.1.b L-Dansyl-phenylalanine ethyl ester (7)

L-phenylalanine ethyl ester HCl salt was neutralised by base treatment (NEt_3) for coupling to dansyl chloride.

3.2.2 Synthesis of functional monomers

The monomers **(8 - 11)** were obtained straightforwardlly by addition of the acid chloride (acryloyl or methyl acryloyl) at 0°C to the corresponding amine (benzylamine or ethylamine). The reactions led to the expected compounds in yields of about 60%, probably due to the instability of the acid chloride and competing Michael reaction. The isolation of *N*-(2-Hydroxyethyl)methacrylamide **(13)** and its acrylamide derivative **(15)** required an additional step. In this case, despite using different amounts of amine, the product obtained was a mixture of the expected mono-substituted compound and the di-substituted species due to esterification. It was decided to produce the di-substituted product with an excess of amine (2.2 eq.) to yield 2-Methylacrylamidoethyl methacrylate **(12)** and 2-Acrylamidoethyl acrylate **(14)**. Saponification (sodium hydroxide (1 M)) yielded the expected compounds **(13)** and **(15)**.

3.2.3 Synthesis of the mini-MIPs in vials

3.2.3.a Polymerisation procedure

The thin polymer films were prepared on the bottom of glass vials by photoinitiation at 15°C for 12 h followed by an additional 13 h at 60°C to complete the polymerisation. It has been reported that polymerisation at low temperature increases the strength of electrostatic interactions,[235] but also increases the amount of unreacted double bonds (between 7 and 9%).[111] An additional polymerisation step performed at higher temperatures is claimed to limit this effect. The standard volume of the polymerisation mixture was 120 μL including EGDMA as the cross-linking agent (87 molar %), a functional monomer (17 molar %), the template (12.5 μmol) and the porogenic solvent according to the experiment. Unless otherwise stated the functional monomer was present at 4 eq. relative to the template. The mixtures were degassed at 0°C prior to the actual polymerisation in order to remove oxygen which could stop the polymerisation process trapping the free radical during the propagation step.

3.2.3.b Effect of functional monomers on polymers imprinted with Boc-D-Phe-NHPh (2) in DCM

In this experiment the capability of monomers **(8 – 11, 13** and **15)** to bind to Boc-D-Phe-NHPh **(2)** has been investigated after polymerisation in DCM by a two step-based method: first screening then a template rebinding experiment. The template Boc-D-Phe-NHPh **(2)** was known to interact by hydrogen bonds via the carboxyl and carbamate functionalities with some monomers having hydrogen bond donor and acceptor groups. MAA was the most commonly used monomer having this property, but the acrylamide derivatives synthesised here would widen the available range. Acrylamide monomers, and their methyl acrylamide counter parts, were synthesised to investigate the effect of the vinyl methyl group on the binding capacities. The donor and acceptor hydrogen bond capacity of the monomers was also modulated by the presence of groups with either a positive or negative inductive effect. The aromatic ring would be able to give additional interaction points by π-π stacking with the template. The acrylamide derivatives **(14 & 15)** were also synthesised in order to observe the effect of the flexibility of the arm on the binding with the template. The NVP functional monomer was chosen as a "negative" control due to the expected low binding efficiency of its single binding point to the template via the carboxyl group. The first screening was

based on the released level of template after each washing. To this end the polymers were washed successively with dichloromethane under sonication for 1h, overnight with no sonication, at 40°C for 1 h with sonication and finally after addition of acetic acid (5%) and sonication 1h. The supernatant was removed after each of these steps and analysed by analytical HPLC. In Graph. 3.1 the sum of the successive washings is shown for the imprinted polymers (P). It has been suggested that the higher the amount of released template the less selective the polymer due to poorly defined cavity for its template, although rebinding should be kinetically favoured.

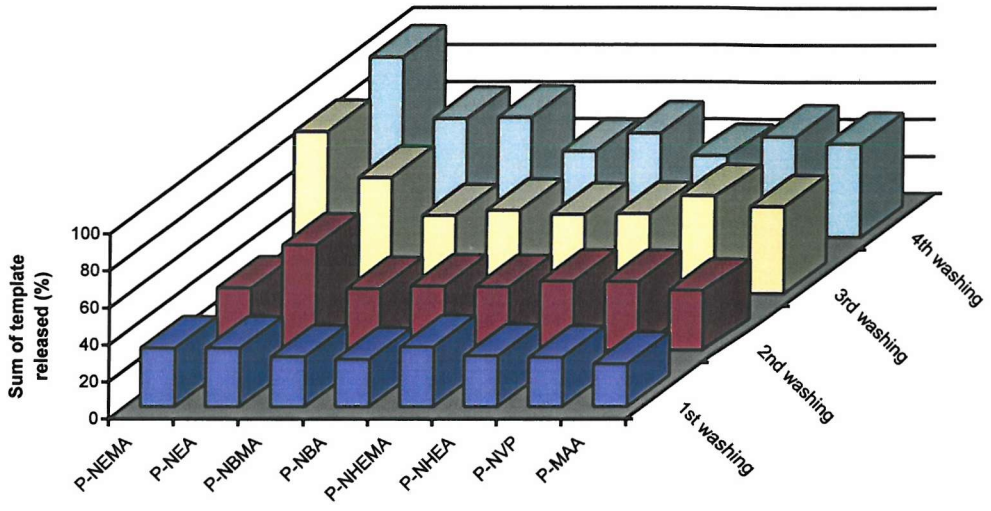

Graph. 3.1: First screening of mini-MIPs in DCM.

After the first washing all polymers showed similar amounts of template in solution but after the second and especially the third it can be seen that the least efficient polymer was the *N*-Ethyl-2-methacrylamide **(10)** (P-NEMA) since nearly 95% of template used for the imprint was released. The corresponding acrylamide derivative **(11)** (P-NEA) was the second least efficient polymer. The absence of groups enhancing the donor or acceptor hydrogen bond capacity, and thus the absence of binding with the template, explains this result. The second group of monomers are those with the benzyl group (**(8 & 9)** P-NBMA and P-NBA), able to interact by л-л stacking with the aromatic rings of the phenylalanine anilide template. The hydroxyethyl monomer derivatives **(13)** (P-NHEMA) and **(15)** (P-NHEA) showed the lowest amount of released template compared to commercial NVP and MAA (50%). A slight difference in each group

between acrylamide and methacrylamide was also observed with the methacrylamide monomer releasing slightly more template than the corresponding acrylamide. The observation made during monomer synthesis that the vinyl methyl group changes the characteristics of the compound was thus also confirmed by screening. After a series of additional exhaustive washings (sonication in DCM / TFA 0.04% (1 mL) until no more template could be observed by analytical HPLC then twice in DCM to remove traces of TFA), sonication of the polymer in the presence of template (0.1 µmole) for 1 hour was followed by measuring the concentration of unrebound template in solution (analytical HPLC (Graph. 3.2))

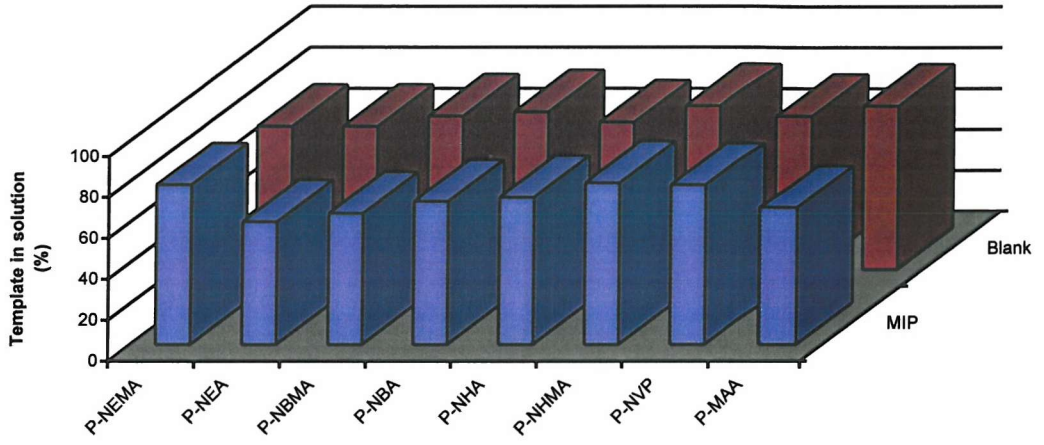

Graph. 3.2: Rebinding experiment of mini-MIPs (template 0.1 µmole in DCM).

Unfortunately, even though a similar profile to the release screening was obtained for this rebinding experiment - polymer made with *N*-Ethyl-2-methacrylamide **(10)** (P-NEMA) gave the highest amount of template in solution - a high amount of template (70%) was still present in the supernatant of the other MIPs. Moreover this binding capacity was unspecific due to binding by the blank polymer (about 20% of template adsorbed). The trend observed during the first screening was maybe too slight to be accurately observable during the rebinding experiment and does not allow any monomer effect during rebinding to be concluded.

3.2.3.c Effect of the functional monomers on polymer imprinted with Boc-D-Phe-NHPh (2) in MeCN

A similar experiment as described above was performed using acetonitrile as the porogenic solvent. The same functional monomers were used, **(8 - 11)** and commercially available MAA and NVP, to compare the effect of the porogenic solvent on the quality of the cavities formed. The effect of HEMA and VPY was also investigated. Finally, TFMA (lower pKa than MAA) which has recently been reported to give strong interactions with this template,[157] and which was thus expected to give a characteristic result to validate the combinatorial approach, included. The first screening was carried out as above and the results are summarised in Graph. 3.3.

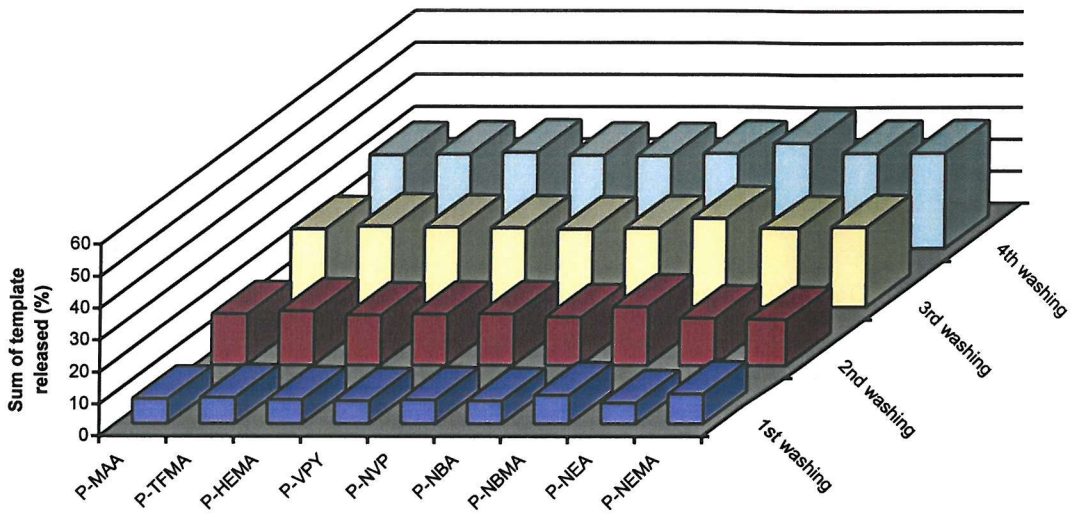

Graph. 3.3: First screening of mini-MIPs in MeCN.

Surprisingly no difference in template release was observed between the functional monomers expected to bind strongly the template (MAA, TFMA) and monomers with the lowest binding capacity (NVP, VPY). Moreover the yield of release for the monomers **(8 – 11 & 13)** was lower than for the previous experiment, suggesting better binding of the cavities for the imprint molecule although MeCN is more polar than DCM and should disturb the template - functional monomer interactions. This result suggests that all functional monomers interact with the same strength with the substrate leading to similar binding cavities. The rebinding experiment was carried out with 0.1

μmole of template in the porogenic solvent MeCN, after a series of exhaustive washings by sonication as in the previous experiment: MeCN / TFA 0.04% then MeCN (Graph. 3.4).

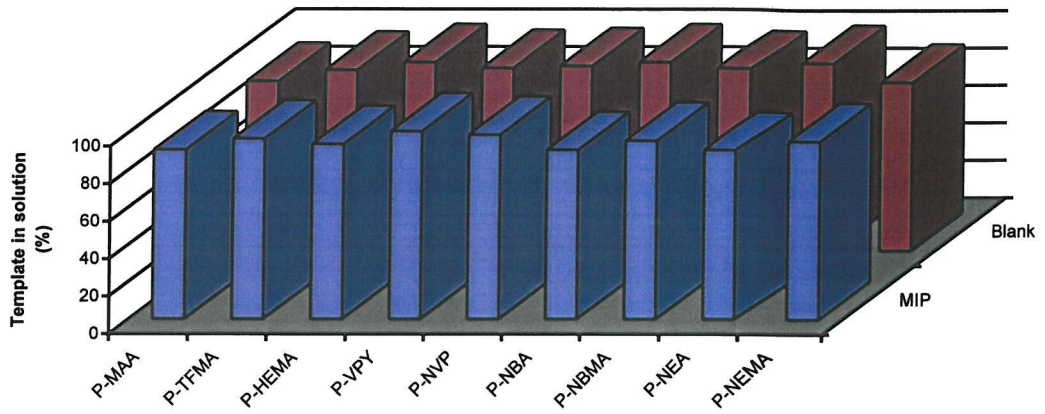

Graph. 3.4: Rebinding experiment of mini-MIPs in MeCN.

The similar profile of the graph for all imprinted polymers and blanks confirms that there was no monomer effect on substrate rebinding. In fact, the extremely high amount of template still present in the supernatant of the MIP samples (about 85 %), quite similar to the blanks, suggests the absence of rebinding cavities. The low template level released by washing during the first screening step suggests that an important proportion of sites in the MIPs are not available for further rebinding experiment due to the permanent presence of the template. A substrate with a chromophore was therefore used to observe small differences in the binding capability of MIPs.

3.2.3.d Effect of the functional monomers on polymer imprinted with Dns-Phe-OEt (49) in MeCN

In order to improve HPLC assessments for small differences in rebinding, a substrate derivative with a strong chromophore system was synthesised: L-Dansyl phenylalanine ethyl ester (**7**). This substrate was expected to lead to strong hydrogen bonding via the sulfonamide group, the carboxyl group of the ester, and л-л stacking. For hydrogen bond interactions MAA was again used. The NVP monomer was used as the "negative"

standard since no interaction was anticipated. Finally *N*-Benzyl-2-methacrylamide **(8)** was chosen for its theoretical л-л stacking capability. We could also expect a shape complementarity effect during the rebinding experiment, due to the bulky group of the dansyl moiety. As with the previous mini-polymers, polymerisation was initiated at 15°C by UV radiation. However only polymers without template (blank polymers) polymerised. The substrate present in the polymerisation mixture of MIP samples absorbed the UV energy preventing the polymerisation. A second experiment was carried out by thermal initiation at 60°C leading to polymerisation of all samples. The first screening was performed in the presence of the porogenic solvent (MeCN) and followed the same sequence as before (Graph. 3.5).

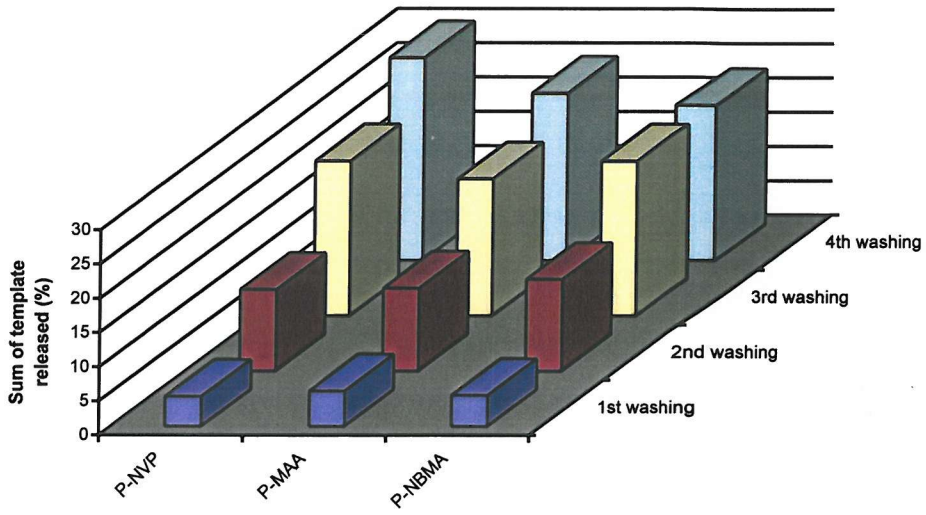

Graph. 3.5: First screening of mini-MIPs in MeCN.

P-NVP released more template than P-MAA and P-NBMA (the latter releasing the least substrate). The hydrophobic interactions developed by the benzyl ring of NBMA **(8)** were thus slightly more efficient in interacting with the template. These led to a more stable pre-polymerisation adduct than with MAA, and therefore resulted in more selective cavities. For all polymers the amount of released substrate was still quite low after four washings. For this reason exhaustive washings by sonication were carried out with different solvent mixtures such as MeOH / MeCN: and MeOH / MeCN / TFA. A final washing sequence was performed with only MeCN to remove traces of MeOH and

TFA that could disturb the interactions between template and cavities. The rebinding experiment was performed with a template solution (0.1 μmole) in MeCN (Graph. 3.6).

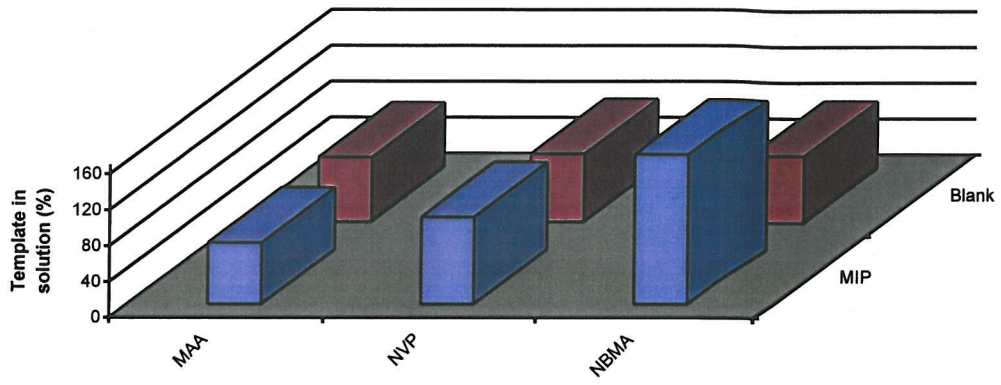

Graph. 3.6: Rebinding experiment of mini-MIPs in MeCN.

Once again the rebinding experiment did not confirm the results of the first screening, since the imprinted polymers showed the same (or worse) absorption levels of template as the corresponding blanks. The imprinted cavities seem to play no role in the binding of the substrate. More intriguing was the inconsistent result obtained for the imprinted polymer synthesised in the presence of NBMA. After the sonication step with the template solution the supernatant shows a concentration 1.5 times higher than the initial solution, although MeOH was used during the exhaustive washing step to remove as much as possible the template.

3.2.3.e Effect of the functional monomers on polymers imprinted with H-Phe-NHC_6D_5 (6) in MeCN

In this experiment the nature of the functional monomers on the selectivity has been investigated by mass spectrometry screening by using H-Phe-NHC_6D_5 **(6)** as template. Many papers report the use of the unlabelled counterpart H-Phe-NHPh in the building of polymers as HPLC stationary phases, to investigate buffer effect in the eluent. This substrate gives one additional type of strong interaction compared to the previous template in the presence of acidic functional monomer (MAA, TFMA...). The amine group of the template deprotonates the carboxylic group of MAA for instance (pKa = 4.6) to give an electrostatic interaction. On this basis it was decided to use the deuteriated derivative H-Phe-NHPh (D_5) **(6)** for a mass spectra assessment of binding. It

was suggested that the resolution by a given MIP of a racemic mixture of the deuteriated template and its unlabelled antipode could be evaluated from the ratio $[MD_5]$ / [M]. The deuterium atoms were attached to the aromatic ring for two reasons. First, the deuteriums on an aromatic ring are not labile (there is nearly no risk for an exchange of deuterium with a proton). Secondly, five deuteriums give a shift big enough to avoid mistakes with the unlabelled compound. To confirm the reliability of the mass spectra evaluation, a control with the deuteriated template and its unlabelled enantiomer was done in a molar proportion of 3 / 1. The same ratio was observed by electrospray positive analysis between the peaks $[MD_5+H]^+$ (template) and $[M+H]^+$. To prepare the library of mini-MIPs, MAA and VPY were used as functional monomers. Finally the accessibility of the sites in the matrix was evaluated using an enhanced level (3 folds) of polymerisation mixture in the vials **(3 VPY & 3 MAA)**. The first screening led to a clear trend in the behaviour of the polymers (Graph. 3.7).

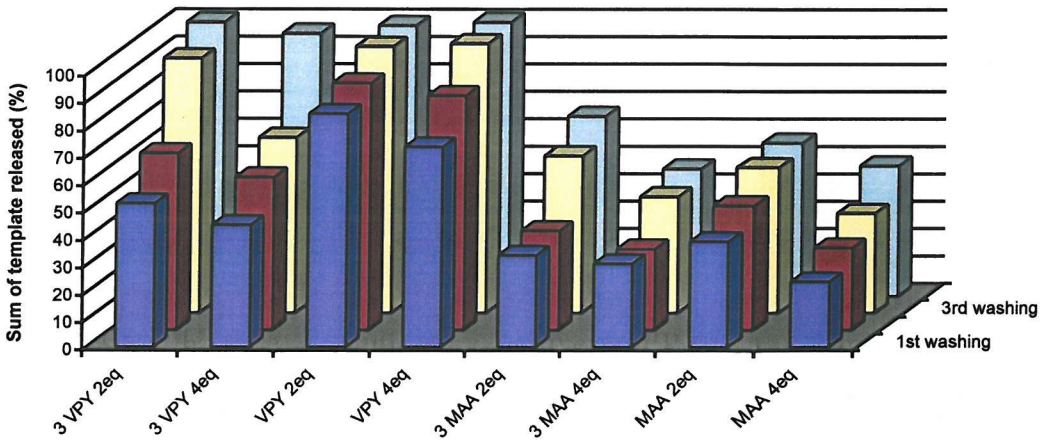

Graph. 3.7: First screening of mini-MIPs in MeCN.

The polymers synthesised with VPY as the monomer showed the highest amount of template released, while MAA showed a very clear ability to retain the template. Although, in theory, two equivalents of MAA are enough to bind the substrate (one for the electrostatic interaction and one for the hydrogen bonds), four equivalents seemed to give the best results. The amount of released template for the MIP synthesised with four equivalents of MAA is consistent with the previous experiments (about 50% after the 4

washings). The levels of VPY did not seem to affect the level of released template in solution. Finally, whatever the thickness of the polymer film, similar percentages of released template were obtained for a given functional monomer, thus the matrix offered good diffusion of the substrate. After an exhaustive washing step (MeCN – TFA 0.04%) until no more substrate was released, a rebinding experiment was performed. A racemic solution (1 mL, 1 mM) of H-Phe-NHC$_6$D$_5$ / H-D-Phe-NHPh in MeCN was added into each vial. A similar profile to the first screening was obtained (Graph. 3.8).

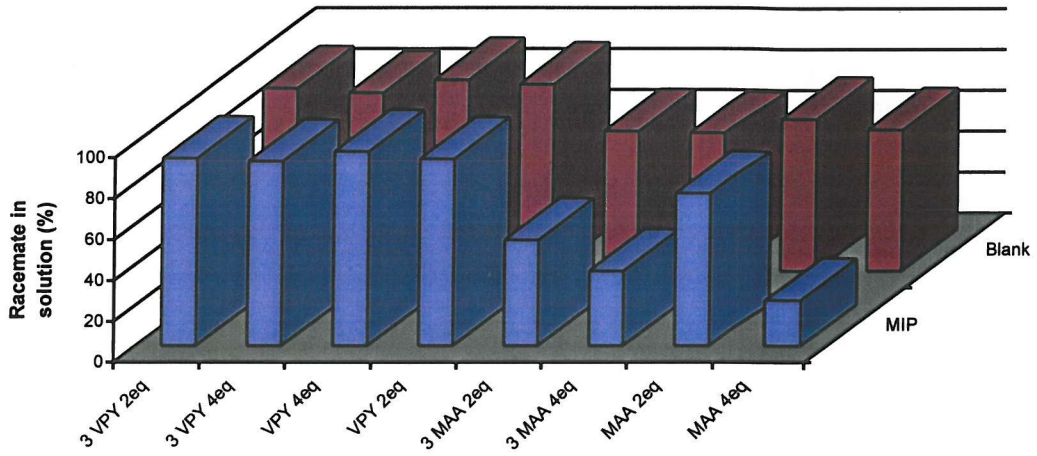

Graph. 3.8: Rebinding experiment of mini-MIPs in MeCN.

The strongest selectivity was obtained with the MIPs that included MAA in the polymerisation mixture. Again, four equivalents of this monomer rebind the substrate significantly better than two. The polymer **(MAA 2eq)** gave much lower binding capacity, due to damage during the exhaustive washings steps (the film was broken and small particles were lost after each supernatant removal step). The results for the polymers imprinted in the presence of VPY confirmed, perfectly, the results of the first screening. Interestingly the rebinding profile of the blank polymers (with MAA) followed roughly those of the MIPs. The blank polymer **(MAA 4eq)** rebound more than **(MAA 2eq)**, and the blank polymer **(3 MAA 4eq)** more than **(3 MAA 2eq)**. The important difference between the MIP and blank binding capacity is, however, due to the imprint process. Finally, a slightly lower rebinding effect was observed for the MIP **(3 MAA 4eq)** than for the MIP **(MAA 4eq)**. Apparently access to all the free cavities

for a thick film is lower than in the case of a thin one, although the first screening gave similar results for both. From these HPLC assessments nothing can be concluded about the selectivity of the cavities towards H-Phe-NHC_6D_5 **(6)** or its enantiomer H-D-Phe-NHPh **(4)**. This assessment was performed by LC-MS (Graph. 3.9). The relative abundance (%) of both species in solution was deduced from the sum of the intensity of the peaks $[M+5D]^+$ and [M] (= 100%).

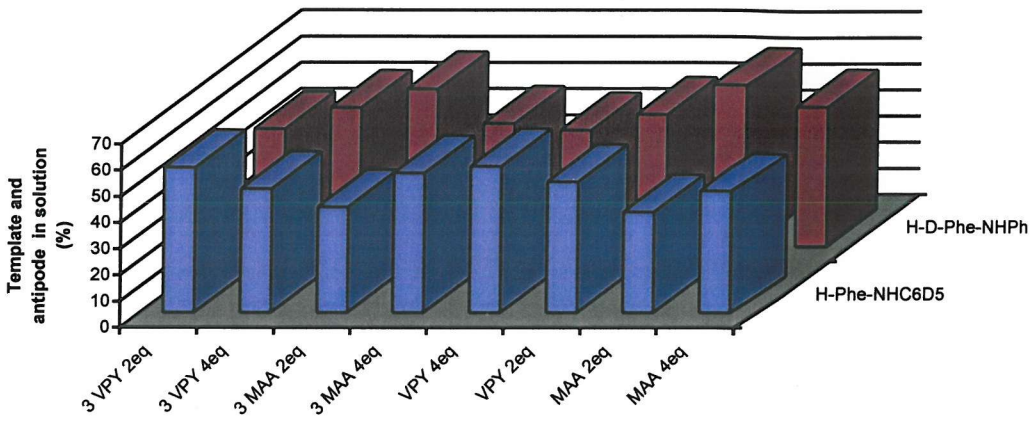

Graph. 3.9: Relative abundance (%) of ***(6)*** *and* ***(4)*** *in solution for imprinted polymers* ***((6)*** *+* ***(4)*** *= 100%).*

The relative abundance of the template and its enantiomer in solution was about 50% for the VPY polymers, which confirms the absence of selective binding for this monomer. The selectivity for the polymers synthesised with MAA was higher, except for polymer **(3 MAA 4eq)**. The polymers **(MAA 2eq)** and **(3 MAA 2eq)** showed by mass spectra similar preference for the template (40% in solution cf to 60% of enantiomer). By a combinatorial approach it was possible to determine the best polymerisation mixture (MAA 4eq.) in a library of 8 members.

3.2.4 Polymerisation in a 96-well plate

3.2.4.a Polymerisation procedure

Fom these encouraging results, the combinatorial approach was extended to the use of a 96-well plate. Thin film polymers, coated onto the bottom of the wells of a micro-plate, were prepared by thermal initiation in a thermostatic bath at 60°C for 18 h followed by 10 h at 75°C to complete the polymerisation.[244] The standard volume of the polymerisation mixture was 120 μL and included EGDMA as a cross-linking agent, the functional monomer, template (12.5 μmol) and the porogenic solvent. The solutions were degassed for 3 minutes at 0°C before loading the mixtures in the wells.
An array of photoinitiated polymerisation was attempted in a 96-well plate, but a cover on the top of the plate to limit evaporation prevented this.

3.2.4.b MIP library with the template Dns-Phe-NHPh (7) in different porogenic solvents and with different functional monomers

The porogenic solvent utilised for molecular imprinting is one of the most important factors which determines effective molecular recognition, especially in a noncovalent approach. The tightness or accuracy of the assembly of template molecules and the host monomer functionality should be dominated by the physical and chemical characteristics of the porogenic solvent used in a system. In order to evaluate quickly the effect of a large series of porogens (DMF, CH_3CN, THF, $CHCl_3$, CH_2Cl_2, hexane) in the imprint process, a library of mini-polymers were prepared following the approach described above. In this case however a 96 micro-well plate was used instead of the individual vials. At the same time the effect of monomers was also investigated for each porogen, with the use of the following commercially available monomers: MAA, NVP, VPY, HEMA, MMA. Finally the shape complementary importance of molecular recognition was investigated by a polymerisation mixture without functional monomer. The main challenge in the combinatorial approach of the plate MIP libraries is, like always in combinatorial chemistry, a reliable and fast screening method. In this case the first screening (assessment of concentration of released template in solution after washing) was carried out using a micro-plate reader. To this end the template already used in the film polymer in vials was used: Dns-Phe-OEt (**7**). After each washing of the 96 micro-well coated films the supernatants were transferred into another 96 well-plate for simultaneous reading by a micro-plate reader (λ = 340). The three first washings of

the first screening were carried out in the respective porogenic solvents (300 µL) so as not to affect the measurement of the porogen effect on the imprint process (Graph. 3.10).

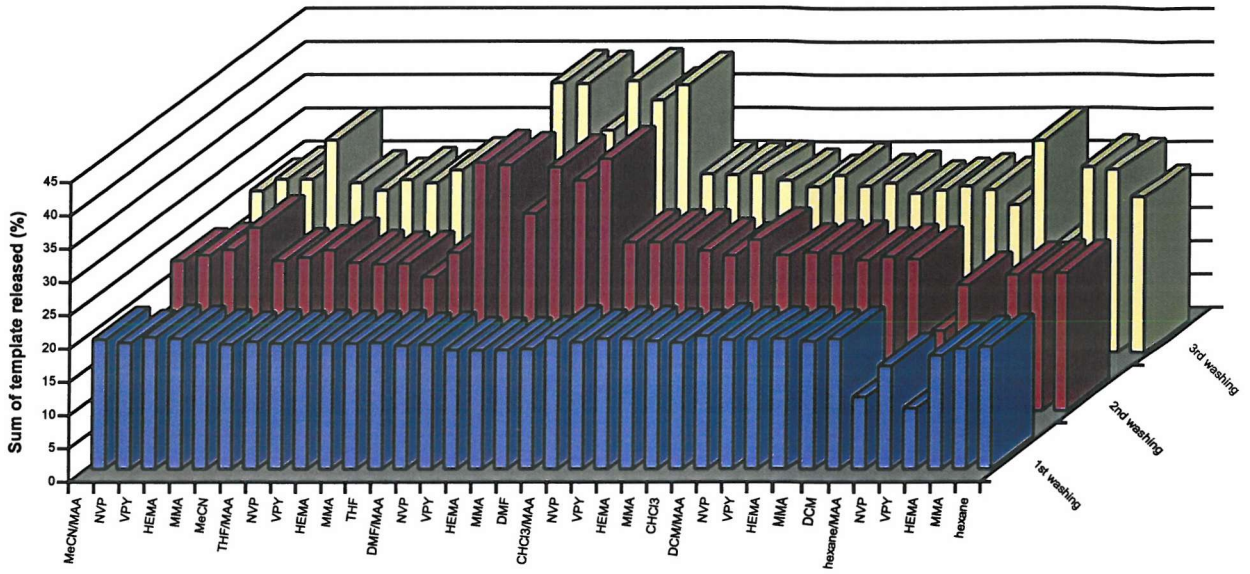

Graph. 3.10: First screening of mini-MIPs in different porogenic solvents.

Surprisingly most polymers showed a similar amount of released template after the first washing. Only two polymers seemed to show a strong binding behaviour, both were prepared in hexane, one in the presence of MAA **(Hexane / MAA)** and the other with VPY **(Hexane / VPY)**. After the second washing a characteristic behaviour arose for the series of polymers made in DMF, which released the highest amount of template. This trend was confirmed by the last washing in the porogenic solvent. The suggestion can be made that the imprint process in this porogenic solvent is less efficient than the others, which is understandable since DMF is the most polar of the range of solvents used. Here the interactions between template and monomer would be disturbed by the competition effect of DMF. The first screening showed that the polymer imprinted in hexane with VPY had the lowest amount of released template. We can also observed a low level of template extracted for all polymers. Since the porogenic solvent seemed to have an effect, a new range of washing procedures was used. It was thought that the

viscosity could also be a parameter affecting the release of the template for the MIPs in DMF. From the third washing the same solvent (MeCN) of washing was used for all polymers. Graph. 3.11 presents the results of this sequence, with also the third washing of the previous one as a standard.

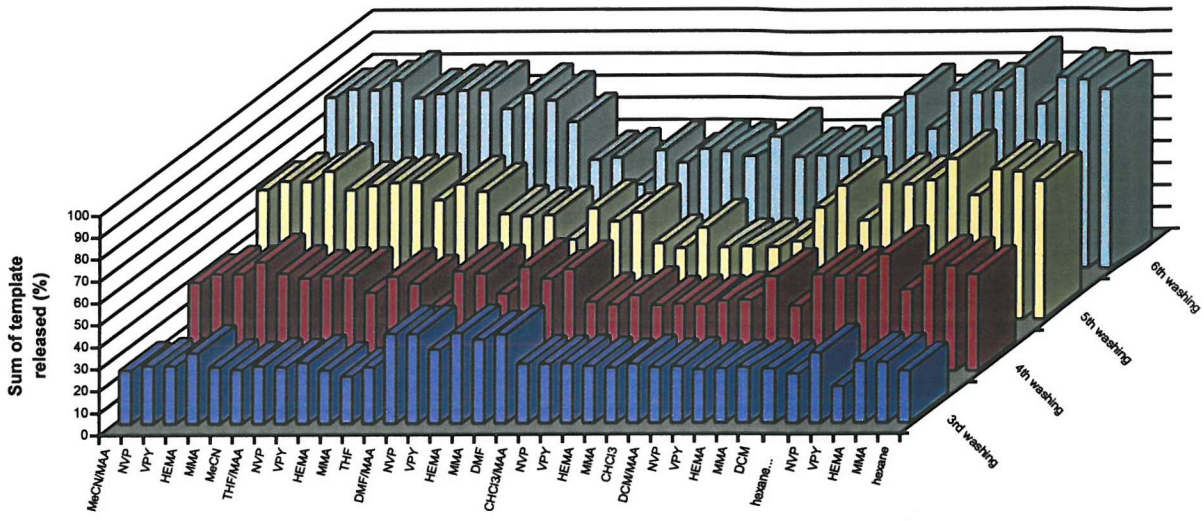

Graph. 3.11: First screening of mini-MIPs in MeCN.

The range of MIPs synthesised in DMF seemed to release no more template into this solvent. The polymers made in chloroform also show a low release of the template under these conditions. On the other hand, acetonitrile improved the yield of extracted template for all the other polymers. MeCN is slightly more polar than the other porogenic solvents (except DMF), and thus this could attenuate binding strength of the substrate to the cavities leading to a higher yield of extraction. In contrast, DMF being more polar than MeCN does not undergo similar competition. To summarize the first screening is noteworthy that the functional monomers surprisingly had no affect on the molecular imprint. In order to confirm this hypothesis the rebinding experiment was carried out as described before with a solution of template (0.1 μmole) in MeCN (Graph. 3.12).

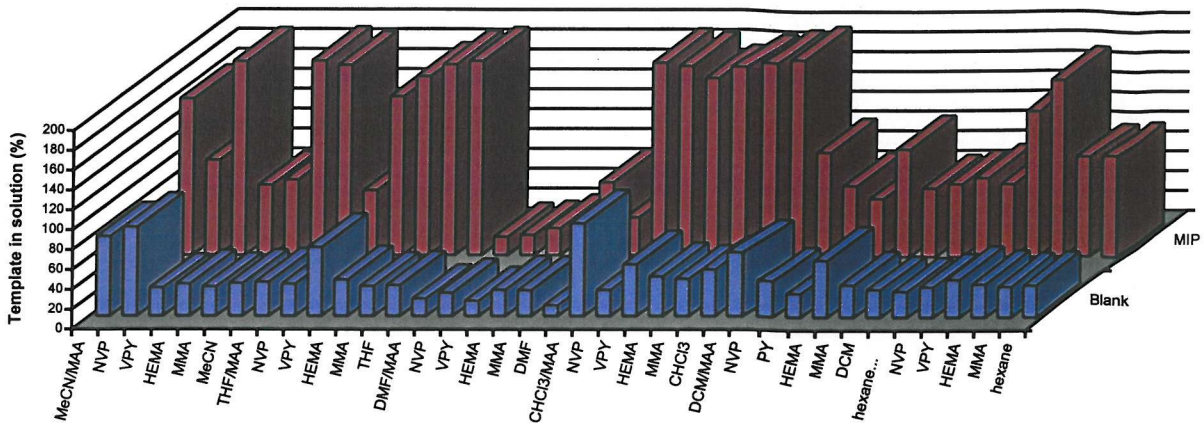

Graph. 3.12: Rebinding experiment of mini-MIPs in MeCN.

Unfortunately this graph gave inconsistent results since the blank polymers absorbed more template than MIPs, with only about 30% of the initial concentration of substrate in solution after one hour of sonication. To try to explain such results, it was suggested that the amount of template used was too small and consequently the blank polymers by unspecific binding led to an apparent higher binding. More surprising is the result obtained for some MIPs with an absorbance corresponding to 160% of the initial amount of template in solution. If we consider a background noise of released template equivalent to or even higher than the amount used for the rebinding experiment we could observe more template in solution than initially added. However an exhaustive washing sequence was carried out before the rebinding experiment. The MIPs that absorbed the most template corresponded to the range of polymers with DMF, which confirms the results from the first screening in MeCN. Thus a new series of washings was performed before a rebinding experiment with a template solution (1 μmole) in MeCN. Once again similar results were obtained with blank polymers binding more than the corresponding MIPs, and for some MIPs the yield of free template evaluated in solution exceeded 100%. But it was not always the same polymers as during the first rebinding experiment. This "random" aspect suggested that the plate-reader approach was not the most appropriate method for such an assessment.

3.2.4.c Library with H-Phe-NHPh with different porogens and with different functional monomers

The aim of this experiment was to determine the effect of changing the porogenic solvent and the functional monomer. To overcome the lack of discrimination observed, it was proposed to carry out the screening of the polymer library by automated HPLC. The retention time for the template, avoids any potential problem due to contamination by side products (unreacted cross-linker, monomer, etc.). A range of assays was carried out in deep polypropylene well plates (1 mL) to improve washing. The polymerisation mixture consisted of the same functional monomers as 3.2.4.b (MAA, NVP, VPY, HEMA, MMA) and porogen solvents (DCM, CH_3CN, $CHCl_3$, hexane, DMSO) in the presence of H-Phe-NHPh **(3)** as a template. The choice of porogenic solvents was however limited, due to the incompatibility of items of the HPLC with certain solvents (THF, DMF), as the evaluation was to be performed by direct injections of the supernatant. In spite of several assays to find the optimum conditions to screen the library (method of elution, type of column, size of cell detector) the screening failed due to unexpected HPLC traces. Parallel screening by analytical HPLC showed the presence of many side products, due to the thermal initiation of polymerisation. The chemical stability of the deep well plate was checked. Unfortunately this stability seemed quite poor at 70°C for 48 hours. Consequently, borosilicate plates were used to make the MIP libraries. Unfortunately, despite the short runs (4 min. for the analysis and 4 min for the post run) and the order in which runs were made (starting with the most volatile solvents in the wells), the small volume of solvent added into the wells for the first screening had evaporated before the end of the assessments.

3.2.4.d Library with H-Phe-NHPh (3) in toluene and with different functional monomers and different ratios of EGDMA

This experiment investigated the effects of the nature and the amount of functional monomer, and the degree of cross linking of the polymer, on the imprint process. To resolve the problem of evaporation during HPLC analysis, toluene was used as the porogenic solvent. The polymerisation mixture consisted of the template (H-Phe-NHPh) **(3)**, the porogenic solvent, different functional monomers (MAA, NVP, VPY, HEMA, MMA) in different proportions (2 or 4 eq.) and the cross-linker ethylene glycol dimethacrylate (EGDMA) present at 83%, 70% and 50% (mol %). In order to obtain

this range, the amount of monomer was kept fixed and the amounts of cross-linker and template werevaried. The influence of polymer morphology could therefore be evaluated. The first screening was performed by measurement of the released template in the porogen solvent (300 µL) after a sequence of three washings by sonication. The evaluations were made *in situ* after each washing by automated HPLC on the supernatant from each well (Graph. 3.13).

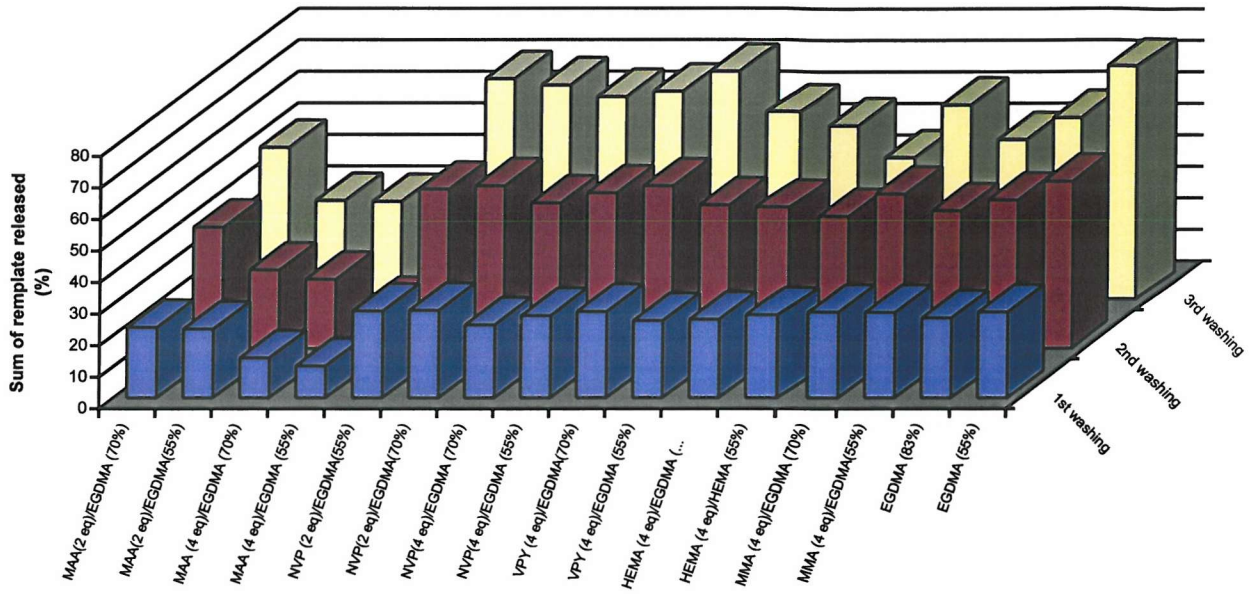

Graph. 3.13: First screening of mini-MIPs in toluene.

This graph shows that the amount of template released was lowest for MAA, indicating that the strongest binding with the template was obtained for this functional monomer. When using the same number of MAA equivalents (mole template equivalent) the polymers made with the lowest amount of cross-linker (55%) seemed to give the best binding capacity, though we can assume that the network of the macroporous polymer would be less well defined. If the amounts of released template are compared to polymers made with 70% cross-linker and either 2 or 4 equivalents of functional monomer (MAA) the latter seemed, after the first washing, to bind more efficiently to the template. For polymers made with NVP the binding capacity seemed to be constant whatever the polymerisation mixture. For other polymers (with VPY, HEMA and

MMA) the polymers prepared with 55% of cross-linker also gave the strongest binding. Finally, polymers without functional monomer were made to evaluate the capability of the cross-linked polymer networks to memorise the shape of the template. In this case the polymer synthesised with the higher amount of EGDMA (83%) showed the best binding capacity. To prove the accuracy of the direct screening from the 96-well plates, parallel assessments were performed preparing samples (10 μL of supernatant in 1 mL of MeCN). Similar results were obtained, confirming that the direct screening approach could be used in future screening of MIPs. Finally, after an exhaustive sequence of washings, a rebinding experiment was performed with the template solution (H-Phe-NHPh **(3)**, 0.1 μmole in toluene) to confirm this first screening. Unfortunately despite the short time of the runs (8 min) and the high boiling point of the porogen the evaluation of the 96 wells by automated HPLC failed due to the evaporation of the samples. But as for the first screening, a parallel assessment was carried out by analytical HPLC. To this end the samples were prepared by adding 5 μL of solution to 100 μL of MeCN (Graph. 3.14).

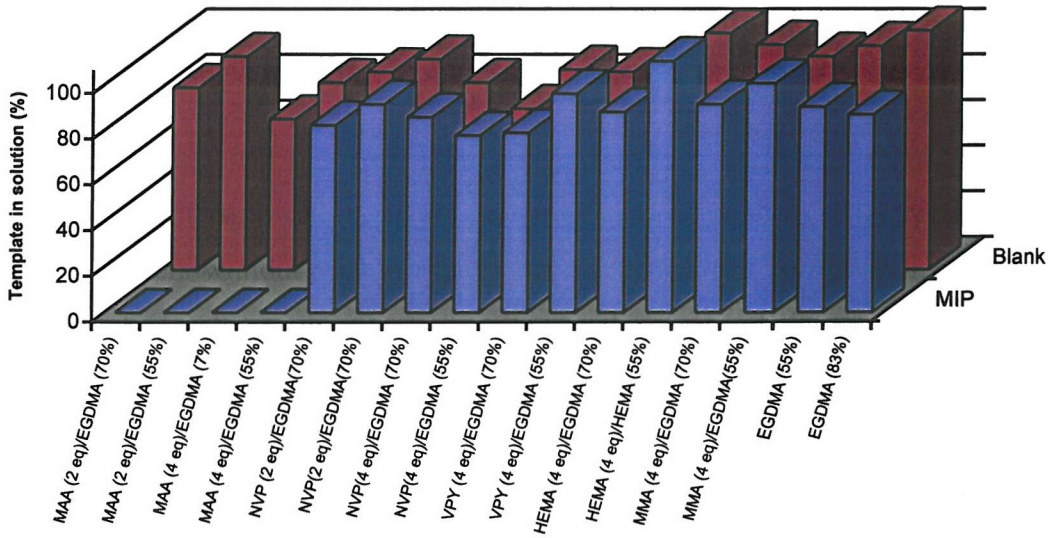

Graph. 3.14: Rebinding experiment of mini-MIPs in toluene.

The polymers made using the functional monomers NVP, VPY, HEMA and MMA showed poor rebinding ability similar to the blank polymers. On the other hand, as

expected the best rebinding behaviour was observed for the polymers made with MAA (owing to its capacity for electrostatic interactions with the template), although it was not possible to draw conclusions on the best mixture due to the small amount of template in the supernatants (under the sensitivity level of the HPLC). These excellent results were consistent with those obtained during the evaluation of a HPLC stationary phase prepared from a similar polymerisation mixture (see Chapter 2, Spectra 2.5).

3.2.4.e Effects of solvatation and amount of functional monomer on the imprint process

From the previous results it was decided to investigate if the combinatorial approach using a 96 well-plate could discriminate between polymers of a close composition. A series of MIPs, and the corresponding blanks, were made with different equivalents of MAA (2, 4, 6 or 8 eq. per mole of template) in the presence of different volumes of porogen (toluene) given by the molar ratio toluene / MAA (50, 27, 13 and 9), keeping the amount of monomer constant while changing the volume of porogen and the amount of template (H-Phe-NHPh **(3)**). In order to compare the different polymers, a volume of polymerisation mixture corresponding to 12.5 μmol of template was poured in the wells. The evaluations were made *in situ* from each well by HPLC and from samples prepared in MeCN to evaluate the accuracy of the method. Graph. 3.15 presents the results obtained by the direct screening of the plate.

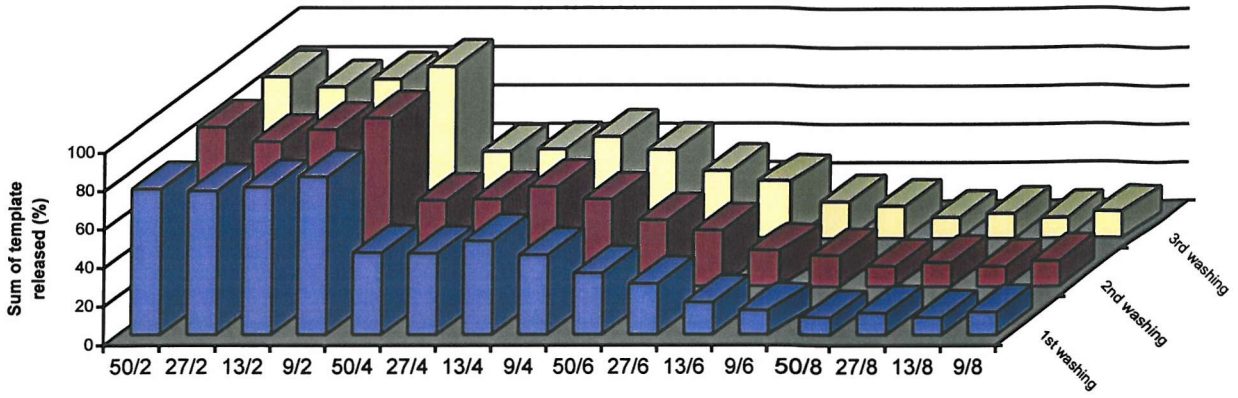

Graph. 3.15: First screening of mini-MIPs in toluene (A / B: A = ratio (toluene / MAA), B = MAA eq.).

It was observed that the most efficient MIPs were obtained for the polymers made with 8 eq. of MAA (with less than 15% of released imprint molecule). For 2 eq. of monomer the polymer had no apparent binding ability. The results obtained for the polymer with 4 eq. (about 50% of imprint molecule extracted) are quite consistent with the previous experiments. For a given amount of MAA (value B on Graph. 3.15) no difference was observed between the polymers. It should be noted that toluene, when used at high ratios for the polymerisation with 6 eq. of MAA, altered the template – MAA interaction. The same results were obtained by analytical HPLC. The rebinding experiment performed with a template solution (H-Phe-NHPh **(3)**, 1 µmole in toluene) was made after an exhaustive template extraction (Graph. 3.16).

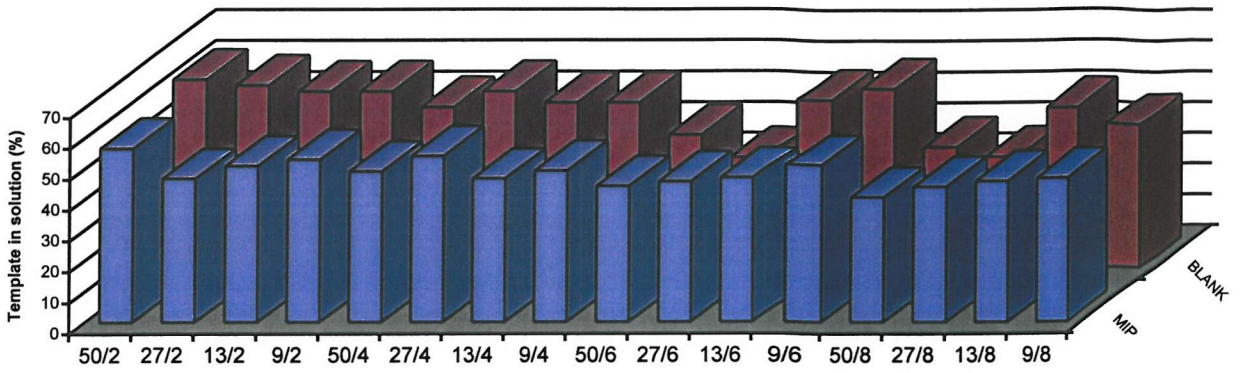

Graph. 3.16: Rebinding experiment of mini-MIPs in toluene (A / B: A = ratio (toluene / MAA), B = MAA eq.).

Unfortunately the expected selectivity was not observed. All the MIPs had a similar ability to rebind the template at about 50% of the initial amount. The high level of unspecific binding observed with the blank polymers suggested that the molecular recognition of MIPs was not reliable. The use of a too high concentration of substrate for this rebinding experiment was assumed to be saturating the sites. A solution at 0.1 µmole of template (H-Phe-NHPh (**3**)) was used but no selectivity was still observed. It was further suggested that the results of the first screening were an artefact of the different amounts of template used in the polymerisation mixture to yield the apparent different equivalent. A control experiment was carried out with a series of polymers imprinted with a constant amount of template in the presence of different equivalent of MAA. However from the previous results the capability of polymers to bind strongly the template is directly proportional to the equivalents of MAA used.
The first screening is reliable but apparently the discrimination between polymers having similar composition is not possible by this combinatorial approach.

3.3 Conclusion

In conclusion the influence of the porogen affecting the template-monomer complexes as well as the nature and ratio of the functional monomer and the degree of the matrix cross-linking, has been addressed. Some monomers were specially designed for these

studies, but did not give strong binding with the templates used for the assessments. It was concluded that:

- the monomer methacrylic acid (MAA) with toluene as porogenic solvent was found to be the best polymerisation mixture for the templates used in this chapter, which is consistent with the results obtained by the conventional method (Chapter 2).
- new types of screening (plate reader, mass spectrometry, direct screening from 96-well plates by automated HPLC) were investigated for high throughput assessments but the lack of reproducibility for some of them limited their use.
- it could be suggested that the thin film coating approach did not mimic exactly the behaviour of the polymer used under dynamic HPLC conditions, especially during the rebinding experiment.[243]
- new screening tools, methods of synthesis, washing, etc. need to be developed.

Nonetheless, since many variables, mostly still unknown, play a role in the formation of the pre-polymerisation complex. this combinatorial approach remains the most promising tool, compared to the conventional approach, for the discovery of the best MIP for a given template in the shortest time.

CHAPTER 4: CYCLIC PEPTIDE SYNTHESIS USING A METAL TEMPLATE

4.1 INTRODUCTION

4.1.1 Why cyclic peptide chemistry?

Cyclic peptides and their derivatives have drawn the interest of chemists and biologists for many years. A significant number of naturally occurring cyclic peptides possess powerful and useful biological activities; examples include the antibacterial agents valinomycin[245] (Fig. 4.1), kawaguchipeptin B[246], octraeotide[247] and the immunosuppressive drug cyclosporin A.[248]

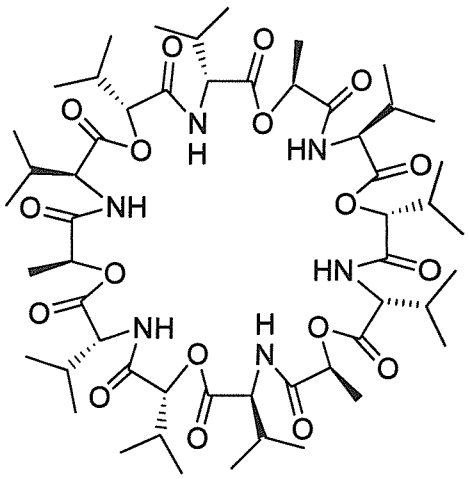

Fig. 4.1: Valinomycin.

The main characteristic of cyclic peptides is their increased stability in comparison to their linear counterparts.[249] The reduced flexibility due to cyclisation can increase receptor specificity. Another characteristic that contributes to the attention of cyclic peptides, is the conformational constraint, imposed by cyclisation,[250] often used a as useful and predictable model of various protein structural motifs such as the β-sheet.[251] The emergence of peptide nucleic acids (PNAs),[252] as novel oligonucleotide analogues used in the antigene strategy against genetic diseases, has led to the discovery that certain PNAs can be cyclised to improve the nuclease stability.

It is, therefore, not surprising that many methods have been developed in the area of cyclic peptide synthesis. They can be summarised in two general approaches: classical

solution phase under high dilution condition and solid phase synthesis. A common feature of both methods is the use of protecting groups to prevent unwanted coupling reactions with, for instance, side chains of amino acids (Scheme 4.1).

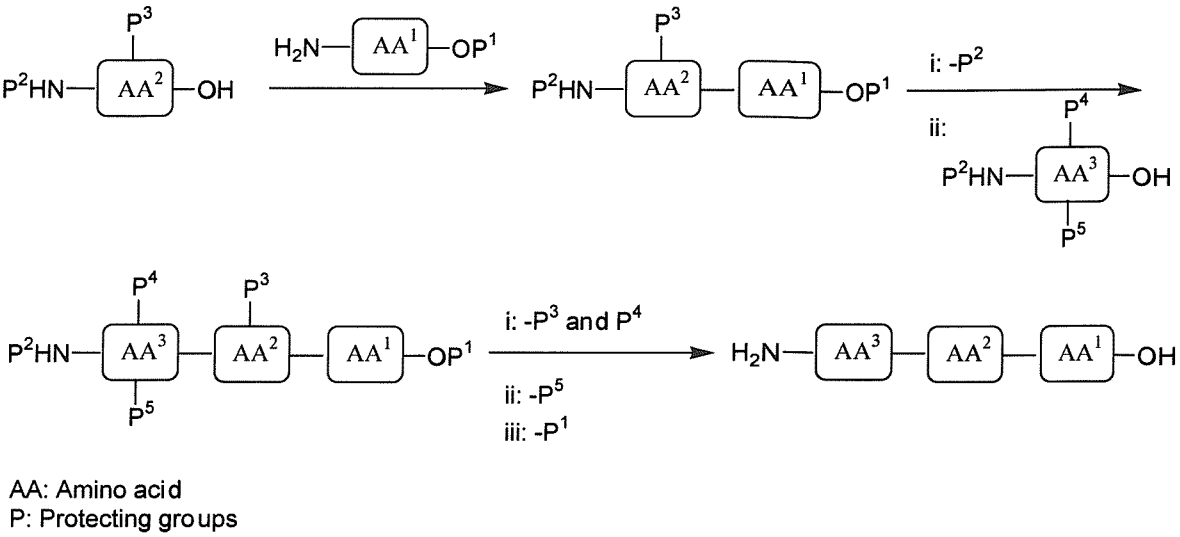

Scheme 4.1: Principle of peptide synthesis.

4.1.2 Synthesis in solution

An important part of the synthesis of cyclic peptides in solution has been the total synthesis of natural products and analogues. Among the three main methods of cyclisation, sidechain-to-sidechain, sidechain-to-backbone and head-to-tail, the last has been investigated most extensively. The most convenient and straightforward strategy is macrocyclisation of linear precursors activated on the carboxy terminal group. Several strategies are available such as activation to the acid chloride, symmetrical and unsymmetrical anhydrides. The chemist has an arsenal of activating reagents: DCC and DIC being the most common examples. However, these reagents lead to the racemisation via oxazolone formation. To overcome this loss of chirality the addition of HOBT, or similar compounds, is used in order to reduce the formation of the oxazolone intermediate.

However, the solution phase approach suffers from limitation since cyclisation must be performed under high dilution conditions to prevent intermolecular oligomerisations, and the expected cyclic peptide must be extracted from the complex reaction mixture,

where unreacted starting materials and activating agents can still be present. Solid phase synthesis is a convenient method to overcome these drawbacks.

4.1.3 Synthesis on solid supports

The concept of using a solid support to perform peptide synthesis (SPPS) was first reported by Merrifield in 1963.[253] Since this date the field has been widely investigated and the preparation of numerous peptides and small proteins has become possible. The method has been successfully applied to the preparation of cyclic peptides. One approach to the formation of immobilised cyclisation precursors is to commence peptide synthesis with an amino acid that has been anchored via its side chain (in bold on Scheme 4.2) to a linker on a resin, then subsequent steps require deprotection of the amino terminal group of the growing peptide followed by activation of the carboxy terminal group of the amino acid. A linker is defined as a bifunctional spacer that serves to attach the initial residue to the solid support. One end of the linker incorporates features of a smoothly cleavable protecting group, and the other end allows facile coupling to a previously functionalised support.

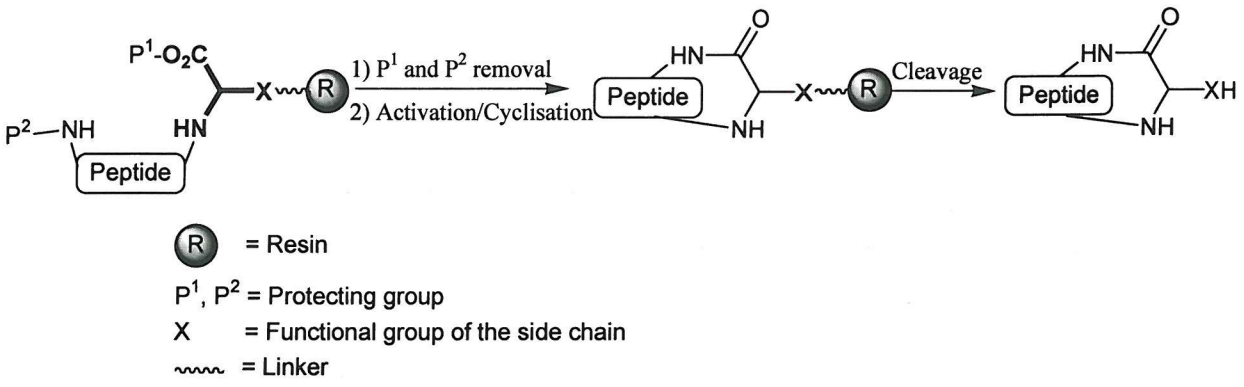

Scheme 4.2: Peptide cyclisation using an amino acid side chain anchored to the solid support via a linker.

Several amino acids (Asp, Glu, Asn, etc.) have been used for head-to-tail cyclisation.[254] The phenolic hydroxy group of tyrosine has also served as a useful point of attachment for certain cyclic peptides. But this approach is obviously limited to those amino acids with reactive side chains. Another approach has been developed for both Boc and Fmoc chemistry by way of a backbone amide linker (BAL) attachment (Scheme 4.3).[255]

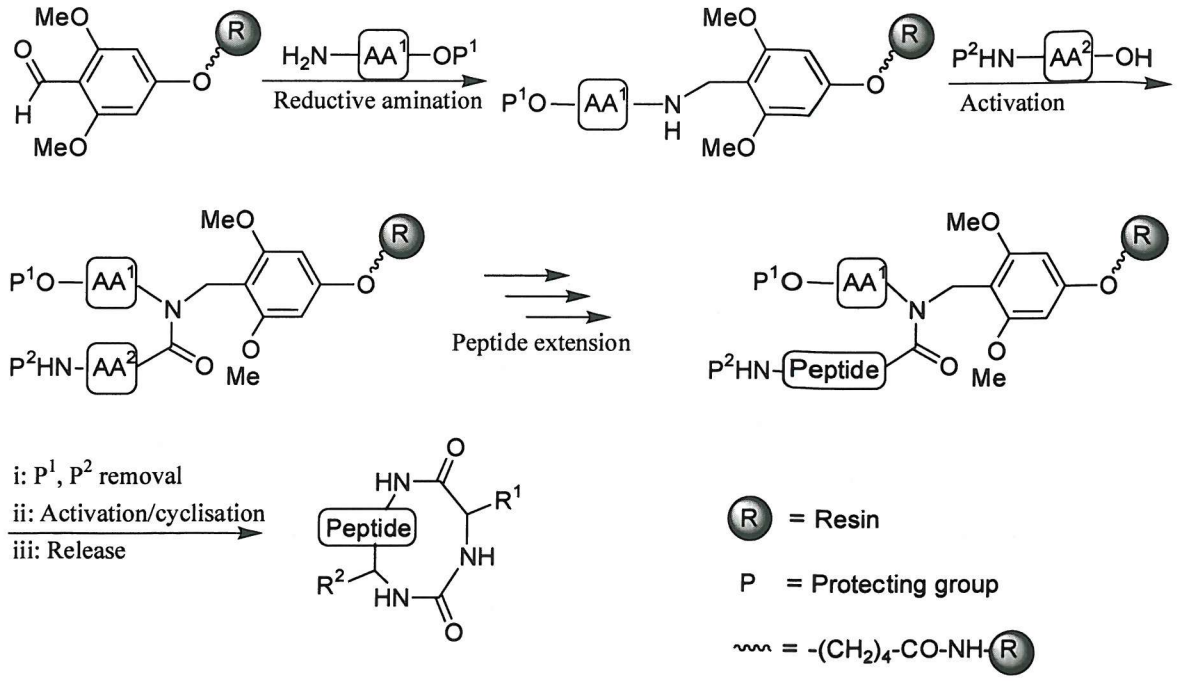

Scheme 4.3: Peptide cyclisation on solid support using a BAL linker.

In this process, the first amino acid AA^1 (usually as a methyl or allyl ester) is introduced by reductive amination of an aromatic aldehyde. Once loaded on the resin, the secondary benzylic amine is acylated with the next amino acid and so on until the linear precursor is assembled. The removal of the protecting group P^1 of the *C*-terminal carboxylate is followed by cyclisation and cleavage to deliver the cyclic peptide. Although many different mechanisms have been used for linker cleavage, for example photolysis, fluoridolysis and base-catalysed β-elimination, the most common method is acid treatment to release the final peptide.

A conceptually different approach to head-to-tail cyclisation is one where the cyclisation and cleavage are intimately connected. Such strategies involve immobilisation of the first amino acid, via its C^{α}-carboxy group, on a specific linker called a "safety-catch" linker. Using this strategy, Yang *et al.* performed the synthesis of cyclic hexapeptide using the Kenner's linker (Scheme 4.4).[256]

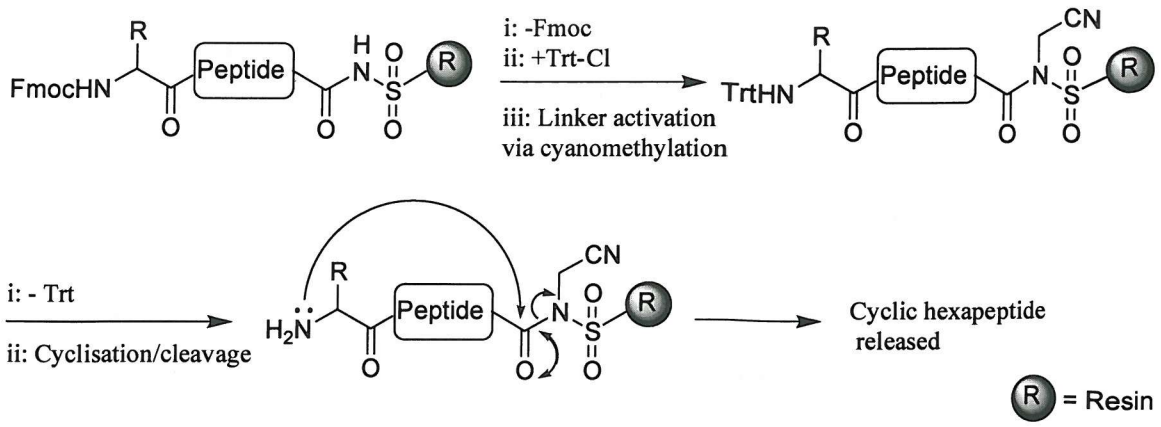

Scheme 4.4: Kenner's safety-catch linker.

This safety-catch sulfonamide linker that is stable to nucleophilic attack until activation, is compatible with Fmoc peptide synthesis. Following assembly of the linear precursors and activation of the linker via cyanomethylation, intramolecular aminolysis of *C*-terminal cyanomethylsulfonamides delivers cyclic peptide products under basic conditions. Similar approaches have been performed via a Kaiser oxime resin attachement[258] and thioester linkages.[257]

More recently, Borne *et al.* reported a different approach with the development for Boc chemistry of a linker bearing an *O*-benzyl (Obn).[249] The activation of the linker relies on the removal of the Obn group as the last step of the linear peptide precursor synthesis to lead to the cyclic peptide by intramolecular aminolysis.

4.1.4 Some reactions used in cyclic peptide synthesis

Many routes have been investigated to obtain chemoselective cyclisation reactions. Aminolysis of the carboxy terminal group of the linear precursor, as previously described, is the most trivial. Another approach reported by Tam *et al.* involves intramolecular transthioesterification by the thiol group of a cysteine residue allowed by ring contraction (Scheme 4.5).[259] It is noteworthy that the linear peptide precursor was used in a unprotected form in relatively high concentration (20 mM).

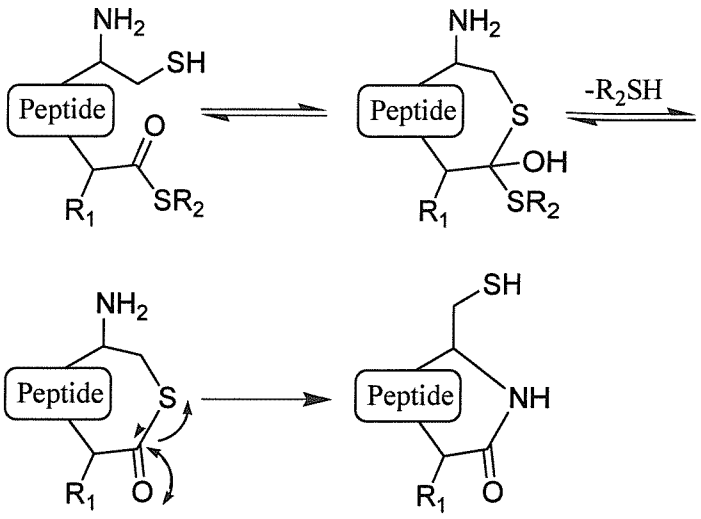

Scheme 4.5: Thiol-mediated cyclisation.

A thiolactone intermediate is generated by a ring-chain equilibrium between the *N*-terminal cysteine and a *C*-terminal thioester which subsequently undergoes an irreversible proximity-driven ring contraction through an *S*- to *N*-acyl migration, resulting in the formation of an amide linked cyclic peptide. Tam adapted this ring contraction to a "thiazip" cyclisation.[260] In this case intermediate states, involving transthioesterification between one or several internal thiols by successive thiol-thiolactone exchanges, lead to the amino lactone that finally underwent irreversible *S*- to *N*-acyl migration.

The obvious drawback of the approach of Tam is the insertion of an *N*-terminal cysteine. To overcome this limitation several approaches have been proposed. For instance, Kent *et al.* have described the use of a removable oxyethanethiol, attached to the α-amine of an *N*-terminal glycine.[261] Thioalkylation reactions have been also successfully used. In a solution approach the thiol of a *C*-terminal cysteine was used to displace an *N*-terminal acetyl bromide[262] or chloride[263] to form a cyclic thioether. The solid phase counterparts of these reactions also yielded the cyclic products, after cleavage of the halogenated linear precursors from the resin followed by cyclisation under basic conditions.[264] The thioether strategy has also been reported to enable cyclisation and cleavage of a linear precursor from the solid support in a one-pot operation.[265]

Another approach widely used is intramolecular disulfide formation. These bridges are present in naturally occurring peptides. The method has several advantages. First of all

disulfides are easy to form under oxidising conditions from the free thiols.[266] The disulfide bonds are also stable at low pH and present a character intermediate between that of a single bond and a partial double bond. In the formation of the disulfide the linear precursor must undergo the deprotection step of the protected cysteine side-chains. Deprotection and oxidation can be performed separately or in "one pot" reaction, the last approach avoids the formation of non-desired regioisomers or polymers (Scheme 4.6).

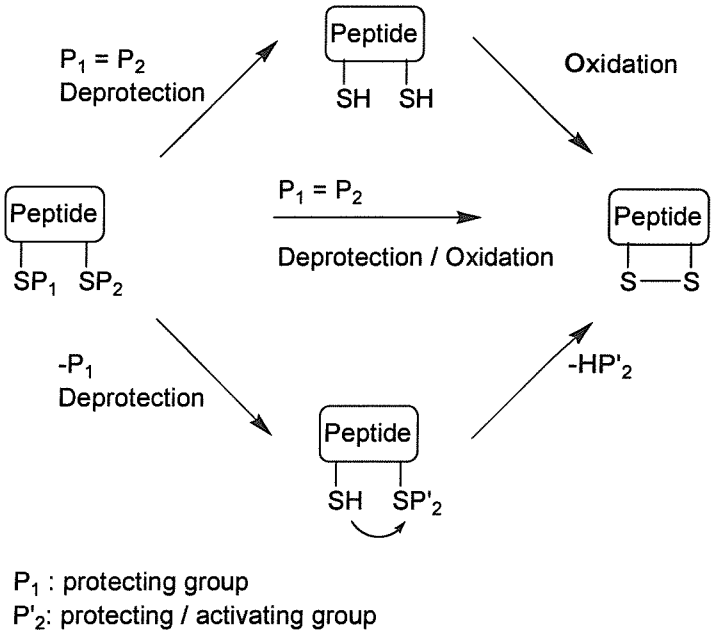

Scheme 4.6: Routes to obtain disulfide bridges.

A third approach for disulfide formation involves a displacement reaction. In this case, one of protecting groups also acts as an activating group to allow the attack of the free sulfhydryls (Scheme 4.6). The preparation of peptides containing multiple disulfide bonds will often require the concomitant use of several of the methods outlined above. A common general approach to the regioselective formation of intramolecular disulfide bridges in the corresponding linear precursor is to protect each pair of cysteine residues with the same group, but to use different protecting groups for different pairs. Disulfide bonds are then specifically formed by staged deprotection and oxidation of pairs of cysteine residues. Numerous synthetic cyclic peptides have been obtained following this

approach such as antamanide mimics, valinomycin analogues and relatively rigid cylindrical α-helical peptides.[266]

One method where the critical ring closure step involves the formation of an ester (lactonisation) has been reported in the work of Ranganathan *et al.* This methodology has been applied to the synthesis of depsipeptides, an important class present in marine natural products.[267-268]

Another common approach in cyclic peptide chemistry relies on oxime formation. The work of Tam and Pallin provides an interesting example of the synthesis of an unprotected linear peptide precursor, generated on a solid support, bearing an *N*-terminal *O*-alkylhydroxylamine and an N^{ε}-lysyl glyoxaldehyde serine, has been reported (Scheme 4.7).[269] Following cleavage and deprotection steps, the *in situ* condensation of the nucleophilic hydroxylamine with the glyoxaldehyde yields the target cyclic oxime.

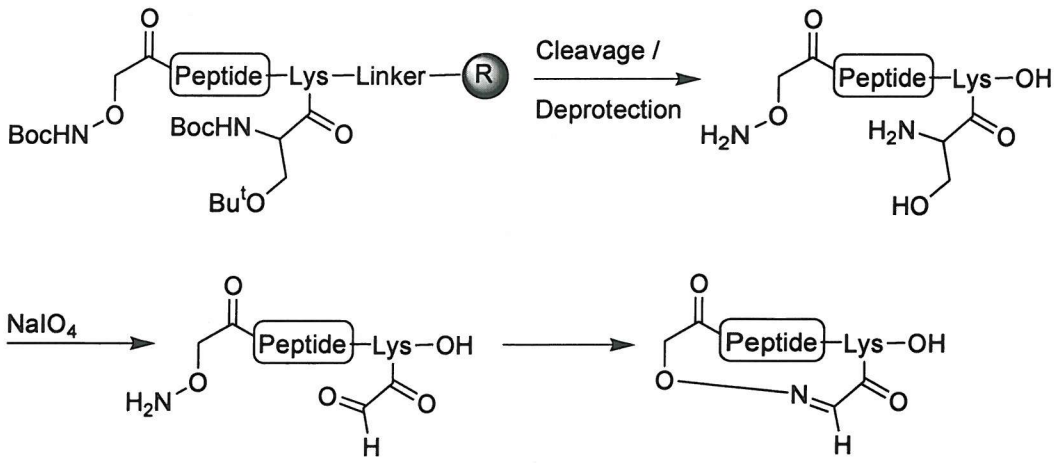

Scheme 4.7: Peptide cyclisation involving oxime bond.

Based on a similar approach cyclic peptide formation via intramolecular thiazolidine bond was also reported where a *N*-terminal cysteine was used instead of the *O*-alkylhydroxylamine.

Finally ring-closing olefin metathesis,[270] nucleophilic aromatic substitution on aromatic[271-272] and Suzuki cross coupling reactions have all been reported to be also efficient methodologies in the synthesis of cyclopeptides.

Based on the observation that some cyclic peptides display metal ion carrier function,[245] it has been suggested that metal ions could facilitate the formation of macrocycles via a templating effect.

4.1.5 Synthesis via templated chemistry

There are three topological classes of templates: interweaving, linear and cyclisation. The classical examples for the interweaving and linear template are catenane synthesis and DNA in replication, respectively. The simplest type of template in the cyclisation category is the metal cation. The range of substrates used for cyclisation is wide. The syntheses of catenanes and rotaxanes have already been mentioned in chapter one. An unexpected application of cyclisation templating is to scavenge cyclisable material in a reaction mixture to promote the formation of linear oligomers. A number of reports have described cyclo-oligomerisation reactions where, when presented in appropriate conditions, simple peptides undergo spontaneous assembly to yield cyclic products. A noteworthy feature of this methodology is the use of unprotected linear precursors. Tam *et al.* have adapted the concept of ring-chain equilibrium[259] for Ag^+ ion-assisted peptide cyclisation, in order to investigate the role of a metal in the enthalpic activation of *C*-terminal carbonyl of the linear precursor (Scheme 4.8).[273]

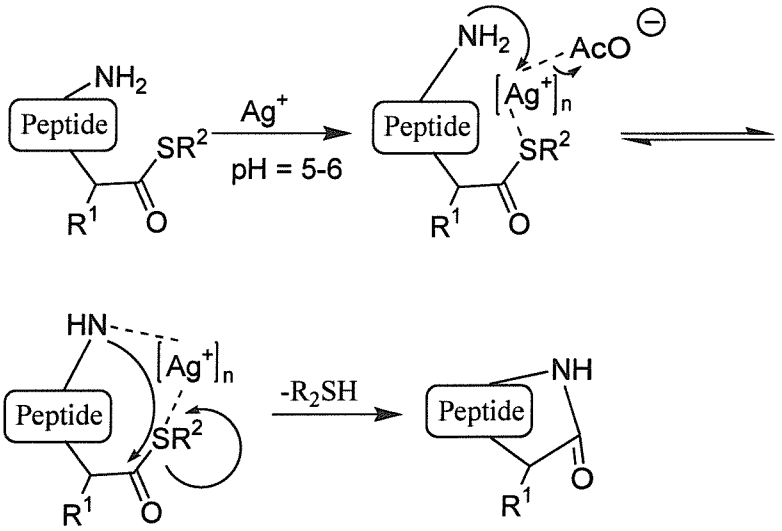

Scheme 4.8: Ring-chain equilibrium templated by metal cation.

The effect of the nature of the metal on the cyclo-oligomerisation process has also been investigated using a series of templates: Li^+, Na^+, K^+, Cs^+, Zn^{2+}.... The *Lissoclinum* family of marine metabolites, which includes a group of heterocyclic rings, was chosen as the target.[274] Depending on the size of the metal template, the product of cyclo-oligomerisation contained three or four motifs of the amino acid thiazole precursor. A

direct relation between the size of the metal, defined as its ionic radius, and the ring size of the cyclic peptide was drawn: the proportion of tetramer being formed increasing with the ionic radius of the metal. Haas and co-workers have reported tetrapeptide synthesis templated by palladium,[275] nickel and copper[276] using non-activated precursors.

In this chapter the principle of the metal cation-assisted cyclo-oligomerisation was applied to a peptide library. By a combinatorial approach, the rate of tetrapeptide synthesis was studied as a function of the chain length and nature of the residues of the linear precursor.

4.2 RESULTS AND DISCUSSION

Using the template approach attempts were made to carry out a cyclo-oligomerisation. To this end the metal Ni^{II} was used as guest in the presence of a series of dipeptides to yield the corresponding cyclic tetrapeptides. The effect of bulky amino acids on a suitable prearrangement around the metal template for cyclisation was investigated. The flexibility was also investigated by different chain lengths. The amino acids used in the synthesis of dipeptides had no reactive side chains to minimise the side coupling reactions.

4.2.1 Solution phase dipeptide synthesis

Three amino acids were used as starting materials for the synthesis of the dipeptide library: β-Alanine (H-βAla-OH), 4-Aminobutyric acid (H-γAba-OH) and 6-Aminocaproic acid (H-εAhx-OH). These amino acids were converted by activation of the carboxylic acid group with thionyl chloride in methanol into the respective amino acid methyl ester HCl salt derivatives **(16)**, **(17)** and **(18)** (Scheme 4.9).[277]

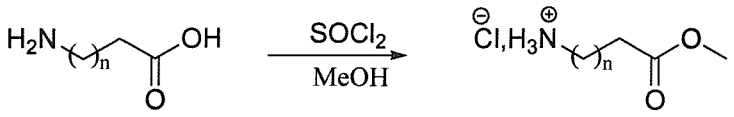

n = 1: H-βAla-OMe, HCl **(16)**
2: H-γAbu-OMe, HCl **(17)**
4: H-εAhx-OMe, HCl **(18)**

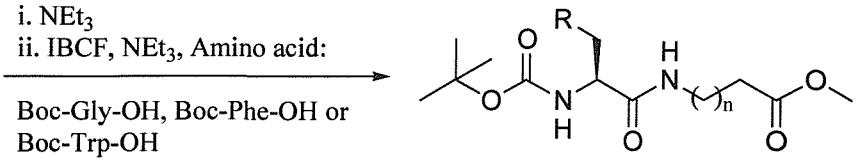

	(16)	**(17)**	**(18)**
Boc-Gly-OH	Boc-Gly-βAla-OMe **(19)**	Boc-Gly-γAbu-OMe **(20)**	Boc-Gly-εAhx-OMe **(21)**
Boc-Phe-OH	Boc-Phe-βAla-OMe **(22)**	Boc-Phe-γAbu-OMe **(23)**	not cross-reacted
Boc-Trp-OH	Boc-Trp-βAla-OMe **(24)**	Boc-Trp-γAbu-OMe **(25)**	Boc-Trp-εAhx-OMe **(26)**

Scheme 4.9: Synthesis of the dipeptide library.

Each salt was neutralised and reacted with an activated carboxylic acid group using isobutyl chloroformate (IBCF) to give the Boc protected dipeptides **(19 – 26))** (Scheme 4.9). The ^{t}butyl carabamate was cleaved from the dipeptides using trifluoroacetic acid (TFA) (8 eq.) in DCM to give the expected dipeptide TFA salts **(27 – 34)** (Table 4.1).

	n = 1	n = 2	n = 4
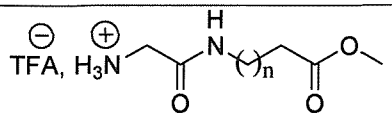	**(27)** (88%)	**(28)** (66%)	**(29)** (40%)
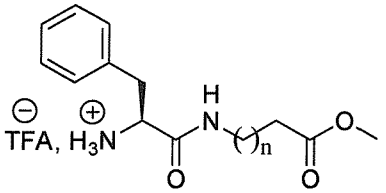	**(30)** (71%)	**(31)** (58%)	Not synthesised
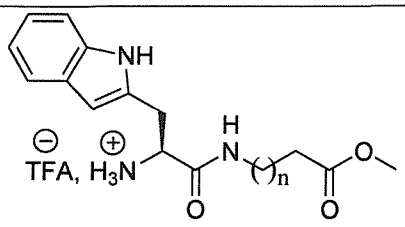	**(32)** (26%)	**(33)** (65%)	**(34)** (30%)

Table 4.1: Yield of the linear dipeptides synthesised in solution phase.

The compounds **(27)** to **(29)** were purified by precipitation from cold ether. The dipeptides containing phenylalanine and tryptophan were purified by semi-preparative HPLC.

4.2.2 Solid phase dipeptide synthesis

A similar dipeptide library as above was prepared on both hydroxymethyl Polystyrene and Quadra Gel resins. The latter was expected to show better swellability properties in MeOH, the solvent used for the head-to-tail coupling reactions (see later in chapter). The hydroxymethyl groups of the polymeric matrix were acylated with Fmoc-βAla-OH following a standard DIPEA / oxalyl chloride coupling method. The difference compared with usual solid phase chemistry is that in this case no linker was used between the resin and the amino acid. The *N*-terminal Fmoc protecting group of the amino acid was removed using a 20% piperidine / DMF solution to yield after washing with DMF and DCM the resins **(54)** and **(55)** (Scheme 4.10).

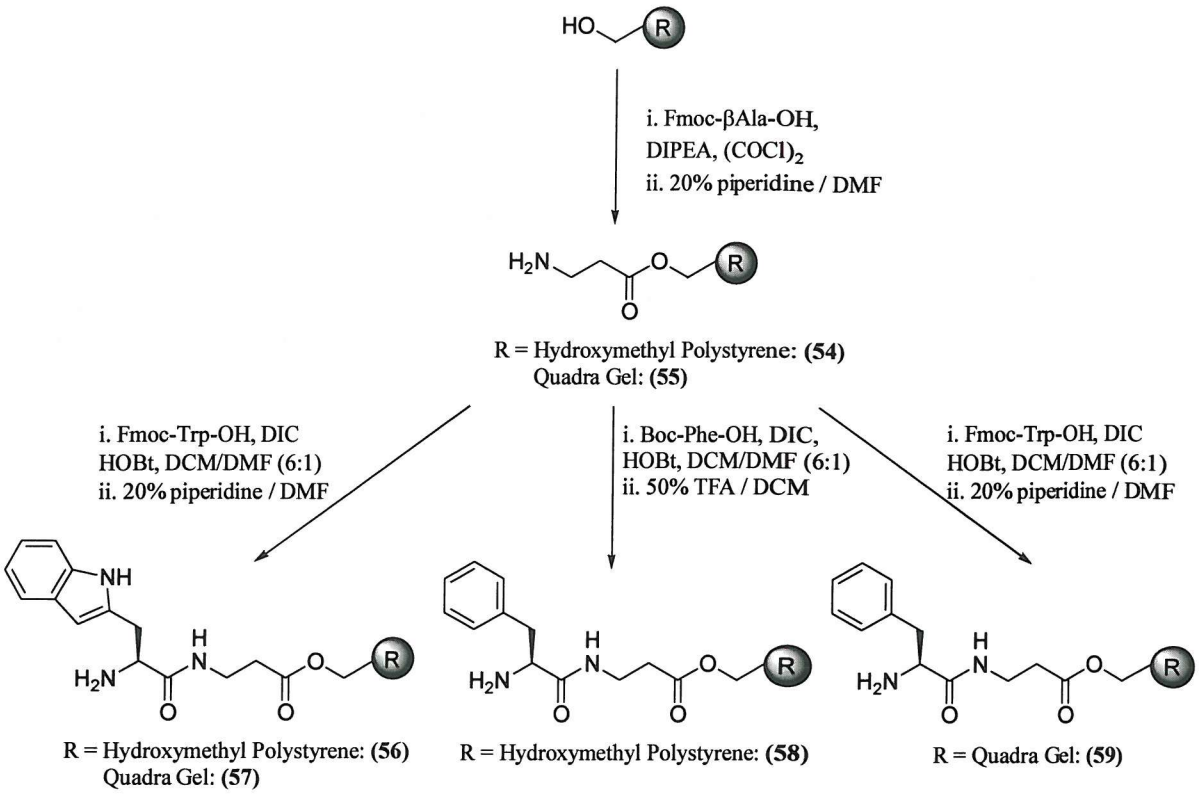

Scheme 4.10: Dipeptide synthesis on solid support.

A series of linear dipeptides was synthesised on the resins **(54)** and **(55)** using Fmoc-Trp-OH and Fmoc or Boc protected Phe-OH. The protecting groups were cleaved from the dipeptides using either 20% piperidne / DMF or 50% TFA / DCM to give quantitatively the resins **(56)** to **(59)** (Scheme 4.10).

4.2.3 Attempted cyclo-oligomerisation in solution around Ni^{II} template

In the first set of experiments each dipeptide (H-Gly-βAla-OMe **(27)**, H-Gly-γAbu-OMe **(28)** and H-Gly-εAhx-OMe **(29)**) was allowed to react with itself in the presence of a metal template ($NiCl_2 \cdot 6H_2O$), in a methanolic solution of sodium methoxide (NaOMe), to give only one type of tetrapeptide. Unfortunately the products of the coupling reaction were not observed by the UV detector of the HPLC due to the absence of any strong chromophore. Hass reported a procedure to collect the cyclic tetrapeptides as crystalline solids by the addition of a counter cation and water.[276] The work-up with the cation Bis(triphenylphosphoranylidene) ammonium chloride ([PPN]Cl) led to the

cyclic tetrapeptide as crystalline structure only for the reaction performed with H-Gly-βAla-OMe **(27)** as reported in literature.[276]

To overcome the lack of chromophore the experiment was repeated with the dipeptide H-Trp-βAla-OMe **(32)** bearing an aromatic ring. By HPLC monitoring, 10 minutes after the beginning of the reaction, a new compound was observed with a retention time of 7.4 min that slowly disappeared showing this intermediate was consumed, giving another product observed at a retention time of 7.0 min. The compound at 7.4 min showed surprisingly after HPLC purification a new retention time at 7.0 min.

According to the scheme 4.11, after prearrangement of the dipeptides around the metal template, nucleophilic attack of a co-ordinated terminal amino group onto the carbonyl group of a neighbouring dipeptide was anticipated.

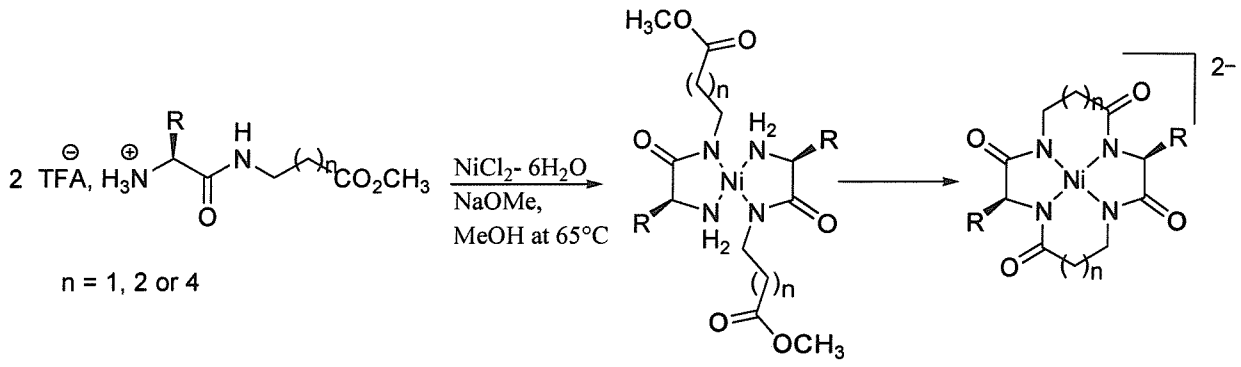

Scheme 4.11: Expected peptide cyclisation mechanism.[276]

However, NMR spectrometry for the product of the cyclisation reaction of the dipeptide H-Trp-βAla-OMe **(32)** on itself gave two distinct signals for the chiral carbons although only one was expected for the symmetric product. It was first thought that it was due to an effect of the flexibility of the macrocycle structure. NMR studies at high temperatures were performed but still showed two distinct chiral carbons. This suggested that the peptide formed was not symmetrical and that in fact only a single peptide bond was formed and no macrocyclisation occurred. Mass spectra confirmed that the intermediate obtained during the reaction was the linear methyl ester tetrapeptides H-Trp-βAla-Trp-βAla-Ome **(35)** (R_T = 7.4 min) and the hydrolysed derivatives H-Trp-βAla-Trp-βAla-OH **(36)** (R_T = 7 min) (Table 4.2). The intermediate

tetrapeptide **(35)** was not isolated due to its instability during the HPLC purification (hydrolysed to **(36)**).

	Tetrapeptide (Retention time: min)	Purity (%, λ = 220 nm) after:					
		10 min	30 min	1h	2h	3h	20h
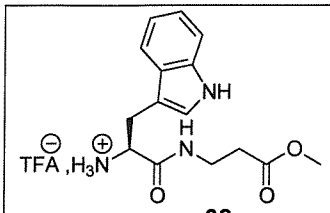 **32**	H-Trp-βAla-Trp-βAla-OMe **(35)** (7.4)	58	58	56	78	51	42
	H-Trp-βAla-Trp-βAla-OH **(36)** (7.0)	0	7	8	21	25	51

Table 4.2: Purities (%) of tetrapeptides obtained during the reaction.

Attempts to force the reaction to completion, i.e. to form the cyclic peptide, by the addition of metal template and base failed. The use of a microwave synthesiser (Personal Chemistry®) also did not give the expected compound. Reflux of the reaction seemed to be an important factor since a sample of H-Trp-βAla-OMe **(32)** left for 30 minutes at room temperature did not give formation of H-Trp-βAla-Trp-βAla-OMe **(35)**. However at 65°C the solution turned orange in a few minutes due to the oxidation of the metal template by complexation with the dipeptides and the linear tetrapeptide **(35)** was observed by HPLC monitoring. It is also noteworthy that the cyclisation reactions involving H-Trp-βAla-OMe **(32)** carried out without metal template failed to yield the linear tetrapeptide. Thus, surprisingly the template was required to bring close together two molecules of dipeptide to synthesise one peptide bond but, unexpectedly the second one, leading to the macrocyclic compound, did not occur. The formation of a macrocyclic tetrapeptide from two dipeptides is disfavoured entropically and might prevent cyclo-oligomerisation. It was also reported that the cyclisations can be correlated with the ionic radii of the metals[276]: Ni^{II} could be too small (ionic radius 63 pm) to bring close together the ends of the linear tetrapeptide. A steric hindrance of the dipeptide precursors could also be mentioned.

Another observation made was that no linear polymerisation was observed in the presence of the metal template.

The use of chromophoric dipeptides was then extended to H-Phe-βAla-OMe **(30)**, H-Trp-γAbu-OMe **(33)** and H-Trp-εAhx-OMe **(34)**.

The results obtained with the dipeptide H-Phe-βAla-OMe **(30)** were similar to H-Trp-βAla-OMe **(32)**. A peak with a retention time of 7.2 min was observed 10 minutes after the beginning of the reaction and identified by mass spectroscopy as the linear tetrapeptide H-Phe-βAla-Phe-βAla-OMe **(46)** (Table 4.3). This tetrapeptide, which formed only in the presence of the metal template, was hydrolysed into the derivative H-Phe-βAla-Phe-βAla-OH **(47)**.

	Tetrapeptide (Retention time: min)	Purity (%, λ = 220 nm) after:					
		10 min	30 min	1h	2h	3h	7h
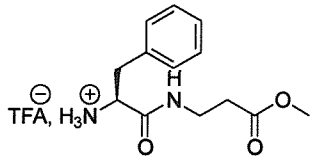 **30**	H-Phe-βAla-Phe-βAla-OMe **(46)** (7.2)	67	100	100	100	100	nd
	H-Phe-βAla-Phe-βAla-OH **(47)** (6.2)	Obtained after HPLC purification					
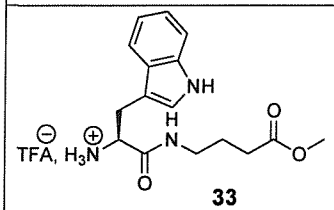 **33**	H-Trp-γAbu-Trp-γAbu-OMe **(45)** (7.5 min)	0	0	0	17	20	30

Table 4.3: Purities (%) of tetrapeptides obtained during the reaction (nd: not determined).

The dipeptide H-Trp-γAbu-OMe **(33)** gave also similar result as above with first the formation, in the presence of metal template, of the tetrapeptide H-Trp-γAbu-Trp-γAbu-OMe **(45)** (7.5 min) yielding slowly a compound at 7 minutes not identified by mass spectra but assumed to be the hydrolysed tetrapeptide (Table 4.3). The tetrapeptide formation with the dipeptide **(33)** seemed to be slower than for the previous dipeptides since after one hour **(33)** was still present in the solution. Finally for the dipeptide H-Trp-εAhx-OMe **(34)** no reaction occurred. From these experiments it was concluded that short tetrapeptide synthesis was favoured.

4.2.4 Crossed reactions between dipeptides with and without aromatic rings

The effect of the bulkiness of the amino acid on peptide coupling was investigated by mixing two different dipeptides in an equimolar ratio, under the same conditions as previously described, to generate a potential library of tetrapeptides bearing different residues. Three peaks by HPLC were expected: two for the product of reaction between same species (H-aa^1-aa^2-aa^1-aa^2-OMe and H-aa^3-aa^4-aa^3-aa^4-OMe), and a single peak corresponding to two products (H-aa^1-aa^2-aa^3-aa^4-OMe and H-aa^3-aa^4-aa^1-aa^2-OMe). The linear tetrapeptides obtained in the previous library were used as standards to identify the species formed in these crossed coupling reactions.

First of all H-Trp-βAla-OMe **(32)** was treated with the dipeptide H-Gly-βAla-OMe **(27)**. It was observed by HPLC that the mixed tetrapeptide H-Trp-βAla-Gly-βAla-OMe **(38)** was formed more quickly than H-Trp-βAla-Trp-βAla-OMe **(35)**. To be compared with intensity of the peak for **(38)**, H-Trp-βAla-Trp-βAla-OMe **(35)** must be divided by two since this tetrapeptide contained two aromatic rings. Therefore **(38)** should have a rate of formation two fold higher than **(35),** which was confirmed by the ELS detector (Table 4.4).

	H-Trp-βAla-OMe **(32)** (retention time: min)	Purity (%, λ = 220 nm) after:			
		10 min	30 min	2h	21h
H-Gly-βAla-OMe **(27)**	H-Trp-βAla-Trp-βAla-OMe **(35)** (7.4)	14	16	14	12
	H-Trp-βAla-Gly-βAla-OMe **(38)** (5.9)	32	34	23	23

Table 4.4: Dipeptide obtained during crossed coupling reaction. The tetrapeptide H-Gly-βAla-Gly-βAla-OMe was not observed by HPLC due to the lack of chromophore.

The favoured formation of tetrapeptides containing only one Trp-βAla motif was confirmed with cross-coupling reactions between the dipeptide H-Trp-βAla-OMe **(32)** and the dipeptides H-Gly-γAbu-OMe **(28)** and H-Gly-εAhx-OMe **(29)** (Table 4.5). The derivative H-Trp-βAla-Gly-εAhx-OH **(44)** was observed during reaction.

	H-Trp-βAla-OMe **(32)** (retention time: min)	Purity (%, λ = 220 nm) after:					
		10 min	30 min	1h	2h	5h	21h
H-Gly-γAbu-OMe **(28)**	H-Trp-βAla-Trp-βAla-OMe **(35)** (7.4)	19	19	18	15	15	12
	H-Trp-βAla-Gly-γAbu-OMe **(41)** (6.2)	35	37	36	32	33	26
H-Gly-εAhx-OMe **(29)**	H-Trp-βAla-Trp-βAla-OMe **(35)** (7.4)	17	17	18	17	15	10
	H-Trp-βAla-Gly-εAhx-OMe **(43)** (6.7)	37	38	40	38	37	27

Table 4.5: Dipeptides obtained during crossed coupling reactions. Tetrapeptides H-Gly-γAbu-Gly-γAbu-OMe and H-Gly-εAhx-Gly-εAhx-OMe were not observed due to the lack of chromophore.

When the intensity of the peaks for H-Trp-βAla-Gly-βAla-OMe **(38)**, H-Trp-βAla-Gly-γAbu-OMe **(41)** and H-Trp-βAla-Gly-εAhx-OMe **(43)** were compared after ten minutes, similar values were obtained (Tables 4.4 and 4.5). The chain length did not affect the rate of the linear tetrapeptide synthesis.

In similar cross-reactions involving H-Phe-βAla-OMe **(30)** it was also observed that tetrapeptides H-Phe-βAla-Gly-βAla-OMe **(48)**, H-Phe-βAla-Gly-γAbu-OMe **(51)** and H-Phe-βAla-Gly-εAhx-OMe **(53)** were synthesised more quickly than H-Phe-βAla-Phe-βAla-OMe **(46)**. It was deduced from this series of experiments that the synthesis of the less bulky tetrapeptide was favoured.

4.2.5 Crossed coupling reactions in solution between two bulky dipeptides

4.2.5.a Dipeptides with the same bulky group

In the previous series of experiments the cross-coupling reactions seemed to be controlled by the presence of the bulky group (indole or phenyl) on one or both dipeptides, rather than by the chain length. The effect of the chain length was therefore investigated in a cross-coupling reaction involving two dipeptides bearing the same bulky group (indole); H-Trp-βAla-OMe **(32)** and H-Trp-γAbu-OMe **(33)**. 30 minutes after the beginning of the reaction it was observed that the dipeptide **(32)** has been consumed while **(33)** was still present and that the tetrapeptides, identified as H-Trp-

βAla-Trp-βAla-OMe **(35)** and H-Trp-βAla-Trp-γAbu-OMe **(39)**, were present in the same proportion (Spectra 4.1).

a) at t = 0

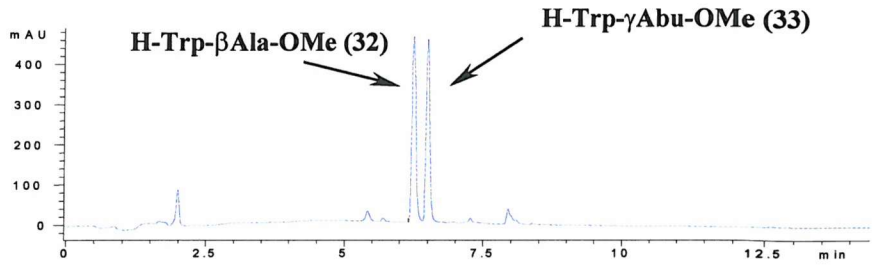

b) at t = 10 min

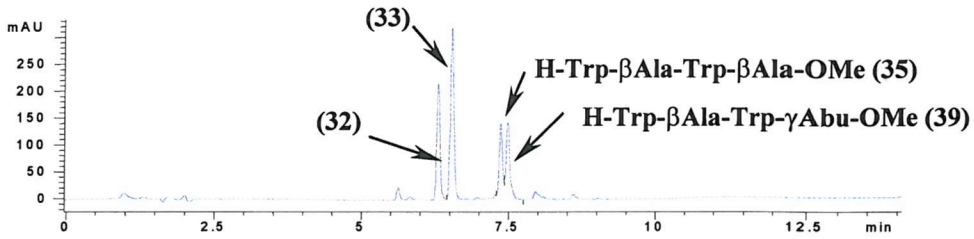

c) at t = 30 min

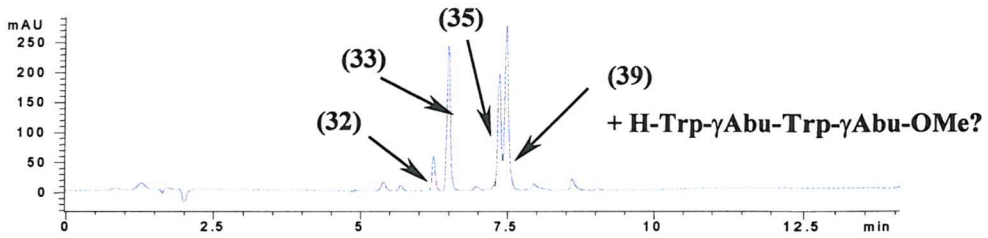

f) at t = 5 h

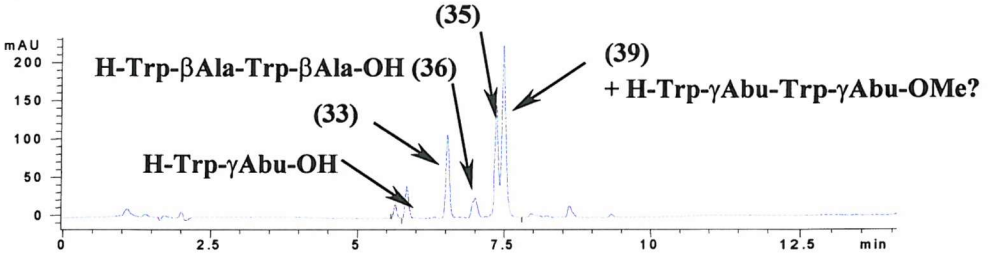

*Spectra 4.1: HPLC monitoring of cross-coupling reactions between H-Trp-βAla-OMe **(32)** and H-Trp-γAbu-OMe **(33)** (λ = 220 nm).*

Thus dipeptide H-Trp-βAla-OMe **(32)** reacted more quickly than H-Trp-γAbu-OMe **(33)**, and **(32)** reacted faster on it self than on **(33)**.

The reaction between H-Trp-βAla-OMe **(32)** and H-Trp-εAhx-OMe **(34)** led to H-Trp-βAla-Trp-βAla-OMe **(35)** and H-Trp-βAla-Trp-εAhx-OMe **(42)** (H-Trp-εAhx-Trp-εAhx-OMe was not observed consistent with earlier results (section 4.2.3)). Similarly H-Phe-βAla-OMe **(30)** and H-Phe-γAbu-OMe **(31)**, gave the tetrapeptides H-Phe-βAla-Phe-βAla-OMe **(46)** and H-Phe-βAla-Phe-γAbu-OMe **(49)**, while the tetrapeptide H-Phe-γAbu-Phe-γAbu-OMe was not observed. It was deduced from these results that from dipeptides with similar bulky groups, the synthesis of the shorter tetrapeptide was favoured.

4.2.5.b Dipeptides bearing different bulky side chains

In the previous experiments it was demonstrated that when two dipeptides bearing the same bulky group were mixed the shorter tetrapeptide was preferentially synthesised. The coupling reaction between H-Phe-βAla-OMe **(30)** and H-Trp-βAla-OMe **(32)** (same chain length but different bulky groups) was then investigated. Since tetrapeptides synthesised during the cross-coupling reactions bore different chromophores (indole and phenyl), analysis by UV detector could distort the results. The physical properties could also change preventing a reliable use of ELS detector. For these reasons the study relied on the rate of consumption of starting materials. The dipeptide H-Phe-βAla-OMe **(30)** was consumed faster (in 10 minutes) than H-Trp-βAla-OMe **(32)** (30 min), suggesting that a small aromatic ring favours the prearrangement of the species around the metal template (by decreasing steric hindrance) to give H-Trp-βAla-Trp-βAla-OMe **(35)** (30%), H-Trp-βAla-Phe-βAla-OMe **(37)** (16%) and H-Phe-βAla-Phe-βAla-OMe **(46)** (15%).

Dipeptides with different chain lengths and bulky groups were mixed together. First of all H-Phe-βAla-OMe **(30)** (short chain length and small bulky group) was reacted with H-Trp-γAbu-OMe **(33)** and yielded H-Trp-γAbu-Trp-γAbu-OMe **(45)** (3%), H-Phe-βAla-Phe-βAla-OMe **(46)** (9%) and H-Phe-βAla-Trp-γAbu-OMe **(50)** (30%). After ten minutes **(30)** was no longer observed, while **(33)** was still present after thirty minutes, suggesting once again that small and little unhindered dipeptides can react quickly. The coupling involving H-Trp-εAhx-OMe **(34)**, instead of H-Trp-γAbu-OMe **(33)**, confirmed this observation, while the dipeptide **(34)** was still present in solution after 5

hours. As expected, only two tetrapeptide were synthesised, H-Phe-βAla-Phe-βAla-OMe **(46)** and H-Phe-βAla-Trp-εAhx-OMe **(52)**, while H-Trp-εAhx-OMe **(34)** did not react with itself.

The coupling between the short bulky petdide H-Trp-βAla-OMe **(32)** and the longer but less hindered H-Phe-γAbu-OMe **(31)** also gave the same conclusions.

It was concluded from these experiments that from dipeptides with different chain lengths and bulky groups, the synthesis of the shorter and less hindered tetrapeptide was favoured.

4.2.6 Attempted cyclo-oligomerisation on the solid phase using a Ni^{II} template

The assay of peptide cyclisation was extended to the coupling between a dipeptide in solution and another attached to a resin. The expected reaction mechanism is described in Scheme 4.12.

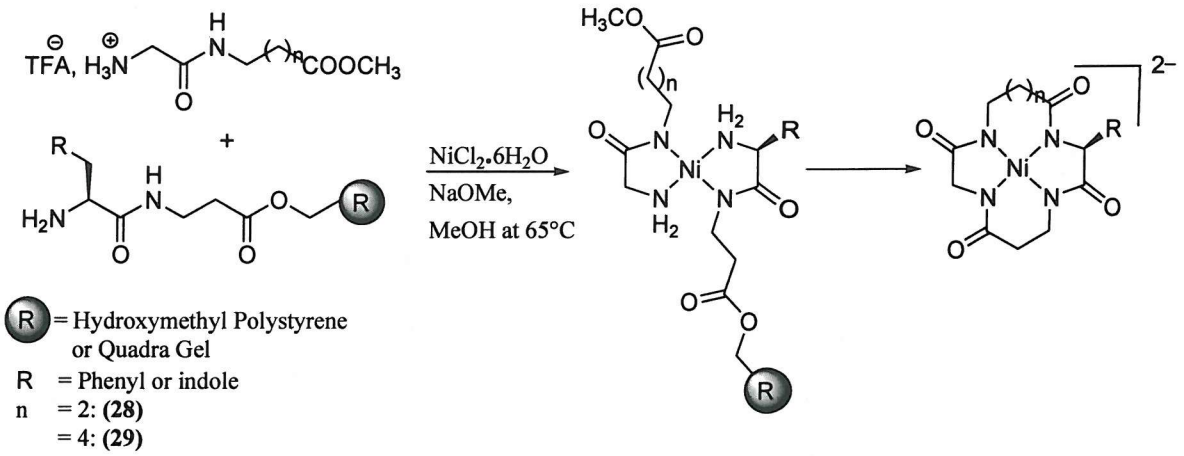

Scheme 4.12: Expected peptide cyclisation mechanism between a dipeptide in solution and one loaded on solid support.

To minimise intermolecular reactions between species in solution, it was decided to use dipeptides with long chain lengths such as H-Gly-γAbu-OMe **(28)** and H-Gly-εAhx-OMe **(29)**. To identify easily the tetrapeptide synthesised, the beads were loaded with dipeptides bearing chromophores: H-Trp-βAla-OResin and H-Phe-βAla-OResin. Two resins, hydroxymethyl Polystyrene and Quadra Gel, were investigated due to their

different swelling properties. The reactivity of resin bound functional groups depends on the resin swelling in a given solvent. MeOH, the solvent used in these coupling reactions, has little swelling effect on the hydroxymethyl Polystyrene resin. Quadra Gel resin that presents a better swellability in MeOH was used to overcome this problem.

In the first experiment an equimolar mixture of H-Gly-γAbu-OMe **(28)** and H-Trp-βAla-OResin (Quadra Gel) **(57)** was reacted with a metal salt template ($NiCl_2 \cdot 6H_2O$) in a methanolic solution of sodium methoxide (NaOMe) at 65°C for four days. During the reaction, HPLC monitoring showed no trace of the expected H-Trp-βAla-Gly-γAbu-OMe **(26)**, and no cyclic tetrapeptide. After filtration of the resin beads, NMR data of the solution confirmed the presence of an aromatic compound with broad signals between 6.5 and 8 ppm. IR monitoring of the beads also confirmed the release of the dipeptide.

The same results were obtained when the experiment was repeated with H-Phe-βAla-OResin **(58)** and H-Gly-εAhx-OMe **(29)** instead of **(28)**, and also when the reactions were extended to H-Phe-βAla-OResins **(58)** and **(59)** reacting with H-Gly-γAbu-OMe **(28)** and H-Gly-εAhx-OMe **(29)**.

When the coupling reaction was performed between H-Gly-εAhx-OMe **(29)** and Polystyrene resin **(56)**, tetrapeptides were observed after 2 hours and assigned by mass spectrometry to H-Trp-βAla-Gly-εAhx-OMe **(43)** and H-Trp-βAla-Trp-βAla-OH **(36)**. The presence of dipeptide **(43)** in solution suggested a nucleophilic attack of the terminal amino group of the glycine onto the carbonyl group of the β-Alanine attached to the resin, cleaving the tetrapeptide from the solid support. The coupling mechanism between two dipeptides "H-Trp-βAla" loaded onto the resin to give the tetrapeptide H-Trp-βAla-Trp-βAla-OH **(36)** was less obvious (Scheme 4.13).

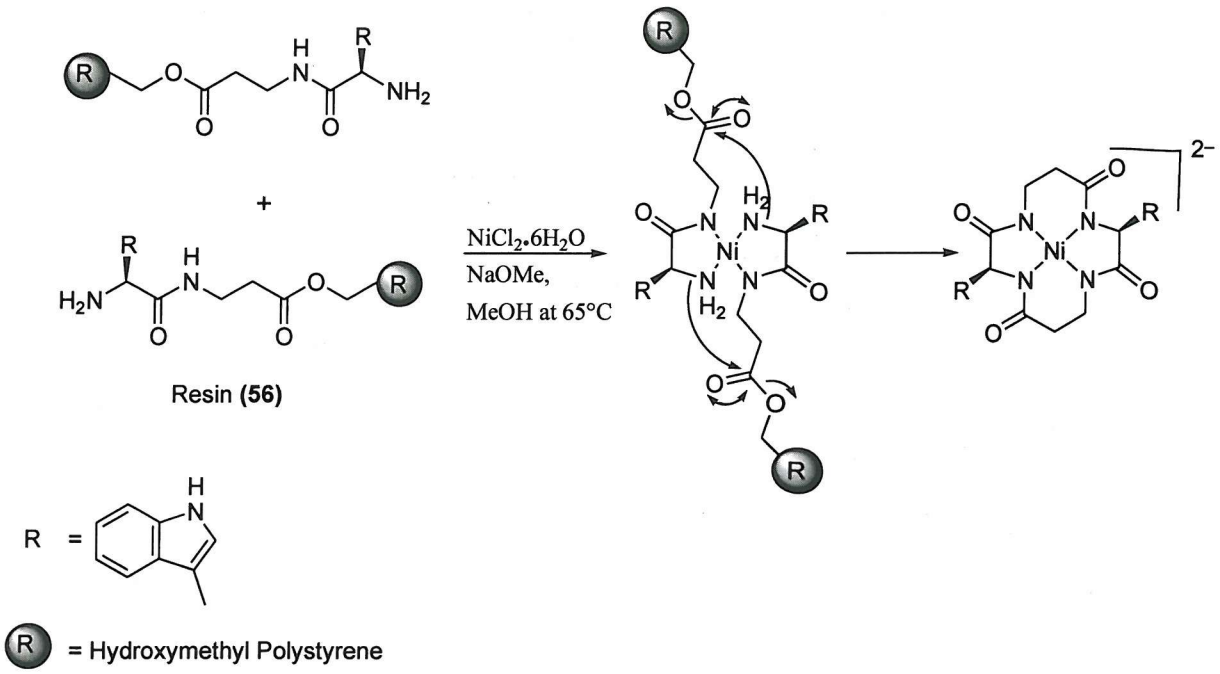

Scheme 4.13: Proposed cyclo-oligomerisation mechanism between dipeptides attached to the resin (56).

In the case of the linear tetrapeptide another cleavage mechanism must have taken place. The explanation was found when a series of reactions was performed to investigate the role of the metal template.

The coupling between H-Trp-βAla-OResin (hydroxymethyl Polystyrene) **(56)** and H-Trp-γAbu-OMe **(33)** in the presence, or not, of metal template was performed. Surprisingly, in both conditions the presence of H-Trp-βAla-OMe **(32)** was observed by HPLC monitoring and confirmed by mass spectroscopy. In absence of metal no linear tetrapeptide was observed but the presence of the cation metal yielded Trp-βAla-Trp-βAla-OMe **(35)** and Trp-βAla-Trp-βAla-OH **(36)**. The dipeptide loaded on the resin was cleaved by hydrolysis of the ester bound in the presence of the base in solution (NaOMe) to yield H-Trp-βAla-OMe **(32)**. The coupling was then performed in solution as described in section 4.2.3, the metal playing no role in the cleavage step but only in the prearrangement of the dipeptides. This mechanism explains also the formation of the dipeptide H-Trp-βAla-Trp-βAla-OH **(36)** reported above.

4.3 CONCLUSION

A library of dipeptides, in solution and on solid support, was successfully synthesised to investigate the effect of the chain length and the bulkiness of the dipeptide on the cyclo-oligomerisation rate around a template metal ($NiCl_2 \cdot 6H_2O$). It was concluded that:

- the metal acted as negative template, to prevent the linear polymerisation of the dipeptides and yielded only linear tetrapeptides bringing close together two dipeptides.
- failure to obtain cyclo-oligomerisation could be due to a too small metal template (ionoc radius 63 pm), or could come from steric hindrance of the dipeptide precursors since no bulky dipeptides yield cyclic tetrapeptides.[276]
- linear tetrapeptides with short chain length and small bulky group were formed preferentially.
- the basic conditions (NaOMe) cleaved the dipeptides of the resin to lead to a conventional peptide coupling in solution.

CHAPTER 5: OVERALL CONCLUSION

In this thesis two rather diverse fields of chemistry were brought together: supramolecular and combinatorial chemistry. Lehn defined supramolecular chemistry as the chemistry of the intermolecular bond, resulting from the reversible association by non-covalent bonds, between two or more chemical species. Combinatorial chemistry is a recent approach to organic synthesis by which various compounds (called libraries) can be obtained straightforwardly.

The first aim of this project was the synthesis, by a conventional approach, of several molecular imprinted polymers (MIPs) as chiral stationary phases for HPLC columns, by varying the nature of the porogenic solvent (MeCN, DCM and toluene). The capability of these polymers to resolve enantiomeric mixtures (L- and D-Phe-NHPh) was investigated by HPLC monitoring under different elution conditions (mobile phase composition, flow rate and column size). It was found that:

- the more selective polymer was prepared in toluene as porogenic solvent.
- by changing the nature of the mobile phase the selectivity of the column was modified.
- unexpectedly acetone, commonly used to determine the void volume of columns, interacts with the stationary phase, distorting the selectivity factor assessment.
- the size of the column did not seem to have an effect on resolution while higher flow rates decreased the selectivity value.
- the conventional approach to obtain polymers had serious limitations (time consuming for polymer grinding, problem of back pressure due to polydispersity of the particle shape, etc) for finding quickly the best polymer of the three developed.

The second aim of this project was to investigate an alternative approach to speed-up this process. Libraries of MIPs as thin films were obtained by a combinatorial approach to address the influence of the porogen, the nature and ratio of the functional monomer and the degree of the matrix cross-linking. From the screening of hundreds polymers, it was concluded that:

- the monomer methacrylic acid (MAA) with toluene as porogenic solvent was the best polymerisation mixture for the templates used in the combinatorial

approach, which is consistent with the results obtained by the conventional method (Chapter 2).

- new types of screening (plate reader, mass spectrometry, direct screening from 96-well plates by automated HPLC) were investigated for high throughput assessments but in some cases lack reproducibility limiting their usefulness.

These experiments demonstrated the advantages of the combinatorial chemistry approach, compared with the conventional method, for the design of a large variety of polymers and screening for the best candidate. Nonetheless new screening tools, methods of synthesis, washing, etc. need to be developed.

A third aim of this project was the application of the combinatorial approach to another area of the supramolecular chemistry: metal templated cyclo-oligomerisation of peptides. Synthetic cyclopeptides are an interesting target molecule because of their biological activity. Present methods for the cyclisation of peptides generally require a completely protected peptide precursor, under high dilution conditions to avoid oligomerisation. In this work (Chapter 4) presented the synthesis in a combinatorial manner of a library of dipeptides was explored, in solution and on solid supports, in order to investigate the effect of the chain length and the bulkiness of the dipeptide on the cyclo-oligomerisation rate around a template metal ion ($NiCl_2 \cdot 6H_2O$). It was concluded that:

- the metal ion acted as negative template, preventing the linear polymerisation of the dipeptides and yielding only linear tetrapeptides.
- the failure to obtain cyclo-oligomerisation could be due to a too small metal template (ionic radius 63 pm), or to steric hindrance of the dipeptide precursors since no bulky dipeptides yielded cyclic tetrapeptides.[276]
- linear tetrapeptides with short chain lengths and small bulky groups were formed preferentially.
- the basic conditions (NaOMe) cleaved the dipeptides from the resin resulting in conventional peptide coupling in solution.

CHAPTER 6: EXPERIMENTAL

6.1 General Information

NMR spectra were recorded using a Bruker AC300 spectrometer operating at 300 MHz for ^{1}H and 75.5 MHz for ^{13}C, a Bruker DPX 400 spectrometer operating at 400 MHz for ^{1}H and 100 MHz for ^{13}C (δ scale in parts per million). Coupling constants (J) were measured in Hz.

ESI mass spectra were recorded using a VG platform Quadrupole Electrospray Ionisation mass spectrometer, measuring mono-isotopic masses.

Infra-red spectra were recorded on a BIORAD Golden Gate FTS 135. Samples were run as either neat solids or oils.

Analytical HPLC was carried out on a Hewlett Packard HP 1100 Chemstation, using a Phenomenex C18 prodigy 5 μm (150 mm x 3 mm) column. The conditions were:

Flow: 0.5 mL/min.

A = H_2O (TFA 0.1%); B = MeCN (TFA 0.04%).

T = 0 min, 90% A; t = 10 min, 90% B; t = 15 min, 90% B; t = 20 min, 90% A; t = 21 min, 90% A.

Preparative HPLC was carried out on a Hewlett Packard HP 1100 Chemstation with an automated fraction collector using a Phenomenex C_{18} prodigy 5 μm (150 mm x 10 mm) column. The conditions were:

Flow: 2.5 mL/min.

A = H_2O (TFA 0.1%); B = MeCN (TFA 0.04%).

T = 0 min, 100% A; t = 20 min, 100% B; t = 25 min, 100% B; t = 30 min, 100% A.

Monitoring of HPLC columns packed with MIP, and corresponding blanks, was carried out on a Hewlett Packard HP 1090 Chemstation at λ = 260 nm.

Screening of the library of mini-MIPs imprinted with dye labelled template was carried out on microplate reader Benchmark (Bio-rad). The absorbance from each well was recorded at λ = 340 nm.

Aluminium backed silica plates (0.25 mm layer of silica gel 60 with the fluorescent indicator Alugram Sil G/UV_{254}) were used for thin layer chromatography (TLC). UV (254 nm) was used to visualise compounds unless stated otherwise.

All amino acids used were configured L unless stated otherwise.

6.2 General Experimental Procedures

6.2.1 Qualitative ninhydrin test (Kaiser test)[277]

A few of beads of resin were treated in a small test tube with 6 drops of reagent A (described below) and 2 drops of reagent B (described below) and heated at 110°C for 5 min. The blue colour of the beads proved the presence of free amine groups.

Reagent A:

Solution 1 – Reagent grade phenol (40 g) was dissolved in absolute ethanol (10 mL) with warming and then stirred over Amberlite mixed-bed resin MB-3 (4 g) for 45 min. The mixture was then filtered.

Solution 2 – Potassium cyanide (65 mg) was dissolved in water (100 mL). A 2 mL aliquot of this solution was diluted with pyridine (freshly distilled from ninhydrin) and stirred over Amberlite mixed-bed resin MB-3 (4 g). The solution was filtered and mixed with solution 1 to form reagent A.

Reagent B:

Ninhydrin (2.5 g) was dissolved in absolute ethanol (50 mL).

6.2.2 Quantitative Fmoc test[278]

To a known mass (3-5 mg) of dry resin was added a solution of 20% piperidine / DMF (2 mL). The mixture was shaken for 10 min then the solution was filtered through glass wool. The filtrate was diluted to 25 mL with a solution of 20% piperidine / DMF. The absorbance at 302 nm was recorded against a blank (20% piperidine / DMF). The experimental loading was calculated using the following equation:

Substitution (mmol/g) = $(A_{302} \times V) / (\varepsilon_{302} \times W) \times 1000$

A_{302} = absorbance of the piperidyl-fluvene adduct.

V = volume of the volumetric flask.

ε_{302} = extinction coefficient (7800 M^{-1} cm^{-1}).

W = mass of resin (mg).

6.2.3 General procedure for Oxalyl Chloride coupling on solid support

A given mass of dry resin was swollen in DCM in the presence of DIPEA (2.7 eq.). To a Fmoc amino acid (2.7 eq.) dissolved in DCM (40 mL) was slowly added oxalyl

chloride (3.2 eq.) then the reaction was initiated by a few drops of DMF. The solution was stirred for 1 h. Excess oxalyl chloride was removed *in vacuo* and the residue dissolved in DCM (3 mL). The solution was transferred to the resin and the mixture was shaken for 3 days. Finally the resin was filtered, washed with DMF, DCM and MeOH and dried overnight *in vacuo*.

6.2.4 General procedure for DIC / HOBt coupling on solid support

A given mass of dry resin was swollen in DCM. Protected amino acid (3 eq.) was dissolved in a small volume of DCM / DMF (6 / 1) and HOBt (3 eq.) was added followed by DIC (3 eq.) 10 min later. The solution was stirred for 10 min then transferred to the swollen resin shaken for 24 h at RT. The resin was filtered, washed with DCM, DMF and MeOH and dried *in vacuo* overnight.

6.2.5 General procedure for Fmoc cleavage on solid support

To a batch of swollen resin in DMF a solution of 20% piperidine / DMF (1 mL for 5 mg of resin) was added and left to shake for 10 min. The resin was filtered before repeating the procedure then the resin was washed with DMF, DCM and MeOH before drying *in vacuo* overnight.

6.2.6 General procedure for Boc cleavage on solid support

To a batch of swollen resin a solution of DCM / TFA (1/1) was added and shaken for 25 min then the resin was filtered. The procedure was repeated and finally the resin was washed with DCM, 5% DIPEA / DCM and MeOH before drying *in vacuo* overnight.

6.2.7 General procedure for monitoring of imprinted and blank polymers as HPLC stationary phase

The columns were heated at 60°C in column oven and the following solutions used as an isocratic eluent:

A = MeCN-AcOH 5%

B = MeCN-TFA 0.041%

at different ratios as isocratic eluent: 100/0 98/2, 95/5, 90/10, 75/25, 50/50, 0/100.
The flow rate was at 0.3 or 0.5 mL/min.

The column sizes used were: 60 x 4.6 mm, 150 x 4.6 mm and 250 x 4.6 mm.

The capacity factor (K') and the selectivity (α) were calculated using the following equations:

$$K' = (t_r - t_0) / t_0$$

$$\alpha = K'_1 / K'_2$$

6.3 EXPERIMENTAL TO CHAPTER 2

6.3.1 Synthesis of templates

6.3.1.a Synthesis of Boc protected phenylalanine anilide (1 & 2)[242]

General protocol for the synthesis of substituted amino acids

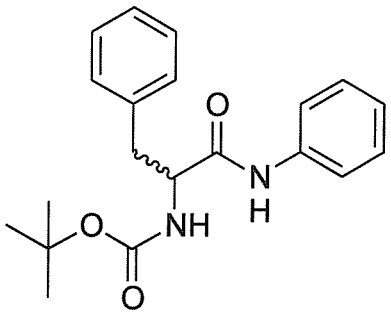

1: Boc-Phe-NHPh
2: Boc-D-Phe-NHPh

To a stirred solution of N-[(t-butyl)carbonyl]-L or D-phenylalanine (3g, 11.3 mmol) (Boc-L or D-Phe-OH) in ethyl acetate (30 mL) cooled to -10°C were added N-methylmorpholine (1.2 mL, 11.3 mmol) and isobutyl chloroformate (1.7 mL, 11.3 mmol). The mixture was stirred for 30 min, then aniline (1 mL, 11.3 mmol) was added at 0°C. The solution was allowed to come to room temperature. then stirred for 3 h. The suspension was poured onto ice (6 g) and water (10 mL). The organic phase was retained and dried with magnesium sulfate. The solution was filtered, the filtrate was concentrated *in vacuo* and the residue was recrystallised from cold diethyl ether overnight to yield the title compound.

^{1}H (300 MHz, $CDCl_3$): δ = 1.45 (s, 9H, $((C\underline{H}_3)_3C)$, 3.17 (d, 2H, J = 7, $C\underline{H}_2$-$C^{\alpha}\underline{H}$), 4.50 (m, 1H, CH_2-$C^{\alpha}\underline{H}$), 5.25 (br s, 1H, N$\underline{H}$), 7.08 – 7.15 (m, 1H, C$\underline{H}$ aromatic), 7.30 (m, 9 H, C$\underline{H}$ aromatic), 7.75 (br s, 1H, N$\underline{H}$).

^{13}C (75.5 MHz, $CDCl_3$): δ = 28.4 ($(\underline{C}H_3)_3C$), 38.7 (Ph-$\underline{C}H_2$-$C^{\alpha}H$), 56.8 (Ph-CH_2-$\underline{C}^{\alpha}H$), 80.6 ($(CH_3)_3\underline{C}$), 120.3 (C$\underline{H}$ aromatic), 124.4 (C$\underline{H}$ aromatic), 127.1 (C$\underline{H}$ aromatic), 128.8 (C$\underline{H}$ aromatic), 129.0 (C$\underline{H}$ aromatic), 129.1 (C$\underline{H}$ aromatic), 129.5 (C$\underline{H}$ aromatic), 136.8 (C aromatic), 137.5 (C aromatic), 156.0 (O$\underline{C}$O), 170.0 ($\underline{C}$O-NH).

IR: ν = 3326 - 3274 (N-H), 3005 - 2930 (alkyl), 1696 (C=O urethane), 1682 (C=O amide), 1600 (C=C aromatic) cm^{-1}.

M/z (ES^+): 341.3 (30%) $[M+H]^+$, 363.3 (15%) $[M+Na]^+$.

Mp.: 124 – 126°C (Lit.: 126 – 128°C).[242]

R_f: 0.15 (Hexane / AcOEt: 9 / 1).

HPLC (λ = 260): 11.7 min.

Yield: 63% (2.43 g) for Boc-Phe-NHPh **(1)** and 63% (2.42 g) for Boc-D-Phe-NHPh **(2)** as white solids.

6.3.1.b Synthesis of phenylalanine anilide (3 & 4)[242]

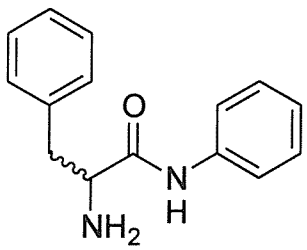

3: H-Phe-NHPh
4: H-D-Phe-NHPh

To a solution of Boc-Phenylalanine anilide (2.42 g, 7 mmol) in DCM (55 mL) was slowly added TFA (10.5 mL, 136 mmol) at 0°C. The mixture was allowed to come to room temperature then stirred for 2 hours. The solution was washed with $NaHCO_3$ aqueous solution (15 mL), the layers separated and the organic phase dried over magnesium sulfate. The organic layer was filtered and concentrated *in vacuo* to yield the expected

^1H (300 MHz, $CDCl_3$): δ = 1.80 (s, 2H, $N\underline{H}_2$), 2.81 (ABX system, 1H, J^{AX} = 9, J^{AB} = 14, $CH\underline{H}$-$C^{\alpha}H$), 3.39 (ABX system, 1H, J^{BX} = 4, J^{BA} = 14, $CH\underline{H}$-$C^{\alpha}H$), 3.77 (ABX system, 1H, J^{XB} = 4, J^{XA} = 9, CH_2-$C^{\alpha}\underline{H}$), 7.15 (m, 1H, C$\underline{H}$ aromatic.), 7.24 – 7.39 (m, 7H, C$\underline{H}$ aromatic), 7.61 (m, 2H, C$\underline{H}$ aromatic), 9.45 (m, 1H, N$\underline{H}$).

^{13}C (75.5 MHz, $CDCl_3$): δ = 40.7 (Ph-$\underline{C}H_2$-$C^{\alpha}H$), 56.9 (Ph-CH_2-$\underline{C}^{\alpha}H$), 119.6 ($\underline{C}H$ aromatic), 124.3 ($\underline{C}H$ aromatic), 127.1 ($\underline{C}H$ aromatic), 129 ($\underline{C}H$ aromatic), 129.1 ($\underline{C}H$

aromatic), 129.4 (CH aromatic), 137.7 (C aromatic), 137.8 (C aromatic), 174.1 (CO-NH).

IR: ν = 3382 (NH_2), 3255 (NH), 3055 - 3027 (alkyl), 1661 (C=O), 1595 (C=C aromatic) cm^{-1}.

M/z (ES^+): 241.2 (100%) $[M+H]^+$, 282.2 (53%) $[M+H+MeCN]^+$.

Mp.: 70 – 72°C (Lit.: 73 –75°C).[242]

Rf: 0.5 (AcOEt).

HPLC (λ=260 nm): 7.2 min.

Yield: 52% (873 mg) for H-Phe-NHPh **(3)** and 22% (367 mg) H-D-Phe-NHPh **(4)** as white solids.

6.3.2 Bulk polymerization

6.3.2.a General procedure for bulk polymerisation of an imprinted polymer[218]

Ethylene glycol dimethacrylate (9.43 g, 48 mmol), functional monomer (10 mmol), template (H-Phe-NHPh) (600 mg, 2.5 mmol), and AIBN (103 mg, 627 μmol) in a porogenic solvent (33 mL) were mixed in 2 glass test tubes (100 x 12 mm) sealed with rubber septum. After degassing with N_2 for 5 minutes at room temperature, the tubes were left at 15°C for 1 hour, then exposed to UV light for 24 hours at 15°C in a thermostatic bath then heated for an additional 18 hours at 65°C. To obtain a homogenous polymerisation the tubes were slowly rotated (50 rpm) during the UV polymerisation process. Subsequently the polymers were carefully ground with a pestle in a mortar dried *in vacuo* overnight and sieved for 30 min. The fraction 45 – 75 μm was retained for slurry packing of a stainless steel HPLC column. A blank polymer was prepared as described above without template in the preparation.

6.3.2.b General procedure for slurry packing.

A suspension of the polymer (particle size: 45-75 or ≤ 30μm) in MeCN (20 mL) was sonicated for 30 min. then transferred to a column reservoir connected to an empty HPLC column. The mass of polymer was in excess compared to the size of the column: 600 mg for a 60 x 4.6 mm, 1.2 g for a 150 x 4.6 mm and 2 g for a 250 x 4.6 mm

column. On top of the reservoir was applied a flow of MeCN under high pressure (3500 psi) delivered by a packer (Alltech® model 1666 Slurry packer). When a volume of 60 mL of MeCN was run the HPLC column was disconnected from the reservoir.

6.3.2.c Bulk polymerisation of imprinted materials (P1 – P4) and blanks (B1 & B2)

A series of imprinted polymers **(P1 – P4)**, and blanks **(B1 & B2)**, were prepared following the standard procedure of bulk polymerisation and packed in different sizes of column according to the conditions listed in Table 6.1.

	Porogen	**Functional monomer**	**Range of particle size (μm)**	**Size of column (mm)**
P1	MeCN	MAA	45 – 75	60 x 4.6
				150 x 4.6
B1	MeCN	MAA	45 - 75	60 x 4.6
P2	DCM	MAA	45 - 75	60 x 4.6
			≤ 30	150 x 4.6
B2	DCM	MAA	45 – 75	60 x 4.6
P3	Toluene	MAA	45 – 75	60 x 4.6
				150 x 4.6
				250 x 4.6

Table 6.1: Composition of polymers and columns used (template: H-Phe-NHPh (3)).

The selectivity of the columns was monitored using several eluents under an isocratic gradient at different flow rates (0.3 and 0.5 mL/min) as described in the general procedures.

6.3.2.d Polymerisation *in situ* of imprinted polymers (P5 – P8)[202]

Two polymerisation mixtures were prepared mixing phenylalanine anilide **(3)** (100 mg, 416 μmol), methacrylic acid (142 μL, 1.67 mmol), AIBN (17 mg, 103.5 μmol) and EGDMA (1.48 mL, 9.89 mmol) in MeCN or toluene (2.27 mL). The suspensions were degassed for 3 min with N_2 at 0°C then transferred to columns screwed at one extremity (Table 6.2). After tightly screwing the second extremity the columns were immersed in thermostatic bath at 70°C for 20 hours.

	Porogen	**Size of column (mm)**
P5	MeCN	60 x 4.6
P6	MeCN	150 x 4.6
P7	Toluene	60 x 4.6
P8	Toluene	150 x 4.6

Table 6.2: Porogen and size of columns used during monolith synthesis.

The assessment of the columns was carried out as described in the general procedure.

6.4 EXPERIMENTAL TO CHAPTER 3

6.4.1 Synthesis of templates

6.4.1.a Synthesis of Boc-Phe-NHC$_6$D$_5$ (5)[242]

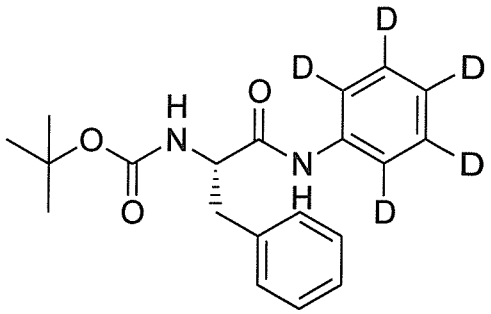

To a solution of Boc-Phe-OH (5g, 19 mmol) in ethyl acetate (50 mL) was added *N*-methylmorpholine (2 mL, 19 mmol), isobutyl chloroformate (2.45 mL, 19 mmol) and aniline 2, 3, 4, 5, 6-d_5 (1.7 mL, 19 mmol) following the reaction and work-up conditions as described for **(1)**. The title compound was isolated as a white solid.

^{1}H (300 MHz, CDCl$_3$): δ = 1.45 (s, 9H, (C$\underline{H}_3$)$_3$C), 3.08 – 3.22 (br m, 2H, C$\underline{H}_2$-C$^{\alpha}$H), 4.50 (br s, 1H, CH$_2$-C$^{\alpha}\underline{H}$), 5.25 (br s, 1H, NH), 7.15 – 7.40 (m, 5H, C$\underline{H}$ aromatic), 7.9 – 8.1 (br s, 1H, NH).

^{13}C (75.5 MHz, CDCl$_3$): δ = 28.4 ((C$\underline{H}_3$)$_3$C), 38.6 (C$\underline{H}_2$-C$^{\alpha}$H), 57 (CH$_2$-C$^{\alpha}\underline{H}$), 127.2 (C$\underline{H}$ aromatic), 129.0 (C$\underline{H}$ aromatic), 129.5 (C$\underline{H}$ aromatic), 138.0 (C aromatic), 170.0 (C$\underline{O}$-NH).

IR: ν = 3347 - 3314 (NH), 2991 - 2935 (alkyl), 1665 (C=O amide), 1601 (C=C aromatic) cm^{-1}.

M/z (ES$^+$): 346 (100%) [M+H]$^+$.

Mp.: 125 – 127°C (Lit.: 126 – 128°C).[242]

R$_f$: 0.12 (Hexane / AcOEt: 90 / 10).

Yield: 98% (6.8 g) as a white solid.

6.4.1.b Synthesis of H-Phe-NHC$_6$D$_5$ (6)[242]

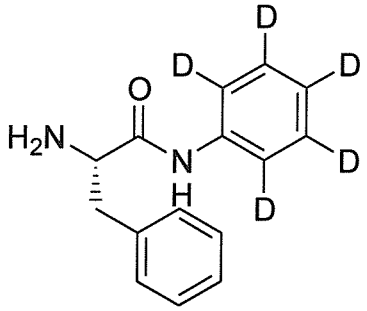

The title compound was prepared by treatment of **(5)** (6g, 17 mmol) in DCM (40 mL) with TFA (15 mL, 195 mmol) to give the title compound according to the procedure used for **(3 & 4)**.

^{1}H (300 MHz, CDCl$_3$): δ = 1.70 (s, 2H, NH$_2$), 2.80 (ABX system, 1H J^{AX} = 9, J^{AB} = 14, CHH-C$^{\alpha}$H), 3.32 (ABX system, 1H, J^{BX} = 4, J^{BA} = 14, CHH-C$^{\alpha}$H), 3.70 (ABX system, 1H, J^{XB} = 4, J^{XA} = 9, CH$_2$-C$^{\alpha}$H), 7.20 - 7.40 (m, 5H, CH aromatic), 9.55 (br s, 1H, NH).

^{13}C (75.5 MHz, CDCl$_3$): δ = 41.0 (CH$_2$-C$^{\alpha}$H), 57.0 (CH$_2$-C$^{\alpha}$H), 127.1 (CH aromatic), 129.0 (CH aromatic), 129.5 (CH aromatic), 138.0 (C aromatic), 173.0 (CO-NH).

IR: ν = 3254 (NH), 2937 - 2877 (alkyl), 1661 (C=O), 1600 – 1566 (C=C aromatic) cm^{-1}.

M/z (ES$^+$): 246.2 (100%) [M+H]$^+$.

HRMS (ES$^+$): $C_{15}H_{11}N_2O_1D_5$ [M+H]$^+$ Calc. 246.1649, found 246.1649.

Mp.: 68 – 70°C.

R$_f$: 0.52 (AcOEt).

HPLC (λ=220 nm): 7.1 min.

Yield: 67% (2.8 g) as a white solid.

6.4.1.c Synthesis of L-Dansyl-phenylalanine ethyl ester (7)[279]

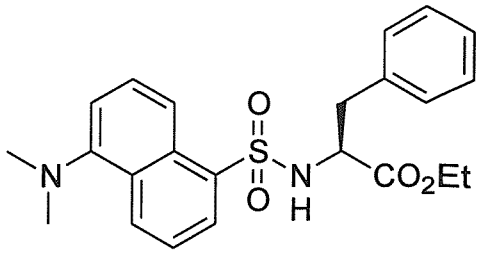

A solution of L-Phenylalanine ethyl ester HCl salt (2 g, 8.7 mmol) in DCM (40 mL) was treated with NEt_3 (366 mL, 19.14 mmol) then a solution of dansyl chloride (2.58 g, 9.57 mmol) in DCM (40 mL) was added under N_2. The mixture was stirred for 4 days and the solvent was removed *in vacuo*. The residue was triturated with AcOEt (10 mL) and the precipitate was collected by filtration. The filtrate was evaporated *in vacuo* to yield the title compound as a yellow solid.

^{1}H (300 MHz, $CDCl_3$): δ = 0.95 (t, 3H, *J* = 7, $CH_2C\underline{H}_3$), 2.87 (s, 6H, $N(C\underline{H}_3)_2$), 2.95 (br d, 2H, Ph-$C\underline{H}_2$-$C^{\alpha}H$), 3.70 - 3.85 (m, 2H, O-$C\underline{H}_2$-CH_3), 4.17 (br s, 1H, CH_2-$C^{\alpha}\underline{H}$), 5.40 (s, 1H, N$\underline{H}$), 6.95 (m, 2H, $\underline{Ph}$-CH_2), 7.15 (m, 3H, $\underline{Ph}$-CH_2), 7.32 (d, 1H, *J* = 7, C$\underline{H}$ aromatic), 7.47 (dd, 1H, *J* = 8, *J* = 8, C$\underline{H}$ aromatic), 7.54 (dd, 1H, *J* = 7, *J* = 7, C$\underline{H}$ aromatic), 8.19 (d, 1H, *J* = 7, C$\underline{H}$ aromatic), 8.23 (d, 1H, *J* = 8, C$\underline{H}$ aromatic), 8.52 (d, 1H, *J* = 8, C$\underline{H}$ aromatic).

^{13}C (75.5 MHz, $CDCl_3$): δ = 13.8 (O-CH_2-$\underline{C}H_3$), 39.4 ($\underline{C}H_2$-$C^{\alpha}H$), 45.6 ($N(\underline{C}H_3)_2$), 57.2 (CH_2-$\underline{C}^{\alpha}H$), 61.7 (O-$\underline{C}H_2$-CH_3), 115.4 ($\underline{C}$H aromatic), 119.1 ($\underline{C}$H aromatic), 123.2 ($\underline{C}$H aromatic), 127.0 ($\underline{C}$H aromatic), 127.2 ($\underline{C}$H aromatic), 128.4 ($\underline{C}$H aromatic), 128.5 ($\underline{C}$H aromatic), 128.7 ($\underline{C}$H aromatic), 129.4 ($\underline{C}$H aromatic), 129.6 ($\underline{C}$H aromatic), 129.9 ($\underline{C}$ aromatic), 130.8 ($\underline{C}$ aromatic), 134.7 ($\underline{C}$ aromatic), 135.1 ($\underline{C}$ aromatic), 152.0 ($\underline{C}$ aromatic), 170.8 ($\underline{C}O_2Et$).

IR: ν = 3281 (N-H), 2981 - 2861 (alkyl), 1733 (C=O ester), 1655 - 1589 (C=C aromatic), 1571 (NH) cm^{-1}.

M/z (ES^+): 427.2 (20%) $[M+H]^+$.

Micro-analysis: $C_{23}H_{26}N_2O_4S \cdot H_2O$ % Calc.: C 64.77, H 6.14, N 6.56, S 7.52. % Found: C 64.32, H 6.42, N 6.43, S 7.83.

Mp.: 52 - 55°C.

R_f: 0.26 (PE / AcOEt: 90 / 10).

HPLC (λ=220 nm): 9.9 min.

Yield: 89% (3 g) as a yellow fluorescent solid.

6.4.2 Synthesis of acrylamide monomers

6.4.2.a Synthesis of *N*-Benzyl-2-methacrylamide (8)[280]

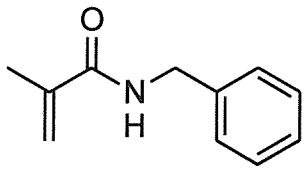

To a stirred solution of benzylamine (5.22 mL, 47.82 mmol) and triethylamine (6.66 mL, 47.82 mmol), in dry tetrahydrofuran (THF) (20 mL) cooled at 0°C, was added very slowly 2-methacryloyl chloride (5 g, 47.22 mmol) dissolved in THF (10 mL). The mixture was stirred for an additional 45 min. at 0°C and concentrated *in vacuo*. The residue was dissolved in DCM (20 mL) and the organic phase was washed with a saturated aqueous solution of sodium bicarbonate (3 x 10 mL). The starting material (benzylamine) was removed from the organic phase by three washings with citric acid 5% (3 x 10 mL), brine (10 mL) and finally the organic phase dried with anhydrous sodium sulphate. The solution was filtered and concentrated *in vacuo*. The product was purified by three recrystallisations from diethyl ether to give the title product.

^{1}H (300 MHz, $CDCl_3$): δ = 2.00 (s, 3H, $C\underline{H}_3$), 4.50 (d, 2H, *J* = 6, NH-$C\underline{H}_2$), 5.35 (s, 1H, H$\underline{H}$C=C), 5.72 (s, 1H, $\underline{H}$HC=C), 6.14 (br s, 1H, N$\underline{H}$), 7.20 – 7.40 (m, 5H, C$\underline{H}$ aromatic).

^{13}C (75.5 MHz, $CDCl_3$): δ = 18.8 ($\underline{C}H_3$), 43.9 ($\underline{C}H_2$), 119.8 ($\underline{C}H_2$=C), 127.7 ($\underline{C}$H aromatic), 128.0 ($\underline{C}$H aromatic), 128.9 ($\underline{C}$H aromatic), 138.4 (CH_2=$\underline{C}$), 140.0 ($\underline{C}$ aromatic), 168.0 ($\underline{C}$=O).

IR: ν = 3281 (N-H), 3061 - 3026 (alkyl), 1652 (C=O), 1605 (C=C) cm^{-1}.

M/z (ES^+): 176.0 (18%) $[M+H]^+$, 193.0 (8%) $[M+NH_4]^+$.

Mp.: 75 - 77°C (Lit.: 73 – 75°C).[280]

R_f: 0.78 (AcOEt).

Yield: 61% (8 g) as a white solid.

6.4.2.b Synthesis of *N*-Benzylacrylamide (9)[281]

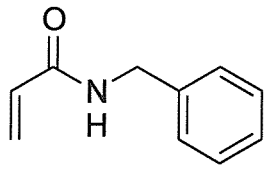

Benzylamine (3.62 mL, 33.14 mmol), triethylamine (4.61 mL, 33.14 mmol) and acryloyl chloride (3 g, 33.14 mmol) were used following the method 4.2.1. The crude product was purified by flash chromatography on silica gel (AcOEt / PE: 25 / 75) to afford the title compound.

^{1}H (300 MHz, $CDCl_3$): δ = 4.48 (d, 2H, J = 6, NH-C$\underline{H}_2$-Ph), 5.65 (dd, 1H, J^{gem} = 1.5, J^{cis} = 10, C$\underline{H}$H=CH), 6.14 (dd, 1H, J^{cis} = 10, J^{trans} = 17, CHH=C$\underline{H}$), 6.31 (dd, 1H, J^{cis} = 1.5, J^{gem} = 17, CH$\underline{H}$=CH), 7.25 – 7.35 (m, 5H, C$\underline{H}$ aromatic).

^{13}C (75.5 MHz, $CDCl_3$): δ = 43.8 ($\underline{C}H_2$), 126.9 ($\underline{C}$H aromatic), 127.7 ($\underline{C}$H aromatic), 128.0 ($\underline{C}$H aromatic), 128.8 ($\underline{C}H_2$=C), 130.8 (CH_2=$\underline{C}$H), 138.2 ($\underline{C}$ aromatic), 165.7 (C=O).

M/z (ES^+): 162.0 (100%) $[M+H]^+$.

Mp.: 58 – 60°C (Lit.: 58 – 60°C).[281]

IR: ν = 3282 (N-H), 3065 - 3030, 1454 (alkyl), 1650 (C=O), 1618 (C=C) cm^{-1}.

R_f: 0.64 (AcOEt / PE: 50 / 50), 0.19 (AcOEt / PE: 25 / 75).

HPLC (λ=220 nm): 7.6 min.

Yield: 61% (3.25 g) as a white solid.

6.4.2.c Synthesis of *N*-Ethyl-2-methacrylamide (10)[282]

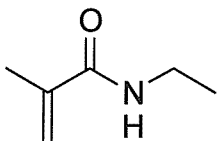

To a stirred solution of ethylamine (14.34 mL, 28.7 mmol) and triethylamine (4 mL, 28.69 mmol) in dry THF (15 mL) cooled to 0°C, was added very slowly 2-methacryloyl chloride (3 g, 28.7 mmol) in dry THF (5 mL). Upon completion of the addition, the mixture was stirred for an additional 30 min at 0°C, concentrated *in vacuo* and the residue was dissolved in DCM (20 mL). The organic phase was washed with a saturated aqueous solution of sodium bicarbonate (15 mL), dried over sodium sulphate, filtered and concentrated *in vacuo*. The residue was purified by flash chromatography on silica gel (AcOEt / PE: 60 / 40) to yield **(10)**.

^{1}H (300 MHz, $CDCl_3$): δ = 1.10 (t, 3H, *J* = 7, CH_2-C<u>H</u>$_3$), 1.90 (s, 3H, C<u>H</u>$_3$), 3.27 (dq, 2H, *J* = 5, *J* = 7, NH-C<u>H</u>$_2$-CH_3), 5.23 (s, 1H, C<u>H</u>H=), 5.62 (s, 1H, CH<u>H</u>=), 6.23 (br s, 1H, N<u>H</u>).

^{13}C (75.5 MHz, $CDCl_3$): δ = 14.8 (CH_2-<u>C</u>H_3), 18.7 (<u>C</u>H_3), 34.6 (<u>C</u>H_2-CH_3), 119.2 (H_2<u>C</u>=C), 140.2 (H_2C=<u>C</u>), 168.6 (<u>C</u>O).

IR: ν = 3316 (N-H), 2976 - 2878 (alkyl), 1654 (C=O), 1611 (C=C) cm^{-1}.

M/z (ES^+): 114.9 (20%) $[M+H]^+$.

R_f: 0.38 (AcOEt / PE: 60 / 40).

Yield: 51% (1.67 g) as a yellow oil.

6.4.2.d Synthesis of *N*-Ethylacrylamide (11)[283]

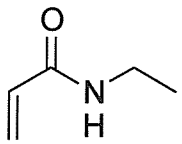

Ethylamine (16.53 mL, 33.14 mmol), triethylamine (4.61 mL, 33.14 mmol) and acryloyl chloride (2.69 mL, 33.14 mmol) were reacted in dry THF (15 mL) following the same reaction and workup conditions as used in 4.2.3 to afford the title compound.

^{1}H (300 MHz, $CDCl_3$): δ = 1.12 and 1.13 (t, 3H, J = 7, CH_2-C<u>H</u>$_3$), 3.31 and 3.32 (dq, 2H, J = 6, J = 7, NH-C<u>H</u>$_2$-CH_3), 5.56 and 5.57 (dd, 1H, J^{gem} = 1.5, J^{cis} = 9.5, C<u>H</u>H=CH), 6.13 (dd, 1H, J^{cis} = 9.5, J^{trans} = 17, CHH=C<u>H</u>), 6.22 and 6.23 (dd, 1H, J^{gem} = 1.5, J^{trans} = 17, CH<u>H</u>=CH), 7.20 (br s, 1H, N<u>H</u>).

^{13}C (75.5 MHz, $CDCl_3$): δ = 14.7 (CH_2-<u>C</u>H$_3$), 34.5 (<u>C</u>H$_2$-CH_3), 126.0 (H_2<u>C</u>=CH), 131.2 (H_2C=<u>C</u>H), 165.8 (<u>C</u>O).

IR: ν = 3280 (N-H), 3073 - 2937(alkyl), 1655 (C=O), 1623 (C=C) cm^{-1}.

M/z (ES$^+$): 100.0 (10%) $[M+H]^+$.

R_f: 0.58 (AcOEt).

Yield: 77% (2.9 g) as a yellow oil.

6.4.2.e Synthesis of 2-Methylacrylamidoethyl Methacrylate (12)[284]

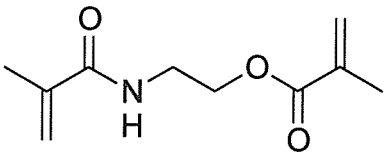

To a solution of ethanolamine (577 μL, 9.56 mmol) and triethylamine (3.34 mL, 24 mmol) dissolved in dry THF (20 mL) cooled at 0°C, was slowly added methacryloyl chloride (2.35 mL, 24 mmol) in dry THF (10 mL), the mixture stirred for 3 hours. The reaction mixture was washed with a saturated aqueous solution of sodium bicarbonate (50 mL) and extracted with a mixture of ethyl acetate / DCM (20 / 3 mL). The organic phase was washed with saturated aqueous solution of sodium carbonate (2 x 15 mL),

and the aqueous phase extracted with DCM (2 x 15 mL). The different organic phases were combined and concentrated *in vacuo*. The residue was redissolved in a minimum amount of DCM and purified by flash chromatography on silica gel (AcOEt) to yield the expected product.

^{1}H (300 MHz, $CDCl_3$): δ = 1.70 (s, 3H, $C\underline{H}_3$), 1.72 (s, 3H, $C\underline{H}_3$) 3.65 (td, 2H, J= 5, J= 6, NH-$C\underline{H}_2$-CH_2), 4.05 (t, 2H, J = 6, NH-CH_2-$C\underline{H}_2$), 5.11 (d, 1H, J^{gem} = 1.5, H$\underline{H}$C=C(Me)(CO)), 5.36 (d, 1H, J^{gem} = 1.5, H$\underline{H}$C=C(Me)(CO_2)), 5.50 (s, 1H, $\underline{H}$HC=C(Me)(CO)), 5.90 (s, 1H, $\underline{H}$HC=C(Me)(CO_2)), 6.36 (s, 1H, N$\underline{H}$).

^{13}C (75.5 MHz, $CDCl_3$): δ = 18.1 (CH_2=C($\underline{C}H_3$)(CO_2)), 18.5 (CH_2=C($\underline{C}H_3$)(CONH)), 39.3 ($\underline{C}H_2$NH), 63.0 ($\underline{C}H_2$O), 119.6 ($\underline{C}H_2$=C(Me)(CO)), 125.9 ($\underline{C}H_2$=C(Me)(CO_2)), 135.7 (CH_2=$\underline{C}$(Me)(CO)), 139.7 (CH_2=$\underline{C}$(Me)(CO_2)), 167.3 ($\underline{C}O_2$), 169.0 ($\underline{C}$O).

IR: ν = 3320 (N-H), 2939 - 2831 (alkyl), 1719 (C=O ester), 1654 (C=O amide), 1638 (C=C) cm^{-1}.

M/z (ES^+): 198.0 (7%) $[M+H]^+$.

R_f: 0.74 (AcOEt).

Yield: 42% (793 mg) as a yellow oil.

6.4.2.f Synthesis of *N*-(2-Hydroxyethyl)methacrylamide (13)[284]

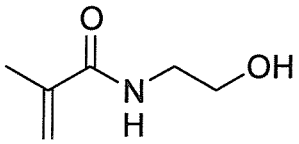

To a stirred solution of 2-(methylacryloylamino)ethyl-2-methyl acryloyl **(12)** (550 mg, 2.8 mmol) in dioxane (5 mL) was added slowly at room temperature an aqueous solution of sodium hydroxide (1M, 10 mL). The mixture was stirred for 2 hours, the solution was concentrated under reduced pressure and the yellow oil residue was triturated with ethyl acetate. The precipitate was filtered and the filtrate was concentrated under reduced pressure to give **(13)**.

^{1}H (300 MHz, $CDCl_3$): δ = 1.87 (s, 3H, $C\underline{H}_3$), 3.48 (dt, 2H, J = 4, J = 5, NH-$C\underline{H}_2$-CH_2), 3.75 (t, 2H, J = 5, NH-CH_2-$C\underline{H}_2$), 5.30 (s, 1H, $CH\underline{H}$=C), 5.60 (s, 1H, $C\underline{H}$H=C), 6.45 (br s, 1H, N$\underline{H}$).

^{13}C (75.5 MHz, $CDCl_3$): δ = 18.7 ($\underline{C}H_3$), 42.7 ($\underline{C}H_2$-NH), 62.3 (CH_2-OH), 120.3 ($\underline{C}H_2$=C(Me)(CO)), 139.7 (CH_2=$\underline{C}$(Me)(CO)), 169.7 ($\underline{C}$O).

IR: ν = 3316 (O-H), 3100 - 2928 (alkyl), 1654 (C=O), 1607 (C=C), 1530 (N-H) cm^{-1}.

M/z (ES^+): 130.0 (25%) $[M+H]^+$.

R_f: 0.3 (AcOEt / MeOH: 97 / 3).

Yield: 84% (302 mg) as a yellow oil.

6.4.2.g Synthesis of 2-Acrylamidoethyl Acrylate (14)[284]

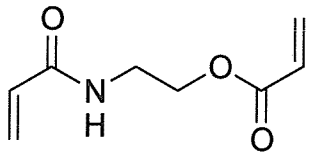

(14) was prepared according to the protocol described for compound **(12)**, with ethanolamine (1.23 mL, 20 mmol), triethylamine (7 mL, 50 mmol) and acryloyl chloride (4 mL, 50 mmol). The purification by flash chromatography on silica gel (AcOEt) afforded the title compound.

^{1}H (300 MHz, $CDCl_3$): δ = 3.61 (dt, 2H, J = 5, J = 6, NH-$C\underline{H}_2$), 4.25 (t, 2H, J = 5, $C\underline{H}_2$-O), 5.61 (dd, 1H, J^{gem} = 1.5, J^{cis} = 10, $C\underline{H}$H=CHC(O)NH), 5.82 (dd, 1H, J^{gem} = 1.5, J^{cis} = 10, $C\underline{H}$H=CHC(O)O), 6.09 (dd, 1H, J^{cis} = 10, J^{trans} = 18, CHH=C$\underline{H}$C(O)O), 6.12 (dd, 1H, J^{cis} = 10, J^{trans} = 17, CHH=C$\underline{H}$C(O)NH), 6.25 (dd, 1H, J^{gem} = 1.5, J^{trans} =17, CH$\underline{H}$=CHC(O)NH), 6.40 (dd, 1H, J^{gem} = 1.5, J^{trans} = 18, CH$\underline{H}$=CHC(O)O).

^{13}C (75.5 MHz, $CDCl_3$): δ = 38.8 (NH-$\underline{C}H_2$), 63.3 ($\underline{C}H_2$-O), 126.8 (OC(O)-$\underline{C}$H=CH_2), 128.0 (HN-C(O)-CH=$\underline{C}H_2$), 130.7 (OC(O)-CH=$\underline{C}H_2$), 131.6 (HN-C(O)-$\underline{C}$H=CH_2), 166.0 (O$\underline{C}$(O)), 166.4 (HN-$\underline{C}$(O)).

IR: ν = 3282 (N-H), 3071 - 2958 (alkyl), 1721 (C=O ester), 1657 (C=O amide), 1626 (C=C), 1542 (N-H) cm^{-1}.

M/z (ES^+): 170.0 (15%) $[M+H]^+$, 192.0 (35%) $[M+Na]^+$.

R_f: 0.6 (AcOEt).

Yield: 25% (500 mg) as a yellow oil.

6.4.2.h Synthesis of *N*-(2-Hydroxyethyl)acrylamide (15)[284, 285]

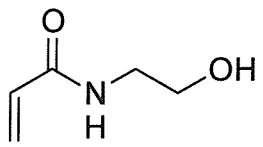

Following the protocol described for the compound **(13)** 2-(acryloylamino)ethyl acrylate (500 mg, 3 mmol) was hydrolysed with an aqueous solution of sodium hydroxide 1M (3 mL). The crude was purified by flash chromatography on silica gel (EtOAc / MeOH: 97 / 3) to afford **(15)**.

^{1}H (300 MHz, $CDCl_3$): δ = 3.44 (dt, 2H, *J*= 5, *J*= 6, C$\underline{H}_2$-NH), 3.65 (bs, 1H, CH_2-O$\underline{H}$), 3.72 (t, 2H, *J*= 5, CH_2-C$\underline{H}_2$-OH), 5.63 (dd, 1H, J^{gem} = 2, J^{cis} = 9.5, C$\underline{H}$H=CH), 6.15 (dd, 1H, J^{cis} = 9.5, J^{trans} = 17, CHH=C$\underline{H}$), 6.26 (dd, 1H, J^{gem} = 2, J^{trans} = 17, CH$\underline{H}$=CH).

^{13}C (75.5 MHz, $CDCl_3$): δ = 42.5 (NH-$\underline{C}H_2$), 61.7 ($\underline{C}H_2$-OH), 127.0 ($H_2\underline{C}$=CH), 130.7 (H_2C=$\underline{C}$HC(O)NH), 167.0 ($\underline{C}$O).

IR: ν = 3516 (OH), 3294 (NH), 2936 - 2881 (alkyl), 1656 (C=O), 1623 (C=C), 1545 (N-H) cm^{-1}.

M/z (ES^+): 115.9 (5%) $[M+H]^+$.

R_f: 0.31 (AcOEt / MeOH: 97 / 3).

Yield: 44% (75 mg) as a yellow oil.

6.4.3 Synthesis of polymers

6.4.3.a General procedure for polymerisation in vials[240]

Mother solutions were prepared mixing EGDMA (4.75 mL, 25 mmol), AIBN (50 mg, 0.3 mmol) and a given porogen (7 mL). To one of the solutions was added a template (1.25 mmol) to give the MIP stock solution, while the other solution was used without template as a blank stock solution. A total of 117.5 µL of each mother solution was dispensed into a 1.5 mL glass vial to give the following composition: EGDMA (47.5 µL, 250 µmol), porogen (70 µL), AIBN (0.5 mg, 3 µmol) and template (12.5 µmol). After the addition of one functional monomer (4 eq.) to the polymerisation mixture, the vials were sealed with a rubber septum, purged with nitrogen for 5 min, cooled to 15 °C in a thermostatic water bath prior to polymerisation by UV radiations for 12 h at 15°C then for an additional 13 h at 60°C.

6.4.3.b General procedure for first screening

After polymerisation the porogen (1 mL) was dispensed into each vial, sonicated for 1 h, left overnight, then sonicated at 40 °C for 1 h. Acetic acid (50 µL) was added to the solution and sonicated again for 1 h. The content of template was quantified after each washing by analytical HPLC (λ = 260 nm with run of 3 min under an isocratic gradient MeCN / TFA 0.04%).

6.4.3.c General procedure for rebinding monitoring

After exhaustive extraction of the template from the imprinted polymer, by a series of washing with 5% AcOH in porogen (1 mL) or 0.042% TFA in porogen until the disappearance of the HPLC trace of the template followed by an additional three washings in porogen (1mL), 1 mL of template solution in porogen (1 mM) was added to each vial and sonicated for 1 h. The content of unrebinded template in each solution was evaluated by analytical HPLC and deduced from the initial concentration (1 mM) to obtain the amount of rebound template.

6.4.3.d Polymer imprinted with Boc-D-Phe-NHPh (2) in DCM

As described above two stocks solutions were made in DCM: one with Boc-D-Phe-NHPh **(2)** (425 mg, 1.25 mmol) to yield the MIP solution and the other without template as a blank. 117.5 µL of each stock solution (MIP and blank) was dispensed into 8 vials then one of the following functional monomers (50 µmol) was added: MAA (4 µL), NVP (5 µL), NEA **(11)** (5 mg), NEMA **(10)** (5.6 mg), NBA **(9)** (8 mg), NBMA **(8)** (8.7 mg), NHEA **(15)** (6 mg) and NHEMA **(13)** (6.5 mg). Polymerisations were achieved following the standard procedure. The first screening and rebinding experiment monitoring (Table 6.3) were performed in 1 mL of DCM as detailed in the general procedure.

	P-MAA	P-NVP	P-NEA	P-NEMA	P-NBA	P-NBMA	P-NHEA	P-NHEMA
First screening experiment with MIP								
1st washing	2553	2913	3466	3756	2958	2809	3013	2558
2nd washing	6083	6964	6213	7293	6588	6574	7008	6087
3rd washing	7711	8190	6861	8443	7645	7729	7749	7715
4th washing	8059	8320	6875	9881	7882	7844	8835	8063
Rebinding experiment								
MIP	1129	1272	1672	1391	1713	1208	1322	1443
Blank	1464	1348	1447	1486	1621	1818	1326	1446

Table 6.3: HPLC data (sum of peak areas of template (mAu at λ = 260 nm)) for first screening and rebinding experiment. (P: Polymer).

6.4.3.e Polymer imprinted with Boc-D-Phe-NHPh (2) in MeCN

A library of 9 polymers imprinted with Boc-D-Phe-NHPh **(2)** (and the corresponding blanks) was prepared as detailed above in the presence of one of the following functional monomers (50 µmol.): MAA (4 µL), NVP (5 µL), VPY (5.4 µL), NEA **(11)** (5 mg), NEMA **(10)** (5.6 mg), NBA **(9)** (8 mg), NBMA **(8)** (5 mg), TFM (7 mg),

HEMA (6.3 µL). The imprint process was evaluated as described in the standard procedure and the data of first screening and rebinding monitoring quoted in Table 6.4.

	P-MAA	P-NVP	P-VPY	P-NEA	P-NEMA	P-NBA	P-NBMA	P-TFM	P-HEMA
First screening experiment with MIP									
1st washing	637	681	5931	548	771	587	741	680	621
2nd washing	1327	1395	1329	1224	914	1240	1512	1402	1300
3rd washing	2012	2079	2048	2049	1790	2030	2287	2094	2059
4th washing	2424	2466	2414	2487	2213	2466	2752	2450	2492
Rebinding experiment									
MIP	700	700	775	787	759	785	759	765	741
Blank	735	735	797	800	778	775	797	765	800

Table 6.4: HPLC data (sum of peak areas of template (mAu at λ = 260 nm)) for first screening and rebinding experiment. (P: Polymer).

6.4.3.f Polymer imprinted with Dns-Phe-OEt (7)

Two stock solutions were obtained by mixing EGDMA (2.28 mL, 22 mmol) and AIBN (24 mg, 144 µmol) in DCM (3.36 mL) with or without Dns-Phe-OEt **(7)** (300 mg, 0.6 mmol). 117.5 µL of each mother solution were transferred into 3 vials and degassed for 3 min at 0°C before adding one of the following functional monomers (50 µmol): MAA (4 µL), NVP(5 µL) or NBMA **(8)** (5 mg). Polymerisation was carried out in a thermostatic water bath at 60°C for 12 h and for an additional 2 h at 75°C. After the first screening performed in 1 mL of DCM as detailed in the general procedure, exhaustive washings were carried out with 1 mL of MeOH / MeCN (7 / 3), MeOH / MeCN / TFA (7 / 2 / 1), MeCN and DCM again. The rebinding experiment was performed as described in the standard procedure and the data listed in Table 6.5.

	P-MAA	P-NVP	P-NBMA
First screening experiment with MIP			
1st washing	480	404	421
2nd washing	1126	1107	1247
3rd washing	1858	2102	2102
4th washing	2265	2745	2109
Rebinding experiment			
MIP	754	1071	1836
Blank	790	835	824

Table 6.5: HPLC data (sum of peak areas of template (mAu at λ = 260 nm)) for first screening and rebinding experiment. (P: Polymer).

6.4.3.g Polymers imprinted with H-Phe-NHC$_6$D$_5$ (6)

The same reaction and polymerisation conditions as detailed in the general procedure were used to prepare 4 polymers imprinted with H-Phe-NHC$_6$D$_5$ **(6)** (102 mg, 447 μmoles), and the corresponding blank, in MeCN in the presence of MAA or VPY (at 2 or 4 eq.). 117.5 μL or 352.5 μL of each stock solution were then dispensed into a 1.5 mL glass vial. The vials were degassed under nitrogen for 3 min at 0°C prior to UV polymerisation for 20 h at 18°C followed by thermal polymerisation at 60°C for 12 h.
After the first screening performed in acetonitrile (1 mL) as previously described, and an additional 60 washings (sonication for 20 min in 1 mL of MeCN / TFA 0.042% removed after each washing), the rebinding experiment was carried out with a mixture (1 mL) of H-Phe-NHC$_6$D$_5$ **(6)** (0.5 mM) and H-D-Phe-NHPh **(2)** (0.5 mM). After 45 minutes of sonication the supernatant contents were monitored by reversed phase HPLC (λ = 260 nm with run time of 3 min under an isocratic gradient MeCN / TFA 0.04%). The ratio of labelled and unlabelled template in solution was evaluated by mass spectroscopy (Table 6.6).

	P-3VPY 2eq	P-3VPY 4eq	P-3MAA 2eq	P-3MAA 4eq	P-VPY 2eq	P-VPY 4eq	P-MAA 2eq	P-MAA 4eq
First screening experiment with MIP								
1st washing	2049	1741	1308	1191	1309	1124	593	367
2nd washing	2524	2181	1415	1157	1386	1316	699	461
3rd washing	3635	2506	2247	1664	1497	1513	819	562
4th washing	3910	3749	2567	1818	1520	1539	862	734
Rebinding experiment								
MIP	1099	1082	621	439	1096	1139	895	270
Blank	1059	1044	820	810	1094	1120	892	831
Mass spectroscopy assessments (ratio : H-Phe-NHC_6D_5 / H-D-Phe-NHPh)								
MIP	1.24	0.90	0.67	1.14	1	1.27	0.62	0.87
Blank	0.90	1	0.93	1.20	3.5	0.76	1	0.60

Table 6.6: HPLC data (sum of peak areas of template (mAu at λ = 260 nm)) for first screening and rebinding experiment and MS data (ratio H-Phe-NHC_6D_5 / H-D-Phe-NHPh) for rebinding experiment. (P: Polymer).

6.4.4 Library of MIP films in a micro-plate

6.4.4.a Library with Dns-Phe-OEt (7) in different porogens and different functional monomer

Synthesis of the library

Six stock solutions were prepared in glass vials (1.5 mL) by adding EGDMA (950 μL, 5 mmol) and AIBN (30 mg, 180 μmol) to one of the following porogens (22 mmol): 1) CH_3CN (1.1 mL), 2) THF (1.8 mL), 3) DMF (1.7 mL), 4) $CHCl_3$ (1.7 mL), 5) DCM (1.4 mL) and 6) hexane (2.8 mL). Each suspension was divided into two equal volumes to give the stock blank solutions and the corresponding stock MIP solutions by the addition of Dns-Phe-OEt **(7)** (56 mg, 125 μmol) to give MIP 1 in CH_3CN, MIP 2 in THF, MIP 3 in DMF, MIP 4 in $CHCl_3$ MIP 5 in DCM and MIP 6 in hexane. The vials were sealed with a rubber septum and degassed for 3 min at 0°C. A volume of each MIP stock solution, corresponding to 12.5 μmol of template, was transferred to the wells of a 96-well borosilicate plate: 105 μL of MIP 1, 136 μL of MIP 2, 132 μL of MIP 3, 135 μL of MIP 4, 118 μL of MIP 5 and 188 μL of MIP 6. The same volume of corresponding blank was dispensed as show in the table 6.7. 50 μmol of the following functional monomer were added to the solutions in the wells (Table 6.7): MAA (4 μL), NVP (5 μL), VPY (5 μL), HEMA (6 μL) and MMA (5 μL). The micro-plate was sealed with an adhesive plastic cover and immersed in a thermostatic water bath at 60°C for 18 h and an additional 10 h at 75°C. The data of first screening and rebinding experiment are quoted in Table 6.8.

	MIP 1 CH_3CN	Blank 1 CH_3CN	MIP 2 THF	Blank 2 THF	MIP 3 DMF	Blank 3 DMF	MIP 4 $CHCl_3$	Blank 4 $CHCl_3$	MIP 5 DCM	Blank 5 DCM	MIP 6 Hexane	Blank 6 Hexane
MAA (50 µmol)	109	109	140	140	136	136	139	139	122	122	192	192
MAA (50 µmol)	109	109	140	140	136	136	139	139	122	122	192	192
NVP (50 µmol)	110	110	141	141	137	137	140	140	123	123	193	193
NVP (50 µmol)	110	110	141	141	137	137	140	140	123	123	193	193
VPY (50 µmol)	110	110	141	141	137	137	140	140	123	123	193	193
HEMA (50 µmol)	111	111	142	142	138	138	141	141	124	124	194	194
MMA (50 µmol)	110	110	141	141	137	137	140	140	123	123	193	193
No functional monomer	105	105	136	136	132	132	135	135	118	118	188	188

Table 6.7: Composition and final volume (µL) of the mixture by well.

Screening of the library

First screening

The template was extracted by sonications (3 x 1 hour) with the porogen (300 μL), twice with MeCN (2 x 1 h) and finally MeCN / TFA 0.042% (1 h). After each sonication, 5 μL of supernatant were diluted into 150 μL of MeCN and transferred to a 96-well plate. The amount of extracted template in solution was measured by the absorbance at λ = 340 nm of each well. A background was carried out by analysis of the washing solutions from the blank polymers (Table 6.8).

Rebinding experiment

After ten exhaustive washings (in 300 μL of MeCN) the rebinding experiment was performed with 300 μL of template solution in MeCN (0.1 μmol) added to each well. The micro-plate was sonicated for 30 min then the amount of free template in solution was recorded at λ = 340 nm (Table 6.8).

	First sreening										
	MeCN/MAA	**MeCN/MAA**	**MeCN/NVP**	**MeCN/NVP**	**MeCN/VPY**	**MeCN/HEM**	**MeCN/MMA**	**MeCN**	**THF/MAA**	**THF/MAA**	**THF/NVP**
1st washing	2,309	2,31	2,254	2,209	2,351	2,327	2,266	2,223	2,329	2,271	2,232
2nd washing	2,672	2,85	2,77	2,913	2,87	3,26	2,675	2,73	2,727	2,86	2,67
3rd washing	2,879	3,127	3,09	3,326	3,089	3,787	3,026	2,89	2,947	3,08	2,93
4th washing	4,837	4,591	5,296	5,532	5,302	5,941	5,321	5,059	5,047	5,18	3,408
5th washing	7,098	5,208	7,551	7,891	7,531	8,084	7,087	7,303	7,015	7,46	5,625
6th washing	9,311	8,978	9,741	9,996	9,703	10,222	9,274	9,482	9,459	9,653	7,821
	THF/NVP	**THF/VPY**	**THF/HEMA**	**THF/MMA**	**THF**	**DMF/MAA**	**DMF/MAA**	**DMF/NVP**	**DMF/NVP**	**DMF/VPY**	**DMF/HEMA**
1st washing	2,24	2,258	2,245	2,239	2,254	2,203	2,184	2,218	2,221	2,121	2,116
2nd washing	2,64	2,61	2,62	2,385	2,82	4,422	4,44	4,38	4,33	3,51	4,34
3rd washing	3,021	3,25	2,85	2,53	3,034	4,809	4,77	4,79	4,76	3,96	4,84
4th washing	5,207	4,266	5,133	4,767	3,535	5,412	5,341	5,303	5,331	4,197	5,65
5th washing	7,489	6,523	7,369	6,971	5,764	5,638	5,627	5,7	5,717	4,372	6,048
6th washing	9,696	8,675	9,524	9,12	7,956	5,914	5,949	6,044	5,972	4,587	6,431
	DMF/MMA	**DMF**	**CHCl3/MAA**	**CHCl3/MAA**	**CHCl3/NVP**	**CHCl3/NVP**	**CHCl3/VPY**	**HCl3/HEM**	**CHCl3-MMA**	**CHCl3**	**DCM/MAA**
1st washing	2,121	2,139	2,332	2,315	2,238	2,26	2,318	2,32	2,279	2,253	2,37
2nd washing	4,1	4,49	3	2,93	2,89	3	3	2,85	2,767	3,04	2,77
3rd washing	4,497	4,77	3,18	3,1	3,089	3,162	3,2	3,067	2,962	3,17	2,974
4th washing	4,998	5,514	3,757	3,709	3,572	3,605	4,1	3,568	3,634	3,603	3,795
5th washing	5,343	5,827	4,158	4,174	3,901	3,914	4,995	3,944	3,988	3,976	4,296
6th washing	5,761	6,48	6,368	6,394	6,107	6,104	7,182	6,103	6,188	6,142	6,539
	DCM/MAA	**DCM/NVP**	**DCM/NVP**	**DCM/VPY**	**DCM/HEMA**	**DCM/MMA**	**DCM**	**C6H12/MAA**	**C6H12/MAA**	**C6H12/NVP**	**C6H12/NVP**
1st washing	2,367	2,264	2,304	2,317	2,321	2,279	2,325	1,863	1,292	1,846	1,286
2nd washing	2,85	2,58	2,827	2,82	2,69	2,756	2,71	2,01	1,43	2,25	1,51
3rd washing	3,048	2,77	3,031	2,85	2,9	2,974	2,908	3,15	2,64	3,78	3,432
4th washing	3,728	3,261	3,832	5,123	3,548	5,24	5,16	5,655	5,156	6,319	5,801
5th washing	5,414	4,664	6,133	7,31	5,414	7,484	7,358	8,054	7,561	8,712	8,161
6th washing	7,643	6,827	8,317	9,492	7,597	9,662	9,518	10,35	9,64	10,909	10,353

Table 6.8: Plate reader data (sum of absorbance (λ = 340 nm)) for first screening and rebinding experiment.

To be continued.

	First screening (to be continued)										
	C6H12/VPY	6H12/HEM	C6H12/MMA	C6H12							
1st washing	1,089	2,031	2,149	2,183							
2nd washing	1,256	2,43	2,465	2,456							
3rd washing	1,957	3,31	3,26	2,78							
4th washing	4,395	5,796	5,675	5,201							
5th washing	6,745	8,137	8,022	7,488							
6th washing	8,905	10,317	10,189	9,68							
	Rebinding experiment										
	MeCN/MAA	MeCN/MAA	MeCN/NVP	MeCN/NVP	MeCN/VPY	MeCN/HEM	MeCN-MMA	MeCN	THF/MAA	THF/MAA	THF/NVP
Blank	0,913	1,172	0,399	1,021	0,325	0,369	0,336	0,377	0,346	0,391	0,3
MIP	1,793	1,767	1,144	1,091	2,223	0,808	0,866	2,233	2,197	2,184	2,247
	THF/NVP	THF/VPY	THF/HEMA	THF/MMA	THF	DMF/MAA	DMF/MAA	DMF/NVP	DMF/NVP	DMF/VPY	DMF/HEMA
Blank	0,368	0,789	0,417	0,343	0,354	0,202	0,15	0,268	0,169	0,175	0,301
MIP	0,745	1,822	2,054	2,192	2,232	0,213	0,268	0,236	0,275	0,31	0,258
	DMF/MMA	DMF	CHCl3/MAA	CHCl3/MAA	CHCl3/NVP	CHCl3/NVP	CHCl3/VPY	HCl3/HEM	CHCl3-MMA	CHCl3	DCM/MAA
Blank	0,296	0,123	1,064	0,306	0,284	0,3	0,594	0,456	0,428	0,534	0,735
MIP	0,836	0,437	2,214	1,436	1,003	2,178	2,036	2,17	2,223	2,265	1,203
	DCM/MAA	DCM/NVP	DCM/NVP	DCM/VPY	DCM/HEMA	DCM/MMA	DCM	C6H12/MAA	C6H12/MAA	C6H12/NVP	C6H12/NVP
Blank	1,156	0,369	0,414	0,27	0,654	0,37	0,318	0,3	0,297	0,346	0,336
MIP	1,221	1,707	0,817	0,67	1,24	0,788	0,838	0,556	0,907	0,836	0,467
	C6H12/VPY	6H12/HEM	C6H12/MMA	C6H12							
Blank	0,431	0,381	0,352	0,366							
MIP	1,674	2,03	1,152	1,164							

Table 6.8: Plate reader data (sum of absorbance (λ = 340 nm)) for first screening and rebinding experiment.

6.4.4.b Library with H-Phe-NHPh (3) in different porogens and with different functional monomers

Synthesis of the library

Six stock solutions were prepared mixing EGDMA (950 μL, 5 mmol) and AIBN (30 mg, 180 μmol) in one of the following porogenic solvents (22 mmol): 1) DCM (1.4 mL), 2) $CHCl_3$ (1.7 mL), 3) CH_3CN (1.1 mL), 4) hexane / CH_3CN (3%) (2.8 and 0.1 mL), 5) DMSO (1.5 mL) and 6) DMSO / CH_3CN (molar ratio 1 / 1: 0.85 and 0.98 mL). Each suspension was divided in two equal volumes to give the stock blank solutions and the stock MIP (by the addition of H-Phe-NHPh **(3)** (30 mg, 125 μmol)): MIP 1 in DCM, MIP 2 in $CHCl_3$, MIP 3 in CH_3CN, MIP 4 in hexane / CH_3CN (3%), MIP 5 in DMSO and MIP 6 in DMSO / CH_3CN. The vials were sealed with a rubber septum and degassed for 3 min at 0°C. A volume of the MIP solution, corresponding to 12.5 μmol of template, was transferred to a well of the 96 well glass plate: 118 μL of MIP 1, 135 μL of MIP 2, 105 μL of MIP 3, 193 μL of MIP 4, 132 μL of MIP 5 and 100 μL of MIP 6. The same volume of corresponding blank solution was also dispensed as show in Table 6.9. The functional monomers were dispensed: MAA (4 μL, 50 μmol), MAA (8 μL, 100 μmol), NVP (5 μL, 50 μmol), VPY (5 μL, 50 μmol), HEMA (6 μL, 50 μmol), MMA (5 μL, 50 μmol) and no functional monomer to give the library. The plate was sealed with a plastic cover and immerged in a thermostatic water bath for 12 h at 50°C and an additional 24 h at 70°C.

Screening of the library

First screening

After polymerisation each polymer was washed with the porogen (300 μL) by sonication of the 96-well plate for 45 min, left overnight in the fridge and sonicated again (2 x 45 min). The content of extracted template was quantified on an aliquot of 5 μL from each well by automated reversed phase HPLC (λ = 260 nm, isocratic gradient MeCN / TFA 0.04% for run time of 4.3 min).

Rebinding experiment

After the usual exhaustive washings, the rebinding experiment was performed with a solution of template 1 mM in MeCN (400 μL) sonicated for 45 min. The amount of free template **(3)** was evaluated by analysing of 5 μL of the solution by automated reversed phase HPLC as above.

	MIP 1 DCM	Blank 1 DCM	MIP 2 $CHCl_3$	Blank 2 $CHCl_3$	MIP 3 CH_3CN	Blank 3 CH_3CN	MIP 4 Hexane / CH_3CN	Blank 4 Hexane / CH_3CN	MIP 5 DMSO	Blank 5 DMSO	MIP 6 DMSO / CH_3CN	Blank 6 DMSO / CH_3CN
MAA (50 µmol)	122	122	139	139	109	109	197	197	136	136	104	104
MAA (50 µmol)	122	122	139	139	109	109	197	197	136	136	104	104
MAA (100 µmol)	126	126	143	143	113	113	201	201	140	140	108	108
NVP (50 µmol)	123	123	140	140	110	110	198	198	137	137	105	105
VPY (50 µmol)	123	123	140	140	110	110	198	198	137	137	105	105
HEMA (50 µmol)	124	124	141	141	111	111	199	199	138	138	106	106
MMA (50 µmol)	123	123	140	140	110	110	198	198	137	137	105	105
No functional monomer	118	118	135	135	105	105	193	193	132	132	100	100

Table 6.9: Composition and final volume (µL) of the mixture by well.

6.4.4.c Library of 96 mini-MIPs with H-Phenylalanine anilide (3) in toluene with different functional monomers at different ratios of EGDMA

Synthesis of the library

Two stock solutions (with or without template) were prepared by mixing AIBN (90 mg, 548 μmol) and toluene (15 mL, 140.5 mmol). The template stock solution contained 1.125 mmol (270 mg) of H-Phe-NHPh **(3)**. Both stock solutions were divided in two equal volumes (7.5 mL) to give solutions MIP 1 and MIP 2 and solutions blank 1 and blank 2.

To MIP 1 and blank 1 solutions was added 1.7 mL of EGDMA (11.25 mmol) to give final volumes of 9.5 mL and a concentration of template in the stock MIP 1 solution of 61.3 mM. Stock MIP 1 and blank 1 solutions were divided (8 x 816 μL) to give MIP 1 (A – H) and blank 1 (A – H). To stock solutions MIP 1 (A – G) and blank 1 (A – G) was added one of the following functional monomers: MAA (8.5 μL, 100 μmol), MAA (17 μL, 200 μmol), NVP (10.7 μL, 100 μmol), NVP (21.4 μL, 200 μmol), VPY (21.6 μL, 200 μmol), HEMA (25.2 μL, 200 μmol) and MMA (21.4 μL, 200 μmol). The stock solutions (H) were used without functional monomer.

To MIP 2 and blank 2 solutions were added 841 μL of EGDMA (5.62 mmol) to give final volumes of 8.32 mL and a concentration of template in the stock MIP 2 solution of 67.5 mM then the stock solutions were divided (8 x 740 μL) to give MIP 2 (A – H) and blank 2 (A – H). The same volumes of functional monomers as above were added to MIP 2 (A - G) and blank 2 (A - G). The solutions (H) were used without functional monomer.

All of these vials were sealed with a rubber septum and degassed with nitrogen for 2 min at 0°C. Finally each solution was deposed in triplet in a well of a 96 well glass plate under nitrogen stream. The following volumes for MIP 1 (A – H) and blank 1 (A – H) were used: 206, 208, 207, 209, 209, 210, 209 and 204 μL. For the MIP 2 (A – H) and blank 2 (A – H) the following volumes were used: 187, 189, 188, 190.3, 190, 191, 190 and 185 μL. The 96 well-plate was placed in thermostatic bath at 5°C at 20 cm of UV lamp for 15 h then the polymerisation was achieved by heating 50°C for 6 h. The composition and the final volume of the mixture by well are shown in Table 6.10.

	MIP 1	Blank 1	MIP 1	Blank 1	MIP 1	Blank 1	MIP 2	Blank 2	MIP 2	Blank 2	MIP 2	Blank 2
MAA (25 µmol)	206	206	206	206	206	206	187	187	187	187	187	187
MAA (50 µmol)	208	208	208	208	208	208	189	189	189	189	189	189
NVP (25 µmol)	207	207	207	207	207	207	188	188	188	188	188	188
NVP (50 µmo)l	209	209	209	209	209	209	190	190	190	190	190	190
VPY (50 µmol)	209	209	209	209	209	209	190	190	190	190	190	190
HEMA (50 µmol)	210	210	210	210	210	210	191	191	191	191	191	191
MMA (100 µmol)	209	209	209	209	209	209	190	190	190	190	190	190
No functional monomer	204	204	204	204	204	204	185	185	185	185	185	185

Table 6.10: Composition and final volume (µL) of the mixture per well.

Screening of the library

First screening

The polymers were washed by sonication for 45 min in 300 μL of toluene as previously described. The supernatant was removed from each well after HPLC monitoring. The first screening made with automated reversed phase HPLC (λ = 260 nm, isocratic gradient: MeCN / TFA 0.042% at 0.5 mL/min with run time of 4 min) was carried out by injecting 5 μL of the supernatant. The screening with analytical reversed phase HPLC (λ = 260 nm, isocratic gradient: MeCN / TFA 0.042% at 0.3 mL/min with run time 3 min) was carried out by injecting 10 μL of sample diluted 100 folds in acetonitrile (Table 6.11).

Rebinding experiment

The rebinding experiment was performed by addition of 300 μL of a solution of H-Phe-NHPh **(3)** (0.1 μmole) in toluene and analysed by analytical reversed phase HPLC as described above (Table 6.11).

	First screening					
	MAA (2 eq)/EGDMA (83%)	**MAA (2 eq)/EGDMA (70%)**	**MAA (4eq)/EGDMA (71%)**	**MAA (4eq)/EGDMA (55%)**	**NVP (2eq)/EGDMA(83%)**	
1st washing	2034	1994	1148	923	2509	
2nd washing	3504	2265	2002	1274	4607	
3rd washing	4391	2850	2823	1624	6370	
	NVP(2eq)/EGDMA (70%)	**NVP(4eq)/EGDMA (70%)**	**NVP(4 eq)/EGDMA (55%)**	**VPY (4eq)/EGDMA (70%)**	**VPY (4e)/EGDMA (55%)**	
1st washing	2531	2113	2377	2490	2230	
2nd washing	4704	4201	4494	4695	4152	
3rd washing	6192	5856	6008	6586	5435	
	HEMA (4eq)/EGDMA (70%	**HEMA (4eq)/HEMA (55%)**	**MMA (4eq)/EGDMA (70%)**	**MMA (4eq)/EGDMA (55%)**	**EGDMA (83%)**	**EGDMA (50%)**
1st washing	2272	2400	2482	2473	248	2314
2nd washing	4096	3834	4476	3991	2610	4295
3rd washing	5028	4098	5632	4626	4521	5257
	Rebinding experiment					
	MAA (2 eq)/EGDMA (83%)	**MAA (2 eq)/EGDMA (70%)**	**MAA (4eq)/EGDMA (71%)**	**MAA (4eq)/EGDMA (55%)**	**NVP (2eq)/EGDMA (83%)**	
MIP	0	0	0	0	72	
Blank	70	82	58	72	76	
	NVP(2eq)/EGDMA (70%)	**NVP(4eq)/EGDMA (70%)**	**NVP(4 eq)/EGDMA (55%)**	**VPY (4eq)/EGDMA (70%)**	**VPY (4e)/EGDMA (55%)**	
MIP	80	75	68	69	84	
Blank	81	72	62	77	76	
	HEMA (4eq)/EGDMA (70%	**HEMA (4eq)/HEMA (55%)**	**MMA (4eq)/EGDMA (70%)**	**MMA (4eq)/EGDMA (55%)**	**EGDMA (83%)**	**EGDMA (50%)**
MIP	77	100	80	88	79	76
Blank	80	91	86,5	82	86	92

Table 6.11: HPLC data (sum of peak areas of template (mAu at λ = 260 nm)) for first screening and rebinding experiment.

6.4.4.d The solvatation effect and the equivalent of functional monomer on the imprint process

Synthesis of the library

Eight stock solutions were prepared by mixing MAA, EGDMA, AIBN and toluene in different proportions to obtain four different molar ratios of solvent / MAA: 50, 27, 13 and 9 (see Table 6.12).

Molar ratio solvent/MAA	Solvent mL, (mmoles)	MAA µL, (mmoles)	EGDMA mL, (mmoles)	AIBN mg, (µmoles)	Final volume (mL)
50	2.6 (24.4)	38 (0.4)	0.17 (1.1)	9 (55)	2.8
	15.6 (146.4)	228 (2.7)	1 (6.7)	54.5 (328)	16.9
27	1.3 (12.2)	38 (0.4)	0.17 (1.1)	9 (55)	1.5
	7.8 (73.1)	228 (2.7)	1 (6.7)	54.5 (328)	9.0
13	0.64 (6.1)	38 (0.4)	0.17 (1.1)	9 (55)	0.85
	3.9 (36.3)	228 (2.7)	1 (6.7)	54.5 (328)	5.1
9	0.43 (4.0)	38 (0.4)	0.17 (1.1)	9 (55)	0.6
	2.6 (24.2)	228 (2.7)	1 (6.7)	54.5 (328)	3.8

Table 6.12: Composition of the stock solutions.

Each solution was divided to obtain stock MIP solution and the corresponding blank solution. The MIP solutions were obtained by adding different amounts of template H-Phe-NHPh **(3)** (Table 6.13).

Ratio solvent/ MAA	Volume of stock solutions (mL)	Volume of MIP solution (mL) / Volume of blank solution (mL)	H-Phe-NHPh (3) (mg) added to MIP solution (corres-ponding eq. MAA)	Volume (µL) of MIP solution and corresponding blank per well
50	2.8	1.4	27 (2)	155
		1.4	-	155
	16.9	2.8 (x 3)	27 (4) 18 (6) 13.5 (8)	311 267 313
		2.8 (x 3)	- - -	311 267 313
27	1.5	0.75	27 (2)	84
		0.75	-	84
	9.0	1.50	27 (4) 18 (6) 13.5 (8)	167 251 336
		1.50	- - -	167 251 336
13	0.85	0.40	27 (2)	47
		0.40	-	47
	5.1	0.85 (x 3)	27 (4) 18 (6) 13.5 (8)	94.5 142 190
		0.85 (x 3)	- - -	94.5 142 190
9	0.6	0.32	27 (2)	35
		0.32	-	35
	3.8	0.63 (x 3)	27 (4) 18 (6) 13.5 (8)	70 104 140
		0.63 (x 3)	- - -	70 104 140

Table 6.13: Composition and volume of the mixture by well.

The composition and the final volume of the mixture by well are shown in Table 6.14.

Molar Ratio / MAA eq.	50			27			13			9		
MIP 2 eq.	155	155	155	84	84	84	47	47	47	35	35	35
Blank 2 eq.	155	155	155	84	84	84	47	47	47	35	35	35
MIP 4 eq.	311	311	311	167	167	167	94	94	94	70	70	70
Blank 4 eq.	311	311	311	167	167	167	94	94	94	70	70	70
MIP 6 eq.	267	267	267	251	251	251	142	142	142	104	104	104
Blank 6 eq.	267	267	267	251	251	251	142	142	142	104	104	104
MIP 8 eq.	313	313	313	336	336	336	190	190	190	140	140	140
Blank 8 eq.	313	313	313	336	336	336	190	190	190	140	140	140

Table 6.14: Composition and final volume of the mixture by well (molar ratio of solvent / MAA).

Screening of the library

First screening

The polymers were washed by sonication for 30 min in toluene (300 μL) as above. The content of extracted template was analysed by automated reversed phase HPLC (λ = 260 nm, isocratic gradient: MeCN / TFA 0.042% for 4.3 min) by injecting 5 μL of the supernatant from each well. The screening with analytical reversed phase HPLC (λ = 260 nm, isocratic gradient: MeCN / TFA 0.042% at 0.3 mL/min with run time 3 min) was carried out by injecting 10 μL of sample diluted 100 folds in acetonitrile (Table 6.15).

Rebinding experiment

The rebinding experiment was carried out by the addition of 300 μL of template solution (1 or 0.1 μmole, in toluene) to each well. The supernatant of each well was monitored by analytical and semi-prep reversed phase HPLC (λ = 260 nm) by runs of 2.5 and 4 min (isocratic gradient: MeCN / TFA 0.042%). For the evaluation by analytical HPLC the samples were prepared from 10 μL of the supernatant added to 1 mL of MeCN (10 μL were injected). For the semi-prep HPLC the supernatant (5 μL) was directly injected from the 96 well-plate (Table 6.15).

	First screening									
	50/2	**27/2**	**13/2**	**9/2**	**50/4**	**27/4**	**13/4**	**9/4**	**50/6**	**27/6**
1st washing	22000	45000	22302	23824	12352	12240	14079	12002	9270	7673
2nd washing	24059	51000	23714	25467	12967	13164	15054	13135	9952	8398
3rd washing	24382	52000	24064	25967	13115	13457	15354	13348	10153	8648
	13/6	**9/6**	**50/8**	**27/8**	**13/8**	**9/8**				
1st washing	4836	3644	2606	3302	2620	3454				
2nd washing	5390	4693	3062	3668	3025	3857				
3rd washing	5574	4893	3173	3748	3102	3988				
	Rebinding experiment									
	50/2	**27/2**	**13/2**	**9/2**	**50/4**	**27/4**	**13/4**	**9/4**	**50/6**	**27/6**
MIP	1574	1300	1414	1472	1366	1504	1300	1371	1232	1271
Blank	1707	1655	1601	1600	1457	1600	1500	1500	1205	1000
	13/6	**9/6**	**50/8**	**27/8**	**13/8**	**9/8**				
MIP	1306	1425	1134	1228	1278	1300				
Blank	1525	1627	1095	1006	1450	1300				

*Table 6.15: HPLC data (sum of peak areas of template (mAu at λ = 260 nm)) for first screening and rebinding experiment. (**A / B**: **A** = molar ratio (toluene / MAA), **B** = MAA eq.).*

6.5 EXPERIMENTAL TO CHAPTER 4

6.5.1 Synthesis of dipeptides in solution

6.5.1.a Synthesis of amino acid methylester HCl salts (16-18)[286]

General procedure for the synthesis amino acid methyl ester HCl salt

The amino acid (18 mmol) was dissolved in methanol (60 mL) at –15°C and thionyl chloride (2 mL, 26 mmol) was added dropwise with stirring. The reaction was allowed to warm to RT for 4 h, then concentrated to afford a white crystalline solid.

H-βAla-OMe, HCl (16)[287]

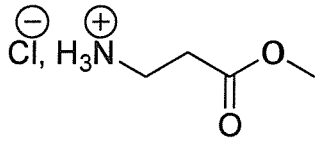

^{1}H (300 MHz, CD_3OD): δ = 2.78 (t, 2H, *J* = 7, $C\underline{H}_2$-CO_2Me), 3.30 (t, 2H, *J* = 7, NH_3^+-$C\underline{H}_2$), 3.75 (s, 3H, O-$C\underline{H}_3$).

^{13}C (75.5 MHz, CD_3OD): δ = 32.4 ($\underline{C}H_2$-CO_2Me), 36.8 (NH_3^+-$\underline{C}H_2$), 53.0 (O-$\underline{C}H_3$), 173.0 ($\underline{C}O_2Me$).

IR: ν = 2884 - 2831 (alkyl), 1725 (C=O ester) cm^{-1}.

M/z (ES^+): 104 (92%) $[M+H]^+$, 145 (100%) $[M+H+MeCN]^+$.

Mp.: 100 – 102°C (Lit.: 103 – 105°C).[287]

Yield: quantitative (2.45 g) as a white solid.

H-γAbu-OMe, HCl (17)[286]

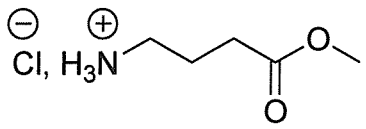

^{1}H (300 MHz, CD_3OD): δ = 1.25 (tt, 2H, *J* = 7, *J* = 7, CH_2-$C\underline{H}_2$-CH_2), 1.80 (t, 2H, *J* = 7, $C\underline{H}_2$-CO_2Me), 2.30 (t, 2H, *J* = 7, $C\underline{H}_2$-NH_3^+), 4.20 (s, 3H, O-$C\underline{H}_3$).

^{13}C (75.5 MHz, CD_3OD): δ = 23.6 (CH_2-$\underline{C}H_2$-CH_2), 31.3 ($\underline{C}H_2$-CO), 40.0 ($\underline{C}H_2$-NH_3^+), 52.2 (O-$\underline{C}H_3$), 174.0 ($\underline{C}O_2CH_3$).

IR: ν = 2952 (alkyl), 1727 (C=O ester) cm^{-1}.

M/z (ES^+): 118 (100%) $[M+H]^+$, 159 (28%) $[M+H+MeCN]^+$.

Mp.: 98 – 100°C (Lit.: 97 – 101°C).[286]

Yield: quantitative (2.9 g) as a white solid.

H-εAhx-OMe, HCl (18)

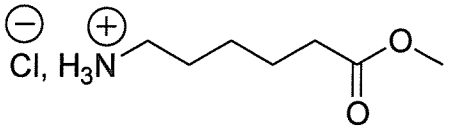

^{1}H (400 MHz, CD_3OD): δ = 1.44 (tt, 2H, *J* = 7, *J* = 7, NH_3^+-$(CH_2)_2$-$C\underline{H}_2$), 1.63 – 1.72 (m, 4H, CH_2-$C\underline{H}_2$ -NH_3^+ and $C\underline{H}_2$-CH_2-CO_2Me), 2.38 (t, 2H, *J* = 7, $C\underline{H}_2$-CO_2Me), 2.94 (t, 2H, *J* = 7, NH_3^+-$C\underline{H}_2$), 3.67 (s, 3H, O-$C\underline{H}_3$).

^{13}C (100 MHz, CD_3OD): δ = 25.3 ($\underline{C}H_2$-CH_2-CO_2Me), 26.8 (NH_3^+-$(CH_2)_2$-$\underline{C}H_2$), 28.1 ($\underline{C}H_2$-CO_2Me), 34.3 (CH_2-$\underline{C}H_2$-NH_3^+), 40.5 (NH_3^+-$\underline{C}H_2$), 52.0 (O-$\underline{C}H_3$), 175.5 ($\underline{C}O_2Me$).

IR: ν = 2952 - 2662 (alkyl), 1727 (C=O), 1516 (NH) cm^{-1}.

M/z (ES^+): 146 (100%) $[M+H]^+$, 187 (20%) $[M+H+MeCN]^+$.

HRMS (ES^+): $C_7H_{15}N_1O_2$ $[M+H]^+$ Calc. 146.1176, found 146.1175.

Mp.: 78 – 80°C.

HPLC (ELS): 3.18 min.

Yield: quantitative (3.78 g) as a white solid.

6.5.1.b Synthesis of the Boc protected methyl ester dipetides (19-26)[288]

General procedure for the synthesis of Boc protected methylester dipeptide

A solution of amino acid methyl ester HCl salt (5 mmol) in dry THF (5 mL) was neutralised with triethylamine (NEt_3) (700 µL, 5 mmol) and stirred for 40 min under nitrogen.

To a solution of Boc protected amino acid (5 mmol) in dry THF (10 mL) cooled at –15°C, was added isobutyl chloroformate (IBCF) (648 µL, 5 mmol), NEt_3 (700 µL, 5 mmol) then stirred for 40 min at this temperature under nitrogen. A solution of the amino acid methyl ester described above was added to the reaction mixture and was allowed to warm to RT and stirred for 2 h. The hydrochloride salt of triethylamine was removed by filtration and the solution concentrated *in vacuo* then purified by silica chromatography to yield the title compound.

Boc-Gly-βAla-OMe (19)[289]

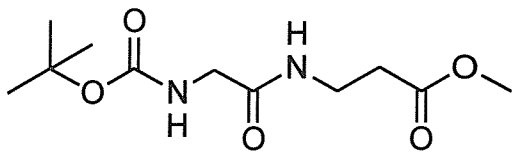

^{1}H (300 MHz, $CDCl_3$): δ = 1.33 (s, 9H, $(C\underline{H}_3)_3C$), 2.45 (t, 2H, *J* = 6, $C\underline{H}_2$-CO_2Me), 3.40 (td, 2H, *J* = 6, *J* = 7, NH-$C\underline{H}_2$-CH_2), 3.55 (s, 3H, O-$C\underline{H}_3$), 3.70 (d, 2H, *J* = 6, NH-$C\underline{H}_2$-CO), 5.70 (br t, 1H, N$\underline{H}$-CH_2-CH_2), 7.40 (t, 1H, *J* = 6, Boc-N$\underline{H}$).

^{13}C (75.5 MHz, $CDCl_3$): δ = 28.3 ($(\underline{C}H_3)_3C$), 33.8 ($\underline{C}H_2$-CO_2Me), 34.9 (NH-$\underline{C}H_2$), 44.1 (NH-$\underline{C}H_2$-CO), 51.8 (CO_2-$\underline{C}H_3$), 71.0 ($(CH_3)_3\underline{C}$), 156.2 (O$\underline{C}$O-NH), 170.0 ($\underline{C}$O-NH), 172.8 ($\underline{C}O_2Me$).

IR: ν = 3308 - 3076 (NH), 2977 - 2933 (alkyl), 1717 (C=O ester), 1655 (C=O amide), 1522 (NH) cm^{-1}.

M/z (ES^+): 261 (15%) $[M+H]^+$, 283 (80%) $[M+Na]^+$.

HPLC (ELS): 7.35 min.

R_f: 0.4 (AcOEt).

Yield: 84% (1.1 g) as a yellow oil.

Boc-Gly-γAbu-OMe (20)[289]

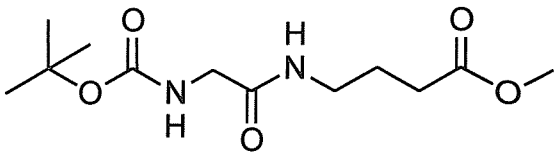

^{1}H (300 MHz, $CDCl_3$): δ = 1.45 (s, 9H, $(C\underline{H}_3)_3C$), 1.85 (tt, 2H, *J* = 7, *J* = 7, NH-CH_2-$C\underline{H}_2$), 2.38 (t, 2H, *J* = 7, $C\underline{H}_2$-CO_2Me), 3.31 (td, 2H, *J* = 6, *J* = 7, NH-$C\underline{H}_2$-CH_2), 3.68 (s, 3H, O-$C\underline{H}_3$), 3.80 (s, 2H, NH-$C\underline{H}_2$-CO), 5.28 (br s, 1H, N$\underline{H}$-CO), 6.65 (br s, 1H, Boc-N$\underline{H}$).

^{13}C (75.5 MHz, $CDCl_3$): δ = 24.6 (NH-CH_2-$\underline{C}H_2$), 28.4 ($(\underline{C}H_3)_3C$), 31.4 ($\underline{C}H_2$-CO_2Me), 39.9 (NH-$\underline{C}H_2$-CH_2), 44.5 (NH-$\underline{C}H_2$-CO), 51.8 (O-$\underline{C}H_3$), 69.8 ($(CH_3)_3\underline{C}$), 157.0 (O$\underline{C}$O-NH), 169.8 ($\underline{C}$O-NH), 173.9 ($\underline{C}O_2Me$).

IR: ν = 3314 (NH), 2973 - 2934 (alkyl), 1717 (C=O ester), 1655 (C=O amide).

M/z (ES^+): 275 (20%) $[M+H]^+$, 297 (100%) $[M+Na]^+$, 313 (8%) $[M+K]^+$.

R_f: 0.47 (AcOEt).

Yield: 93% (1.4 g) as a yellow oil.

Boc-Gly-εAhx-OMe (21)[290]

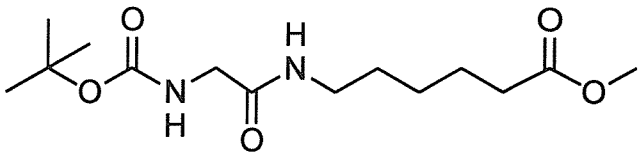

^{1}H (300 MHz, $CDCl_3$): δ = 1.30 – 1.35 (m, 2H, NH-$(CH_2)_2$-$C\underline{H}_2$), 1.42 (s, 9H, $(C\underline{H}_3)_3C$), 1.52 (tt, 2H, *J* = 7, *J* = 7, NH-CH_2-$C\underline{H}_2$), 1.63 (tt, 2H, *J* = 7, *J* = 7, $C\underline{H}_2$-CH_2-CO_2Me), 2.30 (t, 2H, *J* = 7, $C\underline{H}_2$-CO_2Me), 3.25 (td, 2H, *J* = 6, *J* = 7, NH-$C\underline{H}_2$-CH_2), 3.65 (s, 3H, O-$C\underline{H}_3$), 3.75 (s, 2H, NH-$C\underline{H}_2$-CO), 5.35 (br s, 1H, CO-N$\underline{H}$), 6.45 (br s, 1H, Boc-N$\underline{H}$).

^{13}C (75.5 MHz, $CDCl_3$): δ = 24.5 ($\underline{C}H_2$-CH_2-CO_2Me), 26.4 (NH-$(CH_2)_2$-$\underline{C}H_2$), 28.4 ($(\underline{C}H_3)_3C$), 29.2 (NH-CH_2-$\underline{C}H_2$), 33.9 ($\underline{C}H_2$-CO_2Me), 39.3 (NH-$\underline{C}H_2$-CH_2), 44.5 (NH-$\underline{C}H_2$-CO), 51.6 (O-$\underline{C}H_3$), 68.1 ($(CH_3)_3\underline{C}$), 156.3 (O$\underline{C}$O-NH), 169.6 ($\underline{C}$O-NH), 174.2 ($\underline{C}O_2Me$).

IR: ν = 3317 (NH), 2954 - 2873 (alkyl), 1735 (C=O ester), 1718 (C=O urethane), 1655 (C=O amide).

M/z (ES$^+$): 303 (15%) $[M+H]^+$, 325 (100%) $[M+Na]^+$, 341 (7%) $[M+K]^+$.

R_f: 0.5 (AcOEt).

Yield: 92% (1.4 g) as an orange oil.

Boc-Phe-βAla-OMe (22)[291]

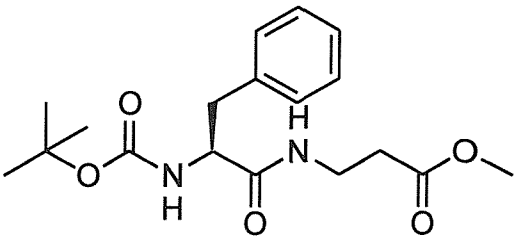

^{1}H (400 MHz, $CDCl_3$): δ = 1.30 (s, 9H, $(C\underline{H}_3)_3C$), 2.23 - 2.42 (m, 2H, $C\underline{H}_2$-CO_2Me), 2.95 (m, 2H, $C\underline{H}_2$-$C^{\alpha}H$), 2.24 - 3.33 (m, 1H, NH-C$\underline{H}$H), 3.37 - 3.46 (m, 1H, NH-CH$\underline{H}$), 3.55 (s, 3H, O-$C\underline{H}_3$), 4.20 (br s, 1H, $C^{\alpha}\underline{H}$), 5.05 (s, 1H, N$\underline{H}$-$C^{\alpha}H$), 6.32 (s, 1H, N$\underline{H}$-CH_2), 7.08 - 7.23 (m, 5H, C$\underline{H}$ aromatic).

^{13}C (100 MHz, $CDCl_3$): δ = 26.8 ($(\underline{C}H_3)_3C$), 32.2 ($\underline{C}H_2$-CO_2Me), 33.3 ($\underline{C}H_2$-$C^{\alpha}H$), 37.0 (NH-$\underline{C}H_2$), 50.3 (O-$\underline{C}H_3$), 54.5 ($\underline{C}^{\alpha}H$), 78.6 ($(CH_3)_3\underline{C}$), 125.5 (C$\underline{H}$ aromatic), 127.2 (C$\underline{H}$ aromatic), 127.6 (C$\underline{H}$ aromatic), 135.3 ($\underline{C}$ aromatic), 154.0 (O-$\underline{C}$O-NH), 169.8 ($C^{\alpha}H$-$\underline{C}$O-NH), 171.1 ($\underline{C}O_2Me$).

IR: ν = 3316 (NH), 3027 (CH aromatic), 2933 (CH alkyl), 1735 (C=O ester), 1694 (C=O amide), 1650 (C=C aromatic) cm^{-1}.

M/z (ES$^+$): 351 (20%) $[M+H]^+$, 373 (100%) $[M+Na]^+$, 389 (5%) $[M+K]^+$.

Mp.: 65 – 68°C.

HPLC (λ=220 nm): 9.7 min.

R_f: 0.78 (AcOEt).

Yield: 91% (1.6 g) as a white solid.

Boc-Phe-γAbu-OMe (23)[291]

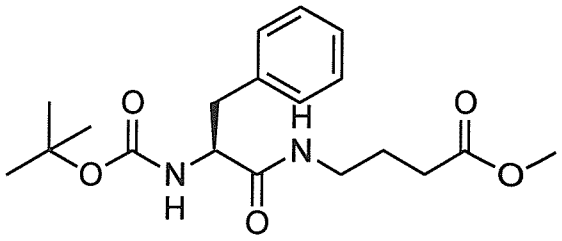

^{1}H (400 MHz, $CDCl_3$): δ = 1.30 (s, 9H, $(C\underline{H}_3)_3C$), 1.63 (tt, 2H, J= 7, J= 7, NH-CH_2-$C\underline{H}_2$), 2.14 (t, 2H, J= 7, $C\underline{H}_2$-CO_2Me), 2.94 (A<u>B</u>X system, 1H, J^{AX} = 7, J^{AB} = 14,C<u>H</u>H-$C^{\alpha}H$), 2.99 (A<u>B</u>X system, 1H, J^{BX} = 7, J^{BA} = 14, C<u>H</u>H-$C^{\alpha}H$), 3.09 – 3.16 (m, 2H, NH-$C\underline{H}_2$), 3.57 (s, 3H, O-$C\underline{H}_3$), 4.20 (AB<u>X</u> system, 1H, J^{XA} = J^{XB} = 7, $C^{\alpha}\underline{H}$), 5.03 (s, 1H, N<u>H</u>-$C^{\alpha}H$) 5.98 (s, 1H, N<u>H</u>-CH_2), 7.10 – 7.24 (m, 5H, C<u>H</u> aromatic).

^{13}C (100 MHz, $CDCl_3$): δ = 19.3 (NH-CH_2-$\underline{C}H_2$), 24.8 ($\underline{C}H_2$-CO_2Me), 28.6 ($(\underline{C}H_3)_3C$), 31.5 ($\underline{C}H_2$-$C^{\alpha}H$), 39.1 (NH-$\underline{C}H_2$), 52 (O-$\underline{C}H_3$), 56.4 ($\underline{C}^{\alpha}H$), 70.1 ($(CH_3)_3\underline{C}$), 127.3 (<u>C</u>H aromatic), 128.9 (<u>C</u>H aromatic), 129.7 (<u>C</u>H aromatic), 137.1 (<u>C</u> aromatic), 155.7 (O<u>C</u>O-NH), 171.6 ($C^{\alpha}H$-<u>C</u>O-NH), 174.0 ($\underline{C}O_2Me$).

IR: ν = 3337 (NH), 3022 (CH aromatic), 2953 - 2874 (CH alkyl), 1731 (C=O ester), 1654 (C=O amide), 1516 (C=C aromatic).

M/z (ES^+): 365 (14%) $[M+H]^+$, 387 (100%) $[M+Na]^+$, 403 (4%) $[M+K]^+$, 428 (8%) $[M+Na+MeCN]^+$, 751 (68%) $[2M+Na]^+$.

HPLC (λ=220 nm): 9.8 min.

R_f: 0.24 (AcOEt / PE: 1/1).

Yield: 90% (1.6 g) as a white solid.

Boc-Trp-βAla-OMe (24)[291]

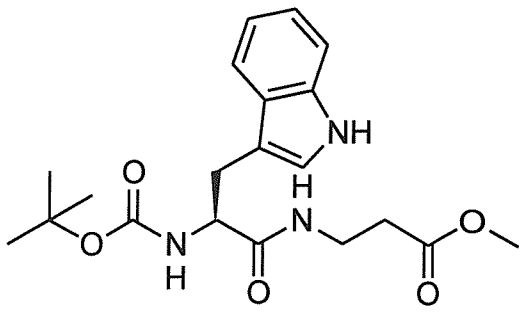

^{1}H (400 MHz, $CDCl_3$): δ = 1.35 (s, 9H, $(C\underline{H}_3)_3C$), 2.08 – 2.20 (m, 1H, $C\underline{H}H\text{-}CO_2Me$), 2.22 – 2.32 (m, 1H, $CH\underline{H}\text{-}CO_2Me$), 3.07 (ABX system, 1H, J^{AX} = 7, J^{AB} = 14, $C\underline{H}H\text{-}C^{\alpha}H$), 3.17 – 3.28 (m, 2H, $CH\underline{H}\text{-}C^{\alpha}H$ and NH-$C\underline{H}H$), 3.35 (m, 1H, NH-$CH\underline{H}$), 3.50 (s, 3H, O-$C\underline{H}_3$), 4.30 (br s, 1H, $C^{\alpha}\underline{H}$), 5.10 (br s, 1H, $N\underline{H}\text{-}C^{\alpha}H$), 6.15 (br s, 1H, $N\underline{H}\text{-}CH_2$), 6.95 (s, 1H, C$\underline{H}$ indole), 7.04 (dd, 1H, J = 8, J = 8, C$\underline{H}$ aromatic), 7.20 (dd, 1H, J = 8, J = 8, C$\underline{H}$ aromatic), 7.28 (d, 1H, J = 8, C$\underline{H}$ aromatic), 7.57 (d, 1H, J = 8, C$\underline{H}$ aromatic), 8.15 (br s, 1H, N$\underline{H}$ indole).

^{13}C (100 MHz, $CDCl_3$): δ = 28.7 ($(\underline{C}H_3)_3C$), 28.9 ($\underline{C}H_2\text{-}C^{\alpha}H$), 33.9 ($\underline{C}H_2\text{-}CO_2Me$), 35.1 (NH-$\underline{C}H_2$), 52.0 (O-$\underline{C}H_3$), 55.7 ($\underline{C}^{\alpha}H$), 80.5 ($(CH_3)_3\underline{C}$), 111.1 (C$\underline{H}$ aromatic), 111.5 (C aromatic), 119.3 (C$\underline{H}$ aromatic), 120.1 (C$\underline{H}$ aromatic), 122.7 (C$\underline{H}$ aromatic), 123.4 (C$\underline{H}$ aromatic), 127.8 (C aromatic), 136.6 (C aromatic), 155.8 (O-$\underline{C}$O-NH), 172.0 ($\underline{C}$O), 172.8 ($\underline{C}$O).

IR: ν = 3319 (NH), 3054 (CH aromatic), 2977 - 2930 (CH alkyl), 1717 (C=O ester), 1657 (C=O amide) cm^{-1}.

M/z (ES^+): 390 (20%) $[M+H]^+$, 412 (100%) $[M+Na]^+$, 801 (55%) $[2M+Na]^+$.

HPLC (λ=220 nm): 9.6 min.

R_f: 0.79 (AcOEt).

Yield: 76% (1.1 g) as a yellow oil.

Boc-Trp-γAbu-OMe (25)[291]

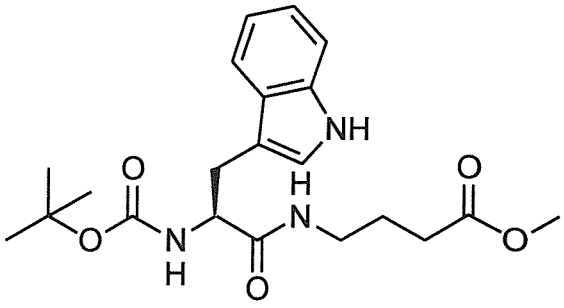

^{1}H (400 MHz, $CDCl_3$): δ = 1.35 (s, 9H, $(C\underline{H}_3)_3C$), 1.51 (tt, 2H, *J* = 7, *J* = 7, NH-CH_2-$C\underline{H}_2$), 2.02 (t, 2H, *J* = 7, $C\underline{H}_2$-CO_2Me), 3.02 (m, 1H, NH-$C\underline{H}$H), 3.04 – 3.16 (m, 2H, $C\underline{H}$H-C^{α}H and NH-CH$\underline{H}$), 3.22 (A$\underline{B}$X system, 1H, J^{BX} = 7, J^{BA} = 14, CH$\underline{H}$-C^{α}H), 3.55 (s, 3H, O-$C\underline{H}_3$), 4.31 (br s, 1H, $C^{\alpha}\underline{H}$), 5.17 (br s, 1H, N$\underline{H}$-C^{α}H), 5.90 (br s, 1H, N$\underline{H}$-CH_2), 6.91 (s, 1H, C$\underline{H}$ indole), 7.03 (dd, 1H, *J* = 8, *J* = 8, C$\underline{H}$ aromatic), 7.10 (dd, 1H, *J* = 8, *J* = 8, C$\underline{H}$ aromatic), 7.28 (d, 1H, *J* = 8, C$\underline{H}$ aromatic), 7.57 (d, 1H, *J* = 8, C$\underline{H}$ aromatic), 8.40 (br s, 1H, N$\underline{H}$ indole).

^{13}C (100 MHz, $CDCl_3$): δ = 26.0 (NH-CH_2-$\underline{C}H_2$), 28.7 ($(\underline{C}H_3)_3C$), 29.0 ($\underline{C}H_2$-CO_2Me), 31.5 ($\underline{C}H_2$-C^{α}H), 39.1 (NH-$\underline{C}H_2$), 52.0 (O-$\underline{C}H_3$), 68.3 ($\underline{C}^{\alpha}$H), 70.1 ($(CH_3)_3\underline{C}$), 111.0 (C$\underline{H}$ aromatic), 111.6 ($\underline{C}$ aromatic), 119.2 (C$\underline{H}$ aromatic), 120.0 (C$\underline{H}$ aromatic), 122.6 (C$\underline{H}$ aromatic), 123.6 (C$\underline{H}$ aromatic), 127.8 ($\underline{C}$ aromatic), 136.6 ($\underline{C}$ aromatic), 155.8 (O$\underline{C}$O-NH), 172.3 ($\underline{C}$O), 174.0 ($\underline{C}O_2Me$).

IR: ν = 3317 (NH), 2953 (CH), 1690 (C=O ester), 1654 (C=O amide), 1648 (C=C) cm^{-1}.

M/z (ES^+): 426 (22%) $[M+Na]^+$, 463 (100%) $[M+CH_3CO_2H]^+$.

R_f: 0.7 (AcOEt).

HPLC (λ=220 nm): 9.72 min.

Yield: 90% (1.82 g) as a yellow oil.

Boc-Trp-εAhx-OMe (26)[291]

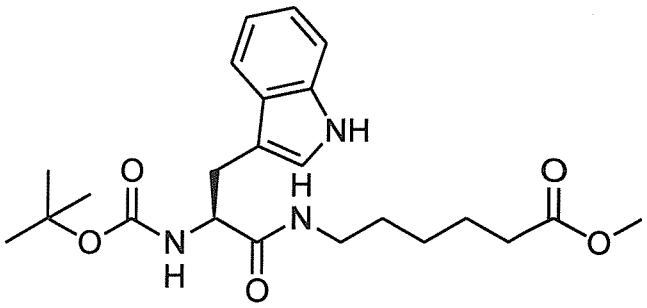

^{1}H (400 MHz, $CDCl_3$): δ = 1.00 (tt, 2H, *J* = 7, *J* = 7, NH-$(CH_2)_2$-$C\underline{H}_2$), 1.23 (tt, 2H, *J* = 7, *J* = 7, NH-CH_2-$C\underline{H}_2$), 1.35 (s, 9H, $(C\underline{H}_3)_3C$), 1.44 (tt, 2H, *J* = 7, *J* = 7, $C\underline{H}_2$-CH_2-CO_2Me), 2.16 (t, 2H, *J* = 7, $C\underline{H}_2$-CO_2Me), 2.93 – 3.12 (m, 3H, $C\underline{H}H$-$C^{\alpha}H$ and NH-$C\underline{H}_2$-CH_2), 3.25 (AB<u>X</u> system, 1H, J^{BX} = 7, J^{BA} = 14, $CH\underline{H}$-$C^{\alpha}H$), 3.60 (s, 3H, O-$C\underline{H}_3$), 3.67 (AB<u>X</u> system, 1H, $J^{XA} = J^{XB}$ = 7, $C^{\alpha}\underline{H}$), 7.05 (dd, 1H, *J* = 8, *J* = 8, C<u>H</u> aromatic), 7.12 (dd, 1H, *J* = 8, *J* = 8, C<u>H</u> aromatic), 7.19 (s, 1H, C<u>H</u> indole), 7.29 (d, 1H, *J* = 8, C<u>H</u> aromatic), 7.80 (d, 1H, *J* = 8, C<u>H</u> aromatic), 8.34 (br s 1H, N<u>H</u> indole).

^{13}C (100 MHz, $CDCl_3$): δ = 24.9 ($\underline{C}H_2$-CH_2-CO_2Me), 26.6 (NH-$(CH_2)_2$-$\underline{C}H_2$), 28.7 (($\underline{C}H_3)_3C$), 29.0 ($\underline{C}H_2$-$C^{\alpha}H$), 29.2 (NH-CH_2-$\underline{C}H_2$), 34.2 ($\underline{C}H_2$-CO_2Me), 39.5 (NH-$\underline{C}H_2$), 51.9 (O-$\underline{C}H_3$), 68.3 ($\underline{C}^{\alpha}H$), 76.1 (($CH_3)_3\underline{C}$), 111.1 (<u>C</u>H aromatic), 111.6 (<u>C</u> aromatic), 119.3 (<u>C</u>H aromatic), 120.0 (<u>C</u>H aromatic), 122.5 (<u>C</u>H aromatic), 123.6 (<u>C</u>H aromatic), 127.8 (<u>C</u> aromatic), 136.7 (<u>C</u> aromatic), 155.8 (O<u>C</u>O-NH), 171.9 (<u>C</u>O-NH), 174.6 ($\underline{C}O_2Me$).

IR: ν = 3313 - 3051 (NH), 2932 - 2868 (CH alkyl), 1733 (C=O ester), 1696 (C=O amide), 1540 (C=C aromatic) cm^{-1}.

M/z (ES^+): 454 (5%) $[M+Na]^+$.

R_f: 0.2 (AcOEt / PE: 1:1).

HPLC (λ=220 nm): 10.5 min.

Yield: 85% (1.7 g) as a yellow oil.

6.5.1.c Methyl ester dipeptide, TFA salt (27-34)

General procedure for the cleavage of the Boc protecting group

To a solution of the protected Boc amino acid in DCM was dropwised TFA (8 eq) and the mixture was stirred for 2 h. The solution was concentrated *in vacuo*. The crude product was purified by crystallisation from cold ether to afford the title compound as a salt.

H-Gly-βAla-OMe, TFA (27)[289]

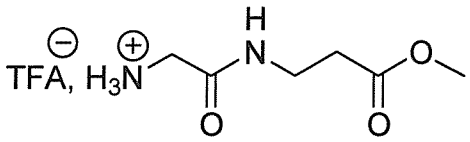

^{1}H (300 MHz, CD_3OD): δ = 2.43 (t, 2H, *J* = 7, $C\underline{H}_2$-CO_2Me), 3.45 (t, 2H, *J* = 7, NH-$C\underline{H}_2$), 3.63 (s, 3H, O-$C\underline{H}_3$), 3.67 (s, 2H, $C\underline{H}_2$-NH_3^+).

^{13}C (75.5 MHz, CD_3OD): δ = 34.4 ($\underline{C}H_2$-CO_2Me), 36.3 (NH-$\underline{C}H_2$), 41.4 ($\underline{C}H_2$-NH_3^+), 52.2 (O-$\underline{C}H_3$), 167.5 ($\underline{C}O$-NH), 173.7 ($\underline{C}O_2Me$).

IR: ν = 3022 (NH_3^+), 2964 - 2837 (alkyl), 1745 (C=O ester), 1670 (C=O amide) cm^{-1}.

M/z (ES^+): 178 (5 %) $[M+Na]^+$.

Mp.: 45 – 47°C.

Micro-analysis: $C_8H_{13}N_2O_3F_3$ % Calc: C 35.04, H 4.78, N 10.21. % Found: C 35.04, H 4.88, N 9.99.

Yield: 88% (894 mg) as a white cream powder.

H-Gly-γAbu-OMe, TFA (28)[289]

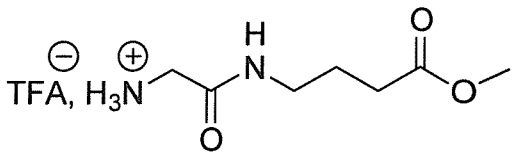

^{1}H (400 MHz, CD_3OD): δ = 1.79 (tt, 2H, *J* = 7, *J* = 7, NH-CH_2-$C\underline{H}_2$), 2.35 (t, 2H, *J* = 7, $C\underline{H}_2$-CO_2Me), 3.23 (t, 2H, *J* = 7, NH-$C\underline{H}_2$), 3.60 (s, 3H, O-$C\underline{H}_3$), 3.60 (s, 2H, $C\underline{H}_2$-NH_3^+).

^{13}C (100 MHz, CD_3OD): δ = 25.5 (NH-CH_2-$\underline{C}H_2$), 31.8 ($\underline{C}H_2$-CO_2Me), 39.6 (NH-$\underline{C}H_2$), 41.3 (NH-$\underline{C}H_2$-CO), 52.0 (O-$\underline{C}H_3$), 167.2 ($\underline{C}O$-NH), 175.1 ($\underline{C}O_2Me$).

IR: ν = 3300 (NH), 3124 (NH_3^+), 2956 - 2851 (alkyl), 1721 (C=O ester), 1664 (C=O amide), 1573 (NH) cm^{-1}.

M/z (ES^+): 175 (7%) $[M+H]^+$, 288 (6%) $[M+TFA]^+$.

Mp.: 55 – 57°C.

Micro-analysis: $C_9H_{15}N_2O_3F_3$ % Calc.: C 37.51, H 5.25, N 9.71. % Found: C 37.66, H 5.28, N 9.72.

Yield: 66% (932 mg) as off white crystals.

H-Gly-εAhx-OMe, TFA (29)[292]

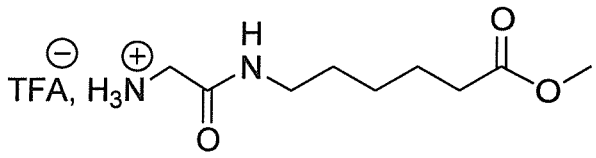

^{1}H (300 MHz, CD_3OD): δ = 1.32 (m, 2H, NH-$(CH_2)_2$-$C\underline{H}_2$), 1.49 (tt, 2H, *J* = 7, *J* = 7, NH-CH_2-$C\underline{H}_2$), 1.58 (tt, 2H, *J* = 7, *J* = 7, $C\underline{H}_2$-CH_2-CO_2Me), 2.29 (t, 2H, *J* = 7, $C\underline{H}_2$-CO_2Me), 3.19 (t, 2H, *J* = 7, NH-$C\underline{H}_2$), 3.60 (s, 3H, O-$C\underline{H}_3$), 3.62 (s, 2H, $C\underline{H}_2$-NH_3^+).

^{13}C (75.5 MHz, CD_3OD): δ = 25.5 ($\underline{C}H_2$-CH_2-CO_2Me), 27.2 (CH_2-CH_2-$\underline{C}H_2$), 29.8 (NH-CH_2-$\underline{C}H_2$), 34.5 ($\underline{C}H_2$-CO_2Me), 40.2 (NH-$\underline{C}H_2$), 41.3 ($\underline{C}H_2$-NH_3^+), 51.9 (O-$\underline{C}H_3$), 167.0 ($\underline{C}O$-NH), 175.7 ($\underline{C}O_2Me$).

IR: ν = 3292 (NH), 3122 (NH_3^+), 2939 - 2861 (alkyl), 1729 (C=O ester), 1665 (C=O amide) 1580 (NH) cm^{-1}.

M/z (ES^+): 203 (32%) $[M+H]^+$, 225 (7%) $[M+Na]^+$, 241 (15%) $[M+K]^+$.

HRMS (ES$^+$): $C_9H_{18}N_2O_3$ $[M+H]^+$ Calc. 203.1389, found 203.1390.

Micro-analysis: $C_{11}H_{19}N_2O_3F_3$ % Calc.: C 41.77, H 6.05, N 8.85. % Found: C 41.66, H 6.11, N 8.78.

Mp.: 50 – 51°C.

Yield: 40% (1.1 g) as a brown powder.

H-Phe-βAla-OMe, TFA (30)[291]

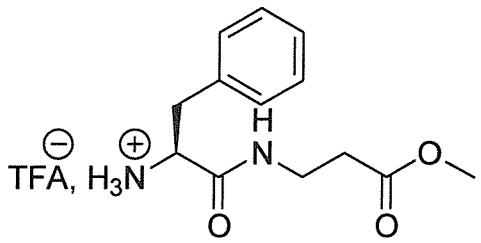

^{1}H (400 MHz, CD_3OD): δ = 2.35 – 2.53 (m, 2H, C<u>H</u>$_2$-CO_2Me), 3.08 (<u>A</u>BX system, 1H, J^{AX} = 7, J^{AB} = 14, CH<u>H</u>-C$^{\alpha}$H), 3.15 (A<u>B</u>X system, J^{BX} = 7, J^{BA} = 14, CH<u>H</u>-C$^{\alpha}$H), 3.36 (m, 1H, NH-CH<u>H</u>), 3.47 (m, 1H, NH-C<u>H</u>H), 3.66 (s, 3H, O-C<u>H</u>$_3$), 4.05 (AB<u>X</u> system, 1H, $J^{XA} = J^{XB}$ = 7, C$^{\alpha}$<u>H</u>), 7.24 – 7.38 (m, 5H, C<u>H</u> aromatic).

^{13}C (100 MHz, CD_3OD): δ = 34.7 (<u>C</u>H$_2$-CO_2Me), 36.7 (NH-<u>C</u>H$_2$), 39.0 (<u>C</u>H$_2$-C$^{\alpha}$H), 52.7 (O-<u>C</u>H$_3$), 56.1 (<u>C</u>$^{\alpha}$H), 129.2 (<u>C</u>H aromatic), 130.4 (<u>C</u>H aromatic), 130.5 (<u>C</u>H aromatic), 130.8 (<u>C</u>H aromatic), 130.9 (<u>C</u>H aromatic), 136.0 (<u>C</u> aromatic), 170.0 (<u>C</u>O-NH), 174.0 (<u>C</u>O_2Me).

IR: ν = 3081 (NH_3^+), 2956 (CH alkyl), 1725 (C=O ester), 1659 (C=O amide), 1561 (C=C aromatic) cm^{-1}.

M/z (ES$^+$): 251 (100%) $[M+H]^+$, 273 (18%) $[M+Na]^+$, 292 (20%) $[M+H+MeCN]^+$, 501 (5%) $[2M+H]^+$, 523 (5%) $[2M+Na]^+$.

HRMS (ES$^+$): $C_{13}H_{18}N_2O_3$ $[M+H]^+$ Calc. 251.1390, found 251.1390.

HPLC (λ=220 nm): 5.53 min.

Yield: 71% (1.2 g) as a brown oil.

H-Phe-γAbu-OMe, TFA (31)[291]

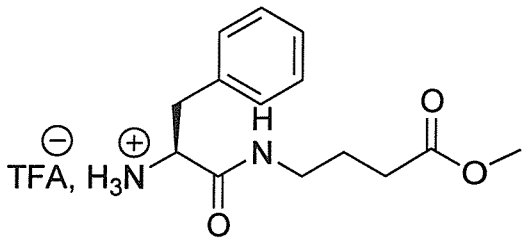

^{1}H (400 MHz, CD_3OD): δ = 1.68 (tt, 2H, *J*= 7, *J*= 7, NH-CH_2-$C\underline{H}_2$), 2.19 (t, 2H, *J*= 7, $C\underline{H}_2$-CO_2Me), 3.08 – 3.16 (br m, 3H, $C\underline{H}_2$-$C^{\alpha}H$ and NH-C<u>H</u>H), 3.20 – 3.28 (br m, 1H, NH-CH<u>H</u>), 3.65 (s, 3H, O-$C\underline{H}_3$), 4.20 (t, 1H, *J* = 7, $C^{\alpha}\underline{H}$), 7.26 – 7.38 (m, 5H, C<u>H</u> aromatic).

^{13}C (100 MHz, CD_3OD): δ = 25.7 (NH-CH_2-$\underline{C}H_2$), 32.2 ($\underline{C}H_2$-CO_2Me), 39.1 ($\underline{C}H_2$-$C^{\alpha}H$), 40.1 (NH-$\underline{C}H_2$), 54.4 (O-$\underline{C}H_3$), 56.3 ($\underline{C}^{\alpha}H$), 129.2 (<u>C</u>H aromatic), 130.4 (<u>C</u>H aromatic), 130.9 (<u>C</u>H aromatic), 136.1 (<u>C</u> aromatic), 170.0 (<u>C</u>O-NH), 175.5 ($\underline{C}O_2Me$).

IR: ν = 3287 (NH), 3087 (NH_3^+), 3032 - 2954 (alkyl), 1715 (C=O ester), 1663 (C=O amide), 1580 (NH) cm^{-1}.

M/z (ES^+): 265 (100%) $[M+H]^+$, 287 (50%) $[M+Na]^+$.

HRMS (ES^+): $C_{14}H_{20}N_2O_3$ $[M+H]^+$ Calc. 265.1546, found 265.1547.

HPLC (λ=220 nm): 6.2 min.

Yield: 58% (1.2 g) as a yellow oil.

H-Trp-βAla-OMe, TFA (32)

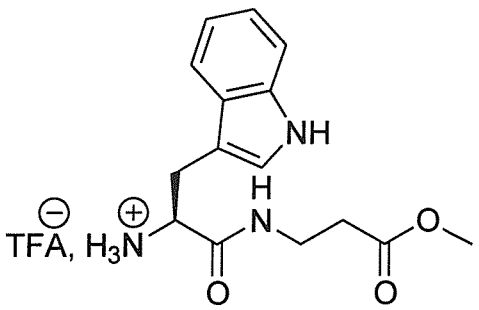

^{1}H (400 MHz, CD_3OD): δ = 2.27 – 2.45 (m, 2H, $C\underline{H}_2$-CO_2Me), 3.23 (<u>A</u>BX system, 1H, J^{AX} = 7, J^{AB} = 14, C<u>H</u>H-$C^{\alpha}H$), 3.30 – 3.38 (m, 2H, NH-CH<u>H</u> and CH<u>H</u>-$C^{\alpha}H$), 3.43 (dt, 1H, *J*= 7, *J*= 14, NH-C<u>H</u>H), 3.53 (s, 3H, O-$C\underline{H}_3$), 4.05 (AB<u>X</u> system, 1H, $J^{XA} = J^{XB}$ =

7, $C^{\alpha}\underline{H}$), 7.06 (dd, 1H, J = 8, J = 8, C<u>H</u> aromatic), 7.15 (dd, 1H, J = 8, J = 8, C<u>H</u> aromatic), 7.20 (s, 1H, C<u>H</u> indole), 7.39 (d, 1H, J = 8, C<u>H</u> aromatic), 7.61 (d, 1H, J = 8, C<u>H</u> aromatic).

^{13}C (100 MHz, CD_3OD): δ = 30.9 ($\underline{C}H_2$-$C^{\alpha}H$), 36.2 ($\underline{C}H_2$-CO_2Me), 38.4 (NH-$\underline{C}H_2$), 54.2 (O-$\underline{C}H_3$), 57.2 ($\underline{C}^{\alpha}H$), 110.1 (<u>C</u>H aromatic), 114.7 (<u>C</u> aromatic), 121.1 (<u>C</u>H aromatic), 121.3 (<u>C</u>H aromatic), 124.9 (<u>C</u>H aromatic), 127.5 (<u>C</u>H aromatic), 130.3 (<u>C</u> aromatic), 140.3 (<u>C</u> aromatic), 172.2 (<u>C</u>O-NH), 175.6 ($\underline{C}O_2Me$).

IR: ν = 3250 (NH), 3061 (NH_3^+), 2954 - 2870 (alkyl), 1719 (C=O ester), 1664 (C=O amide) cm^{-1}.

M/z (ES^+): 290.0 (100%) $[M+H]^+$.

HRMS (ES^+): $C_{15}H_{19}N_3O_3$ $[M+H]^+$ Calc. 290.1499, found 290.1493.

Mp.: 48 - 49°C.

HPLC (λ=220 nm): 6 min.

Yield: 26% (584 mg) as an orange solid.

H-Trp-γAbu-OMe, TFA (33)

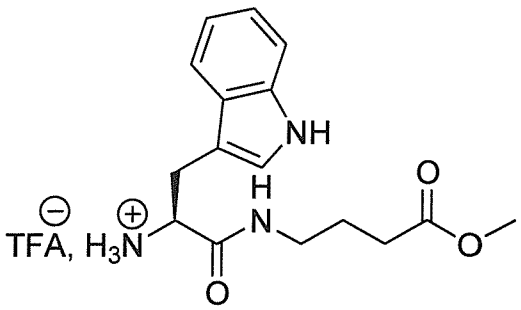

^{1}H (400 MHz, CD_3OD): δ = 1.60 (tt, 2H, J = 7, J = 7, NH-CH_2-$C\underline{H}_2$), 2.11 (t, 2H, J = 7, $C\underline{H}_2$-CO_2Me), 3.08 – 3.20 (m, 2H, NH-CH<u>H</u>), 3.28 (A<u>B</u>X system, 1H, J^{AX} = 7, J^{AB} = 14, C<u>H</u>H-$C^{\alpha}H$), 3.36 (A<u>B</u>X system, J^{BX} = 7, J^{BA} = 14, CH<u>H</u>-$C^{\alpha}H$), 3.63 (s, 3H, O-$\underline{C}H_3$), 4.04 (AB<u>X</u> system, 1H, J^{XA} = J^{XB} = 7, $C^{\alpha}\underline{H}$), 7.07 (dd, 1H, J = 8, J = 8, C<u>H</u> aromatic), 7.14 (dd, 1H, J = 8, J = 8, C<u>H</u> aromatic), 7.20 (s, 1H, C<u>H</u> indole), 7.39 (d, 1H, J = 8, C<u>H</u> aromatic), 7.57 (d, 1H, J = 8, C<u>H</u> aromatic).

^{13}C (100 MHz, CD_3OD): δ = 25.6 (NH-CH_2-$\underline{C}H_2$), 29.2 ($\underline{C}H_2$-CO), 32.1 ($\underline{C}H_2$-$C^{\alpha}H$), 40.4 (NH-$\underline{C}H_2$), 53.5 (O-$\underline{C}H_3$), 55.7 ($\underline{C}^{\alpha}H$), 108.6 (<u>C</u>H aromatic), 113.0 (<u>C</u> aromatic),

119.5 (CH aromatic), 120.6 (CH aromatic), 123.2 (CH aromatic), 125.9 (CH aromatic), 128.7 (C aromatic), 138.5 (C aromatic), 168.2 (CO-NH), 173.3 (CO_2Me).

IR: ν = 3252 (NH), 3027 (CH aromatic), 2953 (alkyl), 1735 (C=O ester), 1684 (C=O amide), 1561 (C=C aromatic) cm^{-1}.

M/z (ES^+): 304.1 (100%) $[M+H]^+$.

HRMS (ES^+): $C_{16}H_{21}N_3O_3$ $[M+H]^+$ Calc. 304.1656, found 304.1656.

Mp.: 45 - 46°C.

HPLC (λ=220 nm): 6.5 min.

Yield: 64.5% (1.21 g) as a brown powder.

H-Trp-εAhx-OMe, TFA (34)

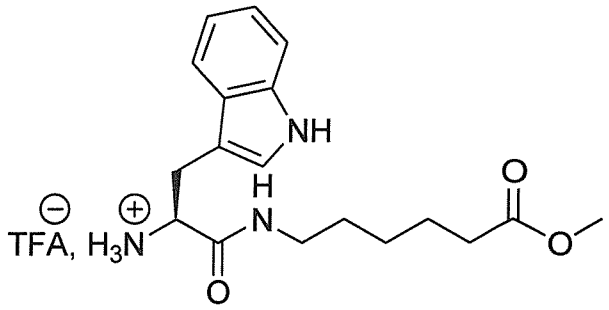

^1H (400 MHz, CD_3OD): δ = 1.10 (tt, 2H, *J* = 7, *J* = 7, NH-$(CH_2)_2$-CH_2), 1.28 (tt, 2H, *J* = 7, *J* = 7, NH-CH_2-CH_2), 1.50 (tt, 2H, *J* = 7, *J* = 7, CH_2-CH_2-CO_2Me), 2.23 (t, 2H, *J* = 7, CH_2-CO_2Me), 3.04 (dt, 1H, *J* = 14, *J* = 7, NH-CHH), 3.15 (dt, 1H, *J* = 7, *J* = 14, NH-CHH), 3.27 (ABX system, 1H, J^{AX} = 7, J^{AB} = 15, CHH-$C^{\alpha}H$), 3.35 (ABX system, 1H, J^{BX} = 7, J^{BA} = 15, CHH-$C^{\alpha}H$), 3.64 (s, 3H, O-CH_3), 4.08 (ABX system, 1H, J^{XA} = J^{XB} = 7, $C^{\alpha}H$), 7.07 (dd, 1H, *J* = 7, *J* = 7, CH aromatic), 7.14 (dd, 1H, *J* = 7, *J* = 7, CH aromatic), 7.21 (s, 1H, CH indole), 7.40 (d, 1H, *J* = 7, CH aromatic), 7.65 (d, 1H, *J* = 7, CH aromatic).

^{13}C (100 MHz, CD_3OD): δ = 27.4 (CH_2-CH_2-CO_2Me), 29.0 (NH-$(CH_2)_2$-CH_2), 30.7 (NH-CH_2-CH_2), 31.4 (CH_2-CO_2Me), 36.4 (CH_2-$C^{\alpha}H$), 42.3 (NH_2-CH_2), 53.9 (O-CH_3), 57.2 ($C^{\alpha}H$), 110.1 (CH aromatic), 114.4 (C aromatic), 121.0 (CH aromatic), 122.0 (CH aromatic), 124.7 (CH aromatic), 127.4 (CH aromatic), 130.3 (C aromatic), 140.0 (C aromatic), 171.8 (CO-NH), 177.8 (CO_2Me).

IR: ν = 3287 (NH), 3061 (CH aromatic), 2939 - 2864 (alkyl), 1715 (C=O ester), 1665 (C=O amide), 1560 (C=C aromatic) cm^{-1}.

M/z (ES^+): 332.1 (100%) $[M+H]^+$, 354.0 (11%) $[M+Na]^+$.

HRMS (ES^+): $C_{18}H_{25}N_3O_3$ $[M+H]^+$ Calc. 332.1955, found 332.1960.

Mp.: 40 – 41°C.

HPLC (λ=220 nm): 7.05 min.

Yield: 30% (675 mg) as a yellow foam.

6.5.2 General procedure for linear tetrapeptide synthesis (35-53) in the presence of a metal salt[276]

A library was synthesised in solution using a multi-reactor carousel device.

A dipeptide (74 μmol), or an equimolar mixture of two dipeptides (37 μmol) for crossed reactions, was dissolved in methanol (5 mL) with the metal salt ($NiCl_2 \cdot 6H_2O$) (8.8 mg, 37 μmol). A methanolic sodium methanolate solution 0.5 M (447 μL, 223 μmol) was added and the mixture was stirred at reflux in a screw top tube for 24 h. A series of crossed reactions was performed by mixing the dipeptide H-Trp-βAla-OMe **(32)** with the dipeptides H-Gly-βAla-OMe **(27)**, H-Gly-γAbu-OMe **(28)**, H-Gly-εAhx-OMe **(29)**, H-Phe-γAbu-OMe **(31)**, H-Trp-γAbu-OMe **(33)** and H-Trp-εAhx-OMe **(34)**. The dipeptide H-Phe-βAla-OMe **(30)** was reacted with the same series of dipeptides and **(32)**. Each of these dipeptides was also reacted with itself to yield symmetrical tetrapeptides.

The products of coupling are listed in Table 6.16.

Linear tetrapeptide	Retention time (min)	Mass spectra (M/z)
H-Trp-βAla-Trp-βAla-OMe (35)	7.4	547 (100%) $[M+H]^+$ 569 (8%) $[M+Na]^+$
H-Trp-βAla-Trp-βAla-OH (36)	7.0	532.9 (100%) $[M+H]^+$ 555.0 (20%) $[M+Na]^+$
H-Trp-βAla-Phe-βAla-OMe (37)	7.3	508.1 (100%) $[M+H]^+$ 530.1 (30%) $[M+Na]^+$
H-Trp-βAla-Gly-βAla-OMe (38)	5.9	418.1 (100%) $[M+H]^+$ 440.1 (20%) $[M+Na]^+$
H-Trp-βAla-Trp-γAbu-OMe (39)	7.5	561.0 (100%) $[M+H]^+$ 582.9 (20%) $[M+Na]^+$
H-Trp-βAla-Phe-γAbu-OMe (40)	7.4	522.0 (100%) $[M+H]^+$
H-Trp-βAla-Gly-γAbu-OMe (41)	6.17	432.0 (100%) $[M+H]^+$ 454.0 (20%) $[M+Na]^+$
H-Trp-βAla-Trp-εAhx-OMe (42)	7.9	588.9 (100%)$[M+H]^+$ 610.9 (25%) $[M+Na]^+$
H-Trp-βAla-Gly-εAhx-OMe (43)	6.7	460.2 (85%) $[M+H]^+$ 482.2 (23%) $[M+Na]^+$
H-Trp-βAla-Gly-εAhx-OH (44)	6	446.1 (35%) $[M+H]^+$ 468.0 (10%) $[M+Na]^+$
H-Trp-γAbu-Trp-γAbu-OMe (45)	7.5	575.2 (100%) $[M+H]^+$ 597.2 (28%) $[M+Na]^+$

Table 6.16: Retention time (min) and mass of linear tetrapeptides. (The linear tetrapeptides H-aa_1-aa_2-aa_3-aa_4-OMe and H-aa_3-aa_4-aa_1-aa_2-OMe were not differentiated. This is also the case for the hydrolysed tetrapeptides).

Continued from previous page.

Linear tetrapeptide	Retention time (min)	Mass spectra (M/z)
H-Phe-βAla-Phe-βAla-OMe (46)	7.2	469.0 (100%) $[M+H]^+$ 491.0 (19%) $[M+Na]^+$
H-Phe-βAla-Phe-βAla-OH (47)	6.2	455.0 (100%) $[M+H]^+$ 477.0 (15%) $[M+Na]^+$
H-Phe-βAla-Gly-βAla-OMe (48)	6.2	379.1 (25%) $[M+H]^+$ 401.1 (15%) $[M+Na]^+$
H-Phe-βAla-Phe-γAbu-OMe (49)	7.3	483 (100%) $[M+H]^+$ 504.9 (25%) $[M+Na]^+$
H-Phe-βAla-Trp-γAbu-OMe (50)	7.3	522.1 (100%) $[M+H]^+$ 544.1 (18%) $[M+Na]^+$
H-Phe-βAla-Gly-γAbu-OMe (51)	5.8	393.1 (100%) $[M+H]^+$ 415.1 (22%) $[M+Na]^+$
H-Phe-βAla-Trp-εAhx-OMe (52)	7.8	550.1 (32%) $[M+H]^+$ 572.1 (8%) $[M+Na]^+$
H-Phe-βAla-Gly-εAhx-OMe (53)	6.5	421.2 (100%) $[M+H]^+$ 443.0 (26%) $[M+Na]^+$

Table 6.16: Retention time (min) and mass of linear tetrapeptides. (The linear tetrapeptides H-aa_1-aa_2-aa_3-aa_4-OMe and H-aa_3-aa_4-aa_1-aa_2-OMe were not differentiated. This is also the case for the hydrolysed tetrapeptides).

A library member **(36)** was purified by semi-prep HPLC to allow full characterisation.

H-Trp-βAla-Trp-βAla–OH (36)

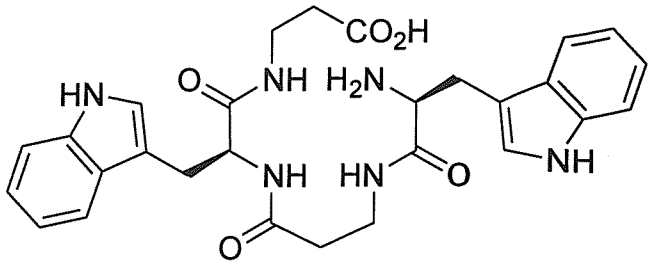

^{1}H (400 MHz, CD_3OD): δ = 2.05 – 2.32 (m, 4H, C<u>H</u>$_2$-CO_2H and C<u>H</u>$_2$-CO-NH), 2.97 (<u>A</u>BX system, 1H, J^{AX} = 7.5, J^{AB} = 14, C<u>H</u>H-C$^{\alpha}$H-NH), 3.07 (<u>A</u>BX system, 1H, J'^{AX} = 8, J'^{AB} = 14, C<u>H</u>H-C$^{\alpha}$H-NH_2), 3.15 – 3.25 (m, 1H, CH<u>H</u>-C$^{\alpha}$H-NH), 3.25 – 3.35 (m, 5H, CH_2-NH, CH_2-NH and CH<u>H</u>-C$^{\alpha}$H-NH_2), 3.90 (m, 1H, C$^{\alpha}$<u>H</u>-NH_2), 4.45 (AB<u>X</u> system, 1H, J^{XA} = J^{XB} = 7.5, C$^{\alpha}$<u>H</u>-NH), 6.90 (ddd, 1H, J = 1, J = 8, J = 8, C<u>H</u> aromatic), 6.96 (dd, 1H, J = 8, J = 8, C<u>H</u> aromatic), 6.97 (dd, 1H, J = 8, J = 8, C<u>H</u> aromatic), 6.99 (s, 1H, C<u>H</u> aromatic), 7.02 (ddd, 1H, J = 1, J = 8, J = 8, C<u>H</u> aromatic), 7.06 (s, 1H, C<u>H</u> aromatic), 7.20 (d, 1H, J = 8, C<u>H</u> aromatic), 7.25 (d, 1H, J = 8, C<u>H</u> aromatic), 7.46 (d, 1H, J = 8, C<u>H</u> aromatic), 7.51 (d, 1H, J = 8, C<u>H</u> aromatic).

^{13}C (100 MHz, CD_3OD): δ = 27.1 (<u>C</u>H_2-C$^{\alpha}$H-NH), 29.3 (<u>C</u>H_2-C$^{\alpha}$H-NH_2), 37.7 (<u>C</u>H_2-CO), 38.3 (<u>C</u>H_2-CO_2H), 38.5 (<u>C</u>H_2-CH_2-CO_2H), 39.0 (CO-CH_2-<u>C</u>H_2-NH), 56.8 (<u>C</u>$^{\alpha}$H-NH), 63.7 (<u>C</u>$^{\alpha}$H-NH_2), 109.3 (<u>C</u>H aromatic), 110.5 (<u>C</u>H aromatic), 110.7, (<u>C</u> aromatic), 111.6, (<u>C</u> aromatic), 117.5 (<u>C</u>H aromatic), 117.8 (<u>C</u>H aromatic), 118.2 (<u>C</u>H aromatic), 119.7 (<u>C</u>H aromatic), 120.3 (<u>C</u>H aromatic), 121.0 (<u>C</u>H aromatic), 123.6 (<u>C</u>H aromatic), 124.0 (<u>C</u>H aromatic), 126.5 (<u>C</u> aromatic), 129.7 (<u>C</u> aromatic), 136.4 (<u>C</u> aromatic), 136.9 (<u>C</u> aromatic), 172.0 (<u>C</u>O-NH), 178.8 (<u>C</u>O-NH), 180.0 (<u>C</u>O-NH), 181.6 (<u>C</u>O_2H).

IR: ν = 3283 (CO_2H), 2931 (alkyl), 1678 (C=O amide), 1563 (C=C aromatic) cm^{-1}.

M/z (ES$^+$): 533.0 (100%) $[M+H]^+$, 554.9 (20%) $[M+Na]^+$.

HRMS (ES$^+$): $C_{28}H_{32}N_6O_5$ $[M+H]^+$ Calc. 533.2498, found 533.2498.

HPLC (λ=220 nm): 7 min.

Yield: 20% (4 mg) as a colourless oil.

6.5.3 Synthesis of dipeptides on solid phase

6.5.3.a Synthesis of H-βAla loaded resins (54 & 55)

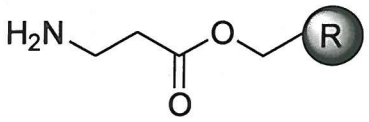

R = Hydroxymethyl Polystyrene: **(54)**
Quadra Gel: **(55)**

Resin (3 g) (Hydroxymethyl Polystyrene: 1.24 mmol/g or Quadra Gel: 1.7 mmol/g) was swollen in DCM (50 mL). Fmoc-βAla-OH (2.7 eq., 3.15 g and 4.75 g, respectively) was coupled to each resin following the standard DIPEA / oxalyl chloride coupling method. After filtration and washing (DCM: 2 x 10 mL, DMF: 2 x 10 mL, MeOH: 2 x 10 mL) the resins were treated with a solution (10 mL) of 20% piperidine in DMF (2 x 20 min) to yield the title resins **(54)** and **(55)**. Loading was measured for each resin by a quantitative Fmoc test.

Resin **(54)**: **IR:** ν = 2920 - 2850 (alkyl), 1732 (C=O ester) cm^{-1}.
Theoretical loading: 1 mmol/g. Found: 0.9 mmol/g. Yield = 90%.

Resin **(55)**: **IR:** ν = 2915 - 2860 (alkyl), 1725 (C=O ester) cm^{-1}.
Theoretical loading: 1.23 mmol/g. Found: 1.2 mmol/g. Yield = 98%.

6.5.3.b Synthesis of H-Trp-βAla loaded resins (56 & 57)

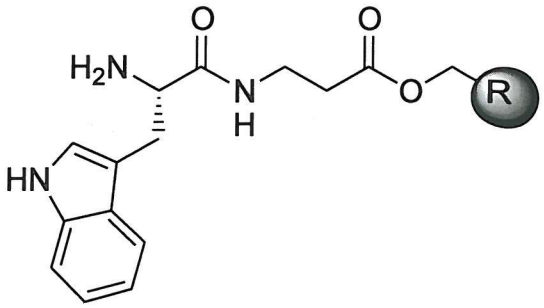

R = Hydroxymethyl Polystyrene: **56**
Quadra Gel: **57**

To 1 g of each resin (**54 & 55**) was added a solution of Fmoc-Trp-OH (3 eq.: 1.11 g and 1.47 g, respectively) and HOBt (3 eq.: 364 mg and 465 mg) in DCM / DMF (6 / 1) (10 mL), followed by DIC (3 eq.: 422 µL and 540 µL) then the mixtures were shaken for 2 days. After filtration and washing (DCM, DMF, MeOH) the resins were treated with a solution of 20% piperidine in DMF (2 x 20 min) to yield the resins **(56 & 57)**. Loading was measured for each resin by a quantitative Fmoc test.

Resin **(56)**: **IR:** ν = 1727 (C=O ester), 1655 (C=O amide) cm^{-1}.
Theoretical loading: 1 mmol/g. Found: 0.9 mmol/g. Yield = 90%.

Resin **(57)**: **IR:** ν = 1730 (C=O ester), 1655 (C=O amide) cm^{-1}.
Theoretical loading: 0.9 mmol/g. Found: 0.9 mmol/g. Yield = quantitative.

6.5.3.c Synthesis of H-Phe-βAla ester resins (58 & 59)

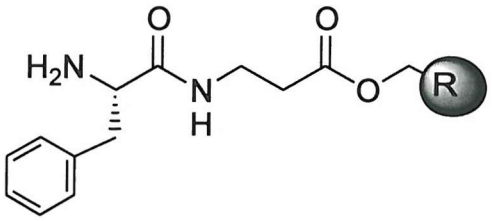

R = Hydroxymethyl Polystyrene: **58**
Quadra Gel: **59**

To 1 g of resin **(54)** was coupled Boc-Phe-OH (3 eq.: 715 mg) and HOBt (3 eq.: 364 mg) in DCM / DMF (6 / 1) (10 mL), followed by DIC (3 eq: 422 µL). Coupling completion was monitored by a negative ninhydrin test (Table 5.5). The resin was treated with a solution of DCM / TFA (1 / 1) (2 x 20 min), filtrated, neutralised with a 5% solution of DIPEA in DMF (2 x 10 mL) and washed with DCM (2 x 10 mL), DMF (2 x 10 mL) and MeOH (2 x 10 mL) to yield the resin **(58)**.
To 1 g of resin **(55)** was coupled Fmoc-Phe-OH (3 eq.: 1.33 g) in the same conditions as described above. The yield of the reaction was evaluated by the standard quantitative Fmoc test. The resin was treated with 20% piperidine in DMF (2 x 20 min) to yield the resin **(59)**.
Resin **(58)**: **IR:** ν = 1730 (CO ester), 1670 (CO amide) cm^{-1}.
Theoretical loading: 0.9 mmol/g. Found: N.D. Yield = complete by ninhydrin test.

Resin **(59)**: **IR:** ν = 1736 (CO ester), 1648 (CO amide) cm^{-1}.
Theoretical loading: 1.04 mmol/g. Found: 0.97 mmol/g. Yield = 93%.

6.5.4 General procedure for peptide coupling between a dipeptide on the solid phase and a dipeptide in solution in the presence of a metal salt.[276]

To each resin (200 µmol) **(56-59)** was added a dipeptide (200 µmol) **(27, 28, 29 & 33)** dissolved in methanol (8 mL) with $NiCl_2 \cdot 6H_2O$ (57 mg, 200 µmol) and a methanolic sodium methanolate solution (1.2 mmol). The mixture was refluxed for 24 h in top-screwed tubes. The crossed reactions are summarised in Table 6.17.

	Retention time (min) of main peaks	Purity (%, λ = 260 nm) after:					
		10 min	1h	3h	5h	21h	24h
56 and Gly-βAla-OMe, TFA (27)	5.9	no	10	no	5	28	15
	6.8	no	11	57	10	19	17
	7.2	no	12	34	11	27	16
56 and Gly-εAhx-OMe, TFA (29)	5.8	18	14	14	nd	30	35
	6.5	7	11	10	nd	5	6
	6.8	4	18	16	nd	23	27
	7.2	no	13	12	nd	18	21
56 and Trp-γAbu-OMe, TFA (33)	6.3	13	18	22	nd	nd	8
	6.5	51	15	20	nd	nd	3
	7.3	6	12	2	nd	nd	10
	7.4	17	16	7	nd	nd	11
57 and Gly-γAbu-OMe, TFA (28)	5.3	38	41	42	nd	nd	41
	6.0	no	18	10	nd	nd	11
	7	no	3	5	nd	nd	3
	7.4	no	4	3	nd	nd	5
57 and Gly-εAhx-OMe, TFA (29)	5.5	24	36	11	35	nd	25
	6	25	12	35	18	nd	32
	6.7	no	9	10	6	nd	12
	7	no	7	8	8.5	nd	9
58 and Gly-γAbu-OMe, TFA (28)	6.6	7.6	nd	4	nd	nd	no
	7.4	6.1	nd	65	nd	nd	100
	8.5	6.2	nd	9	nd	nd	no
58 and Gly-εAhx-OMe, TFA (29)	7.3	8	51	100	100	100	100
59and Gly-γAbu-OMe, TFA (28)	7.3	3	9	23	29	50	40
	8.6	21	20	19	19	19	20
59 and Gly-εAhx-OMe, TFA (29)	6.4	no	3	3	4	nd	no
	7.5	no	14	29	53	nd	85
	8.6	15	17	15	19	nd	no

Table 6.17: Resins and dipeptides mixed to generate the library of tetrapeptides in solution. (no: not observed, nd: not determined).

During the reaction the species formed in solution were characterised by banalytical reversed phase HPLC and mass spectrometry.

After reaction the resins were filtered, washed with DMF (2 x 10 mL), DCM (2 x 10 mL), MeOH (2 x 10 mL) and dried *in vacuo* overnight before IR monitoring. No C=O stretch corresponding to the ester or amide was observed.

REFERENCES

1. Lehn, J. M. *Angew. Chem. Int. Ed. Engl.* **1988**, *27*, 89-112.
2. Cram, D. J. *Angew. Chem. Int. Ed. Engl.* **1988**, *27*, 1009-1020.
3. Benniston, A. C. and Harriman, A. *Synlett* **1993**, 223-226.
4. Pedersen, C. J. and Frensdorff, H. K. *Angew. Chem. Int. Ed. Engl.* **1972**, *11*, 16-25.
5. Szejtli, J. *Chem. Rev.* **1998**, *98*, 1743-1753.
6. Liu, Y.; Han, B. H.; Qi, A. D. and Chen, R. T. *Bioorg. Chem.* **1997**, *25*, 155-122.
7. Breslow, R. and Dong, S. D. *Chem. Rev.* **1998**, *98*, 1997-2011.
8. Rebek, J. *Angew. Chem. Int. Ed. Engl.* **1990**, *20*, 245-255.
9. Amabilino, D. B.; Ashton, P. R.; Balzani, V.; Boyd, S. E.; Credi, A.; Lee, J. Y.; Menzer, S.; Stoddart, F. F.; Venturi, M. and Williams, D. J. *J. Am. Chem. Soc.* **1998**, *120*, 4295-4307.
10. Roh, S. G.; Park, K. M.; Park, G. J.; Sakamoto, S. Yamaguchi, K. and Kim, K. *Angew. Chem. Int. Ed. Engl.* **1999**, *38*, 638-641.
11. Cantrill, S. J.; Youn, G. J. and Stoddart, J. F. *J. Org. Chem.* **2001**, *66*, 6857-6872.
12. Onagi, H.; Easton, C. J. and Lincoln, S. F. *Org. Lett.* **2001**, *3*, 1041-1044.
13. Nielsen, M. B.; Hansen, J. G. and Becher, J. *Eur. J. Org. Chem.* **1999,** 2807-2815.
14. Bom, A.; Bradley, M.; Cameron, K.; Clark, J. K.; Van Egmond, J.; Feilden, H.; MacLean, E. K.; Muir, A. W.; Palin, R.; Rees, D. C. and Zhang, M. Q. *Angew. Chem. Int. Ed. Engl.* **2002**, *41*, 266-270.
15. Feigl, F. *Angew. Chem. Int. Ed. Engl.* **1961**, *73*, 113.
16. van Bekkum, H.; van Rantwijk, F. and van de Putte, T. *Tetrahedron Lett.* **1969**, *1*, 1-2.
17. Hoss, R. and Vögtle, F. *Angew. Chem. Int. Ed. Engl.* **1994**, *33*, 375-384.
18. Thompson, M. C. and Busch, D. H. *J. Am. Chem. Soc.* **1962**, *84*, 1762-1763.
19. Anderson, S.; Anderson, H. L. and Sanders J. K. M. *Acc. Chem. Res.* **1993**, *26*, 469-475.
20. Shanzer, A.; Libman, J. and Frolow, F. *J. Am. Chem. Soc.* **1981**, *103*, 7339-7340.

21. Amabilino, D. B.; Ashton, P. R.; Reder, A. S.; Spencer, N. and Stoddart, J. F. *Angew. Chem. Int. Ed. Engl.* **1994**, *33*, 433-437.
22. Bühner, M.; Geuder, W.; Gries, W.. K.; Hünig, S. and Poll, T. *Angew. Chem. Int. Ed. Engl.* **1988**, *27*, 1553-1556.
23. Kelly, T. R.; Zhao, C. and Bridger, G. J. *J. Am. Chem. Soc.* **1989**, *111*, 3744-3745.
24. Hunter, C. A. *J. Am. Chem. Soc.* **1992**, *114*, 5303-5311.
25. Vögtle, S.; Meier, S. and Hoss R. *Angew. Chem. Int. Ed. Engl.* **1992**, *31*, 1619-1622.
26. Guggisberg, A.; Dabrowski, U.; Kramer, U.; Heidelberger, C.; Hesse, M. and Schmidt, H. *Helv. Chim. Acta* **1978**, *61*, 1039-1049.
27. Breitenbach, J.; Ott, F. and Vögtle, F. *Angew. Chem. Int. Ed. Engl.* **1992**, *31*, 307-310.
28. Breslow, R. and Wiedenfeld, D. *Tetrahedron Lett.* **1993**, *34*, 1107-1110.
29. Rumney, S. and Kol, E. T. *Angew. Chem. Int. Ed. Engl.* **1992**, *31*, 1617-1619.
30. Praseuth, D, Guieysse, A. L. and Helene, C. *Biochim. Biophys. Acta* **1999**, *1489*, 181-206.
31. Ernest, I.; Kalvoda, J.; Sigel, C.; Rihs, G.; Fritz, H.; Blommers, M. J. J.; Raschdorf, F.; Francotte, E. and Mutter, M. *Helv. Chim. Acta* **1993**, *76*, 1539-1563.
32. Pauling, L. *J. Am. Chem. Soc.* **1940**, *62*, 2643-2656.
33. Yilmaz, E.; Haupt, K. and Mosbach K. *Angew. Chem. Int. Ed.* **2000**, *39*, 2115-2118.
34. a) Eschenmoser, A. *Angew. Chem. Int. Ed. Engl.* **1994**, *33*, 2363. b) Lichtenthaler, F. W. *Angew. Chem. Int. Ed. Engl.* **1994**, *33*, 2364-2374.
35. Vidyasankar, S.; Ru, M. and Arnold, F. H. *J. Chromatogr. A* **1997**, *775*, 51-63.
36. Panasyuk, T. L.; Mirsky, V. M.; Piletsky, S. A. and Wolfbeis, O. S. *Anal. Chem.* **1999**, *71*, 4609-4613.
37. Liao, Y.; Wang, W. and Wang, B. *Bioorg. Chem.* **1999**, *27*, 463-476.
38. Kempe, M. and Mosbach, K. *J. Chromatogr. A* **1995**, *691*, 317-323.
39. Sellergren, B. and Shea, K. J. *J. Chromatogr. A* **1993**, *635*, 31-49.
40. Sellergreb, B.; Ekberg, B. and Mosbach K. *J. Chromatogr. A* **1985**, *347*, 1-10.
41. Yoshikawa, M.; Izumi, J.-I., Kitao, T. and Sakamoto, S. *Macromolecules* **1996**, *29*, 8197-8203.

42. Yoshikawa, M.; Izumi, J.-I., Kitao, T. and Sakamoto, S. *Chem. Lett.* **1996**, 611-612.
43. Yoshikawa, M.; Fujisawa, T.; Izumi, J.-I., Kitao, T. and Sakamoto, S. *Anal. Chim. Acta* **1998**, *365*, 59-67.
44. Hedborg, E.; Winquist, F.; Lundström, I.; Andersson, L. I. and Mosbach, K. *Sensors Actuators A* **1993**, *37/38*, 796-799.
45. Ramström, O.; Nicholls, I. A. and Mosbach, K. *Tetrahedron: Asymmetry* **1994**, *5*, 649-656.
46. Kempe, M. and Mosbach, K. *Tetrahedron Lett.* **1995**, *36*, 3563-3566.
47. Klein, J. U.; Whitcombe, M. J.; Mulholland, F. and Vulfson, E. N. *Angew. Chem. Int. Ed.* **1999**, *38*, 2057-2060.
48. Ye, L.; ramström, O.; Manssom M.-O. and Mosbach, K. *J. Mol. Recognit.* **1998**, *11*, 75-78.
49. Shnek, D. R.; Pack, D. W.; Sasaki, D. Y. and Arnold, F. H. *Langmuir* **1994**, *10*, 2382-2388.
50. Norrlöw, O.; Glad, M. and Mosbach, K. *J. Chromatogr. A* **1984**, *299*, 29-41.
51. Arshady, R. and Mosbach, K. *Makromol. Chem.* **1981**, *182*, 687-692.
52. Alexander, C.; Smith, C. R.; Whitcombe, M. J. and Vulfson, E. N. *J. Am. Chem. Soc.* **1999**, *121*, 6640-6651.
53. Wulff, G.; Sarhan, A. andZabrocki, K. *Tetrahedron Lett.* **1973**, *44*, 4329-4332.
54. Mirsky, V. M.; Hirsch, T.; Piletsky, S. A. and Wolfbeis, O. S. *Angew. Chem. Int. Ed.* **1999**, *38*, 1108-1110.
55. Wulff, G. and Lohmar, E. *Isr. J. Chem.* **1979**, *18*, 279-284.
56. Wulff, G.; Sarham, A.; Gimpel, J. and Lohmar, E. *Chem. Ber.* **1974**, *107*, 3364-3376.
57. Wulff, G.; Kemmer, R.; Vietmeier, J. and Poll, H.-G. *Nouv. J. Chim.* **1982**, *6*, 681-687.
58. Wulff, G. and Schauhoff, S. *J. Org. Chem.* **1991**, *56*, 395-400.
59. Mayes, A. G.; Andersson, L. I. and Mosbach, K. *Anal. Biochem.* **1994**, *222*, 483-488.
60. Nilsson, K. G. I.; Sakaguchi, K.; Gemeiner, and Mosbach K. *J. Chromatogr. A* **1995**, *707*, 199-203.
61. Malitesta, C.; Losito, I. and Zambonin, G. *Anal. Chem.* **1999**, *71*, 1366-1370.
62. Spivak, D. A. and Shea, K. J. *Macromolecules* **1998**, *31*, 2160-2165.

63. Spivak, D. A.; Gilmore M. A. and Shea, K. J. *J. Am. Chem. Soc.* **1997**, *119*, 4388-4393.

64. Vlatakis, G.; Andersson, L. I.; Müller, R. and Mosbach, K. *Nature* **1993**, *361*, 645-647.

65. Whitcombe, M. J.; Rodriguez, M. E.; Villar, P. and Vulfson, E. N. *J. Am. Chem. Soc.* **1995**, *117*, 7105-7111.

66. Ramström, O.; Ye, L.; Krook, M. and Mosbach, K. *Anal. Commun.* **1998**, *35*, 9-11.

67. Cheong, S. H.; McNiven, S.; Rachkov, A.; Levi, R.; Yano, K. and Karube, I. *Macromolecules* **1997**, *30*, 1317-1322.

68. Kugimiya, A.; Matsui, J.; Abe, H.; Aburatani, M.; Takeuchi, T. *Anal. Chim. Acta* **1998**, *365*, 75-79.

69. Byström, S. E.; Börje, A. and Akermark, B. *J. Am. Chem. Soc.* **1993**, *115*, 2081-2083.

70. Fischer, L.; Müller, R.; Ekberg, B. and Mosbach, K. *J. Am. Chem. Soc.* **1991**, *113*, 9358-9360.

71. Andersson, L. I. *Anal. Commun.* **1996**, *68*, 111-117.

72. Martin, P.; Wilson, I. D.; Morgan, D. E.; Jones, G. R. and Jones K. *Anal. Commun.* **1997**, *34*, 45-47.

73. Haginaka, J.; Takehira, H.; Hosoya, K. and Tanaka, N. *J. Chromatogr. A* **1998**, *816*, 113-121.

74. Matsui, J.; Nicholls, I. A. and Takeuchi, T. *Tetrahedron: Asymmetry* **1996**, *7*, 1357-1361.

75. Matsui, J.; Doblhoff-Dier, O. and Takeuchi, T. *Anal. Chim. Acta* **1997**, *343*, 1-4.

76. Matsui, J and Takeuchi, T. *Anal. Commun.* **1997**, *34*, 199-200.

77. Zander, A.; Findlay, P.; Renner, T. and Sellergren, B. *Anal. Chem.* **1998**, *70*, 3304-3314.

78. Tanabe, K.; Takeuchi, T.; Matsui, J.; Ikebukuro, K.; Yano, K. and Karube, I. *J. Chem. Soc., Chem. Commun.* **1995**, 2303-2304.

79. Yano. K.; Tanabe, K.; Takeuchi, T.; Matsui, J.; Ikebukuro, K. and Karube, I. *Anal. Chim. Acta* **1998**, *363*, 111-117.

80. Hart, B. R.; Rush, D. J. and Shea, K. J. *J. Am. Chem. Soc.* **2000**, *122*, 460-465.

81. Hong, J.-M.; Anderson, P. E.; Qian, J. and Martin C. R. *Chem. Mater.* **1998**, *10*, 1029-1033.

82. Levi, R.; McNiven, S.; Piletsky, S. A.; Cheong, S.-H.; Yano, K. and Karube, I. *Anal. Chem.* **1997**, *69*, 2017-2021.
83. Wulff, G.; Heide, B. and Helfmeier, G. *J. Am. Chem. Soc.* **1986**, *108*, 1089-1091.
84. Shea, K. J. and Sasaki, D. Y. *J. Am. Chem. Soc.* **1991**, *113*, 4109-4120.
85. Shea, K. J. and Dougherty, T. K. *J. Am. Chem. Soc.* **1986**, *108*, 1091-1093.
86. Shea, K. J. and Sasaki, D. Y. *J. Am. Chem. Soc.* **1989**, *111*, 3442-3444.
87. Piletsky, S. A.; Parhometz, Y. P.; Lavryk, N. V.; Panasyuk, T. L. and El'skaya, A. V. *Sensors Actuators B* **1994**, *18/19*, 629-631.
88. Andersson, L. I.; Mandenius, C. F. and Mosbach, K. *Tetrahedron Lett.* **1988**, *29*, 5437-5440.
89. Jakusch, M.; Jonatta, M. and Mizaikoff, B. *Anal. Chem.* **1999**, *71*, 4786-4791.
90. Kröger, S.; Turner, A. P. F.; Mosbach, K. and Haupt, K. *Anal. Chem.* **1999**, *71*, 3698-3702.
91. Lanza, F. and Sellergren, B. *Anal. Chem.* **1999**, *71*, 2092-2096.
92. Matsui, J.; Okada, M.; Tsuruoka, M. and Takruchi, T *Anal. Commun.* **1997**, *34*, 85-87.
93. Aherne, A.; Alexander, C.; Payne, M. J.; Perez, N. and Vulfson, E. N. *J. Am. Chem. Soc.* **1996**, *118*, 8771-8772.
94. Turkewitsch, P.; Wandelt, B.; Darling, G. D. and Powell, W. S. *Anal. Chem.* **1998**, *70*, 2025-2030.
95. Norrlöw, O.; Mansson, M.-O. and Mosbach, K. *J. Chromatogr.* **1987**, *396*, 374-377.
96. Sellergren, B. *Angew. Chem. Int. Ed.* **2000**, *39*, 1031-1037.
97. Lübke, M.; Whitcombe, M. J. and Vulfson, E. N. *J. Am. Chem. Soc.* **1998**, *120*, 13342-13348.
98. Dickert, F. L.. Tortschanoff, M.; Bulst, W. E. and Fischerauer, G. *Anal. Chem.* **1999**, *71*, 4559-4563.
99. Matsui, J.; Kato, T.; Takeuchi, T.; Susuki, M.; Yokoyama, K.; Tamiya, E. and Karube, I. *Anal. Chem.* **1993**, *65*, 2223-2224.
100. Kugimiya, A. and Takeuchi, T. *Electroanalysis* **1999**, *11*, 1158-1160.
101. Dunkin, I. R.; Lenfeld, J. and Sherrington, D. C. *Polymer* **1993**, *34*, 77-84.
102. Dai, S. *Chem. Eur. J.* **2001**, *7*, 763-768.
103. Nishide, H.; Deguchi, J. and Tsuchida, E. *Chem. Lett.* **1976**, *169-174*.

104. Matsui, J.; Nicholls, I. A.; Takeuchi, T.; Mosbach, K. and Karube, I. *Anal. Chim. Acta* **1996**, *335*, 71-77.
105. Koshland, D. E. *Angew. Chem. Int. Ed. Engl.* **1994**, *33*, 2375-2378.
106. Glad, M., Norrlöw, O.; Sellergren, B.; Siegbahn, N. and Mosbach, K. *J. Chromatogr.* **1985**, *347*, 11-23.
107. Wulff, G.; Grobe-Einsler, R.; Vesper, W. and Sarhan, A. *Makromol. Chem.* **1977**, *178*, 2817-2825.
108. Sagiv, J. *J. Am. Chem. Soc.* **1990**, *102*, 92-98.
109. Mallik, S.; Plunkett, S. D.; Dhal, P. K.; Johnson R. D.; Pack, D.; Shnek, D. and Arnold, F. H. *New J. Chem.* **1994**, *18*, 399-304.
110. Tsukagoshi, K.; Yu, K. Y.; Maeda, M. and Takagi, M. *Bull. Chem. Soc. Jpn.* **1993**, *66*, 114-120.
111. Wulff, G. *Angew. Chem. Int. Ed. Engl.* **1995**, *34*, 1812-1832.
112. Takeuchi, T. and Haginaka, J. *J. Chromatogr. B* **1999**, *728*, 1-20.
113. Lauer, M. and Wulff, G. *J. Chem. Soc. Perkin Trans. 2* **1987**, 745-749.
114. Wulff, G. *Pure Appl. Chem.* **1982**, *54*, 2093-2102.
115. Shea, K. J.; Stoddard, G. J.; Shavelle, D. M.; Wakui, F. and Choate, R. M. *Macromolecules* **1990**, *23*, 4497-4507.
116. Wulff, G. and Vietmeier J. *Makromol. Chem.* **1989**, *190*, 1727-1735.
117. Wulff, G. and Sarhan, A. *Angew. Chem. Int. Ed.* **1972**, *11*, 341.
118. Damen, J. and Neckers, D. C. *Tetrahedron Lett.* **1980**, *22*, 1913-11916.
119. Sellergren, B. and Andersson, L. *J. Org. Chem.* **1990**, *55*, 3381-3383.
120. Shea, K. J.; Thompson, E. A.; Pandey, S. D. and Beauchamp, P. S. *J. Am. Chem. Soc.* **1980**, *102*, 3149-3155.
121. Fuji, Y.; Matsutani, K. and Kikuchi, K. *J. Chem. Soc., Chem. Commun.* **1985**, 415-417.
122. Fuji, Y.; Kikuchi, K.; Matsutani, K.; Ota, K.; Adachi, M.; Syoji, M.; Haneishi, I. and Kuwana, Y. *Chem. Lett.* **1984**, 1487-1490.
123. Pradeep, K. D. and Arnold, F. H. *J. Am. Chem. Soc.* **1991**, *113*, 7417-7418.
124. Pradeep, K. D. and Arnold, F. H. *New J. Chem.* **1996**, *20*, 695-698.
125. Sellergen, B. and Shea, K. J. *J. Chromatogr. A* **1993**, *654*, 17-28.
126. Sellergren, B. *Anal. Chem.* **1994**, *66*, 1578-1582.
127. Sellergren, B. *J. Chromatogr. A* **1994**, *673*, 133-141.

128. Ramström, O.; Andersson, L. I. and Mosbach, K. *J. Org. Chem.* **1993**, *58*, 7562-7564.
129. Andersson, L. I. and Mosbach, K. *J. Chromatogr. A* **1990**, *516*, 313-322.
130. Lepisto, M. and Sellergren, B. *J. Org. Chem.* **1989**, *54*, 6010-6012.
131. O'Shannessy, D. J.; Ekberg, B. and Mosbach, K. *Anal. Biochem.* **1989**, *177*, 144-149.
132. Shea, K. J.; Spivak, D. A. and Sellergren, B. *J. Am. Chem. Soc.* **1993**, *115*, 3368-3369.
133. Mathew-Krotz, J. and Shea, K. J. *J. Am. Chem. Soc.* **1996**, *118*, 8154-8155.
134. Müller-Dethlefs, K. and Hobza, P. *Chem. Rev.* **2000**, *100*, 143-167.
135. Wullf, G.; Vietmeier, J. and Heinz-Günter, P. *Makromol. Chem.* **1987**, *188*, 731-740.
136. Kempe, M. *Anal. Chem.* **1996**, *68*, 1948-1953.
137. Yoshizako, K.; Hosoya, K.; Iwakoshi, Y.; Kimata, K. and Tanaka, N. *Anal. Chem.* **1998**, *70*, 386-389.
138. Berglund, J.; Lindbladh, C.; Nicholls, I. A. and Mosbach, K. *Anal. Commun.* **1998**, *35*, 3-7.
139. Andersson, L. I.; Müller, R.; Vlatakis, G. and Mosbach, K. *Proc. Natl. Acad. Sci. USA.* **1995**, *92*, 4788-4792.
140. Bengtsson, H.; Roos, U. and Andersson, L. I. *Anal. Commun.* **1997**, *34*, 233-235.
141. Ye, L.; Cormack, P. A. G. and Mosbach, K. *Anal. Commun.* **1999**, *36*, 35-38.
142. Haupt, K.; Mayes, A. G. and Mosbach, K. *Anal. Chem.* **1998**, *70*, 3936-3939.
143. Haupt, K.; Dzgoev, A. and Mosbach, K. *Anal. Chem.* **1998**, *70*, 628-631.
144. Takeuchi, T.; Dobashi, A. and Kimura, K. *Anal. Chem.* **2000**, *72*, 2418-2422.
145. Piletsky, S. A.; Piletska, E. V.; Chen, B.; Karim, K.; Weston, D.; Barrett, G.; Lowe, P. and Turner, A. P. F. *Anal. Chem.* **2000**, *72*, 4381-4385.
146. Surugiu, I.; Danielsson, B.; Ye, L.; Mosbach, K. and Haupt, K. *Anal. Chem.* **2001**, *73*, 487-491.
147. Mosbach, K. *TIBS* **1994**, *19*, 9-14.
148. Kriz, D.; Ramström, O. and Mosbach, K. *Anal. Chem.* **1997**, *69*, 345A-349A.
149. Haupt, K. and Mosbach, K. *Chem. Rev.* **2000**, *100*, 2495-2504.
150. Lai, E. P. C.; Fafara, A.; VanderNoot, V. A.; Kono, M. and Polsky, B. *Can. J. Chem.* **1998**, *76*, 265-273.

151. Mirsky, V. M. *Anal. Chem.* **1999**, *71*, 652A.
152. Sergeyeva, T. A.; Piletsky, S. A.; Brovko, A. A.; Slinchenko, E. A.; Sergeeva, L. M.; Panasyuk, T. L. and El'skaya, A. V. *Analyst* **1999**, *124*, 331-334.
153. Lahav, M.; Kharitonov, A. B.; Katz, O.; Kunitake, T. and Willner, I. *Anal. Chem.* **2001**, *73*, 720-723.
154. Haupt, K.; Noworyta, K. and Kutner, W. *Anal. Commun.* **1999**, *36*, 391-393.
155. Kriz, O.; Ramström, O.; Svensson, A. and Mosbach, K; *Anal. Chem.* **1995**, *67*, 2142-2144.
156. Kriz, O. and Mosbach, K. *Anal. Chim. Acta* **1995**, *300*, 71-75.
157. Matsui, J.; Kubo, H. and Takeuchi, T. *Anal. Chem.* **2000**, *72*, 3286-3290.
158. Wang, W.; Gao, S. and Wang, B. *Org. Lett.* **1999**, *1*, 1209-1212.
159. Rathbone, D. L.; Su, D.; Wang, Y. and Billington, D. C. *Tetrahedron Lett.* **2000**, *41*, 123-126.
160. Jenkins, A. L.; Uy, O. M. and Murray, G. M. *Anal. Chem.* **1999**, *71*, 373-378.
161. Damen, J. and Neckers, D. C. *J. Am. Chem. Soc.* **1980**, *102*, 3265-3267.
162. Sarhan, A. and El-Zahab, M. *Makromol. Chem. Rapid Commun.* **1987**, *8*, 555-561.
163. Leonhardt, A. and Mosbach, K. *React. Polym. Ion Exch. Sorbents* **1987**, *6*, 285-290.
164. Whitcombe, M. J.; Alexander, C. and Vulfson, E. N. *Synlett* **2000**, 911-923.
165. Hamase, K.; Iwashita, K. and Zaitsu, K. *Anal. Sci.* **1999**, *15*, 411-412.
166. Davis, M. E.; Katz, A. and Ahmad, W. R. *Chem. Mater.* **1996**, *8*, 1820-1839.
167. Toorisaka, E.; Yoshida, M.; Uezu, K.; Goto, M. and Furusaki, S. *Chem. Lett.* **1999**, 387-388.
168. Ohkubo, K.; Funakoshi, Y.; Urata, Y.; Hirota, S.; Usui, S. and Sagawa, T. *J. Chem. Soc., Chem. Commun.* **1995**, 2143-2144.
169. Kawanami, Y.; Yunoki, T.; Nakamura, A.; Fujii, K.; Umano, K.; Yamauchi, H. and Masuda, K. *J. Mol. Cat. A* **1999**, *145*, 107-110.
170. Robinson, D. K. and Mosbach, K. *J. Chem. Soc., Chem. Commun.* **1989**, 969-970.
171. Ohkubo, K.; Urata, Y.; Honda, Y.; Nakashima, Y. and Yoshinaga, K. *Polymer* **1994**, *35*, 5372-5374.
172. Sellergren, B. and Shea, K. J *Tetrahedron: Asymmetry* **1994**, *5*, 1403-1406.

173. Wulff, G.; Gross, T. and Schönfeld, R. *Angew. Chem. Int. Ed. Engl.* **1997**, *36*, 1962-1964.
174. Heilmann, J. and Maier, W. F. *Angew. Chem. Int. Ed. Engl.* **1994**, *33*, 471-473.
175. Morihara, K.; Kurokawa, M.; Kamata, Y. and Shimada, T. *J. Chem. Soc., Chem. Commun.* **1992**, 358-360.
176. Shimada, T.; Kurazono, R. and Morihara, K. *Bull. Chem. Soc. Jpn.* **1993**, *66*, 836-840.
177. Shimada, T.; Nakanishi, K. and Morihara, K. *Bull. Chem. Soc. Jpn.* **1992**, *65*, 954-958.
178. Beach, J. V. and Shea, K. J. *J. Am. Chem. Soc.* **1994**, *116*, 379-380.
179. Müller, R.; Andersson, L. I. and Mosbach, K. *Makromol. Chem. Rapid Commun.* **1993**, *14*, 637-641.
180. Matsui, J.; Nicholls, I. A.; Karube, I. and Mosbach K. *J. Chem. Soc., Chem. Commun.* **1996**, 5414-5417.
181. Liu, X. C. and Mosbach, K *Macromol. Rapid Commun.* **1998**, *19*, 671-674.
182. Gamez, P.; Dunjic, B.; Pinel, C. and Lemaire, M. *Tetrahedron Lett.* **1995**, *36*, 8779-8782.
183. Morihara, K.; Kurihara, S. and Suzuki, J. *Bull. Chem. Soc. Jpn.* **1988**, *61*, 3991-3998.
184. Tan Z. J. and Ramcho, V. T. *Electrophoresis* **1998**, *19*, 2055-2060.
185. Kriz, D.; Kriz, C. B.; Andersson, L. I. and Mosbach, K. *Anal. Chem.* **1994**, *66*, 2636-2639.
186. Yu, C; Mosbach, K. *J. Mol. Recognit.* **1998**, *11*, 69-74.
187. Wulff, G. and Vesper, W. *J. Chromatogr.* **1978**, *167*, 171-186.
188. Hosoya, K.; Yoshizako, K.; Tanaka, N.; Kimata, K.; Araki, T. and Haginaka, J. *Chem. Lett.* **1994**, 1437-1438.
189. Yoshizako, K.; Shirasu, Y.; Hosoya, K.; Kimata, K.; Araki, T. and Tanaka, N. *Chem. Lett.* **1996**, 717-718.
190. Schweitz, L.; Andersson, L. I. and Nilsson, S. *Anal. Chem.* **1997**, *69*, 1179-1183.
191. Schweitz, L.; Andersson, L. I. and Nilsson, S. *J. Chromatogr. A* **1997**, *792*, 401-409.
192. Levi, R.; McNiven, S.; Piletsky, S. A.; Choeng, S. H.; Yano, K. and Karube, I. *Anal. Chem.* **1997**, *69*, 2017-2021.
193. Haupt, K.; Dzgoev, A. and Mosbach, K. *Anal. Chem.* **1998**, *70*, 628-631.

194. Matsui, J.; Fuliwara, K. and Tackeuchi, T. *Anal. Chem.* **2000**, *72*, 1810-1813.
195. Dauwe, C. and Sellergren, B. *J. Chromatogr. A* **1996**, *753*, 191-200.
196. Remcho, V. T. and Tan, Z. J. *Anal. Chem.* **1999**, *71*, 248A-255A.
197. Matsui, J.; Nicholls, I. A. and Takeuchi, T *Anal. Chim. Acta* **1998**, *365*, 89-93.
198. Sabourin, L.; Ansell, R. J.; Mosbach, K. and Nicholls, I. A. *Anal. Commun.* **1998**, *35*, 282-287.
199. Mayes, A. G. and Mosbach, K. *Trends Anal. Chem.* **1997**, *16*, 321-332.
200. Hosoya, K.; Yoshizako, K.; Shirasu, Y.; Kimata, K.; Araki, T.; Tanaka, N. and Haginaka, J *J. Chromatogr. A* **1996**, *728*, 139-147.
201. Mayes, A. G. and Mosbach, K. *Anal. Chem.* **1996**, *68*, 3769-3774.
202. Svec, F. and Fréchet J. M. *Anal. Chem.* **1992**, *64*, 820-822.
203. Nilsson, K.; Lindell, J.; Norrlöv, O.; Sellergren, B. *J. Chromatogr. A* **1994**, *680*, 57-61.
204. Muldoon, M. T. and Stanker, L. H. *Anal. Chem.* **1997**, *69*, 803-808.
205. Ramström, O. and Ansell, R. *Chirality* **1998**, *10*, 195-209.
206. Norell, M. C.; Andersson, H. S. and Nicholls, I. A. *J. Mol. Recognit.* **1998**, *11*, 98-102.
207. Barett, A. M.; Cullum V. C. *Br. J. Pharmacol.* **1968**, *34*, 43-55.
208. De Camp, W. H. *Chirality* **1989**, *1*, 2-6.
209. Snyder, L. R.; Kirkland, J. J. and Glajch, J. L. in *Practical HPLC Method Development 2nd Edition*, Wiley J. & Sons, New York, 1997, Chapter 12.
210. Bergholdt, A. B. and Lehmenn, S. V. *Chirality* **1998**, *10*, 699-704.
211. Kempe, M. and Mosbach, K. *Int. J. Peptide Protein Res.* **1994**, *44*, 603-606.
212. Miwa, T.; Miyakawa, T. and Kayano, M. *J. Chromatogr.* **1987**, *408*, 316-322.
213. Piletsky, S. A.; Andersson, H. S. and Nicholls, I. A. *J. Mol. Recognit.* **1998**, *11*, 94-97.
214. Han, S. M.; Han, Y. I. and Armstrong, D. W. *J. Chromatogr.* **1988**, *441*, 376-381.
215. Okamoto, Y.; Kawashima, M. and Hatada, K. *J. Am. Chem. Soc.* **1984**, *106*, 5357-5359.
216. Wainer, I. W.; Stiffin, R. M. and Shibata, T. *J. Chromatogr.* **1987**, *411*, 139-141.
217. Pirkle, W. H.; House, D. W. and Finn, J. M. *J. Chromatogr.* **1980**, 192, 143-158.
218. Sellergren, B.; Lepistö, M. and Mosbach, K. *J. Am. Chem. Soc.* **1988**, *110*, 5853-5860.

219. Chirica, G. and Remcho, V. T. *Electrophoresis* **1999**, *20*, 50-56.

220. Lim, C. K. in *HPLC of small molecules: a practical approach*, IRL Press, 1986, 1-3.

221. Asanuma, H.; Kajiya, K.; Hishiya, T. and Komiyama, M. *Chem. Lett.* **1999**, 665-666.

222. Kempe, M and Mosbach, K. *J. Chromatogr. A* **1995**, *694*, 3.13.

223. Sellergren, B.; Dauwe, C. and Schneider, T. *Macromolecules* **1997**, *30*, 2454-2459.

224. Knutsson, M. Andersson, H. S. and Nicholls, I. A. *J. Mol. Recognit.* **1998**, *11*, 87-90.

225. Piletsky, S. A.; Andersson, H. S. and Nicholls, I. A. *Macromolecules* **1999**, *32*, 633-636.

226. Asanuma, H.; Kakazu, M.; Shibata, M.; Hishiya, T. and Komiyama, M. *J. Chem. Soc., Chem. Commun.* **1997**, 1971-1972.

227. Sreenivasan, K. *J. Appl. Polym. Sci.* **1998**, *70*, 15-18.

228. Andersson, H. S. and Ramström, O. *J. Mol. Recognit.* **1998**, *11*, 103-106.

229. Yano, K.; Nakagiri, T.; Takeuchi, T.; Matsui, J.; Ikebukuro, K. and Karube, I. *Anal. Chim. Acta* **1997**, *357*, 91-98.

230. Nicholls, I. A. *J. Mol. Recognit.* **1998**, *11*, 79-82.

231. Andrews, P. R.; Craik, D. J. and Martin, J. L. *J. Med.Chem.* **1984**, *27*, 1648-1657.

232. Williams, D. H.; Cox, J. P. L.; Doig, A. J. Gardner, M.; Gerhard, U.; Kaye, P. T.; Lal, A; R.; Nicholls, I. A.; salter, C. J. and Mitchell, R. C. *J. Am. Chem. Soc.* **1991**, *113*, 7020-7030.

233. Searle, M. S.; Williams, D. H. and Gerhard U. *J. Am. Chem. Soc.* **1992**, *114*, 10697-10704.

234. Nicholls, I. A. *Chem. Lett.* **1995**, 1035-1036.

235. Nicholls, I.A.; Abdo, K.; Andersson, H. S.; Andersson, P. O.; Ankarloo, J., Dahlström, J.; Jokela, P.; Karlsson, J. G.; Olofssom, L.; Rosengren, J.; Shoravi, S.; Svenson, J. and Wikman, S. *Anal. Chim. Acta* **2001**, *435*, 9-18.

236. Pande, V. S.; Grosberg, A. Y. and Tanaka, T. *Proc. Natl. Acad. Sci. USA.* **1994**, *91*, 12976-12979.

237. Umpleby, R. J.; Baxter, S. C.; Bode, M.; Berch, J. K.; Shah, R. N. and Shimizu, K. D. *Anal. Chim. Acta* **2001**, *435*, 35-42.

238. Andersson, H. S. and Nicholls, I. A. *Bioorg. Chem.* **1997**, *25*, 203-201.

239. Svenson, J.; Andersson, H. S.; Piletsky, S. A. and Nicholls, I. A. *J. Mol. Recognit.* **1998**, *11*, 83-86.

240. Takeuchi, T.; Fukuma, D. and Matsui, J. *Anal. Chem.* **1999**, *71*, 285-290.

241. Lanza, F.; Hall, A. J.; Sellergren, B.; Bereczki, A.; Horvai, G.; Bayoudh, S.; Cormarck, P. A. G. and Sherrington, D. C. *Anal. Chim. Acta* **2001**, *435*, 91-106.

242. Obrecht, D.; Bohdal, U.; Broger, C.; Bur, D.; Lehmann, C.; Ruffieuw, R.; Schönholzer, P.; Spiegler, C. and Müller, K. *Helv. Chim. Acta* **1995**, *78*, 563-579.

243. Kempe, M. and Mosbach, K. *Anal. Lett.* **1991**, *24*, 1137-1145.

244. Svenson, J. and Nicholls, I. A. *Anal. Chim. Acta* **2001**, *435*, 19-24.

245. Patrick, G. L. in *An Introduction to Medicinal Chemistry*, Oxford University Press, 195-197.

246. Ishida, K.; Matsuda, H.; Murakami, M.; Yamaguchi, K. *J. Nat. Prod.* **1997**, *60*, 724-726.

247. Bauer, W.; Briner, U.; Doepfner, W.; Haller, R.; Huguein, R.; Marbach, P. and Petchr, T. J. *J. Life Sci.* **1982**, 1133-1140.

248. Emmel, E. A.; Verweil, C. L.; Durand, D. B.; Higgins, K. M.; Lacey, E.; and Crabtree, G. R. *Science* **1989**, *246*, 1617-1620.

249. Bourne, G. T.; Golding, S. W.; McGeary, R. P.; Meutermans, W. D. F.; Jones, A.; Marshall, G. R.; Alewood, P. F. and Smythe, M. L. *J. Org. Chem.* **2001**, *66*, 7706-7711.

250. Spatola, A, F.; Crozet, Y.; DeWit, D. and Yanagisawa, M. *J. Med. Chem.* **1996**, *39*, 3842-3846.

251. Pitt, N. and Gani, D. *Tetrahedron Lett.* **1999**, *40*, 3811-3814.

252. Fox; K. R. *Curr. Med. Chem.* **2000**, *7*, 17-37.

253. Merrifield, R. B. *J. Am. Chem. Soc.* **1963**, *85*, 2149-2154.

254. Ramanovskis, P. and Spatola, A. F. *J. Pept. Res.* **1998**, *52*, 356-374.

255. Alsina, J.; Jensen, K. J.; Albericio, F. and Barany, G. *Chem. Eur. J.* **1995**, *5*, 2787-2795.

256. Yang, L. and Morriello, G. *Tetrahedron Lett.* **1999**, *40*, 8197-8200.

257. Osapay, G.; Profit, A. and Taylor, J. W. *Tetrahedron Lett.* **1990**, *31*, 6121-6124.

258. Richter, L. S.; Tom, J. Y. K. and Burnier, J. P. *Tetrahedron Lett.* **1994**, *35*, 5547-5550.

259. Zhang, L. and Tam, J. P. *J. Am. Chem. Soc.* **1997**, *119*, 2363-2370.
260. Tam, J. P.; Lu, Y. A. and Yu, Q. *J. Am. Chem. Soc.* **1999**, *121*, 4316-4324.
261. Shao, Y.; Lu, W. and Kent, S. B. H. *Tetrahedron Lett.* **1998**, *39*, 3911-3914.
262. Robey, F. A. and Fields, R. L. *Anal. Biochem.* **1989**, *177*, 373-374.
263. Akamatsu, M.; Roller, P. P.; Chen, L.; Zhang, Z. Y.; Ye, B. and Burke, T. K. Jr. *Bio. Med. Chem.* **1997**, *5*, 157-163.
264. Yu, L. Lai, Y.; Wade, J. V. and, Coutts, S. M. *Tetrahedron Lett.* **1998**, *39*, 6633-6636.
265. Roberts, K. D.; Lambert, J. N.; Ede, N. J. and Bray, A. M. *Tetrahedron Lett.* **1998**, *39*, 8357-8360.
266. Pons, M.; Albericio, F.; Royo, M. and Girald, E. *Synlett.* **1999**, *2*, 172-181.
267. Ranganathan, D.; Haridas, V.; Madhusudanan, K. P.; Roy, R.; Nagaraj, R. and John, G. B. *J. Am. Chem. Soc.* **1997**, *119*, 11578-11584.
268. Ranganathan, D.; Haridas, V.; Kurur, S.; R.; Nagaraj, Bikshapathy, E.; Kunwar, A. C.; Sarma, A. V. S. and Vairamani, M. *J. Org. Chem.* **2000**, *65*, 365-374.
269. Pallin, T. D. and Tam, J. P. *J. Chem. Soc., Chem. Commun.* **1995**, 2021-2022.
270. Blackwell, H. E. and Grubbs, R. H. *Angew. Chem. Int. Ed. Engl.* **1998**, *37*, 3281-3284.
271. Feng, Y. and Burgess, K. *Chem. Eur. J.* **1999**, *5*, 3261-3272.
272. Burgess, K.; Lim, D.; Bois-Choussy, M. and Zhu, J. *Tetrahedron Lett.* **1997**, *38*, 3345-3348.
273. Zhang, L. and Tam, J. P. *Tetrahedron Lett.* **1997**, *38*, 4375-4378.
274. Blake, A. J.; Hannam, J. S.; Jolliffe, K. A. and Paattenden, G. *Synlett.* **2000**, *10*, 1515-1518.
275. Haas, K.; Ehrenstorfer-Schäfers, E. M.; Polborn, K. and Beck, W, *Eur. J. Inorg. Chem.* **1999**, 465-469.
276. Hass, K.; Ponikwar, W.; Nöth, H. and Beck, W. *Angew. Chem. Int. Ed. Engl.* **1998**, *37*, 1086-1089.
277. Sarin, V. K.; Kent, S. B. H.; Tam, J. P. and Merrifield, R. B. *Anal. Biochem.* **1981**, *117*, 147-157.
278. Fields, G. B.; Noble, R. L. *Int; J. Peptide Protein Res.* **1990**, *35*, 161-214.
279. Kuromizu, K.; Higuchi, H.; Abe, O. and Shimokawa, Y. *J. Chromatogr.* **1983**, *267*, 199-208.

280. Puertas, S.; Brieva, R.; Rebolledo, F. and Gotor, V. *Tetrahedron* **1993**, *49*, 4007-4014.

281. Szmuszkovicz, J. and Greig, M. E. *J. Med. Pharm. Chem.* **1961**, *4*, 259-296.

282. Ulbrich, K. and Kopecec, J. *European Polymer Journal*, **1976**, *12*, 183 – 187.

283. Maier, L. *Helv. Chim Acta.* **1973**, *56*, 1252-1257.

284. Chan, G.; Looney, M.; Solomon, D. and Veluayitham, S. *Aust. J. Chem.* **1998**, *51*, 31-35.

285. Honnoraty A. M., Mion L.; Collet H.; Teissedre R. and Commeyras A. *Bull. Soc. Chim. Fr.* **1995**, *132*, 709-702.

286. Holroyd, S. E.; Groves, P.; Searle, M. S.; Gerhard, U. and Williams, D. H. *Tetrahedron* **1993**, *49*, 9171-9182.

287. Fluka catalogue **2001-2002**, 55.

288. Bodanszky in *Principle of Peptide Synthesis*, Oxford, 93-94.

289. Sagara, Y.; Sagara, T.; Mase, T.; Kimura, T.; Numazawa, T.; Fujikawa, T.; Noguchi, K. and Ohtake, N. *J. Med. Chem.* **2002**, *45*, 984-987.

290. Gonsalves, K.E. and Chen, X. *Polym. Commun.* **1990**, *31*, 312-313.

291. Falcomer, C.; Vertuani, G.; Boggian, M.; Scatturin, A.; Spisani, S.; Cavalletti, T. and Traniello, S. *Il Farmaco* **1987**, *42*, 815-822.

292. Paruszewski, R.; Matusiak, R.; Rostafinska-Suchar, G.; Gumulka, S. and Krzascik, P *Pol. J. Chem.* **1987**, *61*, 127-132.

APPENDIX

Compounds Chapter 2

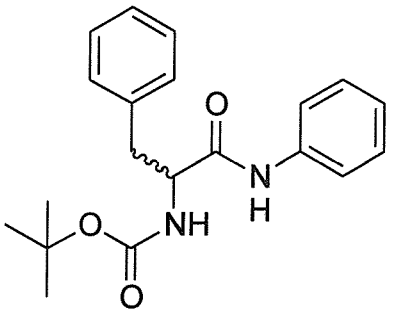

1: Boc-Phe-NHPh
2: Boc-D-Phe-NHPh

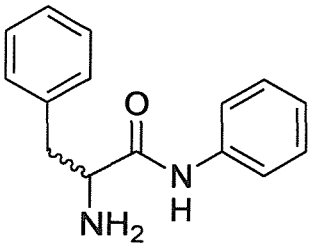

3: H-Phe-NHPh
4: H-D-Phe-NHPh

Compounds Chapter 3

Template

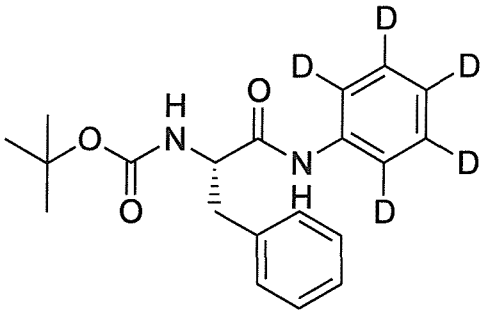

5: Boc-Phe-NHC_6D_5

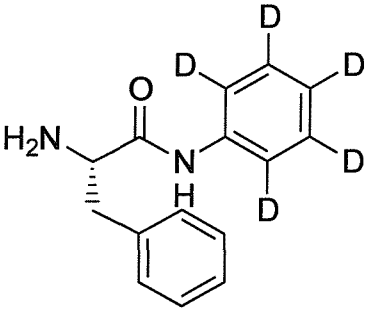

6: H-Phe-NHC_6D_5

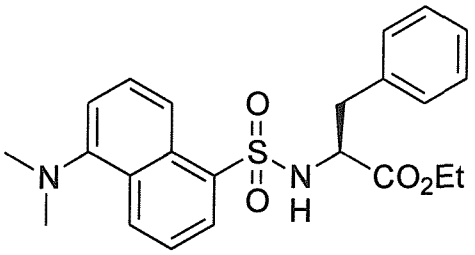

7: L-Dansyl-phenylalanine ethyl ester

Functional monomers (and polymers)

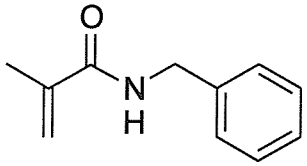

8: *N*-Benzyl-2-methacrylamide
(P-NBMA)

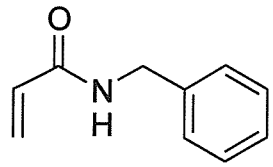

9: *N*-Benzylacrylamide
(P-NBA)

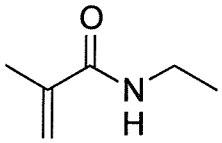

10: *N*-Ethyl-2-methacrylamide
(P-NEMA)

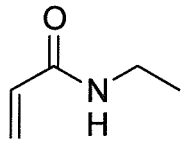

11 : *N*-Ethylacrylamide
(P-NEA)

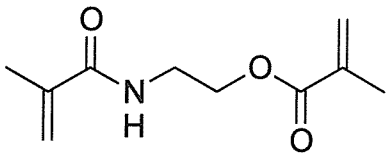

12: 2-Methylacrylamidoethyl Methacrylate

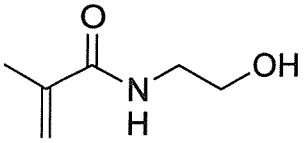

13: *N*-(2-Hydroxyethyl)methacrylamide
(P-NHEMA)

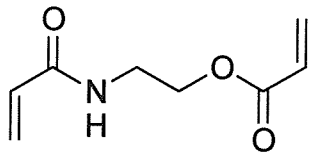

14: 2-Acrylamidoethyl Acrylate

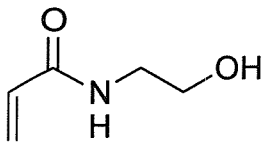

15*: N*-(2-Hydroxyethyl)acrylamide
(P-NHEA)

Compounds Chapter 4

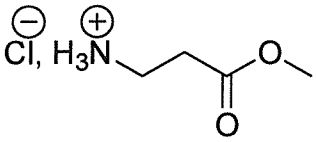

16: H-βAla-OMe, HCl

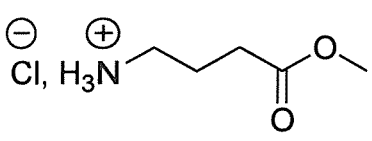

17: H-γAbu-OMe, HCl

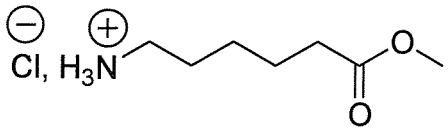

18: H-εAhx-OMe, HCl

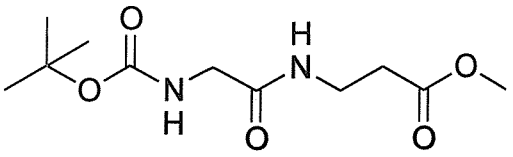

19: Boc-Gly-βAla-OMe

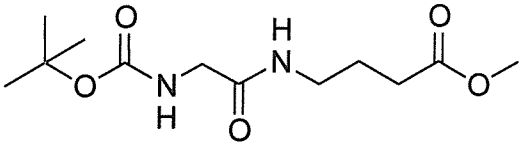

20: Boc-Gly-γAbu-OMe

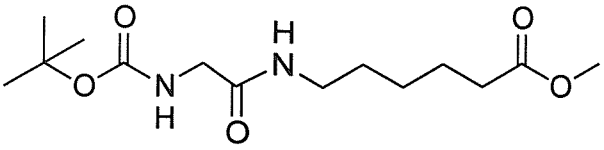

21: Boc-Gly-εAhx-OMe

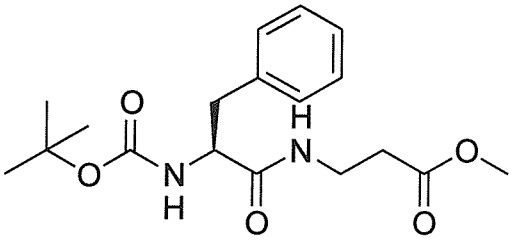

22: Boc-Phe-ßAla-OMe

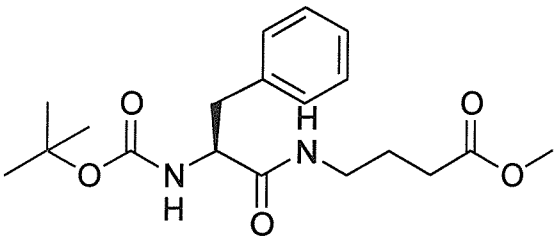

23: Boc-Phe-γAbu-OMe

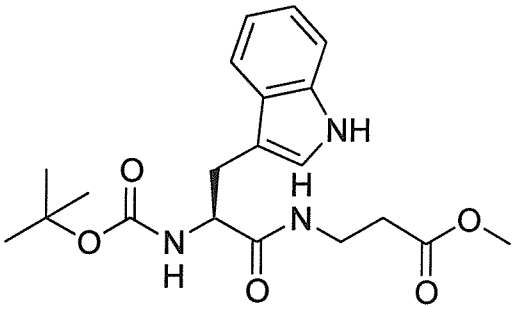

24: Boc-Trp-ßAla-OMe

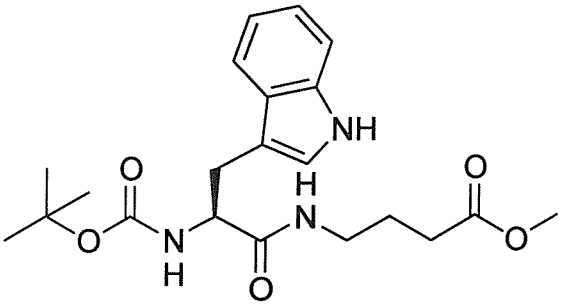

25: Boc-Trp-γAbu-OMe

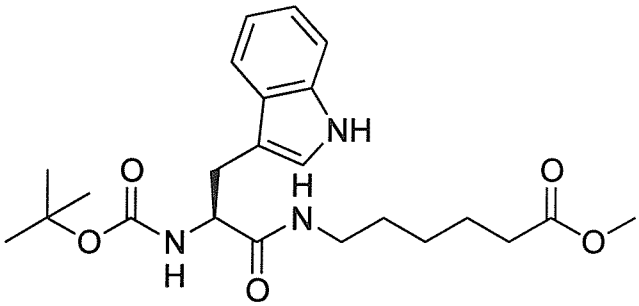

26: Boc-Trp-εAhx-OMe

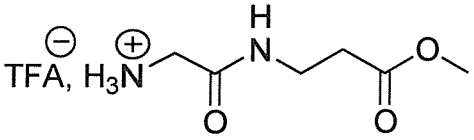

27: H-Gly-ßAla-OMe, TFA

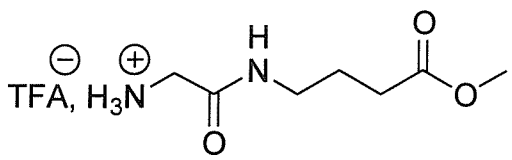

28: H-Gly-γAbu-OMe, TFA

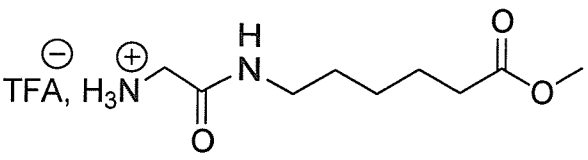

29: H-Gly-εAhx-OMe, TFA

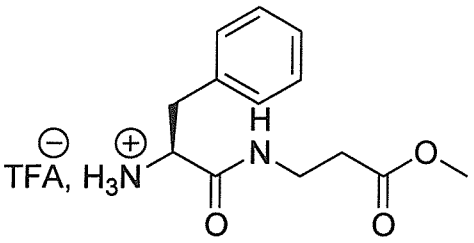

30: H-Phe-βAla-OMe, TFA

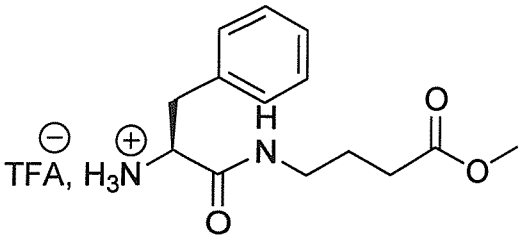

31: H-Phe-γAbu-OMe, TFA

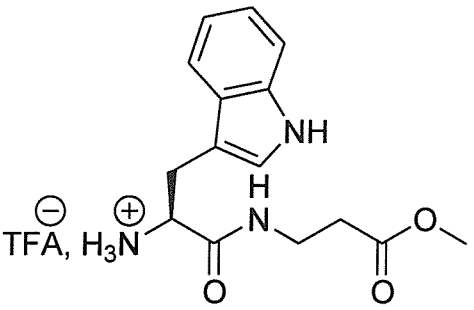

32: H-Trp-ßAla-OMe, TFA

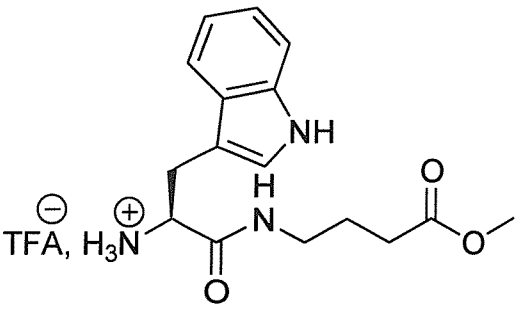

33: H-Trp-γAbu-OMe, TFA

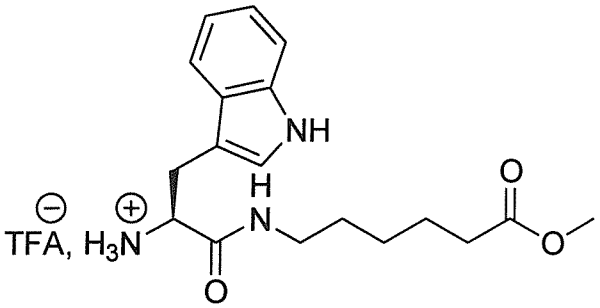

34: H-Trp-εAhx-OMe, TFA

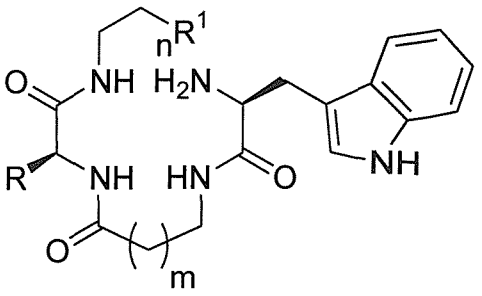

m=1, n=1:

R=CH_2indole, R^1= CO_2Me: **35** H-Trp-βAla-Trp-βAla-OMe
R=CH_2indole, R^1= CO_2H: **36** H-Trp-βAla-Trp-βAla-OH
R=CH_2Ph, R^1= CO_2Me: **37** H-Trp-βAla-Phe-βAla-OMe
R=H, R^1= CO_2Me: **38** H-Trp-βAla-Gly-βAla-OMe

m=1, n=2:
R=CH_2indole, R^1= CO_2Me: **39** H-Trp-βAla-Trp-γAbu-OMe
R=CH_2Ph, R^1= CO_2Me: **40** H-Trp-βAla-Phe-γAbu-OMe
R=H, R^1= CO_2Me: **41** H-Trp-βAla-Gly-γAbu-OMe

m=1, n=4:
R=CH_2indole, R^1= CO_2Me: **42** H-Trp-βAla-Trp-εAhx-OMe
R=H, R^1= CO_2Me: **43** H-Trp-βAla-Gly-εAbu-OMe
R=H, R^1= CO_2H: **44** H-Trp-βAla-Gly-εAbu-OH

m=2, n=2:
R=CH_2indole, R^1= CO_2Me: **45** H-Trp-γAbu-Trp-γAbu-OMe

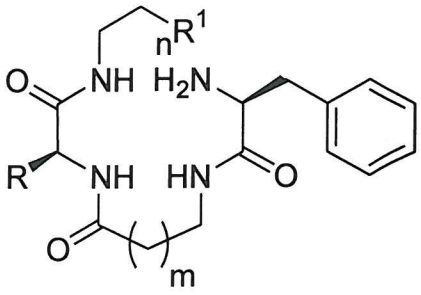

m=1, n=1:

R=CH_2Ph, R^1= CO_2Me: **46** H-Phe-βAla-Phe-βAla-OMe

R=CH_2Ph, R^1= CO_2H: **47** H-Phe-βAla-Phe-βAla-OH

R=H, R^1= CO_2Me: **48** H-Phe-βAla-Gly-βAla-OMe

m=1, n=2:

R=CH_2Ph, R^1= CO_2Me: **49** H-Phe-βAla-Phe-γAbu-OMe

R=CH_2indole, R^1= CO_2Me: **50** H-Phe-βAla-Trp-γAbu-OMe

R=H, R^1= CO_2Me: **51** H-Phe-βAla-Gly-γAbu-OMe

m=1, n=4:

R=CH_2indole, R^1= CO_2Me: **52** H-Phe-βAla-Trp-εAhx-OMe

R=H, R^1= CO_2Me: **53** H-Phe-βAla-Gly-εAbu-OMe

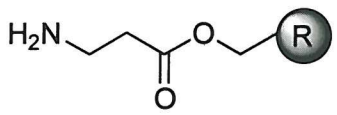

H-ßAla loaded resins

R = Hydroxymethyl Polystyrene: **(54)**

Quadra Gel: **(55)**

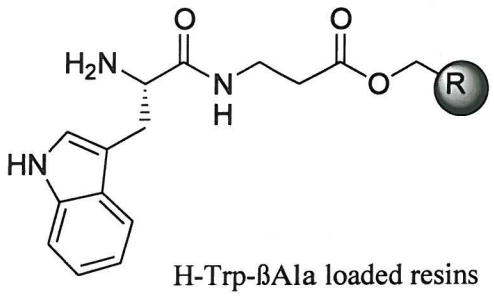

H-Trp-ßAla loaded resins

R = Hydroxymethyl Polystyrene: **56**

Quadra Gel: **57**

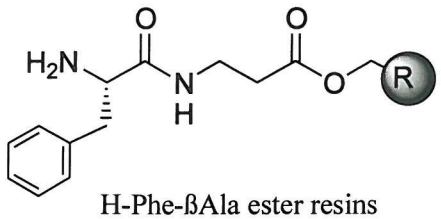

H-Phe-ßAla ester resins

R = Hydroxymethyl Polystyrene: **58**

Quadra Gel: **59**